

No. 293
January 1985

A STUDY OF FLAP-TYPE WAVE ABSORBING DEVICES

by

Robert Mark Scher



Department of Naval Architecture
and Marine Engineering
College of Engineering
The University of Michigan
Ann Arbor, Michigan 48109

ABSTRACT

A class of wave-absorbing devices consisting of one or two thin oscillating flaps is considered from the stand-points of hydrodynamics, design requirements, and engineering economics. A three-dimensional linear hydrodynamic model of flap-type wave absorbers in finite depth water is developed, and the hydrodynamic coefficients necessary to evaluate power absorption and motions are evaluated numerically.

The effects of device dimensions on maximum power absorption and corresponding motion amplitudes are considered. It is shown that for devices that are small with respect to the wavelength the maximum power absorption is a function of the wavelength, varying only slightly with device dimensions, while the corresponding motion amplitude is strongly dependent on device size. In this wavelength range, the flap-type device functions as a "directional point absorber," and absorption cross-sections substantially larger than the device width are obtained, accompanied by extremely large motion amplitudes. In shorter waves the flap functions as a "terminator," approaching the 2-D limit of maximum power absorption per unit width, in normal wave encounter. Power absorption in oblique wave encounter is also considered: flap width is the most important variable. The sensitivity of the device to tuning is also an

issue in choosing dimensions: larger flaps are shown to be inherently less sensitive to mistuning. In addition, increased flap dimensions, especially draft, can alter the added inertia in such a way that the sensitivity of the tuning is reduced. Both of these effects are advantageous in random seas.

The use of linear and nonlinear control forces to reduce the motions occurring near resonant tuning is considered, and the corresponding effect on absorbed power is calculated. The effects of wave environment, water depth, and other site-related factors on device design and operation are examined. Finally, several of the primary design requirements for flap-type devices are considered. A method of approaching the design of a device for a particular location is presented, and the elements of a preliminary cost estimate are proposed.

DEDICATION

For Ellen Beth Katzer.

ACKNOWLEDGEMENTS

There are many people who have contributed mightily to the completion of this work. I am most grateful to the members of my committee, and especially to Armin Troesch, without whose technical advice and encouragement, patience, and force of character, nothing could have levered me off of dead center. I would also like to thank Professor Michael G. Parsons, Chairman of the Department of Naval Architecture and Marine Engineering, for his continuing support, both financial and moral. Mr. Richard O. Wilke, of the Q-Corporation, deserves a medal of some sort for bravery, in that he has stood his ground for a "simple" concept of what a wave-absorbing device should be. Finally, I would like to give my special thanks to Professor T. Francis Ogilvie, who told me long ago that I didn't have the temperament for the task of completing a Ph.D. How I wish I had listened to that man.

PREFACE

It is in the nature of water waves that there are an almost infinite variety of device concepts that can be proposed to absorb energy from them. It is in the nature of humanity in general, and scientists and engineers in particular, to actually propose most of them at one time or another, claiming some particular technical or economic advantage. So many different types have been developed over the past decade or so, with offshoots and refinements of each, that among those familiar with the field it has become customary to speak of "second-generation" devices, even though the majority of the "first generation" have never been built.

The flap-type absorbing device, by comparison with many others, is too simple to be technologically eye-catching. From the early stages of even the first generation, the flap concept was compromised by the idea of "2-D efficiency," that is, the ratio of absorbed power to incident wave power in a two-dimensional problem. For a symmetrical device oscillating in a single degree of freedom, it can be shown that the maximum 2-D absorption is half of the incident power, at optimal tuning and damping. By contrast,

devices that are asymmetric, or that oscillate in two or more degrees of freedom, can be shown to be capable of absorbing all the incident power. Thus, at the outset, the single flap device was commonly judged as "inferior" by a factor of two. Furthermore, the concept had the additional misfortune of being fostered in the United States, which (for many practical reasons) has not been nearly as devoted to wave-energy research as other countries: notably the U.K., Japan, and Norway, all nations in which it isn't very far to the beach.

The preoccupation with maximum power absorption or 2-D efficiency has tended to obscure several key issues: first, something in an absorbing device must move in order to absorb. If the device absorbs power by damping the motion of a body (or a part of the free surface itself), then the motion under certain conditions (including the condition for maximum power absorption) can become larger than most mechanical devices can accept. Therefore, the obtainable absorption of a device may not be limited by its hydrodynamic "efficiency," but by its mechanical arrangements. Second, the very concept of 2-D efficiency is misleading. It implies that more power can always be developed by increasing the width of a device: true enough in normal wave encounter, which is the only kind of wave encounter there is in a 2-D analysis, not true at all in oblique encounter. It also implies that there is a

meaningful denominator in the fraction absorption/incident power, which is also only true in a 2-D case. Third, maximum absorption in regular waves of a given frequency (and amplitude, if motion responses and forces are to be considered) by no means ensures maximum average absorption in a random sea. Fourth, and most obvious, there is no point in incorporating design features that increase the absorption (even the useable absorption), if the cost of the device increases faster.

In any case, early thinking, dominated as it was by the consideration of 2-D efficiency, led to the idea of the twin-flap device, which because of its two independent degrees of freedom, entered the promised land of 100 percent. There were other perceived advantages, too, as there always must be. As it turns out, many of these advantages are partially cancelled by things that happen in the three-dimensional world, and the increased absorption does not appear without larger motions of the flaps, and other problems as well.

The flap-type device, whether single or twin-flap, is merely one (or two) of a myriad of absorbing-body concepts. Brian Count has given what amounts to a design philosophy in a single thought: the absorbing body is only the "antenna," the remainder of the power conversion system constitutes the tuner and receiver. There is no question that the design of the antenna is just one element in the sys-

tem, and not necessarily the most important one. Nevertheless, because it is fundamentally a hydrodynamics problem (as opposed to one of machinery design, control, power generation and transmission, structures, or soil mechanics, some of the elements of the tuner and receiver), the design of the antenna receives a great deal of attention here. Then, too, the antenna may end up driving the design and cost of the tuner and receiver if it becomes either too complicated or too large. For good or ill, this is something to watch out for. And in the design of an antenna there is one cardinal dictum: know your wavelength band, and decide whether you want an antenna that is small with respect to the wavelength (like the ferrite on an AM radio), or large (like a radar dish). As it turns out, a practical wave-absorbing device can be designed from either perspective, under certain conditions, which is perhaps part of the reason why there are so many different kinds.

Finally, there is a well known principal, although it is often disregarded, that every reasonable effort should be made to keep a simple idea from becoming complex. This work is an effort to integrate the hydrodynamics of a flap-type device in three dimensions with some preliminary thinking about the design of practical devices, in the light of that rule.

TABLE OF CONTENTS

DEDICATION	ii
ACKNOWLEDGEMENTS	iii
PREFACE	iv
LIST OF FIGURES	xi
LIST OF TABLES	xvi
INTRODUCTION	1
HYDRODYNAMIC ANALYSIS	9
Measures of Power Absorption	9
Flap Type Absorbers	16
Linear Equations of Motion and Boundary Value Problems	21
Green's Functions	29
Numerical Scheme	38
Validation of 3-D Hydrodynamic Coefficient Predictions	47
EFFECTS OF DEVICE GEOMETRY ON 3-D HYDRODYNAMIC BEHAVIOR	58
Flap Draft	68
Flap Separation	73
Flap Width	78
Pivot Location	84

Flap Dimensions and Nonresonant Tuning	88
NONLINEARITY AND CONTROL REQUIREMENTS	94
Introduction	94
Stroke Limitation and Phase Control by External Forces	96
Upper Bounds on Energy Absorption with Stroke-Limited Response and Phase Control	112
Nonlinear Hydrodynamic Forces Tending to Limit Large Amplitude Motions	117
Suggested Time-Domain Approaches to Motion Prediction	125
ABSORPTION CHARACTERISTICS IN RANDOM SEAS	129
Average Absorbed Power in a Unidirectional Random Sea	135
Directionality Effects on Average Absorption	158
Acceptable Motion Response Criteria in Random Seas	162
MATCHING OF THE SYSTEM AND SITE	167
Wave Climatology	168
Tidal Effects	182
Current Effects	184
Location of Devices with Respect to Breaking Zone	185
Soil Characteristics	186
Other Environmental Factors	187

A DESIGN PHILOSOPHY	191
Floating versus Fixed Structure	192
A Suggested Design Procedure	197
CONCLUSIONS	233
REFERENCES	239
FIGURES	
TABLES	
APPENDIX: PROTOTYPE WAVE ABSORBING SYSTEMS	A1
Type and Arrangement of Power Takeoff Machinery	A3
Power Conversion Machinery and Conversion Efficiency	A16
Restoring Forces	A25
Elements of an Economic Model	A32
A Design Example	A58

LIST OF FIGURES

(All figures are found at the end of the text.)

- Fig. 1. Coordinate system for a terminator.
- Fig. 2. Coordinate system and dimensions for a flap-type absorber.
- Fig. 3. Comparison of Green's function values.
- Fig. 4. Quadrilateral numbering scheme.
- Fig. 5. Application of the Biot-Savart law to the integration of the essential singular part of the Green's function.
- Fig. 6. Half-quadrilateral scheme for the use of midpoint rule integration for the wave part of the Green's function on the local stack of quadrilaterals.
- Fig. 7. Comparison of added mass coefficients versus Kotik's 2-D prediction (sway).
- Fig. 8. Comparison of damping coefficients versus Kotik's 2-D prediction (sway).
- Fig. 9. Comparison of added inertia coefficients versus Kotik's 2-D prediction (roll).
- Fig. 10. Comparison of damping coefficients versus Kotik's 2-D prediction (roll).
- Fig. 11. Comparison of depthwise radiation pressure distribution at midspan versus Toki's 2-D prediction.
- Fig. 12. Comparison of exciting force versus Evans' 2-D prediction (sway).
- Fig. 13. Comparison of exciting force (sway) versus Stiassnie and Dagan's 3-D result, for a flap aspect ratio of 10, normal encounter.

- Fig. 14. Comparison of effect of draft/depth ratio on exciting force, versus Stiassnie and Dagan's 3-D result (normal encounter).
- Fig. 15. Comparison of effect of angle of encounter on exciting force, versus Stiassnie and Dagan's 3-D analytical prediction.
- Fig. 16. Comparison of added mass and acceleration coupling coefficient for a twin flap versus Srokosz and Evans' 2-D prediction.
- Fig. 17. Comparison of damping and velocity coupling coefficient for a twin flap versus Srokosz and Evans' 2-D prediction.
- Fig. 18. Comparison of exciting force magnitudes for a twin flap versus Srokosz and Evans' 2-D prediction.
- Fig. 19. Comparison of absorption cross-section per unit flap width versus experimental results for a finite width twin-flap device.
- Fig. 20. Comparison of flap motion response amplitude operators versus experimental results for a finite width twin-flap device.
- Fig. 21. Typical sensitivity to quadrilateral arrangements for a single flap: added inertia.
- Fig. 22. Typical sensitivity to quadrilateral arrangements for a single flap: damping coefficient.
- Fig. 23. Typical sensitivity to quadrilateral arrangements for a single flap: exciting force.
- Fig. 24. Three-dimensional exciting force magnitude comparisons, single versus twin flap, at three flap widths.
- Fig. 25. Twin flap exciting force magnitudes and phase relationship versus encounter angle.
- Fig. 26. Maximum absorption versus draft for a high aspect ratio flap, deep water.
- Fig. 27. Motion amplitude at maximum absorption versus draft for a high aspect ratio flap,

deep water.

- Fig. 28. Maximum absorption versus draft for a low aspect ratio flap, deep water.
- Fig. 29. Motion amplitude at maximum absorption versus draft for a low aspect ratio flap, deep water.
- Fig. 30. Maximum absorption and motion amplitude versus draft for a low aspect ratio flap, shallow water.
- Fig. 31. Coupling force coefficients versus separation for a twin flap.
- Fig. 32. Exciting force magnitudes and phase versus separation for a twin flap.
- Fig. 33. Absorption cross-section/wavelength ratio, as a function of wavelength/ device width.
- Fig. 34. Absorption cross-section/device width ratio, as a function of wavelength/device width.
- Fig. 35. Maximum absorption versus flap width for a single flap, deep water.
- Fig. 36. Motion amplitude at maximum absorption versus flap width for a single flap, deep water.
- Fig. 37. Maximum absorption versus flap width for a single flap, shallow water.
- Fig. 38. Motion amplitude at maximum absorption versus flap width for a single flap, shallow water.
- Fig. 39. Exciting force versus encounter angle for single flaps.
- Fig. 40. Required spring constant versus tuned frequency, showing the effect of flap draft on tuning.
- Fig. 41. Required spring constant versus tuned frequency showing the effect of flap width on tuning.
- Fig. 42. Exciting force magnitudes and phase versus flap width for a twin flap.

- Fig. 43. Maximum absorption and motion amplitude versus pivot depth/draft ratio.
- Fig. 44. Absorbed power with a maximum stroke constraint ($RAO = 1$) obtained by overdamping, versus flap width.
- Fig. 45. Bouncing off the stops with a nonlinear spring stroke limiter at low exciting-force frequencies.
- Fig. 46. Instability of a time-step simulation at resonant frequency with a nonlinear spring stroke limiter.
- Fig. 47. Energy budget schematic for a twin-flap system.
- Fig. 48. Exciting force versus flap top submergence, deep water.
- Fig. 49. Maximum absorption versus flap top submergence.
- Fig. 50. Motion amplitude at maximum absorption versus flap top submergence.
- Fig. 51. Two spectra for 2 m significant wave height, showing both variance spectral density and power density.
- Fig. 52. Specific power absorption curves for a 5 x 10 m flap, water depth 7.5 m, tuned to a frequency of 0.9 rad/sec, at various dampings.
- Fig. 53. Motion amplitudes for a 5 x 10 m flap, water depth 7.5 m, tuned to a frequency of 0.9 rad/sec, at various dampings.
- Fig. 54. Specific power absorption curves for a 5 x 10 m flap, water depth 7.5 m, at various tunings and dampings.
- Fig. 55. Motion amplitudes for a 5 x 10 m flap, water depth 7.5 m, at various tunings and dampings.
- Fig. 56. Average power absorption in 2-m significant wave height versus damping for three device sizes, various tunings.

- Fig. 57. Root-mean square motion in 2 m significant wave height versus damping for three device sizes, various tunings.
- Fig. A1. Flap device arrangement with a top-mounted airbag and turbine power takeoff system.
- Fig. A2. Flap device arrangement with a top-mounted positive-displacement hydraulic power takeoff.
- Fig. A3. Flap device arrangement with a bottom-mounted hydraulic power takeoff in an underwater enclosure.
- Fig. A4. Stiffened single plate flap with a buoyant member for restoring force.
- Fig. A5. Double plate boxlike flap.
- Fig. A6. Pendulous top-pivoted flap.
- Fig. A7. Arrangement of a positive displacement hydraulic power takeoff and auxiliary systems inside a bottom pivoted boxlike flap.

LIST OF TABLES

(All tables are found at the end of the text, following the figures.)

Table I. Typical comparisons of power absorption and flap motions for single and twin flap devices, normal encounter.

Table II. Typical comparison of single and twin flap directionality effects.

Table III. Typical comparison of twin flap variations near an optimum tuning and damping.

Table IV. Summary of effects of spectral parameters on design parameters.

INTRODUCTION

Within the last decade there has been a significant amount of research activity in the field of energy production from ocean waves. In several nations, notably Japan and the United Kingdom, these efforts have extended to the construction and testing of large-scale prototypes, some of them capable of electrical-power generation on the order of 100 kW, or more (Refs. 1-3).

Because of the nature of water waves, there is an almost unlimited number of possible configurations for converting the motion of water into mechanical response and ultimately into useful work, as an inspection of patent claims will show. A large part of the published work has tended to dwell on the relative merits of various body geometries in absorbing power from ocean waves. In particular, proposed devices are often compared in terms of their absorption "efficiency," which is in a sense an unfortunate concept to begin with when describing a system that has an essentially infinite potential input.

Such comparisons, while they are not meaningless, should be considered without losing sight of one important fact: As stated most succinctly by Count and Jefferys (Ref. 4), "...linear hydrodynamic theory demonstrates that

all shapes are potentially equivalent in their ability to absorb energy from water waves. Therefore, the main feature with which one concept may be separated from another will be their engineering characteristics..." Somewhat more informally, but still in the words of Brian Count, "You can put a teddy bear out in waves, and it will absorb energy."

This is a remarkable restatement of the Haskind relation, but the implication is simply that if a body can radiate large amplitude waves by its forced motion, then it can also absorb large amplitude waves by its motion in response to incident waves. The principal questions remaining are as follows: (1) How much does the body have to move? and (2) How much does the body (and the power conversion machinery attached to it) cost? To these questions might be added a third: To what extent does linear theory explain the situation with the accuracy required for a decision? The answer, of course, depends in great measure on the answer to question (1), above.

As a result of the relatively large number of device concepts competing for research and development funds (the aptly-named "trade-mark war," which is also Count's phrase) research efforts in the area of wave-energy extraction systems have developed what might be called "national character," with each active country committing itself primarily to one, or at most two, concepts. In the U.K., for example,

the elegant but complex Salter "duck" (Ref. 5) became a national standard bearer after a strong challenge by two promising competitors, the Farley triplate (Ref. 6) and the Cockerell articulated raft (Ref. 7). In Japan, the tuned air-chamber buoy was ultimately developed to the point of an operating large-scale prototype, Kaimei (Ref. 8). Subsequent designs, incorporating resonant air or water columns, are still leading contenders in several countries. In Norway, much of the research work has concentrated on the refinement of control systems for arrays of point absorbers (Ref. 9).

In spite of recent budgetary setbacks in wave energy programs (and in most speculative energy technologies, as well, in a period of stagnant or falling fuel price) in all of these countries interest remains active, particularly with regard to local applications in areas where fuel costs are high and wave energy is accessible and plentiful.

During 1981 and early 1982, a series of model experiments were performed with a twin-flap wave-energy absorbing device in the towing tank of the Department of Naval Architecture and Marine Engineering at The University of Michigan (Ref. 10). Without wishing to contribute any further to the trade-mark war, it may be mentioned briefly that the twin-flap concept was believed to offer several potential engineering advantages, including simplicity of design and construction, considerable freedom in design parameters for

adapting the device to a range of seastates, and at least the theoretical possibility of minimizing resultant mooring forces under certain conditions.

In these experiments, measurements were made of absorbed power, incident wave power, flap motion responses, and forces. All experiments were performed with the supporting structure rigidly fixed, with normal wave encounter. Both 2-D and finite flap-length experiments were conducted. One of the principal objectives of these experiments was to obtain a direct comparison with the earlier analytical work of Srokosz and Evans (Ref. 11).

Generally, fair agreement was obtained between theory and experiment with regard to two-dimensional absorption efficiency, although a slight but consistent tendency for theory to underestimate measured efficiency was apparent. Maximum two-dimensional efficiencies approaching 100% (as predicted analytically) were confirmed. Further, the predicted behavior of curves of efficiency versus wavenumber and versus applied damping coefficient was generally matched by experimental results. Results for flap motion responses and forces showed good agreement with theory.

In the course of these experiments and the associated analytical work, however, it became apparent that the feasibility of any wave-power concept would depend on its characteristics under conditions that could not be studied experimentally at the University's facility, due to the limit-

ations of the towing tank and its wavemaker. These conditions are:

- (1) Oblique wave encounter with finite device length.
- (2) Shallow water.

The principal aim of this work is to investigate the effects of a 3-D wave environment on the design and operation of flap-type absorbing devices.

The remainder of this work can be outlined as follows:

In the first chapter, "Hydrodynamic Analysis," a numerical method is derived to estimate the motion and power absorption responses of a flap-type device (either single or twin-flap), incorporating the 3-D linear hydrodynamic effects of oblique encounter and finite device length in the presence of a bottom. Appropriate measures of power absorption are defined and the geometry of flap-type absorbers is introduced. Next, the hydrodynamic coefficients needed to determine the power absorption and motion responses are identified, and the technique used to determine them is described in detail. The testing of this method against available theoretical and experimental results is the subject of the closing section of the first chapter.

The second chapter, "Effects of Device Geometry on 3-D Hydrodynamic Behavior," begins the process of applying hydrodynamic results to the design of flap-type devices.

In this chapter, the principal aim is to determine how the geometrical characteristics of the device influence the power absorption and motion behavior in waves of a particular frequency. It will be shown that to design a system for a regular wave, the amplitude as well as the frequency must be specified, if correct decisions regarding device dimensions are to be made. The influence of device dimensions on the ability to obtain resonant tuning using hydrostatic restoring forces is discussed, as well as the sensitivity of various devices to tuning. The conditions for maximum power absorption are shown to correspond to extremely large values of the motion response of the flaps, often greatly exceeding the reasonable limits of linear theory, when small flap dimensions are specified. Some preliminary conclusions regarding the relative merits of single and twin-flap systems from the standpoint of practical design are also offered. Based on examples, it is shown that the twin-flap device can be set up to absorb approximately twice as much power as a single flap of equivalent width, at a particular design frequency, as is the case in two dimensions. However, in most respects, the general conclusions regarding the influences of dimensions on performance hold equally for twin and single-flap devices.

In the next chapter, "Nonlinearity and Control Requirements," one of the first engineering considerations

associated with flap-type absorbers will be discussed in greater detail, namely, the need to impose limitations on the stroke of the device for practical reasons when predicted motions at maximum absorption are large. The sources of the large motion predictions of linear theory are identified: primarily, the use of an exciting force based computationally on a body boundary condition linearized on the mean position of the flap. The effect on absorbed power of using external forces to limit the device response is calculated. In addition, some nonlinear hydrodynamic forces that may tend to limit the flap motion will be discussed.

The next chapter, "Absorption Characteristics in Random Seas," introduces methods for evaluating the average absorbed power in a spectrum, directional effects due to spreading or misalignment, and some criteria for "acceptable" motions when the flap response is a random process.

In the chapter "Matching of the System and Site," an attempt is made to catalog and discuss the more important environmental factors related to the design of flap-type devices. The long-term wave climatology is of primary importance, naturally, but several other site-related factors are also presented as related to components of the design.

In the next chapter, "A Design Philosophy," a few basic design issues for flap-type absorbers are raised. Then, a preliminary design procedure for prototype flap ab-

sorbing devices is proposed, based on the results of preceding chapters. A simple example of the method is presented as an Appendix, together with arguments for some additional design features of a prototype power-generating system, and the elements of a model for economic evaluation.

Finally, some over-all conclusions regarding the design and feasibility of flap-type devices are offered.

HYDRODYNAMIC ANALYSIS

Measures of Power Absorption

As has been mentioned, proposed devices are often compared on the basis of absorption "efficiency," which is a somewhat ill-defined term in this particular application. For "terminators," finite-length devices that are intended to lie essentially parallel to incident wave crests (as opposed to so-called "point absorbers" or "attenuators"), the absorption efficiency is most often interpreted as the power output per unit width of a device, divided by the energy flux per unit width of wavefront. The "efficiency" of a particular device, then, may be given as a function of wave frequency and angle of encounter.

Unfortunately, the prevalent use of the term "absorption efficiency" has tended to obscure several important facts:

(1) The efficiency of absorption is a function only of the hydrodynamics of the absorbing device, and implies nothing about the efficiency of the mechanical, hydraulic, pneumatic, or electrical equipment used to convert the absorbed power into a useful form. (The type and arrangement of conversion machinery, however, is often dictated by the form of the absorbing device. Therefore, the two parts of

the conversion process, though distinct, are not wholly independent).

(2) "Efficiency" is not necessarily a paramount concern in determining either the feasibility of a concept device or the relative merit of competing devices. In fact, the only proper measure of merit for such an energy-conversion system must be an economic one, and absorption efficiency may not be the crucial component in the analysis, when placed against unit costs, complexity of manufacture, and reliability.

(3) The concept of efficiency, while it has the advantage of being dimensionless, is not particularly useful when there is no obvious definition for power input. A unique definition of power input exists only in the case of a strictly 2-D experiment. There is no such definition in a 3-D situation, unless one adopts the convention of defining power input as the energy flux across an extent of wavefront equal to the length of the device. This definition is completely arbitrary, however, and has nothing to do with the power actually absorbed by a device in a 3-D environment.

(4) Most importantly, the use of an "efficiency" definition seems to imply that an increase in device length must result in an increase in power absorbed. For any device modelled as a rigid body, in 3-D, with the possibility of oblique wave encounter, this is not necessarily true.

For practical situations, therefore, a more suitable measure of potential power output must be invoked. This is particularly necessary if any kind of comparison is to be made between different choices of design variables, including device dimensions and geometry, tuning, and power-takeoff details, as well as the location and orientation (facing) of the device. One such measure is the absorption cross-section, often referred to as "capture width." This measure can be defined according to the following argument.

Consider a wave-energy absorbing device of the "terminator" type, that is, a device designed to be oriented essentially normal to the direction of wave travel. The device is assumed to be of finite (fixed) dimensions, length, breadth, and draft, and the water depth is denoted by h .

The "tuning" of the device (i.e., the masses and restoring force coefficients of the various elements) is given. Similarly, the externally applied damping coefficients of the power takeoffs (which are assumed here to act as linear dampers) are given.

The coordinate system is shown in Fig. 1. The device is subject to regular incident waves of frequency ω and amplitude ζ_A , from direction β , where $\beta=0$ implies normal incidence. The average power absorbed by the device is P .

Next, define the average incident power density, Q , for regular waves as the average energy flux per unit length crossing a line normal to the direction of wave travel.

For water of infinite depth, Ref. 9 gives this quantity as:

$$Q = (1/4) \rho g^2 \zeta_A^2 / \omega \quad (1)$$

In water of depth h , a modified expression (Ref. 9) is

$$Q = (1/4) \rho g^2 (\zeta_A^2 / \omega) \tanh kh (1 + 2kh / \sinh 2kh) \quad (2)$$

where k is the solution of $k \tanh kh = \omega^2 / g$. Note that in the limit $kh \rightarrow \infty$, the terms involving the hyperbolic functions approach unity, giving the previous, simpler expression for the incident wave energy density in deep water.

Since the average power absorbed by the device is P , and the average power density represented by the incident waves is Q , we may now define an absorption cross-section for the device as follows:

$$\sigma(\omega, \beta) = P/Q \quad (3)$$

Note that the quantity σ is dimensional, with units of length. Furthermore, a value of σ is determined not only by the explicit dependency on wave frequency and encounter angle, but also by the geometry, tuning, and power-takeoff damping coefficients selected. That is,

$$\sigma(\omega, \beta) = \sigma(\omega, \beta; \underline{G}, \underline{T}, \underline{D}) \quad (4)$$

where the vectors \underline{G} , \underline{T} , and \underline{D} represent design or operating parameter spaces corresponding, respectively, to the geometry of the device (as length, breadth, draft, spacing of elements, etc.), the tuning of the device (as masses and restoring force coefficients on the various elements), and the external damping coefficients imposed by the power takeoffs on the various elements.

The reason for separating the design parameter space into the three vectors \underline{G} , \underline{T} , and \underline{D} is a practical one. In a plausible system, the over-all geometry of the device would be fixed, or at best, variable only slowly and with some difficulty. By contrast, the tuning (masses and spring constants), could be varied somewhat more rapidly by, for example, flooding or deballasting buoyancy tanks in the oscillating elements of the device. Finally, the external damping coefficients can be controlled rapidly and continuously by increasing or decreasing the power generating load on the system. Before leaving this description of the design parameters, however, we should introduce one additional parameter, namely, the "facing" of the device, which we will signify by θ_0 . This design parameter, although absent from the above definition of $\sigma(\omega, \beta)$, is obviously a key element in determining the performance of the absorber in situations where normal wave encounter cannot be assumed, as will be discussed in detail subsequently.

The absorption cross-section is a measure of the device's potential power output in a wave system of given average power density. For the purposes of assessing various devices in an ocean environment, that is, in random and often short-crested (i.e., directionally spread) seas, the absorption cross-section has a certain advantage over the more commonly used measure (for terminators) of 2-D efficiency. Specifically, the use of the quantity $\sigma(\omega, \beta)$

rather than some variant of 2-D efficiency, avoids the very erroneous idea that an increase of device length necessarily results in increased power absorption. This conclusion is justified only in a strictly 2-D sense, but it is just plain incorrect for oblique wave encounter.

Consider a directional sea spectrum $S^+(\omega, \theta)$, representing a sea state in which the incident waves (and hence, wave energy) are distributed over a range of frequencies and arrive from a distribution of directions. The usual way of constructing such a spectrum is as follows:

$$S^+(\omega, \theta) = S^+(\omega) F(\omega, \theta) \quad (5)$$

Here, $S^+(\omega)$ is the usual nondirectional spectrum that could be obtained by analyzing time histories from a single wave probe, and $F(\omega, \theta)$ is a spreading function, noting that θ is an angle with respect to a fixed geographic direction, or a specified principal wave direction. The spreading function F , in principle, can be evaluated by analyzing the cross-correlations or cross-spectra from an array of wave probes, as described by Haddara (Ref. 12).

For a nondirectional spectrum $S^+(\omega)$, the time-averaged power density \bar{Q}_S can be defined as follows, for deep water:

$$\bar{Q}_S = \frac{1}{4} \rho g^2 \int_0^{\infty} [S^+(\omega)/\omega] d\omega \quad (6)$$

where \bar{Q}_S now represents the average power density integrated over the entire frequency content of the spectrum.

In order to have a consistent definition of power den-

sity for a directional spectrum $S^+(\omega, \theta)$, however, the total power density at a single frequency ω_0 , integrated over all directions in the directional spectrum, must be identical to the single-probe result given in terms of $S^+(\omega_0)$. That is, the spreading function $F(\omega, \theta)$ must be normalized such that

$$\int_{-\pi}^{\pi} \frac{S^+(\omega_0, \theta)}{\omega_0} d\theta = \frac{S^+(\omega_0)}{\omega_0} \quad (7)$$

and

$$\int_{-\pi}^{\pi} \int_0^{\infty} [S^+(\omega, \theta)/\omega] d\omega d\theta = \int_0^{\infty} [S^+(\omega)/\omega] d\omega. \quad (8)$$

In the directional spectrum, the integrand is the average energy flux per unit length, per unit frequency, per unit plane angle, crossing a line oriented normal to the direction θ .

The total power absorbed by the device is then given by

$$\bar{P}_S = \frac{1}{4} \rho g^2 \int_{-\pi}^{\pi} \int_0^{\infty} [S^+(\omega, \theta)/\omega] \sigma(\omega, \beta) d\omega d\theta, \quad (9)$$

where the direction argument β in the cross-section function is given by the fixed orientation of the device θ_0 , $\beta = \theta - \theta_0$.

Up to this point, no particular type of absorbing device was assumed, other than to specify the broad category of terminators. In fact, even this limitation was not strictly necessary, as the idea of an absorption cross-section applies equally to attenuators or point absorbers. Presumably, individual symmetric point absorbers

are omnidirectional in performance, that is, $(\omega, \beta) = \sigma(\omega)$.

Flap Type Absorbers

Now, consider a specific type of wave absorbing device, namely, a single or twin-flap absorber. The problem is to establish a method for determining the absorption cross-section (or simply the power absorption) for this type of device. As it turns out, because of the simple, flat-plate geometry of these absorbers, the hydrodynamic analysis is more straightforward than for some other classes of absorbers.

The geometry of the device and the coordinate system are shown in Fig. 2. The desired cross-section function is

$$\sigma(\omega, \beta) = \sigma(\omega, \beta; \underline{G}, \underline{T}, \underline{D}, h) \quad (10)$$

where now the design-variable vectors \underline{G} , \underline{T} , and \underline{D} may be given specific meanings, as follows:

$$\begin{aligned} \underline{G} &= (a, b, p, w) \\ \underline{T} &= (m_1, m_2, c_1, c_2) \\ \underline{D} &= (d_1, d_2) \end{aligned} \quad (11)$$

where a , b , p , and w are the flap draft, half-spacing, pivot depth, and half-width, respectively, m_i and c_i are the flap inertias and restoring force coefficients for the two flaps, ($i = 1, 2$), and d_i are the damping coefficients of the power takeoffs fitted to the two flaps. (Note that for a single-flap device, the half-spacing b is set to zero, while the coefficients m_2 , c_2 , and d_2 can simply be

omitted.) The remaining variable, h , is the water depth, which may or may not be considered a design variable, depending on circumstances. The additional design variable θ_0 , the "heading" of the device, does not figure in the hydrodynamic analysis of $\sigma(\omega, \beta)$.

Primarily for the purposes of simplifying the hydrodynamic analysis, the following assumptions will be made:

(1) The flaps are of equal width and draft, parallel, and set one behind the other, rather than partially overlapping.

(2) The flaps are considered as rigid bodies, pivoting about a horizontal axis that need not be on the body, at a depth p below the free surface.

(3) The flaps are "thin."

(4) The pivot of each flap is assumed fixed, i.e., the supporting structure of the flaps does not respond to either direct wave forces or reactions to the flap motions.

(5) The water is of uniform depth h , and of infinite horizontal extent. No other bodies are considered. Thus, the free surface, the bottom, and the flaps themselves are the only boundaries in the problem.

(6) Linear wave theory and potential flow are assumed for the purposes of the analysis.

Some justification for these assumptions will be given here. Assumption (1) might be defended on the basis of yielding practical designs, but it also provides a substan-

tial saving in computational requirements due to the symmetries invoked. There is no loss of generality and, in any case, the underlying methods used here would permit the relaxation of this assumption.

Assumption (2) is made for practical reasons as well. By hypothesis, a single power takeoff unit would be attached to a single flap. Thus, if large-amplitude flexing of the flap were permitted, it is conceivable that substantial energy might be absorbed in unusable modes of motion. The more general problem of a long, continuous, but compliant flap attached to multiple power takeoffs will not be undertaken here.

The assumption of thinness is made solely to permit the modelling of the flaps as planar arrays of normal dipoles. In reality, the flaps will probably be substantially less than 1% of a wavelength in thickness, and less than 15% of the flap draft. The effect of actual flap thickness on the hydrodynamic coefficients will be considered subsequently.

Assumption (4) contains a very strong but implicit statement about the construction and placement of the wave absorber, namely, that it is built on a massive foundation in relatively shallow water, rather than moored in deep water. Under the large forces encountered by a terminator, almost any conceivable free-floating structure will move significantly. This would add to the complexity of the

hydrodynamic problem, although not insurmountably. More to the point, ship-like responses of the supporting structure, in general, decrease the power absorption of the device, as found in Ref. 13. The assumption of a fixed supporting structure, while it does limit the applicability of the model, has the merit that it simplifies the analysis immeasurably, and corresponds to a probably desirable form and location for wave-power absorbing devices.

Assumption (5) contains a number of statements, each of which deserves a brief comment. First, in terms of its effect on the local hydrodynamics of the flaps, the slope of the bottom is neglected. In practical terms, this is no great limitation. Second, the influence of the shore is felt, if at all, only in the form of reflections of the waves incident from the open ocean, not through changes in the hydrodynamic coefficients of the absorber itself. Third, and most important, the model in its present form does not take account of interactions between independent members of an array of absorbing devices. Thus, we have an implicit assumption that the members of an array would be widely spaced.

Finally, in assumption (6), again, a number of relatively strong statements have been made. In fact, it is not at all obvious that viscous forces may be neglected: much of the conventional wisdom in offshore structures engineering indicates the opposite. Clearly, the existence

of viscous damping forces on the flaps may have a considerable effect on their motions, and therefore on the power absorption. However, in experiments (Ref. 10), reasonable agreement was obtained with theoretical results based on an ideal fluid. Therefore, at this point, we will assume that if viscous forces due to waves and flap motions are to be included at all, they will be incorporated in the form of an "effective linear damping coefficient."

By contrast, the influence of viscous forces due to a tidal current may be of great importance in increasing the total loads on the structure, and in causing a steady drift of the flaps toward the stops. Similarly, second-order wave drift forces will contribute to these effects. However, these forces will not contribute to the power output of the twin-flap system, being at essentially zero frequency. In effect, then, these steady forces will require only the provision of suitable spring constants (or differential damping coefficients) to prevent the flaps from being gradually driven to the limits of their stroke, and sufficient structure to withstand the additional loads. The magnitudes of these forces could be estimated, in the case of tidal currents, by applying drag (and perhaps lift) coefficients for flat plates. For second-order wave forces, an estimate may be based on the work of Evans (Ref. 14).

Linear Equations of Motion and Boundary Value Problems

The task at hand is to develop the coupled linear equations of motion for the two flaps, and to describe the method to be used for evaluating the coefficients in these equations of motion.

Let x_1 and x_2 denote the positions of flaps 1 and 2, in general, in either linear or angular coordinates, as appropriate. The coupled equations of motion in the frequency domain for the two flaps are then as follows:

$$\begin{aligned}
 -\omega^2(m_1+a_{11})x_1 + i\omega(d_1+b_{11})x_1 + c_1x_1 -\omega^2a_{12}x_2 \\
 + i\omega b_{12}x_2 = F_1e^{i\omega t} \\
 -\omega^2(m_2+a_{22})x_2 + i\omega(d_2+b_{22})x_2 + c_2x_2 -\omega^2a_{21}x_1 \\
 + i\omega b_{21}x_1 = F_2e^{i\omega t} \qquad (12)
 \end{aligned}$$

where a_{ij} and b_{ij} are the hydrodynamic added inertia and damping coefficients, respectively, corresponding to the force (or moment) on flap i in phase with the acceleration and velocity of flap j , and F_i are the complex exciting force (or moment) amplitudes on the two flaps.

The solutions of the equations of motion have the form

$$\begin{aligned}
 x_1 &= X_1 e^{i\omega t} \\
 x_2 &= X_2 e^{i\omega t} \qquad (13)
 \end{aligned}$$

where X_1 and X_2 are the complex amplitudes of the motions of the flaps, in either linear or angular motion. The resulting solutions of the equations of motion, in terms of the unknown hydrodynamic coefficients, are:

$$\begin{aligned}
 X_1 &= \frac{F_1 K_{22} - F_2 K_{12}}{K_{22} K_{11} - K_{12} K_{21}} \\
 X_2 &= \frac{F_2 K_{11} - F_1 K_{21}}{K_{12} K_{11} - K_{12} K_{21}}
 \end{aligned}
 \tag{13}$$

where

$$K_{11} = -\omega^2(m_1 + a_{11}) + i\omega(d_1 + b_{11}) + c_1,$$

$$K_{22} = -\omega^2(m_2 + a_{22}) + i\omega(d_2 + b_{22}) + c_2,$$

$$K_{12} = -\omega^2 a_{12} + i\omega b_{12},$$

$$K_{21} = -\omega^2 a_{21} + i\omega b_{21}.$$

The coefficients m_1 , m_2 , c_1 , c_2 , d_1 , and d_2 are arbitrary, so K_{11} and K_{22} are independent. However, because of the assumed symmetry of the flaps, we have $a_{11}=a_{22}$, $b_{11}=b_{22}$, $a_{12}=a_{21}$, and $b_{12}=b_{21}$, so that $K_{12}=K_{21}$. Thus,

$$\begin{aligned}
 X_1 &= \frac{F_1 K_{22} - F_2 K_{12}}{K_{22} K_{11} - K_{12}^2} \\
 X_2 &= \frac{F_2 K_{11} - F_1 K_{12}}{K_{22} K_{11} - K_{12}^2}
 \end{aligned}
 \tag{14}$$

Furthermore, the power absorbed can be shown to be

$$P = \frac{1}{2} \omega^2 (d_1 |X_1|^2 + d_2 |X_2|^2). \tag{15}$$

With the assumption of symmetry, therefore, there are six unknown hydrodynamic coefficients to be evaluated, namely, the four real coefficients a_{11} , b_{11} , a_{12} , and b_{12} , and the two complex exciting force amplitudes F_1 and F_2 .

Note that the coefficients a_{11} , b_{11} , a_{12} , and b_{12} are functions of ω only, independent of β , while F_1 and F_2 depend on both ω and β . That is, the four real coefficients

result from the solution of the radiation problem, in which one flap is forced to move in the absence of an incident wave but in the presence of the other flap (for a twin-flap device) while the exciting force amplitudes result from the solution of the diffraction problem, in which the flaps are held fixed in the presence of an incident wave. Both of these problems can be approached in the same way, and many of the computations are redundant, as will be shown below.

Under the assumptions of inviscid, irrotational flow, there exists a total potential $\phi(x,y,z,t) = \phi(x,y,z) e^{i\omega t}$, with the governing equation $\nabla^2 \phi = \nabla^2 \phi = 0$ in the fluid.

First, consider the radiation problem with flap 1 moving with amplitude θ in roll about a pivot at depth $z=-p$, and flap 2 fixed. The linearized boundary conditions are as follows:

$$\text{On flap 1: } \phi_x = i\omega(z+p)\theta \quad \text{on } x=-b, -w \leq y \leq w, -a \leq z \leq 0$$

$$\text{On flap 2: } \phi_x = 0 \quad \text{on } x=+b, -w \leq y \leq w, -a \leq z \leq 0$$

For a single-flap device the boundary condition on flap 2 is dropped, of course, and $b=0$.

On the free surface:

$$\phi_{tt} + g\phi_z = 0 \quad \text{on } z=0$$

$$\text{that is, } -\omega^2 \phi(x,y,0) + g\phi_z \Big|_{z=0} = 0$$

On the bottom:

$$\phi_z = 0 \quad \text{on } z=-h$$

In addition, the potential for the radiation problem must satisfy a radiation condition at infinity correspond-

ing to outgoing waves.

For the diffraction problem, both flap 1 and flap 2 are fixed in the presence of an incident wave from direction β , with respect to the x-axis, as shown in Fig. 2. The potential of the incident wave is then:

$$\phi_0 = \frac{g\zeta_A \cosh k(z+h)}{\omega \cosh kh} e^{i(-kx \cos \beta - ky \sin \beta + \omega t)} \quad (16)$$

where ζ_A is the amplitude of the incident wave, and k is the wavenumber given by the solution of the shallow water dispersion relation $\omega^2/g = k \tanh kh$.

In the diffraction problem we must find a diffraction potential ϕ_7 such that the total potential $\phi = \phi_0 + \phi_7$ satisfies the following boundary conditions:

On flaps 1 and 2: $\phi_x = 0$ on $x=\pm b$, $-w < y < w$, $-a < z < 0$

On the free surface:

$$\phi_{tt} + g\phi_z = 0 \quad \text{on } z=0$$

On the bottom: $\phi_z = 0$ on $z=-h$

In both cases the solution will be found numerically by defining a set of quadrilateral elements on the mean position of each flap. On each quadrilateral element a distribution of normal dipoles of unknown constant density will be constructed. For these discrete quadrilateral elements, then, a set of simultaneous equations will represent an approximation to the following integral equation for the dipole strength:

$$\frac{\partial \phi}{\partial x}(x, y, z) = \frac{1}{4\pi} \iint_S \gamma(\xi, \eta, \zeta) \frac{\partial}{\partial x} G_D(x, y, z; \xi, \eta, \zeta) dS \quad (17)$$

where γ is the dipole strength, G_D is the Green's function for a unit dipole in finite depth water beneath a free surface, and the surface S constitutes the entire dipole distribution whether on one or two flaps. Notice that the left-hand side of this integral equation can be equated to the boundary condition normal velocity on the flaps. The corresponding system of simultaneous equations for discrete elements will be solved for the unknown dipole strengths, satisfying the required boundary conditions on the flaps at the centroids of the elements.

With this solution, the resulting total potential ϕ and its time derivative $\partial\phi/\partial t = i\omega\phi$ can be calculated at any point. Since it can be shown that the quantity $i\omega\phi$ is the linearized pressure, this can be integrated over the surface of the flap to give the total force, or moment, if weighted by a suitable lever arm. By definition, this complex force, or moment, resolved by phase, gives the required real added mass and damping force coefficients from the radiation solution, and the complex exciting forces from the diffraction solution. These coefficients, then, will give a solution of the coupled equations of motion according to Eq. 14. Note that the Green's function and the radiation boundary condition must be calculated only once for each combination of \underline{G} , h , and ω ; they do not

depend in any way on β , T , or D . The diffraction body boundary condition, however, depends on both ω and β .

A numerical scheme for solving the potential due to an arbitrary body in finite depth water has been developed by Faltinsen and Michelsen (Ref. 15). The Green's function used in that work corresponds to a distribution of sources. However, the corresponding Green's function for distributed normal dipoles will be found by differentiation with respect to the normal coordinate at the singularity.

With a solution of the equations of motion the power absorbed by the system can be determined, and the absorption cross-section is established. In addition, the total reaction forces acting on the flap and the supporting structure can be calculated. These forces are needed for structural considerations, and for determining in detail the required size and costs of moorings or foundations.

For a boxlike flap having significant thickness, of course, a more suitable model of the flow near the body could be developed using source distributions on both front and back surfaces of the flap, as well as on the bottom and sides. However, the use of a source panel method would require at least twice as many panels for a given resolution. Furthermore, a source panel approach for relatively thin flaps would have presented serious numerical difficulties, some of which have been discussed by Troesch, Ref. 16.

For the purposes of the boundary value problems posed

above, the numerical analysis is of course greatly simplified by the fact that all the dipoles are oriented in the x direction, and that the only normal velocity imposed by the linearized body boundary conditions is the x component. For a known distribution of normal dipoles on the mean positions of the flaps, the x component of the fluid velocity at any point (x,y,z) is given by Eq. 17.

The linearized pressure jump across a sheet of normal dipoles can be shown to be related to the dipole strength as follows:

$$p_0 = i\omega\rho\gamma \quad (18)$$

Thus, the numerical solution of the boundary value problems to arrive at the linearized pressures involves only the normal derivative of the dipole potential; the value of the potential itself need not be calculated.

The pressures on the flap can now be integrated to obtain the total forces or moments on the flap. Solving for the required hydrodynamic coefficients in terms of the dipole strengths, we may write for a twin-flap device with the flaps pivoted to roll about axes at a depth p below the free surface:

$$a_{11} = \frac{\rho}{\omega} \iint_{S_1} \text{Im}\gamma_R (p+\zeta) ds$$

$$a_{12} = \frac{\rho}{\omega} \iint_{S_2} \text{Im}\gamma_R (p+\zeta) ds$$

$$b_{11} = -\rho \iint_{S_1} \text{Re}\gamma_R (p+\zeta) ds$$

$$b_{12} = -\rho \iint_{S_2} \text{Re}\gamma_R (p+\zeta) ds$$

$$\begin{aligned}
 F_1 &= i\omega\rho \iint_{S_1} \gamma_D (p+\zeta) ds \\
 F_2 &= i\omega\rho \iint_{S_2} \gamma_D (p+\zeta) ds
 \end{aligned}
 \tag{19}$$

where γ_R and γ_D are the dipole strengths found to satisfy the radiation and diffraction boundary conditions, respectively, and S_1 and S_2 are the dipole sheets corresponding to flaps 1 and 2, respectively. The relationships shown above for a_{11} , b_{11} , and F_1 are equally applicable in the case of a single flap. Of course the boundary value problems are then solved in the absence of a second flap.

In this modelling of the flaps as dipole distributions, only the nonlifting solution is desired. Therefore, the only requirement to make the solution unique is that there be no circulation. No further edge conditions (analogous to a Kutta condition) are required.

The following section contains the derivation of the required Green's functions for the normal velocity due to a sheet of normal dipoles in the presence of a free surface and a bottom. In addition, a numerical check of the consistency of the Green's function results is described.

Green's Functions

The Green's function for the normal (x-component) velocity due to a dipole is derived from the Green's function for the potential due to a source, by differentiation: once with respect to the singularity coordinate ξ , to obtain the potential for a dipole oriented in the x direction; then with respect to the field coordinate x, to obtain the normal velocity.

The Green's function for a source in finite depth water can be written in the following form, Ref. 15:

$$\begin{aligned}
 G(x, y, z; \xi, \eta, \zeta) &= \frac{2\pi(v^2 - k^2)}{h(k^2 - v^2) + v} \cosh k(z+h) \cosh k(\zeta+h) [Y_0(kr) - iJ_0(kr)] \\
 &+ 4 \sum_{j=1}^{\infty} \frac{\mu_j^2 + v^2}{h(\mu_j^2 + v^2) - v} \cos \mu_j(z+h) \cos \mu_j(\zeta+h) K_0(\mu_j r)
 \end{aligned}
 \tag{20}$$

where

$$r = [(x-\xi)^2 + (y-\eta)^2]^{1/2}$$

$$v = \omega^2/g$$

h is the water depth

k is the solution of $k \tanh kh = v$

and

μ_j are the solutions of $\mu_j \tan \mu_j h = -v$

$$(j = 1, 2, \dots)$$

while J_0 , Y_0 , and K_0 denote the Bessel and Modified Bessel functions following the nomenclature of Abramowitz and

Stegun, Ref. 17.

It will be noted that in this form of the potential there is no separate term representing the essential $1/R$ singularity of the source, where

$$R = [(x-\xi)^2 + (y-\eta)^2 + (z-\zeta)^2]^{1/2}$$

Rather, the essential singularity in the source behavior is contained in the singular behavior of the Y_0 and K_0 Bessel function terms. Furthermore, this form of the potential cannot be directly evaluated at $r = 0$, even when R is not zero. For computational purposes, then, a second form of the source potential is adopted from Ref. 15:

$$\begin{aligned} G(x, y, z; \xi, \eta, \zeta) = & \frac{1}{R} + \frac{1}{R'} + \frac{1}{R''} \\ & + \int_0^{u_1} \frac{2(ku + v) e^{-khu}}{u \sinh khu - (v/k) \cosh khu} \\ & \qquad \qquad \qquad \cosh k(z+h) \cosh k(\zeta+h) J_0(kru) du \\ & - \int_0^{u_1} e^{ku(z+\zeta)} J_0(kru) du \\ & + \int_{u_1}^{\infty} \frac{2v e^{ku(z+\zeta)}}{u - v/k} J_0(kru) du \\ & + i \frac{2\pi(k^2 - v^2)}{h(k^2 - v^2) + v} \cosh k(z+h) \cosh k(\zeta+h) J_0(kr) \end{aligned} \quad (21)$$

In this representation, the limit of integration u_1 is an "arbitrary" constant, which must however be chosen such that $u_1 > 4.5/kh$, so that $\cosh kh$ and $\sinh kh$ can be written as $(1/2) \exp(kh)$ for $u > u_1$. Furthermore, since the principal

value integral is singular at $u=1$, and the integral will be evaluated following the method of Monacella (Ref. 18), this will also require that $u_1 > 2$.

The radii from the images in the free surface and the bottom are denoted by

$$R' = [(x-\xi)^2 + (y-\eta)^2 + (z+\zeta)^2]^{1/2}$$

$$R'' = [(x-\xi)^2 + (y-\eta)^2 + (z+2h+\zeta)^2]^{1/2}$$

respectively.

In this form of the potential, the essential singularity is completely disjoined from the wave terms, and the Green's function can be evaluated at $r = 0$, provided that R is nonzero. However, a computational difficulty still exists in the form of the infinite integral term. Conveniently, following Ref. 15, this term can be rewritten in a finite integral form, in terms of the exponential integral function E_1 , as follows:

$$\int_{u_1}^{\infty} \frac{2ve^{ku(z+\zeta)}}{u - v/k} J_0(kru) du \quad (22)$$

$$= \frac{2v}{\pi} \int_0^{\pi} \exp[v(z+\zeta) + ivr \cos\theta] E_1\{-[k(z+\zeta) + ikr \cos\theta] (u_1 - v/k)\} d\theta$$

Differentiation of the series form of the Green's function, Eq. 20, with respect to the singularity coordinate ξ , gives the following result for the potential due to a dipole:

$$G_D(x, y, z; \xi, \eta, \zeta)$$

$$= \frac{2\pi k(v^2 - k^2)}{h(k^2 - v^2) + v} \cosh k(z+h) \cosh k(\zeta+h) \quad (23)$$

$$\frac{x-\xi}{r} [Y_1(kr) - iJ_1(kr)]$$

$$+ 4 \sum_{j=1}^{\infty} \frac{\mu_j(\mu_j^2 + v^2)}{h(\mu_j^2 + v^2) - v} \cos \mu_j(z+h) \cos \mu_j(\zeta+h) \frac{x-\xi}{r} K_1(\mu_j r)$$

Then a second differentiation, with respect to the field coordinate x , gives the required normal velocity:

$$\frac{\partial G_D}{\partial x} = \frac{2\pi k(v^2 - k^2)}{h(k^2 - v^2) + v} \cosh k(z+h) \cosh k(\zeta+h)$$

$$\left\{ \frac{k(x-\xi)^2}{r^2} [Y_0(kr) - iJ_0(kr)] \right. \quad (24)$$

$$\left. + \frac{r^2 - 2(x-\xi)^2}{r^3} [Y_1(kr) - iJ_1(kr)] \right\}$$

$$+ 4 \sum_{j=1}^{\infty} \frac{\mu_j(\mu_j^2 + v^2)}{h(\mu_j^2 + v^2) - v} \cos \mu_j(z+h) \cos \mu_j(\zeta+h)$$

$$\left\{ \frac{-\mu_j(x-\xi)^2}{r^2} K_0(\mu_j r) + \frac{r^2 - 2(x-\xi)^2}{r^3} K_1(\mu_j r) \right\}$$

Of course, the series form of the Green's function still contains the essential singular behavior within the Bessel terms, rather than in a separate term, and therefore blows up computationally at $kr = 0$. Thus, the alternative integral representation, Eq. 21, must be used for small kr .

Differentiation of Eq. 21 with respect to ξ gives the following result for the dipole potential:

$$\begin{aligned}
 G_D(x, y, z; \xi, \eta, \zeta) &= \frac{x-\xi}{R^3} + \frac{x-\xi}{R'^3} + \frac{x-\xi}{R''^3} \\
 &+ \int_0^{u_1} \frac{2ku(ku+v) e^{-khu}}{u \sinh khu - (v/k) \cosh khu} \\
 &\quad \cosh ku(z+h) \cosh ku(\zeta+h) \frac{x-\xi}{r} J_1(kru) du \\
 &- \int_0^{u_1} k^2 u e^{ku(z+\zeta)} \frac{x-\xi}{r} J_1(kru) du \\
 &+ \int_{u_1}^{\infty} \frac{2kvu e^{ku(z+\zeta)}}{u - v/k} \frac{x-\xi}{r} J_1(kru) du \\
 &+ 2\pi i \frac{k(k^2-v^2)}{h(k^2-v^2)+v} \frac{x-\xi}{r} J_1(kr)
 \end{aligned} \tag{25}$$

A second differentiation, with respect to x , gives the normal velocity

$$\begin{aligned}
 \frac{\partial G_D}{\partial x} &= \frac{1}{R^3} + \frac{1}{R'^3} + \frac{1}{R''^3} - 3(x-\xi)^2 \left(\frac{1}{R^5} + \frac{1}{R'^5} + \frac{1}{R''^5} \right) \\
 &+ \int_0^{u_1} \frac{2ku(ku+v) e^{-khu}}{u \sinh khu - (v/k) \cosh khu} \cosh ku(z+h) \cosh ku(\zeta+h) \\
 &\quad \left\{ \frac{ku(x-\xi)^2}{r^2} J_0(kru) + \frac{r^2-2(x-\xi)^2}{r^3} J_1(kru) \right\} du \\
 &- \int_0^{u_1} k^2 u e^{ku(z+\zeta)} \left\{ \frac{ku(x-\xi)^2}{r^2} J_0(kru) \right. \\
 &\quad \left. + \frac{r^2-2(x-\xi)^2}{r^3} J_1(kru) \right\} du
 \end{aligned}$$

$$\begin{aligned}
& + \int_{u_1}^{\infty} \frac{2kvue^{ku(z+\zeta)}}{u - v/k} \left\{ \frac{ku(x-\xi)^2}{r^2} J_0(kru) \right. \\
& \qquad \qquad \qquad \left. + \frac{r^2 - 2(x-\xi)^2}{r^3} J_1(kru) \right\} du \qquad (26) \\
& + 2\pi i \frac{k(k^2 - v^2)}{h(k^2 - v^2) + v} \left\{ \frac{k(x-\xi)^2}{r^2} J_0(kr) + \frac{r^2 - 2(x-\xi)^2}{r^3} J_1(kr) \right\}
\end{aligned}$$

The infinite integral term here can be rewritten in terms of the exponential integral function as

$$\begin{aligned}
& \int_{u_1}^{\infty} \frac{2kvue^{ku(z+\zeta)}}{u - v/k} \left\{ \frac{ku(x-\xi)^2}{r^2} J_0(kru) + \frac{r^2 - 2(x-\xi)^2}{r^3} J_1(kru) \right\} du \\
& = \frac{2v}{\pi} \int_0^{\pi} \exp[v(z+\zeta) + ivr \cos\theta] \\
& \quad \left\{ \frac{(x-\xi)^2}{r^2} k^2 \cos^2\theta \frac{\exp\{-[k(z+\zeta) + ikr \cos\theta][(v/k) - u_1]\}}{k(z+\zeta) + ikr \cos\theta} \right. \\
& \quad \quad \left. \left(\frac{1}{k(z+\zeta) + ikr \cos\theta} - u_1 \right) \right. \\
& \quad \quad \left. + k \cos\theta \left[\frac{(x-\xi)^2}{r^2} v \cos\theta - i \left(\frac{r^2 - (x-\xi)^2}{r^3} \right) \right] \right. \\
& \quad \quad \left. \left(- \frac{v}{k} E_1\{[k(z+\zeta) + ikr \cos\theta][(v/k) - u_1]\} \right. \right. \\
& \quad \quad \left. \left. - \frac{\exp\{-[k(z+\zeta) + ikr \cos\theta][(v/k) - u_1]\}}{k(z+\zeta) + ikr \cos\theta} \right) \right\} d\theta \qquad (27)
\end{aligned}$$

The imaginary parts of both the series and integral representations are identical, consisting only of wave terms, while the real parts are quite different in form. A

numerical check for consistency of the two forms is described below.

For computational purposes, it is convenient to use the series representation, Eq. 24, for large kr . The number of terms required to obtain a specified accuracy in the infinite series drops drastically for increasing kr , and is approximately 90 terms at $kr = 0.2$, for 1 percent accuracy.

By contrast, in the integral representation, Eq. 26, the oscillatory behavior of the Y Bessel functions implies that more points must be used in a numerical integration scheme as kr increases, in order to obtain an accurate approximation of the first three integral terms. Thus, for practical computations, there is a tradeoff point in kr at which the integral and series representation results must overlap in both accuracy and cost. Typically, in the numerical work described below, a cutoff value of $kr = 0.4$ was used in connection with a 10-point Gauss-Legendre integration scheme, and an imposed maximum of 100 terms in the series.

Before proceeding to a numerical scheme for finding an approximate solution of the integral equation for the unknown dipole strength, a check was desired on the computation of the Green's functions. Accordingly, a third representation of the Green's function was derived by differentiation. This was developed from a source Green's function for deep water, Ref. 19:

$$\begin{aligned}
G(x, y, z; \xi, \eta, \zeta) &= \frac{1}{R} + \frac{1}{R'} \\
&+ 2ve^{\nu(z+\zeta)} \int_0^{\nu(z+\zeta)} \frac{e^{-u}}{(\nu^2 r^2 + u^2)^{1/2}} du \\
&- \pi v e^{\nu(z+\zeta)} [H_0(\nu r) + Y_0(\nu r)] \\
&+ 2\pi i v e^{\nu(z+\zeta)} J_0(\nu r)
\end{aligned} \tag{28}$$

where H_0 is the Struve function.

Differentiation with respect to ξ gives the following dipole potential:

$$\begin{aligned}
G_D(x, y, z; \xi, \eta, \zeta) &= \frac{x-\xi}{R^3} + \frac{x-\xi}{R'^3} \\
&+ e^{\nu(z+\zeta)} \left\{ 2\nu^3 (x-\xi) \int_0^{\nu(z+\zeta)} \frac{e^{-u}}{(\nu^2 r^2 - u^2)^{3/2}} du \right. \\
&- \pi \nu^2 \frac{x-\xi}{r} [H_1(\nu r) + Y_1(\nu r) - \frac{2}{\pi}] \\
&\left. + 2\pi i \nu^2 \frac{x-\xi}{r} J_1(\nu r) \right\}
\end{aligned} \tag{29}$$

Finally, a second differentiation with respect to x gives the normal velocity

$$\begin{aligned}
\frac{\partial G_D}{\partial x} &= \frac{1}{R^3} + \frac{1}{R'^3} - 3(x-\zeta)^2 \left(\frac{1}{R^5} + \frac{1}{R'^5} \right) \\
&+ e^{\nu(z+\zeta)} \left\{ 2\nu^3 \int_0^{\nu(z+\zeta)} \frac{e^{-u}}{(\nu^2 r^2 - u^2)^{3/2}} du \right. \\
&- 6\nu^5 (x-\xi)^2 \int_0^{\nu(z+\zeta)} \frac{e^{-u}}{(\nu^2 r^2 - u^2)^{5/2}} du \\
&\left. - \pi \nu^2 \frac{r^2 - 2(x-\xi)^2}{r^3} [H_1(\nu r) + Y_1(\nu r)] \right\}
\end{aligned} \tag{30}$$

$$\begin{aligned}
& - \pi v^3 \frac{(x-\xi)^2}{r^2} [H_0(vr) + Y_0(vr)] \\
& + 2v^2 \frac{r^2 - (x-\xi)^2}{r^3} \\
& + 2\pi i v^2 \frac{r^2 - 2(x-\xi)^2}{r^3} J_1(vr) \\
& + 2\pi i v^3 \frac{(x-\xi)^2}{r^2} J_0(vr) \}
\end{aligned}$$

Several cases of the Green's function computation were checked, comparing the results of the real parts of the finite-depth series and integral representations, Eqs. 24 and 26 against each other, and against the deep water result, Eq. 30, for water depths of at least a wavelength. A sample comparison is shown in Fig. 3.

This checking procedure was also useful in that it provided some graphic evidence of the variation of the real part of the normal velocity Green's function with respect to the horizontal radius r . This information, in turn, can be used to determine appropriate limitations of a simple mid-point rule for approximating the integrated influence of a rectangular patch of dipoles on the fluid velocity at any field point.

In the following section, the numerical procedure used to approximate the unknown dipole distributions, corresponding to solutions of the radiation and diffraction boundary-value problems is described.

Numerical Scheme

A numerical procedure analogous to that of Hess and Smith is used to obtain an approximate solution to the integral equation for the unknown dipole distribution. Each dipole sheet representing a flap is divided into a set of quadrilateral elements, numbered as shown in Fig. 4. On each quadrilateral the dipole density (and hence the pressure) is assumed to be constant. The normal velocity at any point in the fluid can then be written as the summation of the induced velocities due to each quadrilateral:

$$\frac{\partial \phi}{\partial x} = \sum_{j=1}^n \gamma_j \iint_{S_j} \frac{\partial G_D}{\partial x} dS \quad (31)$$

In particular, if the normal velocities on the flaps (imposed by the radiation and diffraction boundary conditions) are to be satisfied at certain points on the flaps, in this case at the centroids of the quadrilaterals, then the integral equation for the unknown dipole strength can be approximated by the following matrix equation:

$$\Gamma G = V \quad (32)$$

In this equation, each element g_{ij} of the coefficient matrix G represents the normal velocity induced at the centroid of the quadrilateral i by a distribution of constant unit dipole density on quadrilateral j . The elements v_i of the right-hand-side vector V are the required boundary-

condition normal velocities at the centroid of quadrilateral i , and the elements of the vector Γ are the unknown dipole strengths γ_j . Since the boundary-condition velocities are simply calculated, the remaining problem consists of computing the elements of the coefficient matrix, and solving the resultant set of complex simultaneous equations to obtain the dipole strength on each quadrilateral, which, as shown above, corresponds directly to the pressure. Finally, the pressures are integrated over the flaps to yield the forces (or moments) and thus the required hydrodynamic coefficients.

In this particular case, the simple geometry of the flaps provides a substantial simplification of these problems. Each quadrilateral, for example, is already planar, requiring no further fitting to the surface. Since the flap is rectangular by assumption, the quadrilaterals can equally well be rectangular, which simplifies many of the calculations. The flap, or an arrangement of two flaps, is symmetrical about $x = 0$ and about $y = 0$. The Green's function itself is also symmetric, that is,

$$\frac{\partial G_D}{\partial x}(x, y, z; \xi, \eta, \zeta) = \frac{\partial G_D}{\partial x}(\xi, \eta, \zeta; x, y, z) \quad (33)$$

so that the elements g_{ij} and g_{ji} of the coefficient matrix are equal if the two quadrilaterals i and j are congruent. Moreover, if all quadrilaterals are made identical, then an

additional order of symmetry equal to the number of vertical "stacks" of quadrilaterals is obtained. For identical quads, arranged in m "stacks" of n "layers", the number of distinct elements to be calculated for the coefficient matrix is $m(n^2 + n)/2$, while the total number of elements is m^2n^2 .

The assumption of constant dipole strength over a quadrilateral is a first approximation which becomes more valid for small quadrilaterals. Thus, the error implied by this assumption can be controlled by increasing the number of quadrilaterals and reducing their size, limited by computational resources, storage and cost. The summation in Eq. 31, however, still involves the integration of the velocity Green's function over each of the quadrilaterals. There are, of course, a number of methods (of various levels of complexity and accuracy) for approximating these integrals numerically, if they cannot be solved in closed form. At the simplest level the integral may be approximated using a midpoint rule; that is:

$$\iint_S \frac{\partial G_D}{\partial x} dS \approx A \frac{\partial G_D}{\partial x} \bigg|_{(P,Q)} \quad (34)$$

where the point Q is taken as the centroid of the quadrilateral, A is the area of the quadrilateral, and $\partial G_D / \partial x |_{(P,Q)}$ is the velocity induced at the field point P by a unit dipole at Q . Alternatively, as suggested by Zhou (Ref. 20) and others, a two-dimensional quadrature can be

performed over the quadrilateral to obtain a more accurate estimate of the integral, following one of the well-known methods outlined in Ref. 17. Naturally, this approach requires multiple evaluations of the Green's function on the quadrilateral, and therefore increases the computational requirements.

For the purposes of this work, it is necessary to consider in more detail the level of approximation implied by using a simple midpoint rule for integration of the Green's function over a quadrilateral. As mentioned above, two distinct forms of the Green's function are used, depending on the horizontal radius (or rather, kr) from the quadrilateral to the field point: namely, an integral representation, Eq. 26, for small kr , and a series representation, Eq. 24, for large kr . In order to evaluate the accuracy of an approximation using midpoint integration, it is necessary to distinguish the behavior of the wave part of the Green's function from that of the essential singularity.

In the integral representation, Eq. 26, the essential singular behavior is contained in separate terms involving $1/R^3$ and $1/R^5$, together with similar terms representing the image dipoles in the free surface and the bottom. The wave part of the Green's function, as shown above, is non-singular and computable at $r = 0$, even if $R = 0$.

The variation of the wave part with respect to r , that is, with respect to the horizontal coordinates x and y , is

contained in the oscillatory behavior of the Bessel terms, and with respect to the depth coordinate z , in the behavior of the exponential and hyperbolic terms. For practical accuracy, a midpoint rule is then adequate to fit the wave part of the Green's function provided that the quadrilateral dimensions are not too large with respect to the wavelength. If a quadrilateral dimension (width or height) is denoted by q , then a midpoint rule for integration of the wave terms gives a good approximation provided that kq is less than about 0.2, although this can be increased with some loss of accuracy up to 0.4.

Obviously, a special and critical circumstance with regard to the accuracy of a midpoint formulation exists around $r = 0$. Here, even the wave part of the Green's function, although continuous, is quite far from being linear with respect to r , as shown graphically in Fig. 3. This situation arises when evaluating the influence of the local quadrilateral and the quadrilaterals directly above or below the field point. A simple approximate numerical procedure for this particular case is described subsequently.

In any case, however, for quadrilaterals which are at all close to the field point, a midpoint rule for approximate integration of the Green's function is inadequate to treat the essential singularity terms in the Green's function. In the method used here, the singular behavior is

integrated exactly for nearby quadrilaterals, using an application of the Biot-Savart law, with a contour integral around the boundary of the quadrilateral replacing the surface integral of Eq. 31. The basis for this treatment is as follows. The Green's function is first written as the sum of the singular and wave parts.

$$\frac{\partial G_D}{\partial x} = \frac{\partial G_{DS}}{\partial x} + \frac{\partial G_{DW}}{\partial x} \quad (35)$$

Then, the influence of the quadrilateral on the field point velocity may be written as

$$\frac{\partial \phi}{\partial x} = \gamma \left[\iint_S \frac{\partial G_{DW}}{\partial x} dS + \int_C \frac{\underline{i} \cdot \underline{R} \times \frac{d\underline{C}}{|\underline{R}|^3} \right] \quad (36)$$

where the vector quantities \underline{i} , \underline{R} , and \underline{dC} are interpreted as shown in Fig. 5.

Note that similar computations are required for the image quadrilaterals in the free surface and bottom. For economy in computation, the exact integrals for the singular part of the Green's function are performed whenever the midpoint value of the radius R (P, Q) is less than five diagonal lengths of the quadrilateral. Elsewhere, a midpoint rule is used for the singular terms as well as the wave terms.

As mentioned above, a modification of the midpoint rule integration scheme is used for the wave terms of the Green's function for the local quadrilateral and those directly above and below it. In this case, use is made of

the symmetry of the Green's function about $(y-\eta) = 0$. The quadrilateral is divided into two half-quads, and the midpoint of each half-quad is then placed at the quarter-width of the original quadrilateral, as shown in Fig. 6. The influence of the entire quadrilateral (wave terms only) on the field point velocity is then taken as twice the resulting influence of the half-quad. Thus if the original quadrilateral dimensions are chosen such that kq is less than 0.2, as mentioned previously, the corresponding range of kr for each of the half-quads formed is no greater than 0.1.

In the case of the series representation, the wave and essential singularity are contained together in the various terms, and so cannot be separated conveniently. However, since R cannot be less than r , the essential singular behavior decreases at least as fast as $1/r^3$. Thus, if the midpoint radius $r(P,Q)$ is sufficiently large with respect to the quadrilateral size, then the wave behavior (which decreases as $1/r^{1/2}$) dominates the Green's function, and the accuracy of the midpoint rule for the singular part can be judged adequately by the behavior of the total Green's function.

However, for short waves (k large), it occasionally happens that kr becomes large enough to mandate the use of the series representation of the Green's function, while R remains less than five quadrilateral diagonal lengths, requiring the use of an exact integration for sufficient ac-

curacy of the essential singular behavior. Since the essential singularity is not represented by separate terms in Eq. 24, it is necessary to extract the midpoint value of the wave part from the total series Green's function by subtracting the value of the singularity term calculated at $R = R(P,Q)$, the radius at the quadrilateral centroid. Then, the exact integral of the singular part over the quadrilateral is calculated using Biot-Savart, and added to the midpoint wave part. That is,

$$\begin{aligned} \frac{\partial \phi}{\partial x} \Big|_P = \gamma \left[\frac{\partial G_D}{\partial x} \Big|_{(P,Q)} - \frac{1}{R(P,Q)^3} + \frac{3(x-\zeta)^2}{R(P,Q)^5} \right. \\ \left. + \frac{i}{c} \int \frac{R \times dC}{|R|^3} \right] \end{aligned} \quad (37)$$

The solution of the complex matrix equation, Eq. 32, is performed in two steps. First, after the distinct elements of the coefficient matrix G have been computed and the matrix filled, the complex LU-decomposition of the matrix is computed, using a standard subroutine package (Ref. 21). This decomposition is required only once for each frequency, regardless of the number of heading angles desired in the diffraction problem, since the Green's function is obviously independent of the wave encounter angle.

Once the decomposition is stored, any normal-velocity boundary condition can be supplied in the vector V , and the solution for the dipole strength is immediately calculated using complex back-substitution in the prestored decomposi-

tion. The body boundary condition velocities for the radiation problem are applied first, and the solution of the system yields the radiation dipole distribution (that is, the radiation pressure) and thus the added mass and damping coefficients. Then, for each desired encounter angle, the appropriate diffraction boundary conditions are applied, and the resulting solution gives the diffraction pressure and the exciting moments on the flaps.

It should be emphasized that the exciting moments are calculated by direct solution of the diffraction problem, rather than by the use of the Haskind relations. This decision was made because the latter method requires that the potential itself be calculated in addition to the normal derivative required for the solution of the radiation problem. Since the calculation of the diffraction problem body boundary condition is so simplified by the geometry of the device, and since the back-substitution routine is fast (once the decomposition is calculated), the repeated solution of the diffraction problem is more efficient, for a reasonable number of encounter angles, than recalculating the elements of a coefficient matrix.

Finally, the added mass, damping, and exciting moments are calculated by the following simple summations, analogous to the integrals of Eq. 19:

$$A_{11} = -\frac{\rho}{\omega} A \sum_{S_1} \text{Im} \gamma_{jr} (p + \zeta_j)$$

$$\begin{aligned}
 A_{12} &= \frac{\rho}{\omega} A \sum_{S_2} \text{Im} \gamma_{jr} (p + \zeta_j) \\
 B_{11} &= -\rho A \sum_{S_1} \text{Re} \gamma_{jr} (p + \zeta_j) \\
 B_{12} &= -\rho A \sum_{S_2} \text{Re} \gamma_{jr} (p + \zeta_j) \\
 F_1 &= i \omega \rho A \sum_{S_1} \gamma_{jd} (p + \zeta_j) \\
 F_2 &= i \omega \rho A \sum_{S_2} \gamma_{jd} (p + \zeta_j)
 \end{aligned} \tag{38}$$

where p denotes the pivot depth, ζ_j is the vertical coordinate of the centroid of the quadrilateral j , the summations over S_1 and S_2 denotes the quadrilaterals representing flap 1 and flap 2, respectively, A is the area of the quadrilateral, assumed equal for all j , and γ_{jr} are the radiation dipole strengths, γ_{jd} the diffraction dipole strengths.

The following section presents a number of comparisons between the results of the present 3-D method for added mass, damping, and exciting forces, and previous analytical work. Recent experimental results are also compared.

Validation of 3-D Hydrodynamic Coefficient Predictions

In certain special cases, comparisons are available by which the 3-D numerical calculations of the present method can be checked against published analytical results, both two and three-dimensional. In addition, some recent experimental data is also applicable.

2-D Comparisons: Added Inertia and Damping

Consider the case of a single flap of relatively high aspect ratio (width/draft), subject to normal wave encounter in deep water. For this condition a logical comparison can be made between the 3-D hydrodynamic coefficients, divided by flap width to obtain equivalent sectional coefficients, and published 2-D results. Figures 7-10 show comparisons, on this sectional basis, of numerically calculated 3-D added mass and damping coefficients versus the 2-D analytical results of Kotik, Ref. 22. Kotik presents the sectional added mass and damping of a 2-D vertical strip moving in either of two modes: namely, (1) sway, (2) roll about a pivot at the free surface.

Although the present method is specifically intended to calculate the coefficients for roll about an arbitrary pivot, a suitable approximation of pure sway can be obtained by placing the pivot at a sufficiently large distance from the flap. (For the comparisons shown here, this distance was 500 flap drafts). Then, to convert the roll added moment of inertia and roll damping torque coefficient into equivalent sway added mass and sway damping force coefficients, it is only necessary to divide by the radius squared (one factor of radius for the conversion from moment to force, and a second for the conversion from angular to linear acceleration or velocity).

Obviously the normalized 3-D results must tend to the

2-D limit as the flap aspect ratio is increased. To indicate this convergence, points are drawn in Figs. 7 and 8 for flap aspect ratios of 10 and 20, in addition to the 2-D limit of Kotik for sway motion. Two important features of this comparison are noted here. First, the sectional added mass approaches the 2-D limit noticeably more rapidly with respect to aspect ratio than does the sectional damping coefficient. At first glance, this difference in behavior may seem incongruous, since the added mass and damping pressures are nothing more than the imaginary and real parts of the same radiation potential jump at the flap. However, on closer inspection it becomes clear why this difference must exist.

An informal example may be used to demonstrate this. Consider an attempt to obtain a first approximation of the added mass and damping coefficient of a single 3-D flap in sway, using the numerical procedure presented above, with only a single quadrilateral. As before, let the dipole strength be assumed constant over the quadrilateral (patently a crude approximation), and let the radiation boundary condition be satisfied only at the centroid of the quadrilateral. The complex equation for the single unknown dipole strength is then

$$V = \frac{\partial \phi}{\partial x} = \gamma \iint_S \frac{\partial G_D}{\partial x} dS \quad (39)$$

where V represents a complex normal velocity. The integral

can be written as some complex constant, C , (not necessarily the value of the integrand at the centroid) multiplied by the area of the quadrilateral, S . Then solving for the real and imaginary parts of the dipole strength:

$$\begin{aligned} \text{Re } \gamma &= \frac{(\text{Re } V \text{ Re } C + \text{Im } V \text{ Im } C) \cdot l}{|C|^2 S} \\ \text{Im } \gamma &= \frac{(-\text{Re } V \text{ Im } C + \text{Im } V \text{ Re } C) \cdot l}{|C|^2 S} \end{aligned} \quad (40)$$

Following the convention used in formulating the radiation boundary condition, we can arbitrarily let V be the pure complex number $i\omega |X|$, where $|X|$ is the magnitude of the flap motion, so that $\text{Re } V = 0$. Then, the real and imaginary parts of the dipole strength (the damping and added mass in Eq. 38) are seen to be proportional to the imaginary and real parts, respectively, of the complex constant C .

For a low-aspect ratio flap, the real part of C is large, being dominated by the essential singularity term in the Green's function. As the flap is made wider, the portion of $\text{Re } C$ containing the singular behavior becomes less dominant, since the far-field behavior of the essential singularity is $O(1/R^3)$ while the wave terms are $O(1/R^{1/2})$. Thus, the added mass, which stems from the imaginary part of the dipole strength, and hence from $\text{Re } C$, must not increase as rapidly as the damping with increasing width. Therefore, at a given low aspect ratio, the damping coefficient can not be as close to the 2-D limit as the

added mass. Physically, all that this implies is that finite end effects are felt more strongly in the wave-making behavior of the flap than in the non-wavemaking (added mass) behavior.

The second important feature of Figs. 7-10 is that the agreement between the 2-D analytical limit and the computed 3-D results, using constant quadrilateral size, is closer for low frequencies than for high frequencies. This computational problem at high frequency must be anticipated because the assumption of constant dipole strength over each quadrilateral becomes less and less tenable as the wavelength becomes shorter with respect to quadrilateral dimensions, resulting in more oscillation of the wave terms in the Green's function over the quad. However, at high frequency the results for 3-D should tend to approach the 2-D limit, so that a full 3-D treatment becomes less important.

Radiation Pressure Distributions versus 2-D Results

With regard to pressure variation over the depth of the flap, a comparison may be made with the 2-D numerical program of Toki, Ref. 23, for deep water. Figure 11 shows a comparison of the chordwise variation of the radiation pressure at the mid-span of a 10:1 aspect ratio flap versus Toki's 2-D prediction, for four wavenumbers. The agreement is good at low frequencies, becoming undependable for fixed quadrilateral size at high frequencies.

Single Flap Exciting Forces versus 2-D
and 3-D Analytical Results

The 3-D calculated wave exciting forces (again normalized by flap width to give equivalent sectional forces) for normal wave encounter in deep water may be compared with the 2-D results of Evans, Ref. 14. A typical comparison is shown in Fig. 12. Again, the agreement is better for long waves than short, as expected for constant quadrilateral size.

As a further check, the exciting force and damping coefficient must also agree, as required by the form of the Haskind relation given in Ref. 24, as follows:

$$B = \frac{\omega k}{4\pi\rho g\zeta_A^2} \int_0^{2\pi} |F(\theta)|^2 d\theta \quad (41)$$

in which the integral of the wave exciting force over all directions is related to the radiative damping coefficient, B. The numerical results for radiative damping have been checked against the calculated exciting forces, and the above relationship was found to be satisfied numerically to three significant figures.

For a 3-D single flap in finite depth water, the exciting force results of the present method can be compared with the analytical treatment of Stiassnie and Dagan, who solved the linearized 3-D boundary value problem using elliptical coordinates, Ref. 25. This comparison is shown for several cases in Figs. 13-15.

Twin-Flap Hydrodynamic Coefficients versus 2-D Analytical Results

For twin-flap devices, two-dimensional comparisons are available in the analytical results of Srokosz and Evans, Ref. 11. Comparisons of normalized hydrodynamic coefficients for flaps of 10:1 aspect ratio with the 2-D results are shown in Figs. 16-18. In general, agreement is good; the major features of the 2-D curves are duplicated, although in less exaggerated form. Finite width effects are again more noticeable in the damping coefficient than in the added mass, and they are also strongly present in the coupling force coefficients, as might be expected and as will be discussed in more detail subsequently. As always, the agreement is closest at low frequencies for a fixed quadrilateral size.

Comparisons with Finite-Width Experimental Results

Finally, experimental results for a 3-D twin-flap device were obtained recently in the model basin of the Department of Naval Architecture and Marine Engineering at The University of Michigan, Ref. 26. The model device used in these tests was free-floating, with flap width of 1.83 m: flap drafts were varied from about 0.65 m to 1.09 m, and separations from about 1.0 m to 1.5 m. In one case, the model was also tested with the supporting structure rigidly fixed, and this case is used for specific compari-

son with the predictions of the present numerical method. (The effect of motions of the supporting structure on energy absorbing performance is discussed subsequently.)

Although the model was not instrumented for direct measurement of the hydrodynamic coefficients, the flap response amplitudes and power absorption were measured. In addition, the external damping coefficients on the flaps were calculated independently for each run, and were found to show some variation from run to run. Figures 19 and 20 show a comparison between these experimental results and predictions based on the calculated hydrodynamic coefficients, and applying the average experimental power-takeoff dampings found in this sequence of runs. The damping on flap 2 is therefore somewhat higher than on flap 1. This particular configuration was found from subsequent calculations to be undersprung for maximum power output, and too highly damped, as well. Nevertheless, the comparison of its performance with numerical predictions is instructive, if only to show some trends.

It will be noted that the numerical prediction of power output tends to be higher than the experimental result, as is the response amplitude of flap 1. Since this overprediction is fairly consistent, at least in the lower wavenumber range of the experiments, it can hardly be attributable to the variation of the experimental damping coefficients. Furthermore, both the power output and the flap mo-

tion predictions show more pronounced variation with respect to wavenumber than was observed experimentally.

The numerical overprediction of power output by as much as 50 percent, or to put it another way, the failure of the model device to produce the predicted power output, can be interpreted in a significant way; detailed quantitative explanation must await further experiments and analysis.

First, in the experiments, power absorption was measured by the force and motion amplitudes at the hydraulic power takeoff. Thus, any frictional or viscous losses were not included in the experimental output, and this of course would tend to lead to some overprediction, since the numerical results were based on the effective power takeoff damping alone.

Second, the experiment does not correspond exactly to the case of an isolated device. Because of the presence of the tank walls (the tank width is approximately 7.7 m, versus the flap width of 1.83 m), the experiment actually corresponds hydrodynamically to the case of an infinitely wide row of interrupted twin flap devices, moving in phase. For these dimensions, the effective gap between adjacent devices is equal to about 2.66 flap widths, and is somewhat shorter than the wavelength of the longest waves tested. Thus, it should be anticipated that the flap forces are affected by the presence of the images. The exact effect on the power output has not been modelled at this point, how-

ever, the trend toward reduced power output is as expected. As the flap width is increased to the width of the tank, resulting in a 2-D experiment, as in Ref. 10, the power output must be bounded by the maximum 2-D result, that is, by a "capture ratio" (or 2-D efficiency) of unity.

Effects of Quadrilateral Arrangements

As already mentioned, the accuracy of the present method is limited by the assumption of constant dipole strength over each quadrilateral. This approximation, of course, is accurate for practical purposes if the quadrilaterals are small and the wavelength is long. For short waves, then, the number of quadrilaterals must be increased to maintain a given level of accuracy.

The effect of number of quadrilaterals on the calculated hydrodynamic coefficients can be shown by comparing the results at a given flap aspect ratio with a number of quadrilateral arrangements. A comparison of this type is shown in Figs. 21-23. Typically, adequate results have been achieved with 50 to 100 quadrilaterals per flap, giving a maximum of about 200 quadrilaterals. The corresponding full coefficient matrix then contains 40,000 complex elements. If all the quadrilaterals are congruent, however, then the matrix is storage symmetric, that is $g_{ij} = g_{ji}$.

However, the "stackwise" symmetry of the Green's function implies that for an arrangement of 5 vertical tiers of

quadrilaterals, 20 stacks of quadrilaterals on each flap, for two flaps, only 600 distinct elements (each requiring a computation of the Green's function) are necessary to fill the 200×200 coefficient matrix. Consider an alternative arrangement giving the same total number of quadrilaterals, namely, 10 tiers, with 10 stacks on each of two flaps: this arrangement requires 1100 distinct elements. For computational cost reasons, it is therefore preferable to increase the number of stacks, rather than the number of tiers, if possible.

At shorter wavelengths, of course, the variation of the Green's function in the vertical direction must be considered as well as the variation in the horizontal plane in sizing the quadrilaterals. In large water depths this vertical variation is essentially exponential with depth, in shallow water the vertical variation decreases to zero, while in intermediate water depths the variation follows the form of $\cosh k(z+h)$. Thus, the need for more tiers of quadrilaterals is less stringent in shallower finite-depth water than in deep water, to obtain a given level of resolution in the vertical direction. This represents an advantage of the present approach in shallow water applications.

EFFECTS OF DEVICE GEOMETRY ON 3-D HYDRODYNAMIC BEHAVIOR

The 3-D hydrodynamic model described in the previous section calculates the added mass, radiative damping coefficient, coupling coefficients, and exciting forces for flap-type absorbing bodies, given the geometry (including water depth). The hydrodynamic coefficients, of course, do not in themselves determine the power absorption of the device: the external forces (namely, the restoring force coefficients and power-takeoff characteristics) must also be specified to solve for the motion response and power absorption, as is apparent from Eqs. 14 and 15. For this reason, a consideration of the hydrodynamic coefficients alone, and as influenced by the choice of device dimensions, provides only an incomplete picture of the device performance and cost.

Nevertheless, some basic design guidance in selecting appropriate device dimensions for a particular site or wave environment can be obtained by considering the purely hydrodynamic characteristics of a device, provided that we are prepared to accept certain intuitive generalizations about what constitutes "desirable" or "undesirable" hydrodynamic qualities. With this acceptance of admittedly incomplete guidance, at least in the opening stages of

design, we may find a rough but simple heuristic method of beginning a rational design. Presumably, refinement of the initial judgment will then require more detailed analysis, including elements of the design other than its basic geometry.

The definition of "appropriate" device dimensions is left intentionally vague at this point. Hopefully, the hydrodynamic qualities themselves will provide some initial clues, while preliminary estimates of the relationship between flap dimensions, power-takeoff ratings, and costs (which will be considered subsequently) will give more precise meaning to the term.

By assumption, the basic device geometry (single or twin-flap, flap draft, separation, pivot location, and width) is fixed at construction, and therefore cannot be varied to respond to changes in the wave environment over time. Mechanical arrangements that would permit variable flap geometry can be envisioned, however, such contrivances would clearly add a great deal to the complexity and cost of the absorbing bodies themselves, their supporting structures, and auxiliary actuating machinery. Since one of the principle "selling points" of the flap-type device is supposedly its geometric simplicity, as compared with other proposed body shapes, the incorporation of complicating features seems to be self-defeating, and will not be considered further at this stage. Therefore, the choice of a

device geometry must be made at the design stage.

The question is this: How can an initial estimate of the device dimensions be chosen on the basis of an inspection of hydrodynamic coefficients? Indeed, can the device dimensions be chosen to secure "better" hydrodynamic qualities, either at a particular wave frequency of interest, or over some range of frequencies presented by a spectrum or a family of spectra? Some 3-D linear hydrodynamic results will be applied to these questions in the following sections. First, however, it seems that we must decide what we will be looking for: What hydrodynamic qualities are "better" in a wave absorber?

For a single-flap device there are only three hydrodynamic quantities to consider: the exciting force magnitude, the radiative damping coefficient, and the added mass. From the point of view of power absorption the exciting force is of primary importance, as it is the only quantity that can generate absorbable work. The significance of the exciting force magnitude is apparent from Eq. 44, 45, and 49, below, or directly from Eqs. 14 and 15 (suitably modified by letting F_2 , K_{22} , and K_{12} go to zero). Other quantities being equal, the maximum power absorption is seen from Eq. 49 to vary as the square of the exciting force, provided that the device stroke is not limited by other imposed forces. (As shown in a subsequent section, if a stroke limit is imposed the power absorption then

varies directly as the exciting force.) Therefore, intuitively speaking, a greater exciting force magnitude represents "money in the bank" if it can be obtained without greatly increasing the size (and cost) of the flap.

Obviously, however, the device must move in order to absorb work from the exciting force, and the phase of the motion with respect to the exciting force determines the actual absorption. This phase of course, is independent of the magnitude of the exciting force, but depends on the damping and tuning. The radiative damping, as can be seen in Eq. 49, always represents an energy loss, namely, the energy carried away by the radiated wave due to the body motion. From Eq. 49, the maximum achievable power absorption (with no stroke limitation) varies inversely with the radiative damping. Thus, Eq. 49 gives one reasonable means of comparing devices in terms of their maximum absorption capacity. However, the maximum absorption cannot be obtained unless the device can be tuned to resonance at the frequency under consideration. This forces the designer to confront the issue of inertia and spring constant, which can become critical if the inertia is large and the maximum restoring force is limited by a dependence on purely hydrostatic forces for springing.

For a single-flap device, resonant tuning is given simply by $C = \omega^2[M + A(\omega)]$, where C is the spring constant, M the intrinsic inertia of the oscillating device, and A the

hydrodynamic added inertia as a function of frequency. As will be shown by subsequent examples in the following section, and as might be suspected from inspection of Figs. 7 and 9, above, the added mass tends to increase with frequency over the range of interest (relatively low values of ka for typical ocean wavenumbers and moderate device drafts). Thus the required spring constant for resonance increases rapidly with the desired tuned frequency. For this reason a large added mass (or, for that matter, a large intrinsic mass) will reduce the resonant frequency that can be obtained with a given maximum spring constant. (As will be discussed below, a dependence on hydrostatic restoring forces, which are relatively small for a thin flap, will tend to limit the ability of the system to reach resonance at higher frequency. By contrast, practical means are available to tune a flap-type device for very low frequency, e.g., adding ballast to increase M and reduce C .) It will also be shown below that increases in flap draft are critical in the relationship between added mass and available spring constant.

Finally, one further hydrodynamic quality may be of concern even in the initial stages of design: this is the directionality of the device. Directionality, of course, is solely determined by the behavior of the exciting force with respect to encounter angle, since the added mass and damping are independent of angle. At the simplest level, a

highly directional behavior might be viewed as an undesirable characteristic, since it would imply a drastic reduction in power absorption for angles off of normal encounter. However, as suggested by Eq. 41, highly directional behavior of the exciting force must be accompanied either by a low radiative damping (for a fixed value of exciting force at normal encounter) or a high value of exciting force at normal encounter (for fixed damping). Thus, a highly directional absorbing device will have better absorption characteristics (subject to proper tuning) along its preferred direction, in much the same way as a directional radio antenna, when oriented correctly, outperforms a whip antenna. For this reason, a preference for highly directional behavior may be reasonable if the wave environment at a particular site is known to be relatively unidirectional. This is not unlikely in coastal locations, where shoaling water will tend to diffract incident waves to align the crests parallel to the contours of depth.

To summarize, then, the following hydrodynamic generalizations can be made regarding "desirable" characteristics for a single-flap absorber, with regard to power absorption.

1. High exciting force at normal encounter.
2. Low radiative damping.
3. Low added mass for wider frequency limits (i.e., the ability to tune to higher frequencies with limited maximum spring constant.

4. Directional characteristics "consistent" with expected uniformity of incident wave direction.

It should be pointed out immediately that both high exciting force and low radiative damping are not obtainable without leading to practical problems. In particular, the former obviously leads to large forces on the device and its supporting structure; both lead to large response amplitudes which may not be achievable in practical systems.

For twin-flap systems the question of "desirable" hydrodynamic characteristics is considerably more complicated. In particular, Eqs. 14 and 15 do not give any unambiguous instruction. Since both K_{11} and K_{22} in Eq. 14 involve the external dampings and spring constants, the capacity for power absorption cannot be judged by inspection of the hydrodynamic coefficients alone. Furthermore, since both F_1 and F_2 appear in complex form in the numerators of Eq. 14, the responses depend not only on the magnitudes of the exciting forces, but on their relative phase as well. Finally, with the coupling term K_{12} in both denominator and numerator, it cannot be made obvious whether large or small magnitudes of the coupling forces are desired; in fact, the phase of the coupling is equally important, since the force acting on one flap due to the motion of the other flap can reinforce or cancel the exciting force.

In spite of these complications over the case of a single flap, a few generalizations can be made. First, the

exciting force magnitudes still represent, in at least an intuitive sense, the mechanism by which work is done on the flaps. Thus, at least one of the flaps must have a large exciting force at the desired frequency. (Results have shown that at low to moderate frequencies, the exciting forces on both flaps tend to be of about the same magnitude, although this does not hold true at higher frequencies, for which the front flap begins to act as a barrier. Furthermore, as a rule each of the twin-flap exciting forces are of about the same magnitude as a single flap of equivalent draft and width, within the low to moderate frequency range, as illustrated for typical cases in Fig. 24.)

The radiative damping coefficient B_{11} may still be interpreted as an energy "loss," in the sense that each flap radiates waves due to its motion; however, there is an important distinction between the twin-flap and the single-flap in this regard. In the single flap, any work done against the radiative damping force is truly lost, radiated outward in the form of radiated wave. For a twin flap, however, some of this energy may be "recaptured" by doing work on the other flap, through the coupling force, if the relative phasing of the flap motions is correct. Since the relative phasing of the motions can be adjusted by choosing values of the spring constants and external damping coefficients, it follows that higher values of B_{11} do not necessarily imply lower values of absorbed power for a twin-flap

device: the result depends on the coupling forces and phase.

This is analogous to the mathematically simpler 2-D requirement that the phases of the flap motions lead to cancellation of all out-going waves, as discussed in Ref. 11, for maximum absorption. Of course, in 3-D, one cannot cancel all waves going out of an arbitrarily large control volume, since this would lead directly to infinite absorbed power for a finite-width device.

By a similar argument, the simple requirement for resonant tuning, which is explicit for a single flap for maximum absorption, as shown in Eqs. 44 and 49, has no particular meaning for a twin flap. Thus, merely setting the spring constant of one or both flaps for "resonance" and the external dampings equal to the radiative damping does not lead to high absorption as it must for a single flap, according to Eq. 44. A typical example illustrating this is given in Table I. In general, the spring constants for maximum absorption are not equal; they are not even necessarily positive. Even the external damping coefficient of one of the flaps can become negative at maximum absorption. The practical implications of negative spring constants and power-takeoff dampings are discussed in a subsequent section; on the whole, they are not favorable. However, because maximum absorption for a twin-flap device does not depend explicitly on obtaining resonance through higher

spring constants, there may be practical cases in which twin-flap devices are better adapted to the reliance on relatively "soft" hydrostatic springs.

A further generalization regarding the directionality of a twin-flap device can be made here. Recall that for a single flap the directional characteristics of the device can be judged by the behavior of the exciting force magnitude alone. Thus the tuning and damping required for maximum power absorption (in the absence of stroke limitation requirements depends only on frequency, and is independent of encounter angle. For a twin-flap device this is not true: the relative magnitudes of the two exciting forces, and their phase difference, vary with respect to angle, as shown in Fig. 25.

In the following sections the influences of device geometry on the hydrodynamic coefficients are considered in greater detail. Wherever possible, in view of the generalizations discussed above, an attempt will be made to derive some form of design guidance from hydrodynamic conclusions.

A device geometry, including the effect of water depth, can be conveniently specified by four dimensionless ratios. For the purposes of data presentation in the following sections, the four ratios are all referred to flap draft as follows (see Fig. 2):

1. Water depth/flap draft, h/a .
2. Flap aspect ratio, $2w/a$.

3. Flap spacing/draft, $2b/a$.
4. Flap pivot depth/draft, p/a .

In interpreting results plotted on a nondimensional wavenumber ka , it must be remembered that the wavenumber k is the local wavenumber as measured in water of depth h , that is, the solution of $k \tanh kh = \omega^2/g$. Thus, for a given value of ka , it is simple to calculate the corresponding frequency once a particular flap draft is selected.

Flap Draft

To judge the effect of flap draft per se on an absorbing device's hydrodynamic characteristics and performance, it will be instructive to begin with the simplest possible case and then proceed to more complicated situations. Clearly, for a practical 3-D device, the choice of flap draft will have to be related to other dimensions, flap width (for structural as well as hydrodynamic reasons), flap separation for twin-flap systems, and water depth (which may be an active constraint in coastal sites). In addition, the flap draft may be restricted by building considerations, and will contribute to the weight and cost of the absorber.

For the moment, however, let us at least try to isolate the primary hydrodynamic effects of varying the flap draft, independent of other dimensions, if possible, and free of all other dimensions, if possible, and free of all other constraints. In order to do this, consider a deep-

water situation, and assure that the device is of high enough aspect ratio to permit arguments to be based on 2-D results, at least for normal wave encounter. Further, assume for the remainder of this discussion that the flaps are pivoted at the lower edge ($p/a = 1$) unless otherwise noted. The question posed is this: under these simplifying assumptions, what is the significance of flap draft in the design?

For a single-flap device, maximum absorption occurs when the tuning is resonant, that is, when $C = \omega^2[M + A(\omega)]$ and when the external damping is equal to the radiative damping, $d = B$, as can be shown by differentiation of Eq. 45 (with Eq. 44 substituted in for X) with respect to C and d . The maximum power absorbed is then given by Eq. 49, while the corresponding motion amplitude is given by Eq. 48.

A typical 3-D result for a long, shallow flap in deep water is shown in Figs. 26 and 27, in which maximum power absorption and motion RAO are plotted versus flap draft for various wavelengths. It will be noted that the maximum cross-section becomes very large for long waves, greatly exceeding the width of the flap (about which more will be said in a subsequent section).

Unfortunately, however, these large absorption values at low frequency are accompanied by correspondingly large amplitude motions. For a reasonable finite wave amplitude

(as opposed to the infinitesimal amplitude presupposed by linear wave theory and by the linearized formulation of the boundary value problems), the resulting motion of the flap will clearly be too large to support linear assumptions. Thus, for an extremely shallow flap, giving very low values of ka at a fixed wavelength, the linear predictions for motion and power absorption cannot be expected to hold in real finite-amplitude waves. (The general problem of imposing realistic stroke limits is discussed at length in a subsequent section.)

However, an interesting thing happens as the designer increases the flap draft:

1. The maximum absorption cross-section varies hardly at all with flap draft, (Fig. 26).
2. The corresponding motion amplitude at maximum absorption is sharply reduced, (Fig. 27).

This result applies across the entire frequency range shown in the figures, and the reduction in motion amplitude is somewhere between the square and the cube of the flap draft.

Thus the principal effect of increasing flap draft, at constant width, is to reduce the motion of the flap at constant power absorption. In practical terms, then, a designer should look not only at a particular frequency of interest, but also at a design wave amplitude corresponding

to that frequency. By deciding in advance that the device motion should be limited to a particular stroke, which may be a rational consequence of the specific power-takeoff machinery fitted, the designer can then size the flap draft to obtain the desired response amplitude in a given wave height, at the frequency of interest, at maximum absorption, which can then be related to the rating of the power takeoff.

This method, of course, can be applied only to a single-flap device, and the assumption of high aspect ratio has been applied in order to reduce the importance of end effects (the lowest aspect ratio on this series was 7.5). However, similar calculations were done for a constant flap width of 5m (versus 30m), for which the highest aspect ratio was 5.0, and the lowest 1.0. The results are shown in Figs. 28 and 29, and the conclusions are identical to those for a wider flap. The absorption cross-sections for the shorter flap series are remarkably wide, as much as four times the flap width at the lowest frequency. Again, this is a matter of the device behaving as a point absorber. Similar results are obtained for a flap in shallow water, as shown in Fig. 30.

Since the maximum power absorption for a twin-flap device cannot be cast in as simple a form as Eq. 49, it is not possible to give as clear cut an example of the influence of flap draft alone. However, numerical experi-

ments tend to confirm that the maximum power absorption remains relatively insensitive to flap draft, while the corresponding motion amplitudes are reduced. (A similar conclusion might be drawn from 2-D results: Srokosz and Evans (Ref. 11) have shown that a maximum absorption, namely, an efficiency of 1, can be obtained at any frequency and draft, provided that separation, springs, and external dampings are chosen correctly, while the damping becomes relatively less important at low values of ka .)

However, there are several practical problems attached to the selection of a flap draft that will give maximum absorption at a suitable low motion amplitude. First, as the flap motion is decreased, the forces on the power takeoff must increase to absorb the same power. Thus the strength of power takeoff components and supporting structures becomes more of an issue. Second, as the flap draft is increased, the added inertia also increases. For a single-flap device, this implies that a stiffer spring will be required for resonant tuning at any given frequency. (No such firm generalization can be made for a twin-flap device, where the frequency response depends on separation as well as spring and damper settings.) As will be shown subsequently, the purely hydrostatic restoring moments of geometrically similar low-pivoted flaps do not increase as rapidly as the inertias with increasing draft, certainly in the large range of practical (low) ka . Thus, the choice of

a large flap draft in order to obtain smaller motions may place the desired frequency out of reach of resonant tuning with a pure hydrostatic spring. In this case, the maximum absorption will decline, which may or may not be acceptable. In shallow water sites, of course, the designer must work within a more rigid draft constraint, and cannot always use an increased draft to get desirable performance and reasonable motions. In this case, a tradeoff exists against flap width.

Finally, the selection of flap draft has an important implication for the assumed linearity of the problem, quite apart from the prediction of large linear responses in small amplitude incident waves. Specifically, consider the case of a relatively shallow flap in waves of finite amplitude. Since the pivot is assumed fixed, it follows that at a certain wave amplitude the variation in immersion between wave crest and trough will become non-negligible with respect to the draft. Clearly, then, the flap draft must at least be large with respect to wave amplitude if linear results are to remain credible. For the present, however, it can only be assumed that the designer will not expect linear behavior in wave amplitudes that drastically alter the flap immersion.

Flap Separation

In a two-dimensional analysis, such as that of Srokosz and Evans, Ref. 11, the principal effect of changing flap

separation is to change the frequencies at which 100% absorption can take place (of course, with optimum spring and damping coefficients). Thus, varying the separation between flaps constitutes an alternative to conventional tuning (by springs and inertias) for a twin-flap device.

However, consideration of 2-D results also shows that, with more widely spaced flaps, the phase relationship between flap exciting forces and coupling forces swings through more of a cycle over the frequency range of interest. This leads to a curve of absorption efficiency versus frequency that has increasingly sharp and closely spaced peaks (of 100% absorption) and valleys (of zero absorption), as was shown graphically in Ref. 11. This highly oscillatory curve of absorption coefficient cannot be desirable from the standpoint of achieving good performance in a typical wave spectrum. For this reason, one important result of the earlier 2-D work (Ref. 10) was the principle that flap separation could not be unduly large if a device were to have a reasonably high and substantially constant absorption efficiency over a wide frequency band. Typically, the flap spacing for such a system was less than a quarter-wavelength of the shortest wave of interest.

In a three dimensional situation, at a given frequency the flap separation has a direct effect on the phase relationships between the exciting forces on the two flaps, both of which appear in the numerators of Eq. 14, and also

on the phase of the coupling term K_{12} . This fact is physically obvious, just as it is in 2-D, although it may be considerably complicated by finite length effects.

Unlike the 2-D case, however, the effect of increased separation in 3-D is also to reduce the magnitude of the total force experienced by one flap as a result of the motion of the other, since the radiation potential decays as $O(1/r^{1/2})$ in the far field. This reduction can be seen in Fig. 31, where the magnitudes of the coupling coefficients A_{12} and B_{12} are plotted versus separation for various wavenumbers. Since the "role" of the coupling force (in an intuitive sense) is to provide a means of recovering some of the energy which would otherwise be lost through radiation, the desirability of fairly close flap spacing should be even greater in 3-D, especially if the flaps are short. The detailed variation of coupling forces with respect to spacing (at a given frequency and width) does not lend itself to stronger generalizations.

The effect of flap separation on exciting force magnitudes and phase difference is similar, and again the details depend strongly on wavelength. It can be noted from Fig. 32 that in moderate to long wavelengths, with fairly close spacing, the exciting force on the rear flap is significantly larger than that on the front flap, a diffraction effect that also occurs in 2-D results (Ref. 11). As the flap spacing is increased, the magnitudes of both ex-

citing forces gradually approach the single-flap limit, as expected. Obviously, for very short flap widths, the diffraction effects are smaller, and the exciting forces approach the single-flap limit more rapidly with increased separation.

For short wavelengths, that is, at large values of ka , the front flap acts as an effective wave barrier, so the rear flap exciting force is substantially less than the front flap at small separations. Again, however, the diffraction potential decays as $O(1/r^{1/2})$, and the two exciting forces will converge on the single-flap limit, even in normal encounter, if the flap separation is large with respect to width.

Flap separation also has a marked effect on the directionality of the device in terms of the flap exciting force magnitudes and phase difference. In particular, large separations cause more drastic phase changes with respect to heading angle, as should be expected from a consideration of the incident wave potential alone.

In summary, design guidance for the selection of an appropriate flap spacing cannot be reduced to a single rule, or even a rule with constraints, as was the case for flap draft. This is especially true because the effects of flap separation are so strongly frequency-dependent and oscillatory (the flap spacing constitutes a kind of "tuning"), and because flap separation cannot be properly con-

sidered independently of flap width or draft, or even water depth. However, a few very broad conclusions can be drawn.

First, 2-D conclusions (as well as the 3-D decay of the radiation potential) indicate that the flap spacing must be much smaller than the shortest wavelength of interest, regardless of width, flap draft, or water depth. Second, if the separation is large with respect to flap width, the exciting forces and radiative dampings will approach single flap values, and the result will be approximately two single-flap devices (at the same cost, we will need to do better than that). Thus, we must know that the flaps cannot be "too far" apart. So, how far is "too far?" This question cannot be answered on the basis of the coefficients alone.

Rather than attempting to answer this question immediately, since it is affected by the other dimensions in the problem, width, draft, and water depth, suppose we ask the opposite questions: Why shouldn't the flaps be quite close together? With a close spacing, the coupling force magnitude is as large as it can be (presumably, the wavelength will be long with respect to the separation over the entire frequency range of interest, so that there is no question of generating large phase shifts of the coupling force with changes in frequency). Depending of course on the flap width, and the ratio of water depth to draft, the exciting force on the rear flap may be somewhat reduced be-

cause the front flap may be effectively sheltering it, but this is not necessarily unfavorable, provided that the flap motions can be phased to cancel part of the radiated wave. (In fact, experience has shown that the exciting force magnitudes tend to be essentially equal for all practical choices of dimensions, even in shallow water, in the frequency range of interest).

The only physical consideration limiting how close the flaps should be is interference. The flaps must not be allowed to come in contact, regardless of the amplitudes or phases of their motion. Clearly, this requirement is satisfied for bottom-pivoted flaps if the separation is greater than twice the draft: the two flaps can then swing even to a horizontal position, head to head, without hitting. (For flaps which may be ballasted to sink, this criterion may not be quite as extreme as it sounds.)

Finally, the practical advantages of close spacing include shorter cable runs between flaps, smaller common foundations or supporting structures, and reduced exposure to damage by vessels or floating objects. Thus, in the absence of clear hydrodynamic objections, and that is the case, the flaps may be conveniently placed as close together as possible, subject only to interference requirements.

Flap Width

In a strictly two-dimensional treatment, the influence

of increased flap width is a foregone conclusion: since the power absorbed is directly related to the incident wave power per unit width, the power output increases directly as the flap width. In three dimensions, however, this is far from the case. In fact, as has been shown by 3-D results, in oblique wave encounter an increase in flap width can actually result in reduced power absorption, due to partial cancellation of the incident wave exciting forces over the length of the flap.

Increasing the flap width at constant draft results in greater radiative damping, and, in normal wave encounter, the exciting force is also increased, as expected. However, as in the case of increased flap draft, the increased damping dominates, and therefore the maximum absorption cross-section (at optimal damping and tuning) does not increase in direct proportion to the flap width in the low frequency regime. In fact, for systems in which the wavelengths of interest are significantly greater than the flap width (which includes most cases of practical interest), the flap continues to act more or less as a point absorber, and the maximum absorption cross-section is primarily a function of wavelength rather than of flap dimensions. At shorter wavelengths the flap begins to act as a terminator, and the maximum absorption gradually becomes a stronger function of flap width, as shown in Figs. 33 and 34. It will be noted that in the limit of short wavelength, the

absorption cross-section becomes half of the flap width, as it must from 2-D results. In the limit of long wavelength, however, the cross-section/wavelength appears to reach a limit of 0.318, which happens to be $1/\pi$. It should be noted that for a symmetrical point absorber (a source rather than a dipole) Falnes and Budal have calculated a long wavelength limit of $\sigma = \lambda/2\pi$ (Ref. 9).

However, while the maximum absorption may vary only slightly with flap width in the long-wave regime, the corresponding motion amplitudes are markedly reduced by increasing flap width, as shown in Figs. 35 and 36 for deep water, and Figs. 37 and 38 for shallow water, at constant flap draft. Thus, at a given draft a longer flap can obtain linear absorbed power in waves of a certain finite amplitude, while a shorter flap, with an inordinately large required response, cannot. Again, the designer can adjust the flap width, given a limit on draft, so as to obtain a reasonable flap response in waves of a given amplitude at the design frequency.

An interesting design question now arises. For single flap devices, variation of flap draft and width are seen to have similar effects, if the width remains small with respect to the wavelength. As the flap becomes wide with respect to wavelength, of course, the device becomes a full terminator again, and thus absorption should begin to be proportional to flap width, for normal encounter. The ques-

tion, however, is this: Is there a basis for making a tradeoff between desired draft and width for a single flap, in other words, for determining a "good" aspect ratio for the flap?

In an economic sense, this tradeoff might be supported by the relative costs of increasing draft and width; presumably, this would involve a detailed analysis of the structural requirements of deep versus wide flaps. A deeper flap would necessarily be subject to greater hydrostatic pressures, which might require some structural reinforcement for a hollow, box-like structure (although not for the other hand, a wide, shallow flap would experience greater longitudinal bending and torsional loads, which might require reinforced structure, or additional pivot points (more than two hinge points gives an alignment problem as well as statical indeterminacy), or even multiple power-takeoff attachment points (a complication that might be best avoided). This level of structural definition will not be attempted here, although the hydrodynamic model can be used, in principal, to give the depthwise and spanwise dynamic pressure distributions to determine the loads.

Apart from such structural arguments, however, there are also purely performance-oriented tradeoffs to be considered in selecting a flap aspect ratio. Obviously, in the case of a shallow-water setting, the "tradeoff" may not be available: the designer may be forced to adopt the

deepest permissible draft, with the bottom of the flap at or just above the seabed. Then, the flap width will become the only remaining decision, and the aspect ratio will be entirely determined by the width required to obtain the desired motion amplitude. However, what if the designer has a free hand on both draft and width? What hydrodynamic considerations will govern the decision? There are two key factors, namely, directionality and maximum tuned frequency. The first tends to limit the desirability of increased width, while the second tends to limit the draft.

In terms of directional performance the short flap is at an advantage, particularly as the wavelength becomes shorter. That is, a shorter flap loses absorption less rapidly with oblique angle of encounters. This is true because the interference effects mentioned previously tend to increase with flap width at any given non-normal angle of wave incidence, for a given wavelength. An example is shown in Fig. 39, in which the exciting force is plotted versus encounter angle, for various flap widths and frequencies. Some directional comparisons between single and twin-flap devices are shown in Table II.

The effect of flap width on tuned frequency is the second element in the design decision. For hydrostatically sprung flaps of constant draft and buoyant thickness, the righting moment will increase strictly as the width, while the intrinsic inertia also may be assumed to vary approxi-

mately as the width (in fact, depending on whether the steel weight is governed by overall bending moments or by surface area or volumetric content, the steel weight may actually increase slightly faster than width, or slightly slower). To a first approximation, then, the added inertia and intrinsic inertia of the flap will also vary directly as the flap width, provided the aspect ratio of the flap is high enough to permit the added inertia to be adequately predicted by 2-D results. In this case, an increase in flap width will have no effect on the maximum tuned frequency.

However, for finite aspect ratio flaps, the added inertia actually increases substantially faster than the width. Thus, for low aspect ratio flaps, an increase in flap width will actually reduce the tuned frequency, although not nearly to the same extent as increasing flap draft. Typical comparisons of the effects of draft and width on tuned frequency, with a fixed spring constant, are shown in Figs. 40 and 41.

For twin-flap devices, the flap width (at constant separation distance) has an extremely complicated effect on all the hydrodynamic coefficients. In particular, increased flap width results in a larger coupling force magnitude, although the phase of the coupling force still depends primarily on the separation to wavelength ratio. Since the maximum absorption depends partly on coupling, greater flap

widths will presumably yield slightly increased maximum sorption of certain frequencies, although no general conclusions can be drawn. In the limit of short flaps (for a given separation), the coupling coefficients go to zero, and the maximum power absorption will tend to approach twice the single flap value.

Flap width, in connection with a given spacing, also has an effect on flap exciting forces, as shown in Fig. 42. In general, experience shows that shorter flaps tend to produce exciting forces more on the order of single flap values, while longer flaps lead to slightly more sheltering of the back flap. It should be noted that at low to medium frequencies, the exciting force on the rear flap is greater than the force on the forward flap in normal wave encounter, although it has not been observed to exceed the magnitude of the exciting force on a single flap of equal width. Toward the limit of short waves, of course, the rear flap is increasingly masked by the forward flap, until for very short waves (high values of ka) the forward flap acts as a total barrier and the rear flap receives no exciting force.

Pivot Location

A final geometric design consideration is the position of the pivot. In general, the pivot location need not be at the bottom of the flap (although there may be sound practical reasons for placing it there). In fact, however,

the pivot may be placed at any vertical location, either on the flap or off. One common suggestion, for example, has been to place the pivot axis well below the bottom edge of the flap, perhaps even on the seabed, the flap then being supported by a system of struts.

The effect of such a "low-pivot" arrangement on the maximum absorption and the corresponding motion amplitude is shown in Fig. 43. As might be expected in view of the results of previous sections, the effects of varying the pivot depth on the exciting force and radiative damping are such that the maximum absorption is unchanged. However, the amplitude of the corresponding angular motion is reduced by a pivot arrangement; the linear motion at the top of the flap is also reduced, although not as drastically. (As mentioned previously, as the pivot depth is increased to very large values, the motion of the flap becomes pure sway, and the linear amplitude should converge to a finite value at a fixed flap draft.)

Thus, in terms of achieving a high absorption together with a reasonable motion amplitude (that is, believable within the context of linear predictions), a low-pivoted flap produced much the same effect as increased flap draft. Therefore, a tradeoff may exist between flap draft and pivot location, given a finite water depth (or some other practical constraint on the maximum depth of the device). A low-pivot device might appear to offer some secondary

benefits, as well; these will be examined in some detail, however, because there may be practical problems, too.

First, it can be observed that the added inertia of a low-pivoted flap (that is, with $p > a$) increases less rapidly with increasing p than that of a bottom pivoted flap with increasing a . Assuming that the supporting struts can be less massive than an equivalent additional extent of flap, then a similar conclusion also extends to the intrinsic inertia. (Of course, it must be assumed that the additional hydrodynamic added inertia of a well-designed strut system can be made relatively small.) This fact has an important implication for the problem of obtaining higher tuned frequencies using a given limited (hydrostatic) spring constant, which, as noted previously, is one practical drawback of increasing flap draft. However, the question cannot be answered without looking at the effect of increasing pivot depth on the hydrostatic restoring moment at constant flap draft a .

For a flap of small waterplane area, the linearized hydrostatic spring constant arises solely from a surplus of buoyancy moment over weight moment, measured about the pivot point. For a full draft flap, where $p = a$, the buoyancy moment increases as a^3 , provided that the flap "thickness" is permitted to remain proportional to the draft. The weight moment is more difficult to assess in such general terms, but can hardly increase more slowly than a^2 . In

fact, this argument follows from the assumption that the center of flap weight remains at a constant fraction of flap draft, and that the weight itself varies only as the draft, which is surely a lower bound in view of required changes in scantlings and internal structure. However, under these assumptions, and depending on the amount of excess buoyancy moment available in a "baseline" configuration, an increase in flap draft will result in an increase in spring constant no less than order a^3 .

By contrast, for a low-pivoted arrangement, if the flap dimensions, buoyancy, weight, and centers remain constant, and if the struts are assumed to contribute negligibly to the excess buoyancy moment, then the effect of lowering the pivot can be shown to be only linear in p . Therefore, the actual relationship between spring constant and inertia is no more favorable than for increasing the flap draft, in terms of retaining the ability to tune to higher frequencies as the device depth is increased.

Of course, for similar device performance, there remains the issue of the relative costs of increasing the draft, versus the costs of the strut system required for a low-pivot arrangement. Depending on the details of the design, an advantage may exist for the strut system. However, structural problems may also arise if the struts can not be arranged to provide satisfactory bending and torsional rigidity, especially if the power takeoff attachment

is at the bottom of the struts. In addition, a low-pivoted arrangement may well increase viscous losses, due to the motion of the bottom edge of the flap and the drag of the struts themselves. In conclusion, it is difficult to prove that a low-pivoted device will offer any significant improvement over a bottom-pivoted flap, at least without a more detailed level of analysis than can be performed here.

For completeness, it should be mentioned that positioning the pivot above the bottom of the flap, for example, at the midpoint of the draft, or at the top of the flap, has a counterproductive effect. While the maximum absorption remains substantially unchanged, the corresponding motion amplitude increases, as shown in Fig. 43 for a typical frequency. Thus, a high-pivot arrangement appears to carry with it certain hydrodynamic drawbacks, although, as will be mentioned in a subsequent section, such a device would also have some desirable features as well.

Flap Dimensions and Nonresonant Tuning

In the preceding sections the effects of varying flap dimensions on maximum absorption and corresponding motion amplitude have been discussed in some detail. The results are consistent for all single-flap dimensions considered, draft, width, and pivot depth: provided that the flap dimensions remain small with respect to the wavelength, the maximum absorption varies only slightly, while the corres-

ponding motion amplitude decreases drastically as flap dimensions are increased.

It will be recalled that maximum absorption for a single-flap device requires resonant tuning, as shown by differentiation of Eq. 45. This tuning results in very simple expressions for the absorbed power and motion amplitude, Eqs. 49 and 48, respectively. If resonant tuning could always be obtained, then the problem of determining a suitable geometry for a particular wave would become merely a matter of selecting one or more flap dimensions sufficiently large to secure a reasonable motion amplitude in waves of the given frequency and amplitude. For the design of a practical ocean wave-absorbing system, however, this ideal situation can hardly exist.

There are two distinct reasons why it cannot be so simple. First, as mentioned above, the pursuit of smaller motions through large flap dimensions can limit the ability to obtain resonant tuning at higher frequencies, due to the unfavorable scaling relationship between inertia and hydrostatic restoring moment. Therefore, the ability to obtain resonance cannot be so blithely assumed, even if there is only a single frequency of interest. Second, in a random sea, basing the selection of flap dimensions on maximum absorption at any single frequency is false strategy. Just how false it is will be shown by examples in a subsequent section.

In either case, the question now at hand is this: what are the effects of flap dimensions on absorption and motion when resonant tuning does not exist? Leaving specific examples aside for the moment, the general answer to this question is contained in the form of Eq. 44. As demonstrated in the preceding sections, short or shallow flaps are characterized by light radiative damping, and consequently by very large amplitude motions at maximum absorption, given by Eq. 48. Being so lightly damped, the motion amplitudes of small devices are therefore more sensitive to tuning than more heavily damped flaps of larger dimensions, which produce virtually the same maximum absorption at a smaller motion amplitude. The effect of missing the resonant condition on the absorbed power can be shown directly from Eqs. 44 and 45. Writing a simpler version of Eq. 45:

$$P_{ABS} = \frac{1}{2} \omega^2 \frac{|F|^2}{T + D} d \quad (42)$$

where $T = (-\omega^2 M + C)^2$ and $D = \omega^2(d + B)^2$, then differentiating $|X|^2$ with respect to the independent non-negative quantity T , we obtain

$$\frac{\partial}{\partial T} P_{ABS} = - \frac{1}{2} \omega^2 d \frac{|F|^2}{(T + D)^2} \quad (43)$$

Evaluated at resonance, $T = 0$, this derivative is proportional to $-|F|^2/D^2$. For equal maximum absorptions, we know from Eq. 48 that $|F|^2/D$ must be constant. Therefore, the decrease in power due to mistuning must be large when D is

small, that is, for the small, lightly damped flap. Furthermore, from Eq. 47, it is apparent that the optimal external damping d^* (for non-resonant tuning) is always larger than the radiative damping B . Thus, since $|X|^2$ falls off more slowly for a large flap, and d^* is larger, the power absorption (Eq. 42) declines substantially more slowly from its maximum value when the flap is large. By contrast, a small flap becomes in effect "transparent" to energy when mistuned.

There is one hydrodynamic quantity that has received only small mention thus far because it has no effect on the maximum absorption when resonance is obtained, although it does determine how difficult it is to obtain resonant tuning. This is the added inertia, and particularly its behavior with respect to frequency. For a flap oscillating at the free surface, 2-D results, such as Kotik's (Ref. 22) the inertia increases initially with frequency, from its zero frequency value, and reaches a peak at some value of ka , typically about 0.9. Beyond this point it decreases over a certain range before finally going to its high-frequency asymptotic value.

In three-dimensional results, this behavior is modified somewhat, but the added mass still increases with frequency in the low-frequency range. Within this range, the effect of tuning too low is made worse at higher frequencies by the fact that the term $\omega^2 A(\omega)$ increases even more rapidly

than ω^2 itself. Thus, for a limited available spring constant, smaller than $\omega^2 A(\omega)$, the absorbed power will drop off very quickly with increasing frequency.

On the other hand, if the added inertia has already passed its peak somewhere in the frequency range of interest, then the further effect of a given undertuning on power absorption will obviously not be so severe, and the curve of P_{ABS} versus ω will not drop off so steeply. Since the peak added inertia tends to occur at a certain value of ka for flaps of a given width, (about 0.9 for infinitely wide flaps, and higher for short ones), it is clear that increased flap dimensions will move the device into the range of peak added inertia at a lower frequency. Therefore, increased dimensions will make the tuning itself less sensitive to frequency. When combined with the effect of increased damping, in making the absorption less sensitive to tuning, this means that larger flaps are inherently better adapted to broad power response in a spectrum, even though the maximum absorption may not be any better than for a smaller flap, and the increased dimensions may decrease the resonant frequency.

Moral: a relatively large flap is inherently less sensitive to mistuning than a small one. As will be shown in subsequent numerical examples, this difference in behavior can become extremely significant in practical cases. In typical random seas, where some degree of mistuning must

exist over much of the frequency content of the spectrum, the ability to absorb useful amounts of energy at non-resonant frequencies may become as much of an argument for increasing flap dimensions as the desire to avoid unduly large responses at the resonant frequency.

NONLINEARITY AND CONTROL REQUIREMENTS

Introduction

As shown in the previous section, both single and twin-flap systems with certain geometric characteristics can develop extremely large motion responses when tuned and damped for maximum power absorption at low frequencies. In fact, as can be shown by a simple consideration of the work done on the flap by an exciting force of given amplitude, large amplitude motions must accompany large values of the absorption cross-section for a given device size. In particular, for small flap widths or draft, extremely large flap responses are predicted by a linear model at frequencies where the radiative damping is relatively light and the exciting force is not small, with resonant tuning.

Obviously, these predictions of extremely large motion amplitudes are a result of the linear analysis, and cannot be expected to occur in actual physical models, for a variety of reasons. The most important of these reasons is that the roll exciting moment cannot be expected to act at nearly its linear magnitude when the flap inclination is at all large. Since the boundary condition is satisfied on the mean position of the flap, however, this large prediction of the moment is inevitable under the linear model.

Furthermore, for large amplitude motions of the device nonlinear damping, whether of viscous or higher-order wave-making origin, may become significant and thus limit the actual stroke. Then, too, nonlinear exciting forces (in large amplitude or breaking waves) may also be less than linear predictions, even when the flap remains at small angles of inclination. For example, Salter (Ref. 27) has found that the moments experienced by a device in breaking waves are significantly reduced from the linear predictions.

Apart from the consideration of those hydrodynamic forces that may be recognized at small amplitudes, the geometry of the device itself in relation to the wave may impose obvious limitations. For example, for a rolling flap-type device pivoted at or near the lower edge, an excursion of much more than 90 degrees is hardly permissible, even if the flap did not actually hit anything solid, such as the bottom. (In very long waves, it is possible to imagine a flap of small draft being inclined to about 90 degrees under a wave crest, at which point the flap would become virtually aligned with the flow, and no further inclining moment would be applied. Presumably, then, the flap would lie in about this attitude until the passage of the crest allowed it to right itself under hydrostatic moment, and then the flow in the trough would swing it back (assuming of course that the trough didn't leave the device almost out of the water).

In addition, the purely mechanical limitations of any practical power-absorbing device must be recognized. For example, high-mounted power takeoff arrangements imply certain fixed stroke limits, at which point the flap encounters a stop, with results that may range from a bounce (as off a system of nonlinear springs) to a catastrophe (as when a hydraulic piston simply hits the cylinder head). In either case, the result may not be what the designer intended. Similarly, for a low-mounted hydraulic spline pump, the flap may end up in the mud.

In any case, if the linear model yields predictions of the motion amplitude that cannot actually be obtained, regardless of the reason, then it also yields unrealistic predictions of the absorbed power. The questions, for practical purposes, are therefore as follows:

(1) What is it that limits the actual stroke of the device when the predicted linear response is very large?

(2) What is the effect of stroke limitation on the absorbed power?

To offer some answers to these questions, several alternatives will be examined in the following sections.

Stroke Limitation and Phase Control by External Forces

In the following argument, assume that the hydrodynamic forces acting on the flap (i.e., exciting forces, added mass, and damping) are those predicted by the linear numer-

ical procedure described above. For the moment, neglect the memory effect due to the free surface, and consider the system as the usual spring-mass-damper, in which, however, both the restoring force coefficient and the portion of the damping coefficient due to external (non-hydrodynamic) forces may be allowed to vary either with time or flap position, or both. Thus, the model consists of linear hydrodynamics combined with either linear or nonlinear mechanical forces.

The most obvious method of limiting the stroke of the device is by increasing the (linear) external damping coefficient until the motion amplitude decreases to a reasonable small value, small enough, that is, to believe that the linear model holds well enough to predict the power absorbed. While this approach, by definition, gives believable results for the motion amplitude and the absorbed power, it can be shown that it also results in a drastic reduction of power output versus the linear predicted output (which is presumably not believable) at "optimum" damping.

This can be seen most clearly for a single-flap device by considering the equations for the motion amplitude and the absorbed power:

$$|X| = \frac{|F|}{[(-\omega^2 M + C)^2 + \omega^2 (d + B)^2]^{1/2}} \quad (44)$$

$$P_{ABS} = \frac{1}{2} \omega^2 |X|^2 d \quad (45)$$

where F is the exciting force, M and C the mass and spring constant and d and B the power takeoff and radiative damping coefficients. Given the hydrodynamic coefficients, the restoring force and external damping coefficient for maximum power output at a given frequency can be derived by differentiation of Eq. 45 with respect to C and d , having substituted Eq. 44 for the magnitude $|X|$:

$$C^* = \omega^2 M \quad (46)$$

$$d^* = \left[\frac{(-\omega^2 M + C)^2}{\omega^2} + B^2 \right]^{1/2} \quad (47)$$

Note that if $C = C^*$, then $d^* = B$. The corresponding motion amplitude and power absorption are then:

$$|X| = \frac{|F|}{2\omega B} \quad (48)$$

$$P_{ABS} = \frac{1}{8} \frac{|F|^2}{B} \quad (49)$$

Thus, provided that the wave amplitude is small enough so that the resulting flap motion is "acceptable" in terms of linear assumptions, the power absorbed is proportional to the wave amplitude squared.

Now, however, suppose that the motion amplitude with tuning and damping for maximum power absorption exceeds some arbitrary limiting value, S . The required damping to obtain a motion amplitude equal to S is

$$d_S = \frac{1}{\omega} \left[\frac{|F|^2}{S^2} - (-\omega^2 M + C)^2 \right]^{1/2} - B \quad (50)$$

or, at resonant tuning,

$$d_S = \frac{1}{\omega} \frac{|F|}{S} - B \quad (51)$$

The corresponding power absorbed is then

$$P_{ABS}(S) = \frac{1}{2} \omega^2 S^2 d_S \quad (52)$$

or, at resonant tuning

$$P_{ABS}(S) = \frac{1}{2} \omega S |F| - \frac{1}{2} \omega^2 S^2 B \quad (53)$$

Thus, when a stroke limit is imposed by increased linear damping, the power absorption can no longer increase with the square of the wave amplitude; in fact, it increases only linearly with the wave amplitude.

As mentioned previously, flap-type devices are often limited in the maximum spring constant that can be obtained hydrostatically. This is the case for many realistic geometries at all but very low frequencies. It will be noted from Eq. (47), however, that as the maximum obtainable spring constant becomes further from resonance the required constrained optimum damping becomes larger, and therefore the motion amplitude at this constrained maximum absorption becomes smaller. It can be noted here that a reduction of the flap motion amplitude to a given value can be obtained by further deliberate "mistuning" of the spring, or by increased damping at the maximum available spring constant. However, the latter method gives a larger absorbed power.

In Fig. 44, the power absorption per meter wave amplitude, with RAO limited to 1 by overdamping, at optimum spring constant for each wavenumber, is shown for several flap widths. The effect of stroke limitation is apparent by comparison with Fig. 37.

For twin-flap devices, the springs and dampings for maximum power absorption cannot be found in simple form, due to the effects of coupling, so that the situation is not so obvious. Furthermore, as mentioned above, these "optimum" settings often include negative spring constants or dampings (Table III), which may not be admissible for practical reasons. Nevertheless, the general conclusion is still valid: the imposition of stroke limitation by increased external damping reduces the power absorbed roughly in proportion to the required excess damping. That is, if the dampings must be doubled from the "optimal" values to get down to the required stroke limit, then the corresponding absorbed power is approximately halved. Again, this concern must be tempered by the fact that the "optimal" values may not be obtainable in the first place, for other practical reasons, such as the desire to avoid negative springs or dampings, and therefore the loss of power is only on paper.

Regardless of whether optimal springing is practically obtainable, the issue raised by the drastic reduction of absorbed power with increased external damping is whether

or not alternative means exist by which the stroke can be limited with smaller losses. Several possibilities have been proposed, and these are discussed below.

Nonlinear Springs

A mechanical method of imposing a limited stroke is to allow the flap (or its power takeoff device) to encounter a stiff progressive spring as it approaches the desired limit. Thus, the damping coefficient can remain smaller for a given stroke limit. This in turn permits the flap to make its excursion from stop to stop in a shorter time than with heavier linear damping. Depending on the phase of this motion with respect to the exciting force (which is, by assumption, still harmonic) more work can be done by the exciting force per stroke, because the exciting force can remain near its peak value over a longer fraction of the limited stroke. However, the question of this phase relationship now becomes crucial.

Time-step simulations were conducted on a spring-mass-damper, with a nonlinear spring "bumper," subject to a harmonic exciting force. While these simulations were not exhaustive, the results showed that without some additional form of phase control (that is, some method of holding the flap at the limit of its stroke until the exciting force approaches its maximum value), the use of nonlinear springs as stroke limiters produces no advantage in power output over increased linear damping. Although it may seem too

obvious to mention, the desired quick throw from stop to stop cannot be achieved merely by keeping the damping light: the flap inertia (including added inertia) must be considered.

Apart from this failure to produce better results in terms of power absorption, there are several practical disadvantages. First, depending on the frequency and the stiffness of the nonlinear springing, the flap may bounce off each stop several times between each complete half-stroke, as shown for typical cases in Fig. 45. During portions of each of these bounces, since it is only the exciting force that decelerates and returns the flap to the stop, the exciting force is actually doing negative work on the flap. This implies that a great deal of motion, with consequent wear and frictional loss, is taking place without producing very much added absorption.

Second, if the applied damping is too light, at a certain frequency the nonlinear system can become unstable in spite of the stroke limit: bouncing from stop to stop, pushing deeper into the nonlinear spring on each cycle. Because of the steep nonlinearity of the spring at the stroke limits, however, a small increase in spring deflection corresponds to a large stored energy. The flap velocities can then become higher and higher until the system is obviously "blown" for practical purposes, as shown in Fig. 46.

Third, as a purely practical consideration, the nonlinear spring places extreme loads on supporting structure, which can be avoided by suitable use of higher dampings. The nonlinear restoring force coefficient must also be provided either by physical springs, or by some controlled application of hydraulic or pneumatic forces, which would presumably require power to actuate. Both of these alternatives represent additional cost. (With purely hydrostatic forces providing the springs for a rolling flap, the restoring moment can in fact be made nonlinear and progressive, but not easily. For example, a flap with outrigger floats that only encounter the free surface at a certain angle of inclination would have such a righting characteristic, but this hardly seems worthwhile. The plain buoyant flap also has a nonlinear righting moment, of course, but the effective spring becomes softer rather than stiffer at very large angles).

A possible alternative to prevent bouncing of the flap on nonlinear springs and provide positive phase control is to incorporate a system of controlled mechanical locking devices in addition to the springs. This arrangement would apply a brake immediately after the flap stops at the limit of its motion, within the nonlinear range of the spring. Because this brake would only engage when the flap is essentially motionless, the power losses in stopping the flap would be small. A practical problem arises in controlling

the time to release the brake. In regular waves, of course, this could be accomplished with a time delay, but such a simple approach would not be at all useful in random seas. Presumably, the control device would have to sense a dynamic variable, such as pressure or holding torque, in addition to flap position, releasing the flap either at maximum holding torque or at a predetermined value.

However, such a braking system and its controls would add a further complication and cost to a device that is already becoming rather complex. The power needed to actuate the brakes would, of course, have to be subtracted from the useful output of the device. Furthermore, the brakes would transmit both wave and compressed-spring loads to different parts of the supporting structure, and these components would then have to be stressed to carry these loads.

A more promising alternative for flap motion control is the use of a variable power-takeoff damping coefficient, which will be discussed in the next section.

Variable or Controlled Damping

As shown in the preceding sections, the power takeoff damping coefficient has a major influence on the flap response amplitude and the absorbed power as functions of wave frequency. For regular waves, of course, the damping coefficient can be set (as a constant) either to obtain a given motion amplitude, or to produce the maximum linear power absorption, depending on wave amplitude and device

limitations. By extension, in a random sea the setting of the damping coefficient for a particular wave spectrum in large part determines the response spectra of the flap motion and the power output, and thus, the root-mean-square motion, the expected extreme values of the motion, and the time-averaged power absorption.

For the purposes of simultaneous stroke limitation and maximum constrained power output, however, setting the damping coefficient as a constant is not necessarily the most effective strategy. Instead, the power takeoff damping may be varied during the course of the stroke, in response to real-time measurements: appropriate kinematic variables might include the sensing of flap position, velocity, and acceleration, as well as the output from separate wave probes.

The power-takeoff damping is a particularly suitable control for oscillating wave absorbers because it can be varied over a wide range, and quite rapidly, on time scales that are significantly shorter than the wave period. This is particularly true for positive-displacement hydraulic systems. There are a number of ways to exercise control of such a system: the fluid delivery rate from the pump to the high-pressure receiver can be controlled by valving the inlet to the receiver. Simultaneously, the flow rate and power output of the swash-plate hydraulic motor coupled to the alternator can be controlled by varying the swash-plate

angle and increasing the excitation of the alternator. The ability to vary both the load on the alternator and the torque and flow on the motor (by varying the piston stroke) may prove valuable in limiting extreme variation of alternator speed, which are detrimental to alternator efficiency. This ability can also be used to compensate for short-term variations in pump delivery rate, on the time scale of a few wave periods, or to adjust the power-takeoff system for longer-term changes in the ambient average wave power density due to changes in the seastate. Power and generator speed variations have been discussed in greater depth by Dawson (Ref. 28), Bishop and Rees (Ref. 29), and Glendennig (Ref. 30). Generator speed variations of a factor of two or more have been reported in simulations for typical random seas, using turbogenerators with an oscillating water column device. The only way to obtain better results with a positive-displacement hydraulic system would be to incorporate a high-pressure receiver, or to continuously vary both the stroke of the motor and the generator load.

A positive-displacement hydraulic system, however, can be used to lock the flap for purposes of phase control by simply throttling the outlet valve from the pump. It should be mentioned, though, that merely throttling the pump outlet alone does not increase the amount of useful power; the extra work is wasted in large viscous losses in the valve while it is partly open and, of course, once the

pump is completely closed off, no work is being done.

The same degree of control cannot be obtained in a practical way by varying the spring constant or inertia of the flap. Presumably, with flaps depending on hydrostatic restoring forces, variation of the stiffness or inertia could be achieved easily by ballasting or deballasting of floodable spaces. In this way, it would be possible to alter the tuning of the flap quite significantly within a matter of minutes or tens of minutes, depending on the amount of flooding or dewatering to be performed and the capacity of the ballast pump (or compressed air source) or water inlets, but it would hardly be practical to alter the tuning continuously over wave periods of 6 to 18 seconds.

A simple variable-damping scheme that might be proposed for stroke limitation is to vary the damping in response to measurements of flap position alone, increasing the damping as the flap approaches the desired limit. Unfortunately, this sensing strategy is a little too simple: it does not provide enough information to tell the control system that the flap has stopped and that the damping must be reduced to permit the flap to accelerate again for the return stroke. Thus, it must be concluded that a useful control system would have to measure and respond to at least one other kinematic variable in addition to flap position: that is, either velocity or acceleration, or both.

The instrumentation required for these kinematic measure-

ments is not necessarily elaborate or costly. For a rolling flap device with a low-mounted hydraulic power takeoff, such as the device proposed in a subsequent section, a potentiometer driven directly off the spline pump shaft could measure angular position, a rate gyro or pendulum-mounted induction coil could be arranged to give a velocity signal, and acceleration could be measured, if necessary, by an angular accelerometer. The damping coefficient itself could then be controlled continuously by varying the load on the generator and the stroke of the hydraulic motor, rather than by simply throttling the pump outlet

The detailed design of a control system or its associated program is beyond the scope of this work. However, a rough estimate of the possible improvement in power absorption in regular waves, versus overdamping to achieve the same stroke limit, can be made for single-flap systems on the basis of time simulations of a spring-mass-damper with a controlled starting phase and systematic variation of damping, subject to a harmonically varying exciting force.

In general, a controlled flap motion can provide some increase in absorbed power at limited stroke, versus the alternative of a higher (constant) damping. A clear distinction must be drawn, however, between the use of a control to obtain better performance subject to a given stroke limitation and the use of a control to increase the stroke (and power absorption) of a device which, for one reason or

another, cannot be tuned to resonance, and therefore has a small linear response. It is the latter problem that has been studied by Count and Jefferys (Ref. 4), and Falnes and Budal (Refs. 9 and 31), among others, demonstrating that extremely large improvements can be obtained in such cases. (Basically, the use of an optimal control force can recreate the motion amplitude that would be obtained from resonant tuning, however, even Count admits that the mechanical systems required to do so could be very complicated.)

In any case, the problem under discussion here is quite different: the stroke is limited, and cannot be increased. Instead, the control force is used to ensure that increased work is extracted from the exciting force as it acts over the limited stroke. As will be shown below, this increase results largely from phase control, that is, in allowing the exciting force to act through a given distance but at a greater average magnitude over a shorter time period, during which more net work can be done on the flap. Basically, with a controlled power takeoff, the flap is allowed to accelerate faster at the beginning of the stroke with the effective damping relatively light. It thus attains a higher midstroke velocity than with a constant damping for the same stroke limit, and it approaches the end of the stroke at a higher velocity. The damping is then increased, and the "excess" kinetic energy is taken out as useful work. As mentioned previously, however, the ability of the

system to respond with a faster throw is limited by its inertia and maximum obtainable spring constant, as well as by the damping coefficient. To achieve the fastest acceleration, the flap must be built light, but added inertia will dominate in any case.

Similar conclusions were reached by Falnes and Budal (Ref. 9) in connection with point absorbers, using the alternative application and release of brakes to control the phase of the motion, although in their case the damping itself is not varied while the flap is in motion. Thus, although the phase of the motion is controlled, the damping coefficient must be set high enough to provide the required stroke limitation; any "excess" kinetic energy at the stroke limit must be absorbed by the brake, resulting in a loss of power. In spite of this disadvantage, a braking system is undoubtedly mechanically simpler than one designed to provide full optimal control of the motion.

In irregular waves, a system permitting effective control is potentially very beneficial. For example, during an encounter with an unusually large wave, which could be sensed by a high acceleration, the control system could respond by increasing the damping coefficient to prevent the flap from responding with an overly large excursion. Conversely, during a smooth interval between large waves, the damping could be reduced to give better average power absorption at full excursion. The quantitative measure of

this advantage cannot be obtained simply from the wave spectrum and the response amplitude operators at various damping settings. Once variable or controlled damping is applied, the motion of the system is by definition no longer linear in wave amplitude: in fact, for a stroke limited system in which the limit is imposed by varying the damping coefficient, the motion response amplitude is supposed to remain constant even when the wave amplitude increases.

As mentioned above, the power absorption of a stroke-limited device at a given frequency does become linear in wave amplitude, in the sense that for any wave amplitude there is a particular constant value of the damping coefficient which limits the stroke to a given amplitude. However, even with this "linear" behavior of the absorbed power, it does not follow that an effective linear response amplitude operator for the absorbed power can be created from the results at each frequency, with a unique damping coefficient applied at each frequency. The required damping coefficient for a given stroke limit is, after all, a function of wave amplitude as well as frequency. Thus, the motion responses and power performance of a system with continuously variable damping in a random sea cannot be obtained by the usual linear-system spectral methods. Rather, it seems that a detailed investigation of this performance will have to depend on time-domain simulation

methods, and that the results will depend on the proposed damping-control strategy. This complicated task has not been undertaken in the present work, however, it will be a worthwhile field for further study.

Upper Bounds on Energy Absorption with Stroke-Limited Response and Phase Control

For a single-flap device that is constrained to a limited stroke, regardless of the precise manner in which the limitation is imposed, the work absorbed by the device over a cycle is bounded by the work done by the exciting force acting on the flap. The differential of work done by the exciting force on the flap in moving through a displacement dx is defined as $dW = F \cdot dx$, where F is the exciting force, which can by assumption be a function of time. The instantaneous power delivered by the exciting force is then defined as

$$P = \frac{dW}{dt} = F \cdot \frac{dx}{dt} \quad (54)$$

and the work done over a cycle is

$$W_C = 2 \int_0^{T/2} P dt = 2 \int_0^{T/2} F \cdot \frac{dx}{dt} dt \quad (55)$$

Now, suppose the flap executes a half-cycle by moving through a stroke of length $2S$, starting at $x = 0$, while being acted on by the force $F(t) = F_0 \sin \omega t$. No particular time history $x(t)$ is required in moving through this half-cycle. However, since the exciting force is by definition

collinear with the coordinate x , the dot product in the definition of work can be replaced by the algebraic product. The following inequalities hold if $F(t)$ is a sinusoidal function of time:

$$F(t) \leq F_0$$

$$W_C \leq 2F_0 \int_0^{T/2} \frac{dx}{dt} dt \quad (56)$$

$$W_C \leq 2 F_0 (2S) = 4 F_0 S$$

Thus, the work done by the exciting force in acting over a full stroke must be bounded by

$$W_C \leq 4 F_0 S \quad (57)$$

As stated before, the work absorbed cannot be greater than the work done by the exciting force: in fact, the work absorbed must be the work of the exciting force on the flap minus the work done by the flap against the radiative damping force. The expression given above is an upper bound on the work that can be absorbed per cycle with a fixed stroke limit, regardless of the details of the motion, and it can only be obtained in the limit of negligible radiative damping losses. The corresponding bound on average power is then obviously

$$P_{UB} = \frac{4 F_0 S}{T} = \frac{2\omega F_0 S}{\pi} \quad (58)$$

This upper bound can be compared with the earlier result (Eq. 52) for the power absorbed by a linear system

with a constant damping coefficient adjusted to give the same stroke limitation. Dividing Eq. 58 by Eq. 53, and neglecting the radiative loss term in Eq. 53, we obtain

$$\frac{P_{UB}}{P_{ABS}} = \frac{(2/\pi) \omega F_0 S}{(1/2) \omega F_0 S} \quad (59)$$

Thus, in the limit of small radiative loss (which implies either $B \rightarrow 0$ or $\omega \rightarrow 0$ or $S \rightarrow 0$), the maximum gain in absorbed power that can be realized by modification of the flap motion (whether by phase control or otherwise) can be seen to be a factor of $4/\pi$, corresponding to a 27 percent increase. For large radiative losses, of course, the issue of stroke limitation becomes less critical, since the stroke will be small even at optimal linear response.

To include the effects of radiative damping losses, however, assume that the radiative damping coefficient is a constant, B . The work done against the damping force in a half-cycle is then, in integral form,

$$W_{RAD} = \int_0^{T/2} B \left| \frac{dx}{dt} \right| \cdot \frac{dx}{dt} dt \quad (60)$$

It can be easily shown that this lost work will have a minimum value if the stroke is executed at a constant speed, which must be $4 S/T$, where T is the period of a cycle. Thus, the work lost per cycle against the radiative damping force is at least $16B S^2/T$, or an average power of $(4/\pi^2)\omega^2 S^2 B$. Thus, Eq. 59 can be rewritten to include the radiative losses as:

$$\frac{P_{UB}}{P_{ABS}} = \frac{(4/\pi) F_O - (8/\pi^2) \omega_{SB}}{F_O - \omega_{SB}} \quad (61)$$

One possibly confusing feature of Eq. 61 deserves a brief explanation here. Clearly, as the radiative losses go to zero, that is, as the quantities ω_{SB} becomes small, Eq. 61 reverts to the form of Eq. 59. However, if the quantity ω_{SB} is arbitrarily increased, then the ratio P_{UB}/P_{ABS} increases without limit, becoming infinite at $\omega_{SB} = F_O$. It must be noted, however, that the quantity ω_{SB} cannot increase arbitrarily for a device which is absorbing work. In particular, Eq. 44 shows that S and B must be related, since if the stroke limitation is to be an actual constraint, then $S < |X|$. Thus, substituting S for $|X|$ in Eq. 48:

$$\omega_{SB} < (1/2) F_O \quad (62)$$

for an optimally tuned and damped device. For a nonresonant tuning, the optimal external damping will be larger, as shown by Eq. 47, and thus S will have to be still smaller. Finally, it should be noted that the radiative loss in P_{UB} is minimized by allowing the device to act at constant speed, which is neither a linear nor a possible response with finite inertia.

The situation is somewhat more complicated for twin-flap devices, in that work can be done on one flap by the hydrodynamic coupling forces due to the motion of the other flap. However, an absolute upper bound for the work done on flap 1 can be written as

$$W = 4S\{F_1 + [(A_{12}\omega^2|X_2|)^2 + (B_{12}\omega|X_2|)^2]^{1/2}\} \quad (63)$$

where A_{12} and B_{12} are the coupling force coefficients. The assumption here is that the resultant coupling force on flap 1 due to the motion of flap 2 is in phase with the wave exciting force on flap 1. Similarly, an absolute upper bound can be written for flap 2. Adding these two upper bounds gives the result, with $|X_1| = |X_2| = S$:

$$W = 4S(F_1+F_2) + 8S(A_{12}^2\omega^4S^2 + B_{12}^2\omega^2S^2)^{1/2} \quad (64)$$

Clearly, though, this is a naive upper bound. From a consideration of the balance that must exist between the energy entering and leaving the twin-flap system, as indicated schematically in Fig. 47, it can be seen that the combined coupling forces cannot actually produce any work that does not ultimately originate from the work done by the exciting forces. Thus, a more realistic upper bound for the twin-flap system would exclude the coupling force terms from the equation above. Coupling forces can only act advantageously in recovering part of the work done by the exciting forces which would otherwise be lost as radiation. This is totally equivalent to saying that two independent flap motions, with suitable spring and damper settings, can be phased in such a way that the radiated waves partially cancel each other; there is no such thing as a free lunch, even in 3-D.

Nonlinear Hydrodynamic Forces Tending to Limit
Large Amplitude Motions

Even with linear external springs and dampings, the motions of an absorbing device at large amplitudes will be affected by nonlinearities in the hydrodynamic forces. Although the numerical results presented here are based on the assumption of linearity, some discussion of the probable effects of nonlinear hydrodynamics may be offered at this point. The magnitudes of these effects have not been calculated, however, the most important of these nonlinearities should tend to reduce the amplitude of the motion (and consequently, the power absorption).

Nonlinear Radiative Damping. From a linear analysis it is clear that the radiative damping coefficient is of primary importance in determining the amplitude of the response. Thus, if nonlinear radiative force increase the effective damping at large displacements, the motion of the flap must be less than linear analysis predicts.

The argument, as always, can be stated most simply in the case of a single flap. For a surface-piercing rolling flap pivoted near the bottom, the wave damping force may be expected to increase for larger angles of inclination, provided that the top of the flap does not submerge. This expected effect of nonlinear damping arises from two geometric effects:

(1) The immersed area of the flap increases with inclination so long as the flap remains surface-piercing, so that a given pressure will produce a greater total damping moment.

(2) A steeply inclined flap will experience increased local pressures due to the increased vertical component of the motion of the surface, analogous to slamming on a ship's bottom or forefoot.

In effect, then, the flap should produce a larger radiated wave than predicted by linear analysis when it oscillates through a large angle, provided that the top of the flap remains above waver.

However, once the flap becomes entirely submerged, as it would in very large amplitude motions, the above arguments will not remain valid. In such a case, the immersed area would obviously become a constant, while the increasing distance from the free surface will reduce the wave-making damping of the flap. Thus, for very large amplitude motions, the principal non-viscous hydrodynamic effect tending to limit the excursion of the flap must be found in the exciting force, rather than the radiative damping.

Based on the substantial agreement of earlier experimental work with linear predictions, Refs. 10 and 11, viscous damping of the flap is not believed to represent a significant contribution to the total damping, although these experiments were performed at relatively small ampli-

tudes. In any case, viscous damping forces, insofar as they are Reynolds-number dependent, should become less important at increased flap size. However, any viscous forces that would arise due to the high flap velocities experienced in large-amplitude motions will tend to further limit the amplitude of the flap motion. (It should be pointed out that the reduction of viscous losses was one of the original rationales for a bottom-pivoted flap configuration, versus a sway or high-pivoted rolling arrangement).

Nonlinear Exciting Force. At very large amplitudes, a low-pivoted rolling flap will end up well below the free surface at the extremes of its motion. Due to the decay of the incident wave potential with distance from the free surface the wave exciting forces will be drastically reduced, especially at shorter wavelengths.

The effect of submergence of the top of a vertical flap on linear exciting forces has been considered by Evans, Ref. 14, for the two-dimensional deep water case. It has been shown, for example, that a top submergence of as little as one percent of the flap draft can produce a marked reduction in the exciting force. Similar results for a 3-D case are shown in Fig. 48. It may be expected that the overtopping of a rolling flap due to its own submergence at large inclination would reduce the effective exciting force, and would be an important factor in limiting the amplitude of the response.

It is therefore surprising that, in deep water at a typical frequency, a moderate submergence of the top of the flap below the still water line also reduces the radiative damping in such a way that the maximum absorption is not substantially changed, as shown in Fig. 49. However, the corresponding motion actually increases, in spite of the reduction in exciting force, as shown in Fig. 50.

Similarly, in shallow water, with the bottom of the flap at the seabed, a submergence of the top of the flap below the still water line can only be accomplished by reducing the flap height. This further increases the resulting flap motion, while causing relatively little change in power absorption, as shown previously, in much the same way as a reduction in flap draft for a surface piercing flap. Thus, the effect of wave overtopping cannot be judged by a naive consideration of the linear problem, with the body boundary condition met on the mean position.

In shallow water, however, large motions of the rolling flap can be viewed as tending to align the flap with the wave-induced fluid velocity, which is essentially horizontal. Thus, the moment on the flap due to the incident wave potential must tend to zero as the inclination increases.

It should be mentioned here that a flap arranged to respond in pure sway, or in roll with a high pivot, would not submerge below the undisturbed free surface due to large excursions. However, this does not imply that no

nonlinear change in wave forces would occur. Depending on the flap freeboard, of course, a large wave crest will overtop the flap regardless of the choice of sway or roll arrangements. This overtopping in a crest should, at least intuitively, entail a "loss" of force on the flap, although the deficit certainly cannot be related to the linear exciting force in any straightforward way. Overtopping of the flap, whether due to extreme excursions carrying it below the free surface or to crest elevation, should at the very least produce nonlinear power losses in the form of local wave breaking as the water spills over the top, and in additional viscous dissipation in the fluid moving over the submerged upper edge of the flap. These "losses" must correspond to some reduction of the total force on the flap.

The leading effect of freeboard may be in the second-order forces. The second-order force on a 2-D surface-piercing flap in deep water has also been analyzed by Evans (Ref. 14). For a flap which is not overtopped (i.e., of arbitrarily large freeboard), the drift force is always positive, that is, in the direction of wave propagation. For a flap of limited freeboard, however, wave overtopping can produce, under certain conditions, a steady second-order force in the opposite direction from that of wave propagation, as shown for other body shapes by Ogilvie (Ref. 32) and Longuet-Higgins (Ref. 33), among others.

The steady force on a cylindrical body has also been measured experimentally by Salter (Ref. 27), and Maeda et al (Ref. 34). In general, the conclusion has been that the steady force on a typical wave absorber of the terminator type is small by comparison with the first-order oscillatory forces, in non-breaking waves. In any case, useful work cannot be absorbed from the steady force by an oscillating device of practical stroke.

However, in large waves, the steady drift force on the flap can become of practical importance in two other respects: (1) to determine the maximum total force to be withstood by the supporting structure or moorings; and (2) to determine the effective restoring force that must be supplied to keep the flap from migrating away from its mean position toward one of the stops.

One final consideration with respect to the force in large waves arises from the effect of natural wave breaking, which would occur particularly in a shoaling coastal site. Clearly, the assumptions of linear hydrodynamics are violated for breaking waves, so that the present hydrodynamic model cannot give any basis for expecting a decrease (or an increase) of the exciting force. However, Salter has found in the experimental work cited above that the exciting force on a floating cylinder in breaking waves is consistently less than linear theory predicts.

The expected reduction in wave-induced forces when flap

rolling inclinations are allowed to become large points out one method of operating in severe seastates without exceeding the rated output of the power takeoff machinery: the flap can be ballasted to obtain a "softer" restoring moment so that it will tend to incline more easily, or even to submerge (with a negative restoring moment). This will have the desired effect of reducing both the wave forces and power absorption, which would keep the power output within the rated capacity of the power takeoff system while also reducing the loads on the flap and its supporting structure. Obviously, ballasting also changes the natural frequency, so that it can be viewed as intentionally tuning the system below resonance with the incident waves.

It should be noted, however, that ballasting the flap until it lolls (giving two equilibrium positions on opposite sides of center) can only be accomplished if these equilibria correspond to inclined surface-piercing conditions: the flap must have enough freeboard to attain these equilibria at a given angle of inclination. As simple geometry will show, there is no stable equilibrium once the flap is fully submerged, other than upright (if the buoyancy moment is greater than the weight moment), or lying on the bottom (if vice versa). In addition, the effect of a slack liquid surface inside the ballast tank will further destabilize the flap (i.e., the weight moment will increase as the ballast shifts outward with increasing

angle).

The presence of two separate equilibrium positions will obviously make the flap motions highly nonlinear, even under linear wave and damping forces, and the resulting motions have not been studied in this work. Presumably, the flap would be able to oscillate between its two equilibrium positions, or about either one. In the former case, the flap could still experience large motions from one equilibrium position to the other, in spite of being so under-sprung. In the latter case, with the flap continuously submerged, the position of the flap would have to be maintained by forces besides simple hydrostatics. In either case, the resulting motion of the flap, and the corresponding power absorption, must be considered in greater detail than can be done at this point.

Nonlinear Coupling Forces. For twin-flap systems, nonlinear waves created by large oscillations of an individual flap must yield correspondingly nonlinear forces on the other flap. Presumably, both the magnitude and the phase of the coupling force would be affected.

The nature of the nonlinear interaction of the flaps has not been considered in the present work, even qualitatively. Therefore, it is impossible to state with assurance whether nonlinear coupling forces would tend to increase or decrease the motion amplitudes. Intuitively, it might be supposed that if nonlinear radiative wave effects

rolling inclinations are allowed to become large points out one method of operating in severe seastates without exceeding the rated output of the power takeoff machinery: the flap can be ballasted to obtain a "softer" restoring moment so that it will tend to incline more easily, or even to submerge (with a negative restoring moment). This will have the desired effect of reducing both the wave forces and power absorption, which would keep the power output within the rated capacity of the power takeoff system while also reducing the loads on the flap and its supporting structure. Obviously, ballasting also changes the natural frequency, so that it can be viewed as intentionally tuning the system below resonance with the incident waves.

It should be noted, however, that ballasting the flap until it lolls (giving two equilibrium positions on opposite sides of center) can only be accomplished if these equilibria correspond to inclined surface-piercing conditions: the flap must have enough freeboard to attain these equilibria at a given angle of inclination. As simple geometry will show, there is no stable equilibrium once the flap is fully submerged, other than upright (if the buoyancy moment is greater than the weight moment), or lying on the bottom (if vice versa). In addition, the effect of a slack liquid surface inside the ballast tank will further destabilize the flap (i.e., the weight moment will increase as the ballast shifts outward with increasing

angle).

The presence of two separate equilibrium positions will obviously make the flap motions highly nonlinear, even under linear wave and damping forces, and the resulting motions have not been studied in this work. Presumably, the flap would be able to oscillate between its two equilibrium positions, or about either one. In the former case, the flap could still experience large motions from one equilibrium position to the other, in spite of being so under-sprung. In the latter case, with the flap continuously submerged, the position of the flap would have to be maintained by forces besides simple hydrostatics. In either case, the resulting motion of the flap, and the corresponding power absorption, must be considered in greater detail than can be done at this point.

Nonlinear Coupling Forces. For twin-flap systems, nonlinear waves created by large oscillations of an individual flap must yield correspondingly nonlinear forces on the other flap. Presumably, both the magnitude and the phase of the coupling force would be affected.

The nature of the nonlinear interaction of the flaps has not been considered in the present work, even qualitatively. Therefore, it is impossible to state with assurance whether nonlinear coupling forces would tend to increase or decrease the motion amplitudes. Intuitively, it might be supposed that if nonlinear radiative wave effects

tended to increase the amplitude of the wave radiated by a single flap oscillating through a large amplitude (that is, increased effective radiative damping), then the coupling force on the other flap would also be increased. However, as mentioned above, for very large amplitudes the effective damping might be decreased by submergence of the flap with a consequent reduction in the radiated wave. The over-all influence on the interaction of the flaps must therefore be quite complicated.

Suggested Time-Domain Approaches to Motion Prediction

A quantitative approach to the nonlinear behavior of the flap-type absorber could involve several levels of sophistication. At the outset, it would be desirable to use the results of the present linear hydrodynamic model (namely, the added mass damping, coupling forces, and exciting forces) to solve convolution-integral equations of motion in the time domain, following the procedure outlined by Takagi et al (Ref. 35), rather than the usual linear differential equations of motion with constant coefficients given in Eq. 11, that is, a frequency-domain solution. This would also allow the direct modelling of nonlinear springs, and other nonlinear control forces.

The refinement offered by the convolution-integral method is the inclusion of the "memory effect" due to the free surface waves in the time-domain equation of motion. The convolution-integral equation of motion is given in

Ref. 30 for a single degree of freedom as follows:

$$[M+A(\infty)]\ddot{x}(t) + D[\dot{x}(t)] + R[x(t)] + \int_0^t K(t-\tau)\dot{x}(\tau)d\tau = F(t) \quad (65)$$

where M is the intrinsic inertia of the body, $A(\infty)$ is the added inertia at infinite frequency, $D[x(t)]$ is the external damping force, which in the simple case of linear external damping can be written as a constant damping coefficient times the velocity, $R[x(t)]$ is the restoring force, $F(t)$ is the exciting force, and $K(t)$ is the so-called memory-effect function, given by

$$K(t) = \frac{2}{\pi} \int_0^{\infty} \cos \omega t B(\omega) d\omega \quad (66)$$

where $B(\omega)$ is the frequency-dependent radiative damping coefficient.

The high-frequency added inertias, of course, cannot be efficiently calculated numerically using the quadrilateral scheme developed for use at lower frequencies: the assumption of quadrilaterals small with respect to wavelength cannot be maintained. However, it would be assumed that in the limit of high frequency the added inertia of the flap could be calculated using only the essential singularity terms of the normal velocity. The restoring force can be an arbitrary function of x . The exciting force for a regular wave is considered as a sinusoidally varying function of time, with a magnitude given by the linear exciting force at the particular wave

frequency.

For the purposes of computation, the problem that arises is the calculation of the memory function $K(t)$. This involves a cosine-weighted integral of the damping coefficient over the entire frequency domain. Since the 3-D damping coefficient must be calculated (for other than high frequencies where a 2-D result could be used as an approximation) using the numerical procedure developed here, which is time-consuming and expensive, the generation of the memory function is presently considered to be too inefficient to be useful.

Even if this were done, however, the method would still be limited by the assumption that the exciting force could be adequately modelled neglecting the changes due to large amplitude excursions. The wave-induced forces on the flap at various angles of inclination could perhaps be estimated, and the time-dependent exciting force term would then have to be written as $F[t, x(t)]$. No solution or time-simulation of this equation has been attempted in this work.

Obviously, for the twin-body problem imposed by a twin-flap absorber, the convolution-integral equation of motion would have to be replaced by two coupled time-domain equations of similar form. In each of these equations two memory effect functions would have to be calculated: one for the self-induced memory effect, and another for the memory

effect due to the motion of the other flap. This computational requirement might be reduced somewhat by symmetry arguments, as was done for the linear differential equations used here. Nevertheless, the computational problem would be an even more difficult one than in the case of a single degree of freedom.

A sophisticated time-stepping numerical approach to nonlinear forces and motion predictions has been developed recently by Newman (Ref. 36). This method is also extremely time-consuming in computation; it requires the computational resources of extremely fast machines, such as the CRAY-1. Therefore, no application of the method has yet been attempted for the present problem.

ABSORPTION CHARACTERISTICS IN RANDOM SEAS

Up to this point, we have been concerned primarily with the determination of the hydrodynamic coefficients, absorption, and motion responses of flap-type absorbers in waves of a given frequency. In addition, because practical design considerations may impose limitations on the motion amplitude that can be accepted, the selection of flap geometry has also been shown to be related to a particular wave amplitude at the given frequency. Finally the size of the absorbing device was found to have an important influence on the absorption characteristics of systems under non-resonant tuning.

In the ocean, of course, wave energy exists, in general, not in the form of regular waves of a single frequency and uniform amplitude, but in the form of a spectrum, with energy content spread over a range of frequencies and, in some cases, incident from a range of directions as well. Since the ultimate product of a practical wave-absorbing system is supposed to be useful energy, it is the time-averaged power output obtained in an actual wave environment that is of economic significance. Therefore, the time-averaged absorption of a device in response to a random sea is a real economic quantity, while the maximum ab-

sorption at some particular frequency is only an intermediate result. Similarly, the loads and motions of the device in an actual seaway are random processes, and the design of structure and machinery are properly based on probabilistic rather than deterministic grounds.

By extension, even the characteristics of a device in a single sea spectrum are not sufficient to describe the overall economics of the situation. Once the device has been constructed and installed in a given location, the energy produced over the long term is given by its responses in a set of spectra that describes the wave environment of the site. Thus, the energy delivered by a system during its entire life, representing in effect the expected return on an investment, can only be determined by the weighted average of its performance in the various spectra characterizing the location statistically over the long term. Similarly, the rational design of supporting structures and mechanical components, insofar as these are related to extreme values of random processes, may also require long-term analysis.

These two facets of the problem, the spectrum and the family of spectra, are related in the sense that both are probabilistic phenomena, and that both define the availability of incident wave energy and its distribution over the frequency domain. The distinction between the two concepts, however, is that the individual sea spectrum, in principle, describes an actual wave environment that can be

observed over a relatively short period of time, say a few hundred wave encounters, and that might be expected to persist, sensibly constant in a statistical sense, for a period ranging from the order of an hour (for rapidly building or decaying seas) to several hours or days.

By contrast, a family of spectra describing a given location does not correspond to a short-term, observable state of the sea, but rather gives a probability distribution of such states. The family, then, can only be "observed" statistically over a relatively long period of time, such as the month of November, or the winter season, or the entire year (or better still, for statistical purposes, over an ensemble of Novembers, or winters, or years). By hypothesis, the family may be viewed as persisting, statistically stationary (within the named calendar intervals for which it is derived, e.g., for all "Novembers," or all "winters," or all "entire years), for a very long period, say a lifetime; for design purposes, forever.

This difference in time scale between the wave period, the typical duration of an individual seastate, and the assumed consistency of the distribution of seastates within a family of spectra has an important implication for the design of various components of a wave energy-absorbing system. It permits, in many cases, the distinction of design features that are related to variations of wave forces over a short time from those that are related to a particular spectral environment, or to a family of spectra.

For example, the large variations of instantaneous power (that is, the product of a varying speed and force) over a single wave cycle may be crucial to the design of those power takeoff components that are subjected to "unsmoothed" input. These components, in general, include the primary conversion device, such as a pump or turbine; the mechanical linkages between the primary device and the flap itself, such as shafting, clutches, or other couplings; and short-term energy storage arrangements, such as a flywheel or a high-pressure receiver with its associated piping and valves. In addition, any subsystems that are intended to provide actual control of the flap motion must be able to respond within a fraction of a wave period. Since such a control may require placing an external force on the flap other than pure "resistive" damping, the peak power required by the control system, and therefore its size and cost, will depend on the detailed motion of the flap over a cycle.

By contrast, certain design problems may be more properly related to the individual wave spectrum. For example, some components of the systems may only be subjected to a "smoothed" or time-averaged input. Depending on the details of the design, secondary conversion devices (such as hydraulic motors, turbines, or electrical generators) may be partly or entirely isolated from cyclic or "wave-group" variations of the flap response, as by the use of an intermediate energy-storage device. The required capacity of

such a device would moreover be related to the characteristics of the spectrum. In addition, some of the dynamic coefficients of the device may be varied in a practical way, but only relatively slowly, in response to changes in the wave environment observed in time averages over many wave encounters, that is, in response to a changed seastate. Thus, for example, the flap inertia and spring constant may be altered, by flooding or dewatering of ballast spaces in the flap, in order to obtain (or in some cases, to avoid) resonant tuning at the spectral peak frequency, as the seastate changes over the course of hours. Similarly, the effective damping of the power takeoff can be adjusted as necessary (in systems where it is not continuously controlled) to obtain a desired level of motion response, or a desired power output (within limits) in a given seastate.

Finally, of course, there are those parameters of the system which must be considered fixed at design or installation and which, through their effects on system costs and long-term energy delivered, determine the system's economic merit. Among these parameters are the overall dimensions and geometry of the flaps, the precise location and direction of the device, and the maximum rating of the power generating machinery. From the standpoint of power production, design decisions regarding these fixed parameters should only be based on a consideration of the entire family of spectra describing a particular site, even though it

may turn out that some individual members of the spectral family are more important than others in driving the decision-making process. In addition, those structural and mechanical components which must be designed according to extreme values may require a probabilistic analysis of many of the seastates within the family, rather than of one particular spectrum, even the nominally most severe one. (The need for a long-term analysis of extreme loads may be more stringent for a wave-absorbing system than for a conventional ship or offshore platform. Unlike them, an absorbing system, with a power output limited by the rating of its generating system, can be operated in severe seastates in such a way that absorbed power and loads are reduced, while the output power remains at rating. Thus, the loads on the system may be maximum for several seastates, and not just for the "extreme" seastate.) Needless to say, these fundamental design decisions are also strongly related to first costs and risks of damage.

Although the economic merit of the system depends on a long-term analysis, the solution of the long-term problem must begin with the assessment of the performance of flap-type absorbers in each individual spectrum. Accordingly, in the following section the absorption characteristics and motion responses of flap-type devices in random seas will be investigated, using linear system theory and the results obtained from the preceding linear hydrodynamic model. In the process, it will hopefully become apparent that lessons

learned in obtaining desirable device characteristics at a particular "target" frequency will not be entirely lost in dealing with a spectrum. Finally, some general conclusions regarding performance in a family of spectra will be drawn.

Average Absorbed Power in a Unidirectional Random Sea

It is convenient to begin the analysis of device performance in random seas by applying the hydrodynamic results of preceding sections to a simple non-directional spectrum. For the present, at least, it is also reasonable to assume normal wave encounter (the effects of oblique encounter, and directional spreading of spectra, will be considered subsequently).

Consider an absorber, single or twin-flap, of given geometry (that is, draft, width, pivot depth and, for a twin flap device, separation). For the moment it is not necessary to describe how these elements of the design (the geometry vector \underline{G} in Eq. 4) have been chosen; it suffices merely to have some particular geometry in mind. Further, assume a water depth h .

Next, consider a non-directional spectral density $S^+(\omega)$. Using the numerical methods described in preceding sections, the required hydrodynamic coefficients (namely, the added mass, radiative damping coefficient, exciting force, and coupling coefficients, if applicable) can be computed at a number of frequencies, spanning the energetic part of the spectrum. In order to calculate the absorption

and motion responses at each frequency, however, we must also assume values for the intrinsic inertias and spring constants of the flaps (the elements of the tuning vector \underline{T} in Eq. 4), and the external damping coefficients representing the power takeoffs (the damping vector \underline{D} in Eq. 4). With all these coefficients known (and single-frequency results may suggest some methods for choosing values, which will be described shortly) the motion amplitudes and power absorption can be calculated directly from Eqs. 12 and 13. Let the power absorption at a particular frequency be denoted by P_{ABS} .

The power density per unit wavefront in a sinusoidal wave can be written (repeating Eq. 2) as

$$Q = \frac{1}{4} \rho g^2 \frac{\zeta_A^2}{\omega} \tanh kh \left(1 + \frac{2kh}{\sinh 2kh} \right) \quad (67)$$

where the wavenumber k is implicitly a function of ω , namely, the solution of $k \tanh kh = \omega^2/g$. Then, the absorption cross-section can be given at the particular frequency as

$$\sigma(\omega) = P_{ABS}/Q \quad (68)$$

Now, the average absorbed power can be obtained by integrating the product of absorption cross-section and spectral power density (that is, the power density, per unit wavefront, per unit frequency), as follows:

$$\overline{P_{ABS}} = \frac{1}{4} \rho g^2 \int_0^{\infty} \sigma(\omega) \frac{S^+(\omega)}{\omega} \tanh kh \left(1 + \frac{2kh}{\sinh 2kh} \right) d\omega \quad (69)$$

This expression, however, still contains the awkward

implicit function $k(\omega)$, and the hyperbolic functions correcting the incident power density, for finite water depth. There is a more convenient computational method by which we can circumvent the need to calculate the power density, and the cross-section, according to the following logic.

The numerical method used in calculating the hydrodynamic coefficients uses the finite-depth form of the incident wave potential, given above, and therefore must contain the correct (linear) finite-depth incident power density. Thus, if a power absorption is based on these hydrodynamic results, it must correspond to the finite-depth situation. Now, if the power absorption is calculated for a wave of a given frequency and amplitude, the power absorption per unit wave amplitude squared can be defined. We will call this quantity the "specific absorption, and denote it by P_{ABS}' . This definition follows directly from the form of Eqs. 14 and 15, since the exciting force magnitudes are, by assumption, linear in ζ_A , while the exciting force phases, as well as the other hydrodynamic coefficients, are independent of ζ_A . It is most convenient to calculate P_{ABS} for a wave of unit amplitude so that numerically $P_{ABS}' = P_{ABS}$, although of course, the two quantities do not have the same units.

Since the power density Q in a sinusoidal wave of a given frequency is proportional to ζ_A^2 , the average power absorption in a spectrum can be rewritten directly in terms of the specific absorption, instead of dividing by a

sinusoidal-wave power density only to multiply by a spectral power density. Thus, we can calculate the average power absorption as

$$\overline{P_{ABS}} = \int_0^{\infty} P_{ABS}'(\omega) S^+(\omega) d\omega \quad (70)$$

Similarly, if the motion amplitude of the flap is denoted by X (or, for a twin-flap, by X_1 and X_2), and the corresponding amplitude per unit incident wave by X' (or X_1' and X_2'), then the spectrum of the response can be written as usual:

$$S_X^+(\omega) = [X'(\omega)]^2 S^+(\omega) \quad (71)$$

There will in fact be two different response spectra for X_1 and X_2 for a twin flap. It should also be emphasized that for a pivoted flap the response X is an angle, since the hydrodynamic coefficients are given as angular quantities: added moment of inertia, exciting torque, damping torque coefficient, etc. Thus, the quantity X' is not dimensionless, but will have units $[L^{-1}]$.

In any case, with the spectrum of the motion response, the root-mean-square, significant, or short-term extreme values of the response can be calculated for the particular seastate. Both the responses and the average power absorption, however, are then applicable only to the particular selection of design variables (\underline{G} , \underline{T} , \underline{D}). Thus, in order to analyze the performance of a particular design in a random sea, we must construct two functions of frequency, namely, the specific absorption, $P_{ABS}'(\omega; \underline{G}, \underline{T}, \underline{D})$ and the res-

ponse amplitude operator $X'(\omega, \underline{G}, \underline{T}, \underline{D})$.

It might be supposed, at this point, that the next task would be to have a look at the behavior of these absorption and response amplitude curves for a typical situation that might confront the designer. We might, for example, choose a set of possible device geometries (\underline{G}), a set of obtainable tunings (\underline{T}), and arbitrary dampings (\underline{D}), and construct the required curves for each resulting combination ($\underline{G}, \underline{T}, \underline{D}$). We should then, hopefully, be in a position to say something about the general effects of design decisions on the forms of $P_{ABS}'(\omega)$ and $X'(\omega)$, and to reach an intelligent method for choosing design parameters to "suit" a particular site and seastate. However, there are two good reasons to avoid this kind of extensive search for some "general" behavior. First, we have not yet defined what a "typical" design situation is. Apart from seastate considerations, the designer is also faced by practical constraints: maximum flap dimensions, limitations on hydrostatic restoring forces and intrinsic inertias, finite power-takeoff capabilities, etc. None of these factors has yet been given formal recognition, and therefore it would be premature to rush off blindly into ($\underline{G}, \underline{T}, \underline{D}$) space. Second, we already know something about the behavior of flap-type absorbers (especially single-flap absorbers) at individual frequencies, and we should allow this information to guide us in our exploration of ($\underline{G}, \underline{T}, \underline{D}$) space. In the process, some methods of design may become clear.

Before giving some examples, it may be worthwhile to catalog the general insights that we do have.

(1) For flaps that remain short with respect to wavelength, flap dimensions (G) have only modest influence on the maximum absorption obtainable with optimal tuning and damping.

(2) On the other hand, flap dimensions have a marked effect on the motion amplitude at maximum absorption. Larger flaps, whether enlarged in draft or width, reduce the required motion at maximum absorption.

(3) Flap dimensions have an important secondary effect in determining intrinsic inertia and hydrostatic restoring moment (spring constant). In general, a larger flap, particularly one of deeper draft, loses the ability to tune to higher frequency, unless the designer can invoke spring constants beyond what hydrostatics can provide.

(4) To mitigate this detuning effect, larger flaps are inherently less sensitive to mistuning than smaller flaps, simply because they are not so extremely lightly damped.

(5) The ability to tune for resonance at low frequency is only limited by second-order effects. A thin flap (or a box-like flap ballasted with water) can be given an arbitrarily small buoyant restoring moment. However, if the flap is very lightly sprung, any steady force (such as second-order drift or a current) may eventually push the flap to its limit.

(6) Finally, we can add one pearl of economic wisdom, which is so obvious that it will be submitted without proof: a large flap dimension costs more than a small one. (The details of the relative cost of increasing flap draft versus width or pivot depth are, of course, part of the designer's baggage at the economic end, so that there should be a rational tradeoff between dimensions, as in ship design. Nevertheless, this fact should not be allowed to obscure the obvious.) Thus, if a designer finds that one can absorb virtually the same power with a small and a large flap, and if both give acceptable motions in a particular wave environment, then the smaller flap should be preferred.

These generalizations, although strictly based on results for single-frequency cases (and simple economics), do permit some extensions to the case of a device in a random sea. However, one important distinction should be discussed immediately. In designing for a regular wave, maximum absorption is obtained for a given geometry \underline{G} by adopting values of tuning \underline{T} and damping \underline{D} that are functions only of the geometry and the frequency. In the case of a single-flap device, the maximum-absorption values of tuning and damping are extremely simple. For an optimal tuning at frequency ω_0 , we need to satisfy $C = \omega_0^2[M + A(\omega_0)]$, where C is the spring constant, M the intrinsic inertia, and $A(\omega_0)$ the added inertia at ω_0 . (We see at once that $A(\omega_0)$ depends on the geometry \underline{G} , as does minimum M , while maximum

C is also fixed by geometry if the design depends on hydrostatics. Thus, there is a practical question of whether the optimal tuning can be obtained for a given \underline{G} and ω_0 , but it certainly exists.) Now, at any tuning, whether optimal or constrained, a corresponding value of \underline{D} can be calculated from Eq. 47, giving maximum absorption at ω_0 , subject to \underline{G} and \underline{T} . That is, there exists a clearly defined optimum damping $D_0 = D_0(\omega_0; \underline{G}, \underline{T})$. Stroke limitation, if required for a particular wave amplitude, entails either a higher than optimal damping (and loss of power) at the original geometry, or a larger device (and presumably increased cost, at essentially constant power).

Thus, in a specified regular wave (ω_0, ζ_A), the designer can be assured of maximum absorption at any given geometry by following two firm rules:

- (1) Tune as close to resonance at ω_0 as practical limitations (primarily spring constant) will permit.
- (2) Damp optimally for that tuning, provided the stroke limit is not exceeded by doing so. If it is, then overdamp minimally, applying just enough additional damping to secure the stroke limit in wave amplitude ζ_A .

Inspection of Eqs. 44 and 45 will be sufficient to prove that less absorption is lost by overdamping than by deliberate mistuning in an attempt to obtain reduced motion amplitude. (However, when there is a reason to reduce absorption as well as motion, as in the case of a conversion

system that would exceed its rated power in a wave of large amplitude, then deliberate mistuning may well be preferable to overdamping, since absorption, motions, and wave loads can be reduced at the same time. The designer should not forget this: a flap that is overdamped "reflects," while one that is undertuned becomes "more transparent.")

This discussion of tuning and damping has been predicated on a regular wave (ω_0, ζ_A). By extension, a similar approach could be argued for a seastate in which the energetic component tends to resemble a regular wave, for example, a spectrum containing a great deal of its power density in the form of narrow-banded swell. However, this is a special case, a specially "easy" one for design, with the power density "gift-wrapped" for absorption. In general, a wave spectrum may contain most or all of its energy in wind-driven seas rather than in nearly monochromatic swell. In this case the power density, basically $S^+(\omega)/\omega$, is distributed over a relatively broad range of frequencies. Faced with such a spectrum, how shall we choose values of tuning and damping for a device of a given geometry? Is there a simple method, analogous to the "rules" for a single-frequency case, by which we can find values of the tuning and damping that give maximum average absorption for a given spectrum and geometry? That is the first issue, and a second may be appended to it: in a regular wave, we were prepared, at least in principle, to define an arbi-

trary (or practical) stroke limit, and then overdamp, if necessary, to obtain it in a wave of given amplitude ζ_A . Since the motion response is now a random process, how shall we even define what constitutes "too much" motion, and what shall we do to reduce the motion if necessary? Finally, and this is a matter not yet settled even for a regular wave, if we have a variety of geometries to choose from, each one with a corresponding tuning and damping which gives maximum absorption subject to all constraints (i.e., achievable tuning and acceptable motions in a particular spectrum), on what grounds shall we pick the "best" device for the spectrum?

Let us start with the first two problems, which are at least posed in strictly physical terms (absorbed power and motion response as functions of T and D) rather than intertwining physics, design details, and economics. The cost implications of tuning and damping, or rather, the design elements needed to obtain certain values of the spring constant and external damping coefficient, will be discussed in some detail in the appendix: prototype wave absorbing systems. For the moment, let us concern ourselves only with the effects of tuning and damping on absorption and motion in a given seastate, for a given device geometry.

Formally, the unconstrained values T₀ and D₀ giving maximum average absorption in a particular spectrum $S^+(\omega)$, given the geometry G, can be written as follows:

$$\underline{T} = \underline{T}_0 (S^+; \underline{G})$$

$$\underline{D} = \underline{D}_0 (S^+; \underline{G})$$

if

$$\overline{P_{ABS}} = \int_0^{\infty} S^+(\omega) P_{ABS}'(\omega; \underline{G}, \underline{T}, \underline{D}) d\omega \quad (72)$$

is maximum. That is,

$$\int_0^{\infty} S^+(\omega) \frac{\partial}{\partial \underline{T}} P_{ABS}'(\omega; \underline{G}, \underline{T}, \underline{D}) d\omega = 0$$

and

$$\int_0^{\infty} S^+(\omega) \frac{\partial}{\partial \underline{D}} P_{ABS}'(\omega; \underline{G}, \underline{T}, \underline{D}) d\omega = 0 \quad (73)$$

(Note that these two relations also apply at P_{ABS}' a minimum, so that some further checking of the function $\overline{P_{ABS}}$ will be needed to discriminate a maximum. Note also that in these equations the specific absorption P_{ABS}' is considered for the purposes of differentiation as a function of the independent variables \underline{T} and \underline{D} , at each value of ω , although the integration must be performed with respect to ω .)

Unfortunately, solutions of these integro-differential equations, Eqs. 73, are not available in closed form. Therefore, to "solve" for the tuning \underline{T}_0 and damping \underline{D}_0 , we must search iteratively.

Alternatively, in the interest of a method for making initial design decisions, or for choosing an initial point for the search, we can adopt an heuristic approach based

directly on single-frequency results. As a starting point, we know that we can obtain maximum specific absorption at a particular frequency ω_0 (for a single-flap device) by adopting the tuning $C = \omega_0^2 M(\omega_0)$, and the external damping $d = B(\omega_0)$, where M is the total inertia (intrinsic plus hydrodynamic at ω_0) and B is the radiative damping coefficient.

Suppose we begin by tuning and damping for maximum P_{ABS} at some "target" frequency, which we will have to define more or less intuitively. To the extent that the spectral density (or power) is concentrated around this frequency, the tuning and damping may then be regarded as near-optimal for the spectrum. Now, however, in an actual sea spectrum, some of the density "slips away" into both higher and lower frequencies. There are two immediate concerns. First, is the idea of selecting a "target" frequency for the spectrum valid, at least to the extent of serving as a starting point? Second, if the concept is worthwhile, what should the target frequency be, given the spectrum?

The validity of the "target-frequency" concept must be accepted as "strong intuition": for most single-peaked spectral forms, a large proportion of the total power content is concentrated within a relatively narrow band of frequencies. (The fact that the power density is proportional to $S^+(\omega)/\omega$ makes the distribution of power "sharper" and narrower than the variance spectrum itself.) If there are

two spectral peaks, usually formed by swell and wind-driven sea components, this argument of course is not very convincing. However, for reasons that will become clear, in cases involving widely separated double peaks, it will usually be necessary to choose one or the other of the components to go after, and fortunately it will usually be possible to choose which one it should be. In any case, it is logical to assume that if a design is to get much absorption out of a spectrum, then it must at least be tuned to give a large cross-section across the range of frequencies that contain most of the energy, if such a range can be found.

Now, what simple measures of the spectrum are available to help point out the "target" frequency range? Consider the following three measures:

(1) The power-peak frequency ω_{pmax} , defined where $S^+(\omega)/\omega$ reaches a maximum.

(2) The power-averaged frequency (usually called energy-averaged), defined as

$$\begin{aligned} \omega_{pavg} &= M_0/M_{-1} \\ &= \int_0^{\infty} S^+(\omega) d\omega / \int_0^{\infty} [S^+(\omega)/\omega] d\omega \end{aligned} \quad (74)$$

(3) The peak frequency of the variance spectrum itself, where $S^+(\omega)$ is a maximum.

Each of these frequencies has something to say about the spectrum, and a case can be made for using each as a first guess for a target frequency. None of them is over-

whelmingly right: besides, the actual "optimal" tuning and damping (say, for maximum $\overline{P_{ABS}}$) does not depend solely on the spectrum in any case, it depends as well on the form of the curve of $P_{ABS}'(\omega)$ over the range of frequencies near the target. Therefore, it is not possible to state unequivocally which of the three measures constitutes a "best" first estimate for the target frequency.

This is serious, because in certain cases the differences between these frequencies can be rather large (for example, in the usual one-parameter spectrum, such as the Pierson-Moscowitz, the power-averaged frequency can be shown to be about 17 percent higher than the variance-peak, and about 22 percent higher than the power-peak). However, if we can't choose a target frequency on some rational basis, then we will have to make our first estimate of \underline{T} and \underline{D} completely blind except for any constraints that we may already have determined. Anything is better than this, so in a sense, it doesn't matter very much which measure of target frequency is chosen.

However we can do a little better than this. Consider the general form of the absorption curve $P_{ABS}'(\omega; \underline{G}, \underline{T}, \underline{D})$, where for simplicity we will let \underline{G} be held constant, establishing particular hydrodynamic coefficients (functions of frequency, of course): the exciting force $F(\omega)$, added inertia $A(\omega)$, and damping $B(\omega)$. For a single-flap device, the tuning \underline{T} is given by the spring constant C , a design

parameter which we vary (hydrostatically speaking) by adjusting the flap weight and buoyancy moments, and the intrinsic inertia M , also a design parameter which we vary by adjusting the flap mass and its distribution about the pivot. The damping \underline{D} is simply the external damping coefficient, D . The specific power absorption can then be written as

$$P_{ABS}'(\omega; \underline{G}, \underline{T}, \underline{D}) = \frac{(1/2) \omega^2 [F(\omega)]^2 D}{\{C - \omega^2 [M + A(\omega)]\}^2 + \omega^2 [D + B(\omega)]^2} \quad (75)$$

directly from Eqs. 44 and 45.

Differentiating this equation with respect to ω , including the derivatives of the hydrodynamic quantities, we obtain the following:

$$\begin{aligned} \frac{d}{d\omega} P_{ABS}' &= \frac{\omega F D [F + \omega(dF/d\omega)]}{[C - \omega^2(M + A)]^2 + \omega^2(D + B)^2} \\ &+ \frac{\omega^2 F^2 D [C - \omega^2(M + A)] [2\omega(M + A) + \omega^2(dA/d\omega)]}{[C - \omega^2(M + A)]^2 + \omega^2(D + B)^2} \\ &- \frac{\omega(D + B)^2 + \omega^2(D + B)(dB/d\omega)}{[C - \omega^2(M + A)]^2 + \omega^2(D + B)^2} \end{aligned} \quad (76)$$

where F , A , and B are still to be understood as functions of ω , although the formal notation has been dropped for compactness. Now at first glance this may not seem to be a very convenient form of the derivative, but for the present purpose it is instructive. Note that the denominators of all three large terms are positive in any case, and they

become larger in magnitude as the system becomes either more "mistuned" at a frequency, $[C-\omega^2(M+A(\omega))]^2$ becoming larger, or more highly damped. This is particularly true of the latter two terms, because of the final squaring of the denominators. The first term, then, is assuredly positive at all frequencies where the derivative $dF/d\omega$ is positive, and even a little past that. This happens to be so throughout the energetic frequency range of ocean waves for practically sized devices. In fact to push "over the top" of the exciting force curve, we must go to deep draft at high frequency, a clear mistake. Importantly, the numerator of this term is independent of both the tuning and the radiative damping.

The last term is negative whenever the derivative $dB/d\omega$ is positive, and even a little past that. This also happens to be the case throughout the frequency range of practical interest, for the same reason. Moreover, the numerator becomes large when the system is highly damped, independent of the tuning.

Thus, these two terms have clearly opposed effects on the shape of the curve of $P_{ABS}'(\omega)$. The first term contributes to an upward slope over the whole frequency range of a typical spectrum; the strength of this contribution becomes greater around resonance, because of the mistuning term in the denominator, and greater also if the radiative damping is light, due to the damping term in the denominat-

or, but the term itself is always positive in practical situations. The last term contributes to a downward slope, also stronger near resonance, but always negative. Therefore, between them, these two terms influence the over-all behavior of the curve in a way that is only slightly affected by the tuning, even near resonance, because their signs are opposite.

At the same time, by considering the form of the function P_{ABS}' itself, as opposed to its derivative, it is clear that the effect of overdamping is to drive the curve down at high frequencies far more strongly than at low frequencies, also regardless of the tuning, and thus to move the peak absorption to a lower frequency.

Finally, and by contrast, the middle term in the derivative is the key to the influence of tuning. Here, the second bracketed expression in the numerator is positive wherever the derivative $dA/d\omega$ is positive: again, this is true over the practical frequency range. The first bracketed expression, however, causes this term to pass through zero at the resonant frequency, from positive below to negative above resonance. It is this term, therefore, that is responsible for peaking the curve of P_{ABS}' at resonance. The other two terms, through their relative magnitudes, also push a peak into the curve, but this has relatively little to do with resonance: it is primarily an effect of the relationship between exciting force and damping as

functions of frequency.

In general, then, the shape of the curve of P_{ABS}' is sharper and narrower when resonance dominates, the peak being somewhere near the resonant frequency. This can happen only when the damping is light in the neighborhood of the resonant frequency, which means only when the tuning is low, or the flap dimensions are small, and the system is not being overdamped by the external damper. This means, in design terms, that a very sharp, resonance-like behavior of the absorption curve corresponds to a low-frequency tuning combined with a small wave amplitude (or, in a spectrum, low energy) for a given device size, so that overdamping is not necessary to limit the resulting motion. On the other hand, if the tuning is higher in the frequency range, or the wave amplitudes are larger with respect to the device size, then either the increased radiative damping or the increased required external damping will begin to reduce the sharpness of the peak, and the curve of P_{ABS}' will become broader and lower at the peak.

However, a curve of P_{ABS}' does not have to be strongly resonant in order to represent a good solution to maximizing the average spectral absorption. In fact, if the energy is spread over a fairly wide frequency range, an overly sharp curve of P_{ABS}' may fail to absorb as much as a broader curve with a somewhat lower peak. The curve can be broadened in the vicinity of the spectrum either by in-

creasing the external damping or by tuning away from the spectrum. However, the latter will also tend to move the peak more strongly on the frequency scale, thereby lowering the values obtained at all the energetic frequencies even while the curve flattens out across them. Therefore, the designer should never deliberately tune away from the spectrum unless his objective is to reduce absorption, along with motions and loads.

On the other hand, cases may arise when the designer is unable to tune up to the spectrum, for example, because there is a limited hydrostatic spring constant available. In this case, although the curve of P_{ABS} ' may be able to reach a fairly high value at some lower tuned frequency, it will be completely unresonant throughout the higher-frequency components of the spectrum. This is not necessarily completely fatal if the degree of mistuning is not too severe. Within the range of energetic frequencies the curve may be almost flat, and what slope it does have will be primarily due to the variation of the exciting force and radiative damping, rather than the distance away from resonance. The slope, in fact can remain positive, though small, even above the resonant condition, while the first term in the derivative remains large enough. A similar effect happens if the tuning is above the spectral energy, although this is certainly less likely to be the case for practical reasons.

So, where does this leave us with respect to defining a "target" frequency? If the curve of P_{ABS}' is going to be flattened in the vicinity of the spectrum because of required overdamping (large seastate, small flap, or low-frequency tuning) then the choice of a target frequency for tuning is not very critical. However, since $S^+(\omega)$ begins to fall off above the peak frequency ω_0 , and the corresponding power decreases above the power-peak frequency ω_{pmax} , there does not seem to be any reason to tune for maximum P_{ABS}' at a higher frequency than ω_0 . So, in such a case, the power-averaged frequency would seem to be too high.

On the other hand, if the seastate is small enough, or the flap large enough, so that overdamping will not be required, and if the tuning itself is not constrained by dependence on weak springs, then there is at least the possibility that resonance can be obtained and used. In this case, at a low-frequency tuning, the curve of P_{ABS}' will tend to be sharp, rather than flat. Accordingly, if the target frequency is set at the lowest proposed value, ω_{pmax} , the resulting tuning may tend to cut off the higher-frequency components too sharply, while the lower half of the peak of the P_{ABS}' curve will be placed on the low-frequency wing of the spectrum, where it falls off more steeply than on the high-frequency side, in most spectral forms. Accordingly, it still seems appropriate to tune for

an initial target frequency of ω_0 . Again, with a very sharp P_{ABS}' curve and a wide spectrum, the best strategy may be to increase the damping to broaden the curve, but never to tune away from the spectrum. In any case, the sharpness of both the spectrum and the P_{ABS}' curve are likely to be reduced for higher-frequency peaks, the former because generally less energetic seastates have higher peak frequencies, the latter because of increased radiative damping at higher frequencies.

This point, however, brings us to a final condition. Suppose the tuning is constrained, for some reason, to below the spectral peak. In this case, the "target" frequency hardly matters, because we cannot reach it anyway. Therefore, the designer will tune as high as he can, and try to increase the values of P_{ABS}' in the vicinity of the spectral peak by increasing the damping, if possible.

To illustrate the effects of some of the design variables on the performance in a nondirectional random sea, typical spectra are selected, with a practical situation of water depth and flap draft. Two spectra, both for a 2-m significant wave height but differing substantially in modal frequency, are shown in Fig. 51. One is an ITTC one-parameter spectrum, having a modal frequency of about 0.89 sec^{-1} , the other an Ochi 2-parameter, with a modal frequency of 0.71 sec^{-1} .

Response curves (specific absorption and flap motion

RAO versus ω) for a flap of 5 m draft and 10 m width in a water depth of 7.5 m have been calculated, and are shown in Figs. 52 and 53 for a number of external dampings at a tuned frequency of 0.9 sec^{-1} . The effect of increased damping is noticeable: reducing the power absorption at peak, while broadening the power absorption curve over the frequency range. Of course, the motion response is always reduced by increased damping, for a single flap device.

Comparable curves showing the effects of both tuning and damping are shown in Figs. 54 and 55. Here, several different tunings are shown, each with a different damping "strategy" adopted. Referring to the order of the figure legends: Curve 1 is tuned and damped for the peak of the ITTC spectrum; curve 2 is tuned for the peak of the Ochi spectrum, and somewhat overdamped; curve 3 is tuned below peak, and underdamped (a tragic mistake in a random sea, just as it is at a single frequency); curve 4 is tuned even farther below the peak than curve 3, but with the damping set higher to broaden the power response.

Finally, curve 5 in Figs. 54 and 55 does not represent a single damping, but rather the obtainable maximum power and response with a fixed tuning, allowing the damping to be set at its optimal value for each frequency. Thus, this curve cannot be obtained by any device with a fixed damping coefficient. However, it would be interesting to see how a device with active control forces would compare to such a

curve. Unfortunately, that analysis cannot be done using a simple, linear model of the flap motion.

Finally, the over-all results for the spectra, that is, the average absorption $\overline{P_{ABS}}$ and the root-mean-square value of the motion response σ_X , are plotted against external damping coefficient in Figs. 56 and 57, for three single-flap device sizes at a number of tunings. It will be noted that there is often a trade-off between increased spring constant (to increase the absorption by better tuning) and flap size (increasing the absorption by making the device less sensitive to mistuning).

It will also be noted that the effect of mistuning is particularly strong for the smaller devices. Furthermore, the optimum damping in each case is substantially larger than the optimum damping for the peak frequency of the spectrum itself, 0.89 sec^{-1} . In fact, the largest flap is typified by a very broad power response curve, an illustration of the difference between designing for a single frequency (or swell) and for a more diffuse wind-driven seastate.

Directionality Effects on Average Absorption

Directional effects on the absorption characteristics of flap-type devices arise from two distinct sources: oblique wave encounter (in unidirectional seas) and directional spreading of a random sea. Needless to say, both of these effects may be experienced at the same time, when the device is not aligned normal to the principal wave direction.

The effect of pure misalignment in a unidirectional sea is easy to deal with. Since the exciting force is the only quantity that changes, at each frequency, a new definition of the specific absorption, $P_{ABS}'(\omega, \beta; \underline{G}, \underline{T}, \underline{D})$, a function of angle of encounter β as well as ω must be computed, using the exciting force corresponding to the angle β . As mentioned previously, the exciting force decreases rapidly with angle, particularly so as the flap width becomes longer with respect to the wavelength, while the power absorption varies as the exciting force squared.

For a directional sea, the expression analogous to Eq. 70 is

$$\overline{P_{ABS}} = \int_{-\pi}^{\pi} \int_0^{\infty} S^+(\omega, \beta) P_{ABS}'(\omega, \beta) d\omega d\beta \quad (77)$$

where $S^+(\omega, \beta)$ is a directional spectral density, $P_{ABS}'(\omega, \beta)$ is the directional specific absorption, and β is measured with respect to the normal to the device.

As an example, consider a directional spectrum of the

typical cosine squared form:

$$\begin{aligned} S^+(\omega, \theta) &= (2/\pi) S^+(\omega) \cos^2 \theta & (-\pi/2 < \theta < \pi/2) \\ &= 0 & \text{elsewhere} \end{aligned} \quad (78)$$

where θ is now defined as the angle from the principal wave direction, and $S^+(\omega)$ is the total spectral density (incident from all directions) at the frequency ω . This form of the spectrum is simple to use, but not very general. The spreading function is zero at 90° from the principal direction, and in the entire semicircle opposite to it. Furthermore, in actual seas the spreading tends to be a function of frequency, as suggested by Dawson (Ref. 28).

Now, the directional specific power absorption can be written as

$$P_{ABS}'(\omega, \beta) = P_{ABS}'(\omega, 0) \frac{F(\omega, \beta)^2}{F(\omega, 0)^2} \quad (79)$$

where $P_{ABS}'(\omega, 0)$ is the specific absorption in normal encounter, and $F(\omega, \beta)$ is the exciting force. Now, clearly the ratio of exciting forces on the right of Eq. 79 is not independent of frequency, even if the spreading function is assumed to be so. Therefore even if there were a cosine power function that adequately fitted the results at one frequency, a different exponent of the cosine would be needed to describe the form at another frequency. However, over the limited range of frequencies covered by the energetic part of a sea spectrum, it may be found that the fitted cosine exponent varies only slightly from high to

low frequency. In such a case, the ratio of exciting forces may be adequately represented by a generalized cosine power expression (in some sense, the exponent used must actually be is "power-averaged" in a particular spectrum, or no judgement can be made). If this can be done, then the directional absorption may be rewritten as

$$P_{ABS}'(\omega, \beta) = P_{ABS}'(\omega, 0) \cos^m \beta \quad (80)$$

where m is an exponent assumed to be constant with respect to frequency. Then the expression for average power absorption in random sea can be rewritten as

$$\begin{aligned} \overline{P_{ABS}} &= (2/\pi) \int_{-\pi/2}^{\pi/2} \int_0^{\infty} S^+(\omega) \cos^2 \theta P_{ABS}'(\omega, 0) \cos^m \beta \, d\omega \, d\theta \\ &= (2/\pi) \int_{-\pi/2}^{\pi/2} \cos^2 \theta \cos^m \beta \int_0^{\infty} S^+(\omega) P_{ABS}'(\omega) \, d\omega \, d\theta \\ &= (2/\pi) \overline{P_{ABS0}} \int_{-\pi/2}^{\pi/2} \cos^2 \theta \cos^m \beta \, d\theta \end{aligned} \quad (81)$$

where $\overline{P_{ABS0}}$ denotes the average power absorption in an unspread spectrum of the same total power. Note that if the device is oriented normal to the principal wave direction, then $\beta = \theta$, and the angular integral in the final expression is just $\int \cos^{(2+m)} \theta \, d\theta$, which can be calculated trivially for m an integer. If the device is oriented away from the principal direction say by an angle θ_0 , then $\beta = \theta - \theta_0$, and the integral must be solved numerically.

Now, in order to make use of the approximation afforded by Eq. 81, we must estimate the exponent m appearing in

the absorption cosine function. The directional effect actually does vary with frequency, being less important for a short device in a long wavelength. Over the range of spectral frequencies in a particular case, then, the exponent m might easily vary from 2 to 4, for moderate angles (it should be noted that at high angles of encounter β , interference effects in short waves produce complications that cannot be modelled by a simple cosine power form). Thus, given normal orientation to the principal direction, the average absorbed power would fall to 75 percent of its value in a unidirectional sea having the same total power density. Due to cosine-squared wave spreading alone, with $m = 2$. This figure becomes 68 percent with $m=3$ (a compromise value), and 63 percent with $m=4$. With non-normal orientation to the principal direction, the average absorption will be even lower.

Finally, having used it for the purposes of illustration only, it should be noted that the cosine-squared spreading function is probably not appropriate for coastal locations having a significant amount of energy reflected from the shoreline.

Acceptable Motion Response Criteria in Random Seas

In a regular wave, the definition of "acceptable" motion may be somewhat arbitrary, but at least the response of the flap is a deterministic quantity. Thus, for example, suppose the designer determines that a particular set of power-takeoff machinery imposes a 30° travel limit on each side of the neutral position and if this limit is hit with high enough flap velocity, the machine will fail. Now, the response of the flap in a given regular wave (ω, ζ_A) happens to be 25° amplitude, at some specified tuning and damping. Then the response of the flap can be said to be within appropriate limits for that wave, with room for a 5° "deceleration" zone at each end, just for safety. On the other hand, if the linear predicted amplitude is 35° , then the designer knows that the tuning or damping must be changed, and can find out how much to change them. The fact of "acceptable" or "unacceptable" motion is clear in any case, once the arbitrary definition is given.

In comparison, what can be said about the "acceptability" of the response in a random sea? Suppose that the machine will fail if the motion record crosses plus or minus 30° with velocity greater than $20^\circ/\text{sec}$. The spectrum of the motion response in a particular seastate is given as $S_X^+(\omega)$, and the spectrum of the velocity as $S_V^+(\omega)$, again at a particular tuning and damping. Now, is the motion acceptable?

Is the motion acceptable? Obviously we can't answer that question in as simple and unambiguous a way as we did for a regular wave. In general, an economically sound answer can only be obtained when we know how much we lose by a failure of the machine: which in turn depends on how much energy (and money) it is bringing in, how much it costs to replace or repair, how long it's supposed to last, and most importantly, how long it does last before it fails.

The general decision theoretic problem of a system with a random cash flow (usually involving a random ending time for the the cash flow) with probability densities that can be altered by design decisions is well known. This problem is too lengthy to set out here, although it will be stated that at least two of the principal variables in the problem come directly from consideration of the responses of the device, and are therefore directly affected by the decision to "accept" the response spectra as they are or to change the tuning and damping.

The first of these is that when the motion spectra are modified by changed tuning and damping, the expected failure rate changes, and therefore so does the distribution of the time of failure. Second, as the motion spectra are changed the average power absorption will also change. As in all risk problems, there is an optimal failure rate that cannot be zero; furthermore, in the case of a wave energy

absorbing system without any form of "smart" damping control, the requirement for an "acceptably" small failure rate, obtained solely by tuning and static damping, will restrict the power output in much the same way as overdamping does in regular waves.

Now, what is the "failure" rate in terms of the response spectra. If a "failure" is defined as an upcrossing of a given positive value of the response motion at or above some threshold value of the velocity, then the problem is completely analogous to that of ship slamming, as discussed by Ochi (Ref. 34), and others. The expected rate of failures for a narrow-band process is then given by:

$$N = (1/2\pi) \frac{\sigma_V}{\sigma_X} \exp \left(-\frac{X_t^2}{\sigma_X^2} + \frac{V_t^2}{\sigma_V^2} \right) \quad (82)$$

where σ_V and σ_X are the root-mean-square velocity and motion, and V_t and X_t are the threshold values of velocity and motion, respectively. It will be noted that the factor $(1/2\pi)$ indicates the assumption of a one-sided failure process. Now, for a flap type device, if an upcrossing of X_t at V_t is a failure then so presumably is a downcrossing of $-X_t$ at $-V_t$. However, if the mean position of the flap is not midway between the two imposed thresholds $\pm X_t$, it is not quite right to simply double the expression above. Instead the down and up thresholds (representing roll

toward and away from the wave direction) should be calculated as two separate quantities, although the random processes X and V will still be considered symmetric about their (non-zero) mean. It should be physically obvious that if the flap's mean position inclines away from the center of the machine stroke, for example, that the rate of failures occurring at the nearer limit is higher than at the farther limit. However, if the two failure processes are regarded as independent, the total of their two failure rates, calculated according to Eq. 82 will be the combined failure rate.

Now, we have been using the term "failure" for an event that occurs, but the definition of the event need not be a failure in the conventional sense of a mechanical or structural catastrophe. In fact, for a flap type absorbing device, we may be able to arrange the system so that, mechanically at least, the flap is able to pivot nearly 90° each side of neutral without destroying itself. In this case, the "acceptability" of the response will be determined more by the desire to maintain the flap motion response small enough so that the linear power predictions can be at least reasonably accurate. What these "reasonable" bounds should be, however, cannot be made clear by linear theory itself. Nevertheless, it seems that there could be hundreds of minor "failures" of linear theory per hour in a random sea without necessarily changing the average power

absorption very much. A second-order analytical treatment, model experiments in large amplitude waves, or preferably both, would certainly help to resolve this issue.

MATCHING OF THE SYSTEM AND SITE

The identification of suitable sites for wave-power systems in general, and the related (but more specific) problem of configuring a system for good performance at a particular site, involve several design factors. A large number of investigators, among them Crabb (Ref. 38), Fang and Hogben (Ref. 39), Houmb and Overvik (Ref. 40), and Mogridge et al (Ref. 41), have presented wave climatological data for various offshore and coastal locations in the UK, Norway, North America, and Japan.

The wave climate in a particular location is obviously a key consideration not only in selecting the site, but also in selecting the dimensions and capacity of a device intended for that site. However, other factors in addition to the distribution of sea spectra may also combine to make site selection or device matching a particularly thorny problem. In the following section, the effects of various site environmental factors on the design and operation of flap-type wave absorbers will be discussed.

Wave Climatology

On the most obvious level, a potential site for wave-power applications can be judged in terms of the average annual incident wave power density. For a parametric family of wave spectra characteristic of the location, and with a suitable probability density function for the parameters of the family, the availability of wave energy can be calculated directly from the expression for time-averaged power per meter of wave front, as follows:

$$\bar{Q} = \frac{1}{4} \rho g^2 \int_{\underline{p}} f(\underline{p}) \int_0^{\infty} \frac{S^+(\omega; \underline{p})}{\omega} d\omega d\underline{p} \quad (83)$$

where the vector \underline{p} denotes the set of parameters characterizing the family of spectra, $f(\underline{p})$ is a joint probability density function for the parameter set, and $S^+(\omega; \underline{p})$ is the variance spectral density associated with a particular combination of the parameters. For practicality, the parametric family of spectra can be approximated by a discrete set of n representative spectra, in which case the above integral can be approximated by the corresponding weighted sum

$$\bar{Q} = \frac{1}{4} \rho g^2 \sum_i f_i \int_0^{\infty} \frac{S_i^+(\omega)}{\omega} d\omega \quad (84)$$

where the subscript i denotes a particular member of the set of spectra, f_i is its frequency of occurrence, and $S_i^+(\omega)$ is the corresponding spectrum.

Obviously, in the choice of a particular spectral family, the resolution to be gained by enlarging the parameter set (e.g., from a single-parameter description, such as the familiar Pierson-Moskowitz, to 2-parameters, 5-parameters, such as JONSWAP, or 6-parameters) must be balanced against the difficulty of obtaining a suitable data set to support the probability density function. Where observational data is relatively sparse, the use of a 1 or 2-parameter family may be the only available choice, and any inaccuracies arising from insufficient detail in the model must simply be accepted.

A widely used 2-parameter spectral family is that adopted by Ochi (Ref. 42):

$$S^+(\omega) = 0.278 \frac{\omega_0^4}{\omega^5} H_S^2 \exp[-0.437(\omega_0/\omega)^4] \quad (85)$$

where H_S is the significant wave height, and ω_0 is the mean frequency m_1/m_0 .

Ochi has also suggested that the long-term joint pdf for a 2-parameter spectrum (with parameters significant wave height and mean zero-crossing period) can be described by a 5-parameter log normal distribution:.

$$f(h, t) = \frac{1}{2\pi(1-\rho_{ht}^2\sigma_h\sigma_t)^{1/2}} \exp\left\{-\frac{1}{2(1-\rho_{ht}^2)} \left[\left(\frac{h-\mu_h}{\sigma_h}\right)^2 + \left(\frac{t-\mu_t}{\sigma_t}\right)^2 - 2\rho_{ht}\left(\frac{h-\mu_h}{\sigma_h}\right)\left(\frac{t-\mu_t}{\sigma_t}\right) \right]\right\} \quad (86)$$

where h and t are the natural logs of the significant wave height and mean zero-crossing period, respectively, μ_h and σ_h are the mean and standard deviation of h from the data, μ_t and σ_t are the mean and standard deviation of t , and ρ_{ht} is the correlation coefficient of h with t .

Ochi's distribution was found to fit the observational data quite well except in the upper range of significant wave heights. Since the primary motivation of Ochi's work was to predict long-term extreme values of the loads or motions of ships and marine structures, and since these are particularly strongly influenced by the nature of the assumed distribution in higher seastates, subsequent work by Fang and Hogben (Ref. 39) introduced an additional skewness parameter intended to improve the fit at low levels of exceedance. However, for the specific purposes of estimating the annual average power output of an energy-absorbing device, the influence of extreme seastates, which occur with very small frequency, is by no means as critical as it is for long-term extrema.

In characterizing the suitability of a particular site for the application of wave-power devices, the annual average power density might seem to indicate relative merit, in the obvious sense of giving some measure of the availability of the "raw material" for energy output. However, the annual average power density, by itself, does not provide direct guidance for the design of the absorber: its arrangement, dimensions, spring constant, or power takeoff

capacity. Clearly, any number of different distributions of seastates, expressed in the form of Eq. 86, can give a single value of the average annual power density, and yet represent widely differing wave environments, in terms of the design of a device.

For example, consider a site characterized by relatively moderate but consistent seastates over the larger portion of the year (such as a trade-wind area), and another characterized by periods of energetic seastate interrupted by lengthy periods of low seastate. Both sites could have the same annual average power density, but the probability density functions of power density are radically different. The two sites would certainly not be equally preferable for the application of wave-power devices in general, nor could the same device perform equally well in both areas.

As an even more extreme example, consider two sites which have not only identical average annual power densities, but identical pdf's of power density. Even with these strong similarities, the two sites could differ substantially in their distributions of wave height and mean period.

From the standpoint of site selection for wave-power applications in general, the wave-climate information that is most significant in judging the relative merit of sites includes the following, based on Ochi's model of the joint pdf for a 2-parameter family of spectra:

(1) Average annual power density. Obviously, a site with extremely low average density must be regarded as unworthy. Regardless of the wave height or modal period distributions, the low power density would require large arrays of absorbers to produce a given output. Consequently, the cost per unit output would then be unjustifiably high.

(2) Variance of power density. Since the power density is a random variable, any device design must be a compromise between the different design conditions. Therefore, a low variance of power density within the family of seastates is clearly to be preferred, in that less compromise is necessary. A high variance of the daily mean power density, for example, would be produced by a prevalence of higher seastates interspersed with calm periods. Thus, a device intended for a high-variance site would have to be given larger power-takeoff capacity and heavier supporting structures, which would then be under-utilized or understressed during the frequent low-energy periods. At the same time, the expected extreme loads on the device would be higher, and the required structures would be correspondingly heavier. Both of these factors would contribute to increased costs for a given annual average output. By contrast, a device in a low-variance environment could be built around a smaller power-takeoff capacity which would be less subject to periodic underutilization, and the structures could be lighter in view of lower extreme loads.

(3) Distribution of wave period. For any class of devices which has a limited range of tuning, such as a flap device depending on hydrostatic restoring force, a small variance of the distribution of mean wave period is clearly preferable. At a given average power density, a distribution of mean periods favoring long-period spectra would also be preferable. For example, although a floodable device can be ballasted to obtain resonance with long waves when desired, there will be some upper limit on the available hydrostatic spring constant. Consequently, waves above a certain frequency will not be absorbed with large cross-section, due to the inability to operate near resonance. This, for a device of fixed size, would tend to favor a distribution heavy in long mean-period seastates.

From the point of view of designing a device for a particular location, distributions of wave height and period have additional implications. In general terms, an increasing prevalence of long-period waves would tend to favor increased flap draft (provided sufficient water depth was available) since shallow flaps would have to be severely stroke limited in long waves. By contrast, an increasing prevalence of short-period waves would tend to favor decreased flap draft. The influence of mean period on desired flap width is more complicated. Since shorter waves are diffracted less strongly, a flap-type device of finite width acts increasingly like a 2-D terminator in short waves. Thus, a larger flap width becomes more desirable in

normal encounter. On the other hand, a long device responding in short waves also becomes increasingly directional, until interference effects begin to cancel the exciting force at all but normal encounter. Therefore, in directional seas, the effects of oblique wave encounter are more detrimental to a wide flap than to a relatively narrow one. The further effects of directionality are discussed below.

(4) Other Spectral Characteristics. In the above discussion, a 2-parameter spectral family was assumed. This restriction implies a spectrum that is unimodal in frequency, generally corresponding to wind-driven seas alone. For many locations, of course, the typical spectrum includes both wind-driven and swell components. Several models, such as the Ochi 6-parameter spectrum (Ref. 42), have been proposed to include the presence of multiple components. In these models, an additional shape parameter is usually incorporated for each component.

Considering each component separately (as a 3-parameter spectrum), the effect of the shape parameter on the potential maximum output of a wave-absorbing device in a given spectrum can be stated. In Ochi's formulation of the spectral components, the shape factor corresponds to the "sharpness" of the spectrum, that is, its tendency to concentrate energy in a narrow range of frequency. For a nearly monochromatic swell component, for example, a high

value of the shape parameter is indicated. Thus, from the standpoint of a wave-energy absorber, a high-valued shape parameter is a favorable characteristic, permitting greater absorption since more of the spectral energy can be placed near a maximum of the power absorption RAO (with an appropriate choice of geometry, tuning, and damping). Furthermore, as has been shown, larger devices are less sensitive to tuning than smaller ones. Accordingly, at a given total energy and peak frequency, a "broader" spectrum requires a larger device to achieve similar absorption.

For an actual multiple component spectrum, however, higher shape parameters for any or all of the components (other parameters being unchanged), may raise a complication. If the spectral components are not too far apart in mean frequency, and not too sharply peaked, the combined spectrum remains unimodal in frequency, with swell and sea components at least partially overlapping. Thus, in designing a device configuration for the particular spectrum, the designer is free to center the power absorption RAO (insofar as possible) to match the high-energy portion of the frequency range. For devices having a unimodal RAO of limited bandwidth, this is a simple heuristic approach to obtaining high absorption. By contrast, for more widely separated swell and sea components, which can appear in connection with high shape parameters, the spectrum becomes bimodal. In such a case, the designer will generally be

forced to shift a unimodal absorption RAO onto either the swell or sea component: the middle ground will contain little energy.

For a device which has a multimodal absorption RAO, however, it would be possible to cover even widely separated spectral peaks with peaks in the RAO itself. Twin-flap devices, in fact, do have such a characteristic when sprung and damped for maximum absorption at certain frequencies, as demonstrated by Srokosz and Evans (Ref. 11) in their 2-D analysis. However, because of the extreme sensitivity of twin-flap RAO's to spring and damper settings and also the requirement for negative spring and damper coefficients for optimal power absorption in many cases, this predicted ability may be quite difficult to achieve in practice.

For an actual multiple component spectrum, a better method of approach to an ideal design might be through a time-domain analysis, explicitly incorporating the ability to control the power takeoff system in real time (by varying the load on the alternator or the flow into the high-pressure receiver) in order to increase time-averaged absorbed power, rather than attempting to argue the merits of a particular absorption RAO in the frequency domain. However, this type of analysis is considerably beyond the scope of the present work.

The wave "groupiness factor" discussed by Mogridge et al (Ref. 41), is a measure which indicates the degree of

variation of the "smoothed instantaneous wave energy history" (basically, a smoothed time history of the wave elevation squared) about its time average for a wave record. In effect, the groupiness factor is a measure of the uniformity of average wave energy over time scales on the order of a few wave periods. The authors suggest that the presence of wave groups may be expected to have an effect on power takeoff systems of wave-energy absorbing devices. In practical design terms, this is no doubt true.

Significant wave grouping implies that packets of relatively large waves, perhaps several cycles, tend to be separated by periods of smaller wave encounter. Thus, the power takeoff system may have to cope with several cycles at overload, followed by a minute or so at lower output. The principle effect of the groupiness factor may be on the desired maximum output of the power takeoff, or on the capacity of output-smoothing components of the power takeoff system, for example, the high-pressure receiver in a hydraulic system. A high groupiness factor implies relatively more variation of the smoothed energy history, and this in turn would require either more temporary energy storage capacity or a higher maximum rating of the power takeoff itself, in order to absorb at the rate predicted for a linear system in a given time-averaged power density.

(5) Directional Effects. For both single and twin-flap devices, exciting forces decline relatively sharply in

oblique encounter. Furthermore, since the maximum absorbed power varies with the square of the exciting force, operation in oblique seas is particularly undesirable from the standpoint of power output. For this reason, to orient a flap-type device for maximum absorption in a particular sea, it is essential to align the device normal to the principal direction of wave travel. Even with this alignment, as the directional spreading of the spectrum increases, the total power absorption of a given directional absorbing device must decrease.

In spite of strong directional effects on the absorption cross-section of a flap-type device, it is not necessarily true that a non-directional device is preferable. As has been pointed out by Count (Ref. 4), the directional absorbing characteristics of a device are directly related to its directional radiation characteristics. By reciprocity, a device with a strongly directional absorption pattern, as it turns out, is always found to have a higher absorption cross-section in its preferred direction, than an omnidirectional absorber of equivalent damping coefficient. This fact can be derived from a consideration of Eq. 41, a form of the Haskind relation. Nevertheless, for a particular directional device, the directional spreading of incident wave energy must entail some reduction of the total absorption, versus the absorption in a unidirectional sea of the same total energy content.

By extension, in a family of spectra characterizing a particular site, the most suitable situation would be one where there is a single predominant direction of wave travel that applies to all of the seastates encountered, with relatively small variance in the principal direction. In the open ocean, even in trade-wind areas, this is not usually the case. Unless a method of reorienting the flaps is provided (which would be quite difficult in a practical full-scale device), the choice of a single fixed orientation for the flap-type device is a very critical and limiting step, and one which "throws out" a great deal of potentially absorbed energy.

Even when there is a predominant wind direction, and therefore a fairly compact distribution of primary direction for the local wind-driven sea, the presence of energetic swell components originating from distant disturbances in various directions may mean that a significant portion of the total wave power is not aligned with a single preferred direction. Thus, in open ocean sites, it may not be possible to choose a single orientation for the device to obtain high average absorbed power in all high-probability conditions. To add to the difficulty, in real two-component seaways the principal directions of the wind-driven and swell components are generally quite different, sometimes even at right angles, giving rise to a cross-sea. In such a case, directional "losses" are likely to be quite

large, regardless of the direction in which the device is pointed.

In coastal sites, on the other hand, a single preferred direction is imposed (to an extent) by wave diffraction due to bottom contours. A good location for a highly directional flap-type device might then be in relatively shallow water, on a gradually shoaling bottom with straight contour lines, with the flaps aligned approximately parallel to the contours.

This diffractive "sheltering" effect would, of course, be most pronounced for longer wave components in any given water depth. It is unfortunately true, however, that the directional absorption characteristics of flap-type devices are strongest for short waves, as shown previously. Thus, the largest benefits due to bottom diffraction would be for long swell components coming into shoal water from the deep ocean, rather than on local, fetch-limited seas. In addition, the straightening effect would become greater in shallower water, where some loss of incident wave energy would also occur due to bottom friction, and other interactions.

A small additional increase in absorption might also be obtained from shore reflections, particularly if the adjacent shoreline were formed by a straight reflecting breakwater or steeply shoaling beach, rather than by a gently inclined or irregular strand. The amount of this

reflected energy has not been estimated, however.

It should be mentioned in this connection that a single-flap device, being symmetric, has equal absorption characteristics from the front and back. On the other hand, while the twin-flap device has symmetric hydrodynamic coefficients, if different spring constants and dampings are set on the front and back flaps, the absorption characteristics do not remain symmetric.

From the point of view of configuring an absorber for operation in unavoidable oblique waves, or in a widely spread directional spectrum, it should be remembered that short flaps tend to be less directionally sensitive than long ones. In fact, in the limit of long flaps (or short wavelength/flap width ratios) the exciting force will eventually go to zero for any oblique encounter (due to lengthwise cancellation effects), provided that the flap continues to respond as a rigid body.

Tidal Effects

One of the important practical distinctions between free-floating and bottom-fixed flap-type energy-absorbing devices lies in the effects of height of tide. While a floating device can be free to operate at constant draft (even a tensioned-leg mooring system could be arranged to vary the cable length), a bottom-mounted device with a fixed pivot point would of necessity be subject to changes in draft equal to the range of tide. Such changes in draft will affect virtually all the dynamic characteristics of the flap.

At low water, for example, with reduced draft both the added mass and damping will be reduced, as will the exciting force. At the same time, the buoyancy moment will decrease until, finally, the flap will loll to a new equilibrium in an inclined position, or rather, two new equilibrium positions. In this state, the basic linearity of the system will be clearly violated, certainly if the flap responds by bouncing from one equilibrium point to the other. Obviously, if the range of tide is very great the device will ground, and all hydrodynamic bets are off.

At high water, on the other hand, increased draft will tend to increase the hydrodynamic forces and static restoring moment, up to the point at which the top of the flap is immersed. Thereafter, with increasing height of tide, the damping and particularly the wave exciting force will begin to decrease, as shown by Evans (Ref. 14), while the restor-

ing moment will become a constant. Even if the flap does not become entirely submerged in still water, the reduced freeboard will contribute to more frequent overtopping by wave crests and large-amplitude motions, with the attendant changes in nonlinear effects discussed previously.

The only method of compensating for these effects is to provide positive vertical mechanical movement of the pivot point in response to tidal variation. The mechanical systems involved would probably be costly and complicated, and it might very well be more economical to just accept the effects, adjusting the tuning and power-takeoff damping as far as possible to minimize the losses of absorbed power. Indeed, the effects of tidal range constitute a possible objection to bottom-fixed devices in general, although these compromises must be weighed against the difficulties of an offshore location in deeper water, with a free-floating device: primarily mooring systems, undesirable shiplike motions, and longer undersea cable runs.

Even if the device itself can be compensated for the effects of tidal range, the effects of height of tide on the wave environment will also be important. At low water, diffractive effects and bottom losses will be greater, so that less incident wave energy will reach the location of the device. The opposite effects will be encountered at high water. The surf zone will also move off or onshore, so that the device's exposure to breaking waves may be

altered. The designer cannot do anything about these factors.

Apparently, then, the best alternative lies in selecting a site with a relatively small range of tide. This will limit the number of suitable coastal sites, perhaps severely.

Current Effects

Tidal currents, particularly components normal to the device, will also be troublesome. The presence of a steady tidal current will tend to drive the flap toward the limit of its travel, in the same way as the steady second-order wave force. For a flood tide acting on a surface piercing flap, the tidal current and the second-order drift will be in the same direction, and consequently the total steady force will be a maximum.

With only a hydrostatic restoring force available to resist this steady force, the flap will tend to assume an equilibrium position at some angle of inclination, which may in severe cases become excessive. Apart from the restoring force, however, it might also be possible to use differential control of the power-takeoff damping to obtain a more upright mean position. Under the linear assumptions, however, this would undoubtedly cause a loss from the maximum absorbed power. Accordingly, the decision to simply allow an "off-center" mean position might be better from the standpoint of power output, provided that the

steady force were not strong enough to bring the flap all the way to its limit at one end of the stroke.

Fortunately, a simple application of continuity will show that maximum tidal current velocity components normal to a straight shoreline must be smaller closer to the shore, for a given water depth. Thus, if the range of tide and the distance from shore are not too large, and the depth at low water not too small, the maximum normal tidal current velocity will be manageable.

Longshore current components will also have some effect on the flap. The current will tend to produce a steady lift force on the flap, which will also add to the total steady force. In addition, the motion of the flap in response to waves will shed eddies into the free stream, increasing the small viscous losses that may already be present due to vortex shedding and dissipation. For small velocities, of course, these effects will be negligible. No quantitative results for current effects on the steady force or on viscous losses have been calculated in this analysis. Similarly, the influence of wave-current interactions on flap responses have been neglected entirely.

Location of Devices with Respect to Zone of Wave Breaking

As mentioned previously, Salter (Ref. 27) has found by experiment that the forces acting on an absorbing body in breaking waves are generally lower than linear theory predicts for non-breaking waves of similar height and frequen-

cy.

For this reason, a desirable site selection would be one in which the zone of breaking waves is well inshore of the location of the device in low seastates, moving out to the location of the device in seastates in which the device begins to exceed its maximum rating. Once the zone of breakers is offshore of the device, the incident energy at the device will be reduced by losses due to wave breaking. A mildly shoaling or flat bottom contour in the neighborhood of the device will tend to produce such a gradual movement of the surf zone better than a steep or abruptly shelved contour.

Soil Characteristics

The principal soil mechanical problem for offshore structures is the foundation or anchor-holding strength of the bottom, and its stability under loads. For a bottom-fixed structure mounted on a relatively large-area, mass-concrete footing, the bottom loading can be made fairly light. In critical soils, pilings under the structure may be needed in any case. Presumably, however, this would increase the installation cost.

A hard sand or gravel bottom would also be suitable, provided that the foundation could be shaped to give adequate resistance to the horizontal forces imposed by the flaps. A relatively light weight precast concrete footing could be used if it were entrenched and backfilled. How-

ever, the costs of these underwater operations would have to be judged against the costs of building and emplacing a heavier substructure depending on pure frictional forces.

Other soil-related problems that may be important for bottom-fixed devices include the buildup of sediments around the flaps, and the possible intrusion of silt into the seals of underwater pivots. Both of these problems may be solved by placing the pivot centerline on short steel or reinforced concrete pylons extending upward a meter or so from the mass-concrete footing. In addition, it may be necessary to prevent silt intrusion by using forced water lubrication of underwater bearing seals. Obviously, a device pivoted at the top, or even above water, would avoid some of these problems completely, but it would then be subject to other structural, mechanical and hydrodynamic problems that have already been discussed in previous sections.

Other Environmental Factors

Several additional potential environmental problems may be dealt with rather briefly. The difficulties are probably minor, or at any rate they can be avoided by suitable site selection.

Wind forces on exposed flap surfaces. With excessive flap freeboard, windage on the above-water portions of the structure will contribute to the steady force tending to drive the flap toward its limit. The wind force is orders

of magnitude less than the first-order wave force, but it may nevertheless become a significant part of the steady inclining moment if too much flap freeboard is incorporated: the moment arm is large.

Ice. Obviously, the exposure of oscillating wave absorbers to drifting sea ice is not a good idea. Unlike other fixed coastal structures, such as navigational aids, wave absorbers cannot be protected by riprap and still function. For this reason, the application of absorbers in areas that are not usually ice free year-round should be viewed with some caution.

The icing of flaps, the above water portions of supporting structure, or exposed components of the power-takeoff system, by spray should not be overlooked. For a free-floating device, substantial top icing could jeopardize the stability of the entire platform, although fixed supporting structures could carry any likely amount of ice with no problem.

For an oscillating flap, however, a heavy load of ice accumulating on the above-water portions could alter the effective hydrostatic restoring force and flap inertia enough to change its absorption characteristics. This problem, if it should prove significant enough to worry about, could probably be dealt with by deicing systems or special coatings. However, it would be better to avoid icing conditions by site selection.

Marine Fouling and Corrosion. An accumulation of marine growth on the flap or its pivots could be a significant problem. Heavy fouling would increase viscous losses, and might also alter the restoring forces or inertia of the flap. More important, perhaps, local fouling of running gear, such as flap pivot seals, might introduce an additional maintenance requirement. Antifouling coatings would probably be necessary in addition to the usual corrosion protection of flap surfaces. Careful design of exposed moving parts, together with self-scraping fittings, might alleviate the critical problem around the pivot seals. Cathodic protection would also be necessary, together with careful isolation of the electrical generating plant from the flap structure.

Institutional Factors and Environmental Impact. A brief summary of the environmental and social effects of large-scale wave-energy absorbing systems is presented by Shaw (Ref. 43). Among the influences considered are:

- The effects on adjacent shoreline (primarily through reduced shoreline erosion leading to local accretion of material).
- The appearance of large, moving, and possibly unsightly objects to the detriment of the coastal scene, especially for devices located fairly close to shore.
- The effects on coastal-zone fish, mollusk, and bird

populations due to the installation and operation of absorbing devices (much of the concern arising from the possible effects of high-voltage transmission lines on the seabed and ashore, as well as from the devices themselves, which might be expected to produce noise and physical emissions, such as hydraulic fluid or lubricants).

- Interference with coastal navigation and the fishing industry (additional protective aids to navigation would have to be considered as part of the over-all costs of the system).
- The effects on the local economy of coastal communities.

There is, of course, no particular reason to suppose that flap-type devices would be more disruptive than other proposed types of ocean-energy installations, except with regard to their possible placement in relatively near-shore locations. It may be reasonably anticipated that environmental and social impacts can be held to an acceptable level, even for a full-scale installation. Certainly, small prototype systems would not offer any substantial problems.

A DESIGN PHILOSOPHY

As indicated in the preceeding sections, the selection of device dimensions must play an important part in the design of flap-type wave absorbers. However, there are several other key decisions that must be made in connection with the choice of dimensions. These basic design decisions are in three principal areas, namely:

1. Floating versus fixed supporting structure.
2. Arrangement of power takeoff (external damping) systems.
3. Arrangement of restoring force (spring) systems.

The first of these issues will be addressed in the section immediately below, since it is a fundamental issue of design philosophy, stemming from hydrodynamic results. The latter two questions, however, are deferred to the appendix on prototype wave absorbing systems, because they are more matters of design detail.

Floating versus Fixed Structure

Many early proposals for wave-energy absorbing devices were predicated on a floating structure arrangement. The principal reasons for this preference were as follows:

1. Average annual incident wave power densities are significantly higher offshore, in deep water, than in shallow-water coastal locations. For this reason, at least at first glance, sites further offshore seemed to offer the most attractive opportunities for generation of large-scale power.

2. With an offshore location, environmental impacts on coastal zones could be minimized.

3. Using a moored system in moderate to deep water, variable headings could be obtained either by suitable control of the mooring system, or by allowing the device to orient itself in response to wave forces.

The first argument, that of higher ambient power density offshore, is undeniable. However, for a given desired total power output, or absorption, the question remains whether it would be more economical to build fewer (or smaller) devices for offshore stations, or to compensate for the lower average power density of nearshore shallow-water locations by installing larger or more numerous devices closer to shore. This trade-off is not an obvious one: however, the problems of successfully mooring large wave-absorbing structures in deep water are immense. The

forces on these structures are extremely large, particularly for "terminators" such as a flap-type system.

In addition, a number of researchers have found experimentally that the absorption characteristics of devices are generally reduced by ship-motion like responses of the supporting structure, Refs. 13 and 26. It should be mentioned here, that in theory motions of the supporting structure need not produce losses of absorbed power. In fact, coupling between ship-motion like degrees of freedom of the structure (which are not arranged to absorb power directly through external damping) and modes which are directly damped by the power takeoff can produce either increased or reduced absorption, just as any two independent modes of motion can produce either cancellation or reinforcement of exciting forces or radiated waves, even when one of the modes is not externally damped (as in a twin-flap system with one of the flaps undamped).

Thus, depending on the phase relationship between exciting forces and coupling, and on the magnitude of radiative losses due to the non-power producing modes, it might be supposed that a free-floating device could absorb as much energy as a fixed, single-degree of freedom device, at certain isolated frequencies. Nevertheless, practical experience has shown that this favorable interaction does not generally occur between ship-like motions and power absorbing degrees of freedom when large frequency ranges are con-

sidered. In addition, if the ship-like motion is heavily damped, it must naturally represent a loss of absorbed power.

Obviously, in the case of flap-type absorbers, certain modes of ship-like response are excluded because they can not be coupled with the flap responses: a clear example of this is the heave response of a supporting structure with symmetric pivoted flaps; platform heave and flap roll (or sway) are uncoupled by inspection. On the other hand, sway and roll of the supporting structure are obviously coupled with sway and roll of the flaps. Therefore, practically speaking, it must be the case that the radiative losses due to hydrodynamic damping of these supporting-structure degrees of freedom dominate any gains that can be achieved through coupling, or that favorable coupling (if it exists at all) is confined to such narrow and isolated frequency ranges that the gains are never seen.

Many recent schemes for wave power absorption, discussed in Ref. 43, especially terminator types, have been based on fixed supporting structures sited in relatively shallow water, for several reasons. First, losses in absorption due to ship-motion like responses cannot be avoided in practice. Second, no practical deep-water mooring system can wholly suppress these responses for a large-scale terminator system. Third, a deep-water mooring system capable of even holding a full-scale device on station

in large waves would necessarily be extremely large and expensive due to the magnitude of the forces involved. Finally, in spite of the higher ambient power densities to be found in distant offshore locations, the cost of power transmission over large distances via underwater cable can constitute a sufficiently strong motive to adopt a site closer to the shore.

Accordingly, in the following applications of the 3-D hydrodynamic results, emphasis will be placed on the performance of flap-type devices in relatively shallow water. In shallow water, certainly, a fixed structure offers a more cost-effective solution to the problem of keeping an absorbing device secured, presumably since such an arrangement could take advantage of simple mass concrete foundations rather than more sophisticated moorings or towers.

The question of variable heading for terminators is closely related, and is similarly dispensed with. Needless to say, a system permitting variable headings for flap-type wave absorbers would entail a substantial increase in cost and complexity, although it probably could be done with either a floating or grounded supporting system.

The 3-D hydrodynamic results with regard to directional effects on flap exciting forces do provide some basis for assessing the potential advantages of this feature. For single flaps, the maximum power absorption (at optimal spring and damper settings) is proportional to the exciting

force squared. Since the added mass and damping coefficients are invariant with respect to heading in any case, the effect of directionality can be judged solely by reference to the exciting force.

For wavelengths that are relatively long compared to device dimensions, as will be the case for practical systems, the exciting force tends to vary over moderate encounter angles at a rate roughly between the cosine and the cosine squared. This can be seen from Fig. 39. Thus, the maximum absorption at optimum tuning and damping, which is proportional to the exciting force squared, must generally vary at a rate between the cosine squared and cosine to the fourth power. Since this represents a very abrupt fall-off in absorption, the potential effect of variable facing might be quite large under certain conditions, although its net value would remain questionable until a system for swinging the device was designed and estimated. For stroke limited applications, in which the response of the device is restrained as necessary by overdamping, the power absorption varies only directly as the exciting force.

The situation for twin-flap devices is more complicated, due to the influence of coupling. Nevertheless, for a fixed flap spacing the flap exciting forces still vary with heading angle at a rate somewhere between the cosine and cosine squared, as shown in in Fig. 25, until the flap width becomes of the same order as the wavelength.

A Suggested Design Procedure

In general, the design problem for any wave-absorbing device begins with following elements, which may be considered more or less as underlying assumptions:

1. A location, as characterized by a discrete family of wave spectra, together with the probability or frequency distribution of the member spectra.

2. A water depth or, at least, a limited range of water depths available at the location. The selection of a particular spot for the device, in a location where a sloped bottom allows some latitude in choosing water depth, is a tradeoff that is too subtle to be discussed in any great detail here. It should be noted, however, that even if the power density is assumed to be invariant over the location (which is a very strong assumption, since it neglects wave attenuation due to breaking and bottom interaction), then the choice of water depth still subtends a number of important factors. Among these are the following:

- (a) Deeper water gives the designer more freedom to increase flap draft, which may be desirable either to increase power absorption at nonresonant tuning or to reduce motions at a given absorption.

- (b) Deeper water gives a longer corresponding wavelength at any frequency, which in turn reduces the directionality for a given device width. At the same time, however, deeper water produces less diffraction of incident waves parallel to the bottom contours, so

that the wave environment may be more directionally spread.

(c) Deeper water, if it involves a site further from shore, will require longer cable runs and consequently increased cost.

(d) For a given flap draft, deeper water entails some additional height of supporting structure, which also translates into increased costs. Presumably, at a certain water depth a floating structure would become a preferred option. but, because of the problems in mooring such a device to resist ship-motion-like responses, or even in mooring it at all, we will simply assume that any water depth that favors floating over fixed structures is deeper than we should go.

Finally, of course, the designer should realize that water depth does affect the ambient power, particularly if the waves are breaking offshore of the device. In fact, in high seastates, this can be an advantage in terms of partially protecting the device from extremely large (and, given a finite generating capacity, unconvertible) power densities, and forces. In any case, however, more detailed oceanographic analysis is required for the water-depth tradeoff than can be provided here.

3. A measure of merit. As in all formal decision problems, the "design problem" is not properly posed without a measure of preference. In the most complete analysis, the designer should be aiming at a combination of flap

geometry, conversion machinery rating, and tuning and damping "strategies" (whether fixed-valued, variable, or actively controlled) which gives a preferable (or as an idealistic designer might put it, an optimal) value of "utility" in the given location and its family of spectra.

The definition of utility, however, depends on the ultimate purpose of the device: for a laboratory test device or a small field-test prototype, we may reasonably adopt a performance criterion, such as maximum average absorption, subject to imposed constraints such as maximum flap dimensions, and maximum cost. This is not a false criterion, only a limited one. On the other hand, if the purpose of the device is to provide a given amount of electrical energy per year to an isolated community, then we might define the utility (to be maximized) as the negative of average annual cost for a device supplying the required average power. Then again, if the purpose of the device is to supplement the generating resources of a utility grid, then we should be interested in maximizing expected annual kilowatt hours per dollar of average annual cost. Finally if the purpose of the device is to make money while selling electricity at a given price, then we should look for a maximum net present value, in dollars (or more properly, net present value per dollar of investment; or return on investment, expressed as an equivalent interest rate). The details of these measures of merit, all of which constitute

proper utilities in their specific applications, can be found in a marine context in Benford, Ref. 44. In general, the ranking of alternatives according to their merit, or (for those high-minded enough to insist on it) the parameters of the optimal design, may be quite sensitive to the choice of measure of merit. (This is only a formal way of saying that a "good" device for delivering 50 kW, with simple technology, to an out-island village in Indonesia, and a "good" device for attracting investment capital in northern California, may be quite different, and the difference does not arise solely from wave spectral densities.)

With these three elements, the family of spectra, the water depth, and an appropriate measure of merit for the purpose of the device, a problem at least is defined. Additional practical constraints, for example, on flap materials and dimensions, machinery specifications and availability, and design details, may also exist in a particular case, but these factors fit immediately into the framework of a decision problem. In fact, such "nuts and bolts" constraints may drive the design from the very outset: this is usually not a good thing from the standpoint of achieving high-tech engineering glory, but it can be a very good thing in terms of simplifying a formal design problem. So much for the problem: now, what about a method of solution?

The rational design process in general, except in certain key cases where a simple closed-form solution exists (such as for a cantilever beam) is an iterative one. Often, the designer may use computer resources to speed the iteration, or he may translate much of the decision-making model into program form, and let the machine run until it finds merit in a design. However, in any application the outline of a design procedure must precede the computer code. Furthermore, physical insight into the problem can often be used to accelerate the search method. In some cases, where the computational requirements at each iteration are quite large (as in the 3-D hydrodynamic model presented in previous sections), this acceleration is not just for the sake of more refined code: it is vital.

In the remainder of this section, the outline of a design method is presented. This procedure, which is fairly detailed, is intended to be applied when confronted with a particular family of spectra, a fixed water depth, and a measure of merit by which to judge alternative solutions. Some of the steps are computational, using the methods described in previous sections. Other are largely heuristic, based on results or, to an extent, on physical intuition. One step in particular, embarrassingly enough, Step 1, is plainly intuitive although it is not without a logical basis. If it works, it may save an eternity of more or less blind computer search time. If it doesn't work, well,

computers have nothing but time, anyway.

Basically, the method depends on starting at the simplest level, with what we know about designing a "suitable" absorbing device for regular waves; extending the physical and economic arguments upward to guide the design process for a particular sea spectrum, given what we know about spectra and finally, using design information for selected spectra to guide the design process for a family of spectra. The entire method, of course, depends on iterative procedures at the various levels: it is not a closed-form solution. However, it is an attempt to capture the "spirit" of a closed-form approach, in the sense that it works from the physics up, using information from lower levels to direct tentative steps at higher levels. The alternative, a direct search through design-parameter space, works in the opposite direction, from the tentative solution down, and in the process, loses much of the opportunity to argue, from either physical or economic principles, what the next step should be.

There is one final note on the philosophy of the design procedure: a prelude to Step 1, as it were. Assume that a "satisfactory" device (that is, near-optimal, subject to compliance with all constraints) can be found for each of a number of spectra, a subset of the family of spectra (possibly for the entire discrete family). Call the set of spectrum-suited devices {SSD}. Now, under what

conditions, if any, can it be said that at least one satisfactory solution for the entire family can be selected from among the members of {SSD}? First, it is necessary that the subset of spectra for which the devices in {SSD} are defined by "representative" of the whole family: otherwise, there may be significant design conditions left out of the picture. On the other hand, it may be that some of the seastates can be logically excluded (or at least deemphasized) as drivers of certain aspects of the design. For example, relatively low-probability states should not be as important in determining gross characteristics, such as flap dimensions and generator capacity, as states with high probability; low-energy states can be excluded as determiners of maximum damping and structural requirements; similarly, states with low-frequency spectral peaks will not drive maximum tuning, etc.

In any case, if {SSD} is representative of the family as a whole (perhaps requiring a device for each spectrum in the family) are there sufficient conditions to choose a design for the family out of {SSD}? Generally, the answer must be no, if all elements of the design are considered at the same time. However, if the elements are considered separately, it may be possible to see a pattern. Flap draft and width, for example, may be driven by moderate seastates that occur with some regularity; tuning limits will certainly be most affected by seastates with high-

frequency peaks; structures by high-energy states. Thus, it may be possible to choose design characteristics from a composite of the members of {SSD}, in an heuristic way. In effect, then, we are looking for a "compromise" design for the family by observing the characteristics of designs for member spectra.

Now, we will turn to a detailed description of the proposed method.

Step 1: Consider the discrete family of spectra and the probability distribution associated with it. Try to determine if there are any individual spectra that can be set aside, at least temporarily, from the analysis leading to certain design elements. Conversely, ask whether there are any seastates that appear likely to drive the gross features of the design (dimensions, maximum tuning, maximum damping, generator capacity) in a particular direction.

Obviously, if there is a pronounced modal seastate, or a group of states which, taken together, constitute a "central" part of the family, then the selection of gross characteristics should begin with these states. At the same time, however, the structure (and weight, and therefore, the maximum tuning) will be affected by more extreme seastates, even if their aggregate probability is low. For a ship design, the more extreme seastates tend to drive the structure, to the exclusion of design influence from moderate states. However, an absorber can shed loads, to a cer-

tain extent, by deliberate mistuning. Therefore, it may be a mistake to design a structure against extreme seastate loads, at the outset, when the forces in more moderate seas may be just as large, due to working at a higher cross-section.

Accordingly, the first few exploratory designs should be aimed at the near-modal seastates. Here are some general "rules" to guide the opening moves within this "design" set:

Temporarily, avoid undue concern about the relative probability of the spectra in the design set: just assume that each of the "design" seastates is important enough to be worth a design.

Next try to discriminate, if possible, between the influences of the spectra on the design. There are three or four measures of spectra that may be useful in this intuitive process:

(a) The design should respond to differences in energy density. Therefore, order the spectra on a scale of total energy density, that is:

$$\bar{Q} = \frac{1}{4} \rho^2 \int_0^{\infty} \frac{S+(\omega)}{\omega} \tanh kh \left(1 + \frac{2kh}{\sinh 2kh} \right) d\omega \quad (87)$$

where $k(\omega)$ is the solution of $k \tanh kh = \omega^2/g$. (Note, however, that if the spectra are actually measured in deep water, or inferred from deep-water spectral forms, rather than measured at the water depth of the site, then the

correction for k_h is not necessary or correct, and must be ignored.) In principle, a prevalence of low-energy seastates will tend to favor a smaller flap device for a given generator capacity, because motion restrictions will not be as severe. Similarly, optimal tuning will be more valuable, for the same reason. By contrast, high-energy seastates will encourage larger devices, possibly uprated generators, and detuning.

(b) The design should respond to some measure of the frequency at which the majority of the energy in the spectrum is located, the "target" frequency discussed in a previous section. Accordingly, we may choose any of the measures of "central" frequency, the power peak ω_{pmax} , the variance peak ω_0 , the power-averaged frequency M_0/M_{-1} , or the zero-crossing frequency $(M_2/M_0)^{1/2}$, for that matter. (Since this first step is only a convenient and intuitive way of sorting the family on a relative scale of central frequency, it is not really important which measure is chosen.) Conceptually, though, a prevalence of "high-frequency" centered seastates will tend to increase the economic value of a higher tuneable frequency. Therefore, it should be expected to put a premium on small flap draft, large buoyant moment, light flap weight, or more sophisticated (and presumably expensive) forms of springing, to supplement the limited hydrostatics. On the other hand, the flap width may be driven upward as well,

because at higher frequencies the absorption becomes a stronger function of width, the device beginning to act as a terminator. To limit this particular tendency, of course, the longer flap will also become more sensitive to directional effects at any given wavelength. By contrast, "low-frequency" centered seastates will be seen as tending to reduce the the need for high tuning, thus favoring increased draft and decreased width, if possible, while maintaining given stroke limits.

(c) The design should respond to some measure of the concentration or dispersion of energy over the frequency scale. That is, a design should recognize the difference between a nearly monochromatic spectrum and a broad-banded spectrum, in terms of power rather than variance. A measure of power "broadness" may be defined as follows. Let ω_C be some "central" frequency measure related to power, such as ω_{pmax} , ω_0 , or ω_{pavg} . Then, a "measure of power broadness" (MPB) can be given as a mean-squared deviation from ω_C , that is:

$$MPB = \int_0^{\infty} \frac{S^+(\omega)}{\omega} (\omega - \omega_C)^2 d\omega \quad / \quad \int_0^{\infty} \frac{S^+(\omega)}{\omega} d\omega \quad (88)$$

which can be arranged as

$$MPB = \frac{M_1}{M_{-1}} - 2\omega_C \frac{M_0}{M_{-1}} + \frac{M_0^2}{M_{-1}^2} \quad (89)$$

Note that if the power-averaged frequency M_0/M_{-1} is used as ω_C , then this expression becomes

$$\text{MPB} = \frac{M_1}{M_{-1}} - \frac{M_0^2}{M_{-1}^2} \quad (90)$$

The effect of a prevalence of spectra in which power is widely dispersed (high MPB) is to put an emphasis on off-tuned absorption, and to make the tuning itself less critical. This in turn will tend to favor larger device dimensions because larger, more heavily damped systems are inherently less sensitive to mistuning. On the other hand, an abundance of concentrated spectra, (such as swell) will tend to favor highly tuned systems, sized to obtain acceptable motions.

(d) Finally, if directional-spectrum information is available, then the design should respond to that, too, in principle. A directional spectrum is usually defined by the following information:

(i) A principal wave direction, θ_p , or possibly even a principal wave direction defined as a function of frequency, $\theta_p(\omega)$.

(ii) A spreading function, generally given such that $S^+(\omega, \theta) = S^+(\omega) F(\theta)$, but also possibly with F a function of frequency as well. Usually, F is given so as to define a symmetric spreading of the spectrum around the principal direction, so that $F(\theta)$ is actually $F(|\theta - \theta_p|)$.

A "power-averaged direction" and a "power-averaged spreading function" could probably be defined in some way,

but this seems to be an unnecessary complication, to say the least. It should suffice, instead, to note that the ideal wave environment for a fixed, directionally sensitive absorber is one in which the principal directions of all spectra are the same, invariant with respect to frequency, and with all spreading functions collapsed to unidirectional seas. To the extent that this isn't so, and it certainly isn't in most real situations, the spectral family and its member spectra would favor shorter flap widths, because these are less sensitive to directionality.

The presence of directional spreading is particularly obnoxious if it occurs at higher frequencies, because of the increased cancellation of the exciting force over the flap width. Although Dawson (Ref. 28) gives suggested spreading functions that show more spreading at lower frequency, reflecting the fact that high-frequency components tend to be aligned with the local wind, in shallow water sites this may be offset by the fact that lower-frequency components may be "despread" by the diffracting effect of bottom contours.

In any case, with some disregard of mathematical rigor, and only vague intuition for that matter, let us try to define a spectral measure of directionality by which we can order the members of the family of spectra according to their principal directions and spreading functions. Let there be some angle α , determined only by the form of the

spreading function, which can be regarded in some sense as an "average" direction from which waves, and therefore power, are incident, relative to the principal direction.

The proposed definition is as follows:

$$\alpha = \int_{-\pi}^{\pi} |\theta| F(\theta) d\theta / \int_{-\pi}^{\pi} F(\theta) d\theta \quad (91)$$

It should be noted that α is not really "power-averaged" unless the spreading function is independent of frequency. If the spreading function is frequency dependent, then a corresponding definition would presumably involve double integration over frequency and direction, and would have to bring in the spectrum explicitly (this is the "complication" mentioned above in connection with a power-averaged direction.) Let's agree to forget it.

Now, one common form of the spreading function $F(\theta)$ is the cosine-power expression

$$F(\theta) = \cos^S \left(\frac{1}{2} \theta \right) \quad (-\pi < \theta < \pi) \quad (92)$$

where the angle θ is to be understood as the angle from the principal direction, as suggested by Dawson. For a coastal sea, this spreading function has the limitation that the directional spectrum must go to zero at $\theta = \pm\pi$, that is, from the direction opposite to the principal. With reflection from a relatively nearby shoreline, it is likely that there would be a "reflected principal direction," as well, with a local maximum of the spreading function. However,

this, too, is a refinement that is not available at present. Dawson further suggests that the exponent S is actually a function of the frequency, but in the interests of simplicity alone, let us use some value of S that "averages" the power. In particular, when $S=0$ we obtain an isotropic sea, with the waves spread uniformly around the entire compass, and $\alpha = \pi/2$. For S extremely large, on the other hand, the spreading function becomes very small except in the principal direction, $\theta = 0$, where it is unity, and α must go to zero. At the spectral peak frequency, Dawson suggests a large exponent, approximately 16, with the exponent decreasing rapidly above and below the peak frequency. For $S = 16$, α is approximately 16° , for example.

Now, for a device oriented normal to the principal wave direction, let us define, as a hypothesis only, a measure of directionality which relates to the effect on power absorption. From previous results, we have seen that the exciting force on a short flap tends to fall off at least as the cosine of the angle of encounter, and therefore the power absorption at least as the cosine squared. Now, let us define the effective angle of encounter in the spread spectrum as $\alpha/2$, since we can say that in an omnidirectional sea ($\alpha = 90^\circ$) equal energy must be incident from each quadrant, at an "average" angle of 45° . Furthermore, let us take the measure of power absorption as

$\cos^2(\alpha/2)$. For a unidirectional sea, α is of course zero, and the measure is unity. At $S=16$, and $\alpha=16^\circ$, the measure is about 0.98. At $S=2$, a typical cosine squared spreading rule, α is approximately 54° , and the measure is 0.80. Finally, at $S=0$, an isotropic sea, the measure becomes 0.5, its minimum.

However, this measure does not include any effect of orienting the device itself at a non-normal angle to the principal direction, say β . By assumption, the power absorption in a unidirectional sea would now be said to vary as $\cos^2 \beta$, where β can go to 90° (edge-on encounter), producing zero absorption. Combining the two effects, spreading and device orientation, we can naively assume that reorienting the device in a directional sea turns the flap more normal to some waves, and further from normal to others, by an amount β . Using a symmetry argument, we can at least postulate that at normal encounter, half the power absorption will be from waves on one side of the normal, and half on the other. Therefore, consider the following combined expression:

$$P = (1/2) [\cos^2 (\alpha/2 - \beta) + \cos^2 (\alpha/2 + \beta)] \quad (93)$$

or, rearranging

$$P = \cos^2 (\alpha/2) \cos^2 \beta + \sin^2 (\alpha/2) \sin^2 \beta \quad (94)$$

Now, this is undoubtedly a very naive way to measure the effect of directionality, and it involves the crudest kinds of assumptions, but it does have theoretically correct

behavior under several limiting conditions. At $\alpha = 90^\circ$, for example, in isotropic waves, the orientation β has no effect on the absorption, as expected. Furthermore, at $\beta = 90^\circ$, edge-on encounter, there is no power absorption unless there is spreading.

To provide a measure of directionality that increases as the situation becomes more directionally critical, we can take $1/P$. Presumably we can now compute a "directionality measure" $DM = 1/P$, for each spectrum in the design set. If the principal directions of all the spectra are essentially parallel, then there will be no problems other than spreading. On the other hand, if not, then the penalty will show up in nonzero angles β for at least some of the spectra, assuming a constant fixed "heading" of the device. In any case, the fact is that larger values of DM should set the design to favor shorter flap width, while very large values of DM will imply almost no absorption at all, regardless of flap dimensions.

Now, having defined rational (or at least semi-rational) spectral measures for power density \bar{Q} , central frequency ω_c , power "broadness" MPB, and directionality DM, how can we use them to guide the first spectral designs? Even within the design set of spectra, there should be a large variation of all these measures. It would be wonderful, of course, if we could average the measures, using the probabilities of the states in the design set as weights,

then reconstruct an "average" design spectrum from them, design a device for this spectrum, and call the result a design for the family. No, that would be a little too intuitive. Besides, even if a family of spectra could be distilled in this way into a single design spectrum, and there is certainly no mathematical or probabilistic reason to believe it, we still lack the means to turn this into a design: we have no transformation that goes from spectral properties to design parameters.

However, we do have some general trends, which we may be able to use. Table IV gives a summary of the general effects of the four spectral measures defined here on the design parameters geometry (specifically flap draft and width), tuning, damping, generator capacity, and structural scantlings. In each cell, the table indicates the effect of an increase in the particular spectral measure, the others remaining constant, on the specific design feature, again, with the other design parameters unchanged. Together with any practical constraints that may exist on the various elements of the design, this summary may help to show which of the constraints are likely to be active in a particular type of spectrum, and therefore, which ones may be "pushed" to greatest advantage.

Of course, in many families of spectra, the spectral measures will not be independent of each other. For example, in the simple one-parameter descriptions, high \bar{Q} is

always accompanied by low ω_C . Clearly, then, in order to have these two measures independent, we will require at least a two-parameter spectral family, involving significant wave height and modal period or frequency, as in Ochi's work (Ref. 42). Even then, the two measures will be correlated. Similarly, the power "broadness" and directionality measures may be found to be related to the wave height and central frequency in some statistically important way.

Furthermore, different combinations of the four measures may represent somewhat special and distinct conditions: e.g., a broad, high-centered spectrum will make somewhat different demands on tuning than an equally broad but low-centered one, quantitatively. Properly, then, Table IV might be extended, with cells accounting for various combinations of spectral characteristics. However, such a refinement is hardly possible at this stage, although it might become so with design experience.

The acquisition and sorting out of "design experience" is an additional function of the spectral measures proposed here. It has been stated that there is no one-to-one function that maps the spectral characteristics into values of design parameters. However, it is possible that after several full family designs have been prepared, iteratively, such a mapping, at least on a regression basis, might begin to show up. In that event, the spectral measures might be-

come quantitatively valuable as design tools.

Since the final economic performance of a proposed device is necessarily based on the power output derived from the entire family of spectra, the "design set" is actually just a convenience. Every member of the family, except an absolute flat calm, contributes something to the total annual power production. Thus, any design for an individual spectrum can only be an intermediate step toward a solution for the entire family. In any case, the designer must get some economic result from every spectrum in the family, even if the result is no power or too much. Thus, there is no way to avoid the necessity for spectral designs, at least several of them, to help define the design for the family. The next step in the design procedure begins that task.

Step 2: Select one spectrum at a time from the design set for analysis. The choice of the first "target" spectrum is not really critical, of course, since we will be returning to this step at least several times, perhaps even until we have exhausted the design set, unless we can somehow reach a rationally satisfying stopping point earlier. However, in terms of making the analysis as efficient as possible, the order of analysis may very well be of some interest. The important thing is to choose the order so that we may at least intuitively expect to acquire design information at each iteration that will be most useful in

the subsequent ones: that is what an heuristic approach means.

For this reason it seems logical to start with a spectrum that comes closest to fitting "typical" values of the spectral measures defined in the previous step (Q , ω_c , MPB, and DM) within the design set. The logic may not be obvious, however, without an argument: after all, there is great deal of information to be gained by trying a design for an extreme member of the design set, as well. Why choose the "middle" first? Implicitly, we are assuming, first of all, that near-optimal design parameters for a particular spectrum should at least vary continuously, although as yet in a quantitatively obscure way, with respect to the over-all characteristics of the spectrum (this had better be true). Second, we must assume that the family of spectra has at least some degree of "compact support" within the probability distribution that describes it. That is, the members of the family, although treated as discrete, must represent some "continuum" of related states with the modal behavior reasonably non-extreme. For example, a sea environment that featured seastate 0 with probability 0.48, seastate 8 with probability 0.48, and rising or decaying seas somewhere in between with probability 0.04, would not be a good family to argue from. On the other hand, it would not be a good family for a wave absorbing device, either.

In any case, if these two assumptions are accepted as valid, then it should follow that a "best" design for the family cannot be completely isolated from the set of "best" designs for at least some of its members, particularly those states near the modal behavior, the "design set" by definition. Thus, it is argued that we can expect to learn more about the design set as a whole, on the first step, by choosing a point "in the interior" rather than "on the boundary." This is particularly justified, of course, if the states nearer the mean or median characteristics within the design set are also of relatively higher weight in probability. In such a case, the states around the "center" of the design set are also more heavily weighted in the over-all economics of the system. Having selected a spectrum as near as possible to "typical," we can subsequently examine the "corners" of the design set to see how much variation of the design results.

Step 3: Consider the spectrum, particularly with regard to its peak frequency, power density (or significant wave height), and concentration. (Directionality may be considered as an afterthought, in the absence of detailed data.) Now, there are two design decisions to make at once, at least on an interim basis: dimensions (specifically flap draft and width) and available tuning (specifically flap buoyancy or springs). Generator rating and maximum external damping coefficient will be considered as a sepa-

rate issue at first.

Unfortunately, the flap dimensions and tuning are generally coupled by hydrodynamic and hydrostatic effects, so that it may be difficult to reach initial decisions independently. However, the difficulty may be resolved in some cases by asking whether there are any constraints on the dimensions, tuning, or both.

The only absolute constraint on flap dimensions that is inherent in the problem (as opposed to arbitrary constraints introduced by construction facilities, etc.) is that the flap draft cannot exceed the water depth. In addition, there is also a good but flexible argument for keeping the flap width small with respect to wavelengths of interest, since only in this way can the maximum absorption cross-section be substantially larger than half the flap width, for a single flap device.

Now, how can we tell whether the water-depth constraint is active, based solely on the spectral information? The answer, generally, is that we cannot, until we obtain some hydrodynamic results. However, there are two factors that would tend to argue immediately for using the maximum flap draft available, subject to constraint, if the water is shallow. These are as follows: (a) large significant wave height, that is, high energy; (b) low peak frequency. It must be remembered, of course, that flap draft can be traded off against flap width for the purposes of stroke

reduction at a given power absorption. However, there is a limit to this process, represented by the two-dimensional problem, that is, even for an infinitely wide flap (in normal encounter, of course) there would be a motion response, determined by the 2-D exciting force, inertia, and damping.

By contrast, increasing the flap draft continues to reduce the motion amplitude, even in 2-D. An infinitely deep flap will not move. Thus, when confronted with either an energetic sea, or a low-frequency one, a first step should be to consider an increase in draft, if possible. In the case of an energetic, high-frequency seastate, however, the increase in draft must be weighed against the adverse effect on maximum tuning. Thus the designer should expect that there are many cases when an essentially "arbitrary" initial assumption has to be made regarding flap draft, as well as other dimensions. In such cases, however, purely practical limitations on dimensions may arise to give an approximate starting point.

Accordingly, we must select an initial estimate of the geometry, \underline{G} , often without much rational basis in hydrodynamics. However, there is no point agonizing over what the dimensions "should" be from the hydrodynamic point of view. The linear hydrodynamic model basically implies that there is no such thing as "wrong" dimensions, independent of tuning, damping, and directionality.

In fact, optimum flap dimensions do exist, from an economic standpoint, even when the power absorption increases monotonically and no formal constraints are invoked. For example, even in normal, completely unidirectional seas, there is no point in pursuing additional absorption by means of flap width, ad infinitum. This only leads to the 2-D result, absorption equal to one-half the incident power, at best. Since it has already been demonstrated that a more favorable cross-section can be obtained by short flaps, even when overdamped as required to satisfy stroke limits, it is clear that dimensions will not be driven out of reasonable bounds. Furthermore, non-normal encounter or directional spreading will hold the optimal flap width down even more stringently.

For the flap draft the problem is even more closely circumscribed, although not for the same reason. In fact, at a fixed, finite flap width, the maximum absorption cross-section per unit of draft (an odd ratio, physically) becomes increasingly large at small draft: the draft has a very small effect on the maximum absorption at optimal tuning and damping. Thus, if the flap draft has a cost associated with it, and it certainly does, then the "optimal" flap draft (for maximum absorption per unit cost in draft) is near zero, regardless of width. Unfortunately, of course, a very small draft implies that the maximum absorption only occurs at an impossibly large motion ampli-

tude, so that this optimum is not obtainable.

However, to move away from this infeasible optimum in the direction of feasibility there is a fairly obvious path to follow. No power is lost by increasing the draft until the motion amplitude is acceptable, or up to the draft limit, whichever comes first, provided that optimal tuning can be maintained as the flap gains inertia. Generally, since this entails an increase in spring constant, the flap buoyancy must be increased faster than the weight. The effects on flap cost, then, arise from the larger draft itself, the required additional buoyancy (which may require an increasingly "thick" boxlike flap), and the increased weight and strength of fixed structure needed to hold the flap down against its excess buoyancy.

However, if the flap draft is constrained (or the tuning starts to become critical) before the motion is sufficiently reduced, the flap width can also be increased. This move has a smaller effect on the required spring constant than the draft, and actually gives some increase in maximum absorption at higher frequencies, although an eye has to be kept on directionality as the flap width is increased. The additional costs of width, however, are somewhat different than for draft. First, the flap is subject to a horizontal bending moment due to wave loads. This will increase at least as width squared if the flap is kept on only two pivots, while the box thickness may not be large

enough to give a sufficient section modulus without increased scantlings. Vertical bending moment also arises from the excess buoyant force, but at least the flap draft is the long dimension of the box section. Thus, there should come a flap width when a third hinge point is cheaper than increased bending stress. Torsional loads (arising from the power takeoff, or from oblique wave encounter) will also become important if the flap becomes too long and "ribbony." Because of these structural effects, it will also be noted that if the flap weight increases too quickly, the tuning will begin to drift away from optimal absorption.

Thus, if the flap has reached one of these practical width limits, or if directionality begins to get critical, then we have run out of dimensions that we can use to control the motion amplitude. The only remaining variables are the tuning and damping. To tune away from the energy will reduce the motion very quickly, but it will also reduce the absorption drastically. On the other hand, overdamping does represent an alternative to increased dimensions, although there will be a loss of absorption roughly in proportion to the required remaining motion reduction.

Now, it should be reemphasized that the influence of flap dimensions on power absorption remains small only when near a resonant tuning: off the resonance, increasing flap

width increases the power with relatively little effect on the motion, which is small anyway because of the nonresonant tuning. Accordingly, if the tuning is forced for practical reasons to be well away from the energetic frequencies of the spectrum, either because of limited hydrostatic spring resources or because the spectrum itself is wide, then the possible paths to increasing the power output will include increased width and draft, as well as increased damping.

Here, finally, are a few simple guidelines for the the initial selection of the flap geometry:

Flap Width

(a) Assume a flap substantially shorter than the shortest wavelength of economic interest (can't be too far above the energy averaged frequency).

(b) Assume a flap width short enough to envision it responding as a rigid body without requiring more than a simple box structure, preferably with only two hinge points and one power-takeoff.

(c) Assume a flap width short enough to build, transport, and install in one piece.

(d) If you can be sure that resonant tuning will be obtainable, either because of a low frequency "target" or the application of additional spring forces (mechanical, pneumatic, etc.), then by all means assume as short a flap as you dare. You will have to increase it by and by, unless

the spectrum is of very low energy.

Flap Draft, Freeboard, and Pivot Location

(a) Assume a flap draft large with respect to the significant wave amplitude, at least 4 or 5 ζ_A .

(b) In shallow water, assume a flap draft as large as possible, unless the wave amplitudes are very small. The flap draft must be considered primarily as an effective and inexpensive cure for excessive motion amplitude, rather than as a bid for increased absorption.

(c) On the other hand, assume a flap draft that is quite small with respect to the "target" wavelength. As a rule, systems with $ka > 0.5$ will prove most difficult to tune, without requiring spring systems in addition to hydrostatics. Note that this suggestion, together with (a) above, implies a maximum wave steepness, height/wavelength, for hydrostatically sprung systems, of about 3 percent. Small waves.

(d) Do not add a lot of flap freeboard. Linear theory has nothing to say about the effect of freeboard per se on either absorption or motion amplitude. Nevertheless, it has a substantial effect on the weight, center of gravity, and intrinsic inertia of the flap. All of these effects are counterproductive for tuning up to higher-frequency wave components. Suggestion: zero freeboard.

(e) On the other hand, do not put the top of the flap below the still water line. (Surprisingly, linear theory

predicts that this will not change the power absorption very much, for reasonably long waves, but it will increase the motion response, which is not a good thing.)

(f) Put the pivot as near as possible to the bottom of the flap for minimum angular motions. A lower pivot point will also reduce motions, but so will increased draft. Therefore, the complication of a system of struts to support the flap does not seem justified.

Flap Thickness and Buoyancy

(a) If the flap is of boxlike construction, choose the thickness to obtain the highest required resonant tuning with hydrostatics only, if possible. From a hydrodynamic point of view, the results of the present model are adapted only to relatively thin flaps, however. From rough estimates (see the appendix) a box flap thickness up to about 40 percent of the draft should still show the right trends.

(b) Relatively large flap thickness is also good for structural reasons, since it makes the flap a more efficient structure against horizontal bending moment and torsion.

(c) On the other hand, if the flap is to be thin, perhaps of stiffened single-plate construction, and will depend either on added buoyancy members or non-hydrostatic springs, then remember that the bending moment still exists, and that additional hinge points and power takeoff points may be required.

Flap Separation for Twin Flaps

(a) For a twin-flap device, keep the separation as small as possible, certainly less than a quarter of the shortest wavelength of interest.

(b) However, for safety against flap collisions, the flaps cannot be less than one flap draft apart, and two drafts would be better.

Step 4: Calculate the required hydrodynamic coefficients, using the initial estimates of flap geometry and the water depth, for several frequencies over the range of the spectrum. The hydrodynamic analysis can also be used to provide estimates of wave loads for detailed structural calculations.

Step 5: Design a flap. Calculate the buoyancy of the flap and its lever arm about the pivot, then estimate the weight and center of gravity. These quantities, then, will determine the maximum linear hydrostatic spring constant that is available. Similarly, a first estimate of the moment of inertia of the flap about the pivot is required, although this is not critical because in most cases the added mass will dominate. However, the weight and center of gravity are very important.

Step 6: Check the tuning. Compare the available hydrostatic spring against the requirement for resonance

near the frequency of the spectral peak. If resonant tuning is available, or very close to it, then proceed directly to Step 7. If not, then consider whether it is advisable or possible to attempt a quick redesign to obtain a more nearly resonant tuning. If the seastate under consideration is small to moderate, then it may be advantageous to try to improve the tuning. However, if the tuning is very deficient, as it may be with a high-centered spectrum, then small modifications to the device, such as weight saving, will not have a great effect on the tuning. A major increase in flap buoyancy might. Other possible revisions include draft reduction, which may not be an option if the spectrum is too energetic, or the addition of external spring forces in addition to hydrostatics, which will add expense, but which should not be overlooked. On the other hand, if the spectrum is very energetic, consider how little might be gained by improving the tuning, since the device will have to be overdamped to maintain a given required level of motions. Now, proceed directly to step 7.

Step 7: Choose the damping for maximum absorption at the peak frequency, and calculate and plot the specific absorption and motion RAO curves at several frequencies, spanning the range of the spectrum. The optimum damping for the spectrum will be considerably higher than this.

Step 8: Calculate the average absorption and motion

response spectrum for the device, using the initial estimate of damping from Step 7. From the response spectrum, calculate the root-mean-square motion. Check for excessive response, as measured by extreme values or number of "over-strokes" per hour, as described in the previous section on random sea response. If the device is exceeding the specified motion, then increase the damping and recalculate the motion, until the motion has been damped to the required value. Then recalculate the average absorption.

Step 9: Increase the damping to broaden the power absorption curve. Several larger dampings should be investigated and the average absorption recalculated. Increased damping is more important in broader spectra. The optimum damping can then be found from a plot of $\overline{P_{ABS}}$ versus damping, at the constant tuning. Never underdamp.

Step 10: Choose or check the generator rating and power-takeoff system. Estimate the conversion efficiency and calculate the average power output corresponding to the average absorption $\overline{P_{ABS}}$. (See the appendix for details.)

Step 11: Estimate the costs of the flap, support, and power takeoff systems and calculate the average cost per kW·hr of energy production in the spectrum under consideration. See the appendix for a suggested cost model.

Step 12: If the system had a near resonant tuning in Step 6 and had to be overdamped in Step 8 in order to reduce the motion response to an acceptable level, then a larger flap may in fact offer better economic performance than severe overdamping. Increase the draft if possible, because that is the less expensive dimension. Return to Step 4 and iterate through Step 11.

Even if the system did not have to be overdamped, a larger flap should be tried once to confirm that smaller is better. If the spectrum is broad enough, then a less sensitive tuning may give better economic performance. Increase the width, if possible, because that will degrade the tuning the least. Return to Step 4 and iterate through Step 11.

Finally, if the system did not have a near resonant tuning in Step 6, why not try new springs or a thicker flap now. Return to Step 6 and iterate through Step 10.

Step 13: When an increase in flap dimensions fails to secure improvement in the economics for a particular spectrum, then there is no point in continuing. (If the starting point was selected properly, then smaller flap dimensions will result in excessive motion and required damping. Furthermore, since a generator capacity has been chosen specifically for the absorption of a given flap size, in Step 10, there can be no issue of increasing flap size to obtain any "hidden" economies of scale in the generator.

Note the that the "design for the spectrum" can be thought of as consisting of only three main elements, each of which may be modified separately when the time comes to consider the "design for the family": (a) the flap geometry; (b) the maximum tuning; (c) the generator rating. Consideration of the family can begin as soon as we start to collect spectral designs.

As each spectral design is arrived at, the over-all economics of that particular design in the family is calculated by determining its performance in each of the other members of the family of spectra, the "off-design" conditions. For each off-design seastate, the tuning may be adjusted from the design condition, subject to its limitation by available spring forces, and the damping may be reset to maximize power output, but the flap dimensions and generator rating are assumed to be constant, for the present. Thus, in many cases, the iterations required for the off-design performance will be limited: for example, in higher frequency off-design states the tuning will be given by inspection as the maximum tuning available; similarly, in higher-energy off-design states, the power output can generally be written down simply as the generator rating.

For comparison purposes in attempting to derive a design for the family, the following information should be attached to each spectrum design after the off-design calculations have been finished: (a) the average annual power

output; (b) the probability (summed over all seastates) of operating at full generator capacity; (c) the probability of operating with tuning set to its maximum constrained value; (d) the average annual cost per kW·hr.

After several spectrum designs have been prepared, a pattern may begin to emerge. If there is a candidate, or a range of candidates, having a particularly favorable annual average cost per kW·hr, then, intuitively, these designs should be developed for the family. However, the designs need not be accepted completely unmodified. First, the marginal value of generator capacity should be examined, considering whether a larger (or smaller) generating plant would improve the over-all performance. Second, the marginal value of maximum spring constant should be checked. If both of these values are small, then the best spectrum designs should be quite close to an optimum for the entire family.

CONCLUSIONS

The purpose of this work has been to establish a method of estimating the performance of three-dimensional flap-type absorbers in finite depth water. This method is intended to enable the designer to take account of the effects of finite device width, and to estimate the degrading influence of oblique wave encounter. Both of these effects are significant in terms of the over-all economic feasibility of this class of devices.

The following general conclusions may be offered with regard to flap-type devices.

(1) In waves that are substantially longer than the device width, these absorbers are capable of developing absorption cross-sections substantially longer than their width. Thus, the 2-D result of 50 percent maximum "absorption efficiency" is misleading. When the device is short with respect to wavelength, it acts as a "directional point absorber," in that the cross-section becomes a function of wavelength alone, while the device still maintains a preferred direction for absorption. In this respect, the situation resembles that of a radio antenna, in which the "frontal area" of the antenna has nothing to do with the

amount of energy that can be absorbed.

(2) By comparison with a symmetric (nondirectional) point absorber, it appears that a directional device can attain twice the maximum absorption cross-section in the long wave limit, in normal encounter. Of course, unlike the nondirectional device, the cross-section of a flap-type absorber decreases for angles of encounter other than normal. For flaps that are short with respect to the wavelength, the reduction in exciting force is approximately as the cosine of the encounter angle, so that the single-flap power absorption decays as the cosine squared.

(3) All flap dimensions have a very strong influence on the motion amplitude of the device at maximum absorption. Since, in the long wavelength regime, the maximum absorbed power is essentially independent of dimensions, while the exciting force is smaller for a small device than for a large one, a small flap must move with very large amplitude in order to absorb the power. To the extent that practical restrictions imposed by machinery, as well as the limitations of the linear prediction, make these large amplitudes unrealistic, a larger flap has an advantage in achievable power absorption that can be weighed against increased cost.

(4) Flap dimensions, and especially draft, have important secondary effects in determining the relationship between inertia and the maximum hydrostatic restoring

moment, and therefore on the ability to adapt the tuning of the device to various wave frequencies without the use of mechanical or pneumatic springs.

(5) In off-tuned conditions, such as over the range of a random sea, the ability to absorb useful amounts of energy is increased by additional damping, well beyond the "optimal damping" at the central frequency of the spectrum.

(7) In designing for a spectrum that is not very narrow, larger flap dimensions, whether draft or width, increase the net absorption. This occurs in two ways. First, the larger flap is not nearly so lightly damped as the smaller. Thus, its power absorption is not as peaked at near-optimum damping. At the same time, a larger flap draft moves the area of peak added mass into the region of reasonable ocean wavenumbers. When the added mass flattens out, the sensitivity to gross undertuning is much reduced.

(8) Nonlinear control is not of great value in situations where the flap motion is arbitrarily limited, for example, by power takeoff machinery limits. By contrast, when the tuning is off, a purely damping-controlled device has a very small resulting motion and absorption. In such a case, the use of an optimal controller to increase the stroke represents an entirely different problem.

(9) By the same token, in random seas a control force, other than straight constant-coefficient damping, can permit the device to function within acceptable motion rest-

rictions without the necessity for perpetual overdamping and consequent loss of absorbed power. On the other hand, the device so controlled cannot be treated analytically by linear theory, using the usual frequency-domain equations of motion.

(10) The twin-flap device, when operated at ideal tuning and damping for a particular frequency, (which are considerably harder to discover than for a single flap) can obtain approximately twice the absorption of a single flap. This added absorption occurs through partial cancellation of the radiated wave and, at certain frequencies, through an increase in the exciting forces due to diffractive effects. However, the twin-flap concept has a number of detailed design problems. First, in order to keep the hydrodynamic coefficients from becoming very sensitive to wavelength, the spacing between flaps must be kept small with respect to wavelengths of interest. For rolling flaps, this requirement may become a constraint on flap draft. Second, in order to achieve a strong cancellation of the radiated wave, the flaps must be fairly wide with respect to their separation. This requirement makes directionality more critical. Third, optimal tunings and dampings for twin-flap devices can include negative values of spring constants and even damping coefficients (as was also noted in 2-D results). Such values may not be obtainable for simple mechanical systems. Finally, for non-optimal

tunings and dampings, the twin-flap device often fails to produce twice the cross-section of a single-flap device. Since, by hypothesis, a twin-flap device (with a power takeoff system on each flap) is approximately twice as expensive as a single-flap of equivalent width, it seems that in general it would be a simpler and better alternative to use the additional flap device as part of an array of single flaps, rather than as a rear element in a twin-flap. However, there may be certain advantages to be gained if one of the flaps can be a passive oscillator, without an external damper. As shown by the economic example included in the appendix, the power takeoff and conversion systems represent a major portion of the system cost (other than transmission cable), while the flaps themselves can be built relatively cheaply, being simple flat-plate structures. This concept deserves further study.

There remain many questions about certain aspects of the flap-type absorber. Suggested avenues for future work include:

- (1) An investigation of the use of control forces, by an application of a time-domain analytical technique.

- (2) A study of nonlinear wave forces on the device, in an attempt to remove (or justify) arbitrary restrictions on flap motion, and to determine whether the achievable power absorption may thereby be increased without violating rel-

evant physical laws or breaking the machine.

(3) An extensive design family can be developed using the analytical and design methods proposed here. This may begin to clarify certain questions that remain, even within the context of linear theory. In particular, optimum values for the geometry, tuning and damping of a device for either a particular seastate or a collection of seastates, may be worth developing.

(4) A more detailed prototype design, together with firm vendor quotations on certain cost items, will be necessary at the next stage of development.

REFERENCES

1. N.N. Panicker, "Review of the Technology for Wave Power Conversion," Marine Technology Society Journal, Vol 10, 1976.
2. Proceedings of the International Symposium on Wave and Tidal Energy, Cambridge, 1979.
3. Proceedings of the Second International Symposium on Wave and Tidal Energy, Cambridge, 1981.
4. B.M. Count and E.R. Jefferys, "Wave Power, The Primary Interface," Thirteenth Symposium on Naval Hydrodynamics, Tokyo, 1980.
5. S.H. Salter, D.C. Jeffrey, and J.R.M. Taylor, "The Architecture of Nodding Duck Wave Power Generators," The Naval Architect, Jan 1976.
6. F.J.M. Farley, "The Triplate Wave Energy Converter," Proceedings Wave Energy Conference, London, 1978.
7. C. Cockerell, M.J. Platts, and R. Comyns-Carr, "The Development of the Wave Contouring Raft," Proceedings Wave Energy Conference, London, 1978.
8. Y. Masuda, G. Kai, T. Miyazaki, and Y. Inoue, "The Sea Trials and Discussions on the Wave Power Generating Ship KAIMEI," Thirteenth Symposium on Naval Hydrodynamics,

Tokyo, 1980.

9. J. Falnes and K. Budal, "Wave Power Conversion by Point Absorbers," Norwegian Maritime Research, Vol 6, 1978.

10. R.M. Scher, A.W. Troesch, and G. Zhou, "Experimental and Theoretical Evaluation of a Twin-Flap Wave Energy Absorbing Device," Ocean Engineering, Nov 1983.

11. M.A. Srokosz and D.V. Evans, "A Theory for Wave Power Absorption by Two Independently Oscillating Bodies," J Fluid Mech, Vol 90, 1979, pp 337-362.

12. M.R. Haddara, "Directional Spectra Estimates for Ship Motion and Stability Calculations," University of California--Berkeley, Department of Naval Architecture, 1971

13. A.D. Carmichael, "An Experimental Study and Engineering Evaluation of the Salter Cam Wave Energy Converter," Sea Grant College Program, Massachusetts Institute of Technology, Report MITSG 78-22, 1978.

14. D.V. Evans, "Diffraction of Water Waves by a Submerged Vertical Plate," J Fluid Mech, Vol 40, 1970, pp 433-451.

15. O. Faltinsen and F.C. Michelsen, "Motions of Large Structures in Waves at Zero Froude Number," International Symposium on the Dynamics of Marine Vehicles and Structures, London, 1974.

16. A.W. Troesch, "The Diffraction Potential for a Slender Ship Moving Through Oblique Waves," The University of Michigan, Department of Naval Architecture and Marine

Engineering, Report No 176, 1976.

17. M. Abramowitz and I.A. Stegun, Eds, Handbook of Mathematical Functions, Dover, New York, 1965.

18. V.J. Monacella, "On Ignoring the Singularity in the Numerical Evaluation of Cauchy Principal Value Integrals," David Taylor Model Basin Report 2356, 1967.

19. J.V. Wehausen and E.V. Laitone, "Surface Waves," Encyclopedia of Physics, Springer-Verlag, Berlin, 1960, Vol 9, pp 446-778.

20. G.J. Zhou, "Documentation of a Fortran Program for Solving Three-Dimensional Free Surface Problems," University of Michigan, Department of Naval Architecture and Marine Engineering (personal communication, 1982).

21. L.J. Harding, "Numerical Analysis and Applications Software Abstracts," University of Michigan, Computing Center Memo 407, 4th ed, 1979.

22. J. Kotik, "Damping and Inertia Coefficients for a Rolling or Swaying Vertical Strip," J Ship Research, Oct 1963.

23. N. Toki, "Documentation of a Fortran Program to Solve the Diffraction Problem of False Bottom," University of Michigan, Department of Naval Architecture and Marine Engineering, (personal communication, 1982).

24. J.N. Newman, "The Exciting Forces on Fixed Bodies in Waves," J Ship Research, Dec 1962.

25. M. Stiassnie and G. Dagan, "Wave Forces on a Sub-

merged Vertical Plate," J Eng Math, Vol 7, 1973, pp 235-247.

26. D. Bauermeister, "Evaluation of a Three Dimensional Wave Energy Recovery Device," University of Michigan, Department of Naval Architecture and Marine Engineering, Ship Hydrodynamics Laboratory, Report 388771 (unpublished).

27. S.H. Salter, "Recent Progress on Ducks," First Symposium on Wave Energy Utilization, Gothenburg, Sweden, 1979.

28. J.K. Dawson, in "Wave Energy", Energy Paper No. 42, H.M. Stationery, 1979.

29. H.W. Bishop and G.R. Rees, "An Electrical Generation and Transmission Scheme for Wave Power," First Symposium on Wave Energy Utilization, Gothenburg, Sweden, 1979.

30. I. Glendenning, "Generation and Transmission," Proceedings Wave Energy Conference, London, 1978.

31. K. Budal and J. Falnes, "Interacting Point Absorbers with Controlled Motion," Power from Sea Waves, Proceedings I.M.A. Conference, Edinburgh, 1979.

32. T.F. Ogilvie, "First- and Second-Order Forces on a Cylinder Submerged under a Free Surface," J Fluid Mech, Vol 16, 1963, pp 451-472.

33. M.S. Longuet-Higgins, "The mean Forces Exerted by Waves on Floating or Submerged Bodies with Applications to

Sand Bars and Wave Power Machines," Proceedings Roy Soc London A, Vol 352, 1977, pp 463-480.

34. H. Maeda, H. Tanaka, T. Kinoshita, "Theoretical and Experimental Study on Wave Power Absorption," Thirteenth Symposium on Naval Hydrodynamics, Tokyo, 1980.

35. M. Takagi, K. Saito, and S. Nakamura, "Comparisons of Simulation Methods for Motions of a Moorde Body in Waves," ASME Third Offshore Mechanics and Arctic Engineering Symposium, New Orleans, 1984.

36. J.N. Newman, "Transient Axisymmetric Motion of a Floating Cylinder," Fourteenth Symposium on Naval Hydrodynamics, Hamburg, 1984.

37. M.K. Ochi, "Extreme Behavior of a Ship in Rough Seas--Slamming and Shipping of Green Water," Trans Soc Naval Architects and Marine Engineers, Vol 72, 1964, pp 143-202.

38. J.A. Crabb, "A Review of Wave Measurement and Analysis and Analysis Methods Relevant to the Wave Energy Programme," Proceedings Wave Energy Conference, London, 1978.

39. Z.S. Fang and N. Hogben, "Analysis and Prediction of Long Term Probability Distributions of Wave Heights and Periods," NMI Ltd Report No R146, 1982; reported in The Naval Architect, Feb 1984.

40. O.G. Houmb and T. Overvik, "On the Statistical Properties of 115 Wave Records from the Norwegian

Continental Shelf," University of Trondheim, Division of Port and Ocean Engineering, 1977.

41. G.R. Mogridge, E.R. Funke, W.F. Baird, and E.P.D. Mansard, "Analysis and Description of Wave Energy Resources," Second International Symposium on Wave Energy Utilization, Trondheim, 1982.

42. M.K. Ochi, "Wave Statistics for the Design of Ships and Ocean Structures," Trans Soc Naval Architects and Marine Engineers, 1978, pp 143-202.

43. R. Shaw, Wave Energy--a design challenge, Ellis Horwood, Chichester, 1982.

44. H. Benford, "The Practical Application of Economics to Merchant Ship Design," The University of Michigan, Department of Naval Architecture and Marine Engineering, Report No 12, 1967.

45. Q-Corporation, "Concept Feasibility Tests and Evaluation of the Tandem-Flap Wave Power Conversion System," Troy, Michigan, 1982.

46. D.V. Evans, "The Submerged Cylinder Wave Device," Proceedings Wave Energy Conference, London, 1978.

47. D.E. Turnbull, Fluid Power Engineering, Newnes-Butterworths, London, 1976.

48. R. Meir, "The Development of an Oscillating Water Column," Proceedings Wave Energy Conference, London, 1978.

49. G.W. Moody, "The N.E.L. Oscillating Water Column--Recent Developments," First Symposium on Wave

Energy Utilization, Gothenburg, Sweden, 1979.

50. P.J. Rance, "The Development of the H.R.S. Rectifier," Proceedings Wave Energy Conference, London, 1978.

51. L.S. Wirt, "Wave-Powered Motor," U.S. Patent 4,152,895, 1979.

52. R.J. Grant, C.G. Johnson, and D.P. Sturge, "Performance of a Wells Turbine for Use in a Wave Energy System," Proceedings Third International Conference on Future Energy Concepts, IEE Conference Publication No 192, 1981.

53. M.J. French, "The Flexible Bag Device," Proceedings Wave Energy Conference, London, 1978.

54. N.W. Bellamy, "A Second Generation Wave Energy Device--The Clam Concept," Proceedings Third International Conference on Future Energy Concepts, IEE Conference Publication No 192, 1981.

55. A.R.S. Wallace and H.R. Whittington, "Routing of Submarine Cables for Wave Power Transmission," Third International Conference on Future Energy Concepts, IEE Conference Publication No 192, 1981.

56. D.S. McIlhagger, "Output Optimization from a Group of Wave Energy Converters," Third International Conference on Future Energy Concepts, IEE Conference Publica-

tion No 152, 1981.

57. J. Korn, (Ed), Hydrostatic Transmission Systems, Intertext, London, 1969.

58. I. Glendenning, "Ocean Wave Power," Applied Energy, Vol 3, 1977, pp 197-222.

59. A. Papanikolaou, "Schwingungen von Schwimmenden Zylindern," Institut für Schiffstechnik, Technische Universität Berlin, 1980.

60. M.K. Ochi, "Principles of Extreme Value Statistics and their Application," Extreme Loads Response Symposium, Arlington, 1981.

61. American Bureau of Shipping, Rules for Building and Classing Steel Vessels.

62. R.M. Scher and H. Benford, "Some Aspects of Fuel Economy in Bulk Carrier Design and Operation," Shipboard Energy Conservation '80, Soc Naval Architects and Marine Engineers, New York, 1980.

63. R.F. Beck and R.M. Scher, "Technical and Economic Feasibility of a Flap-Type Wave-Power Conversion Device," report to Q-Corp, Troy, Michigan, 1979 (unpublished).

64. R.M. Scher, "Economic Comparison of Salter-Cam and Reciprocating Flap Wave-Power Conversion Systems," report to Q-Corp, Troy, Michigan, 1979 (unpublished).

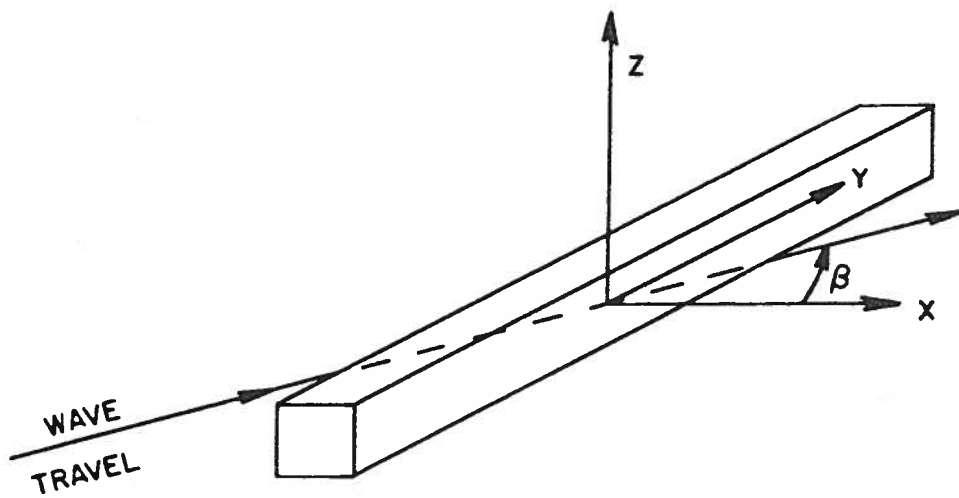


Fig. 1. Coordinate system for a terminator.

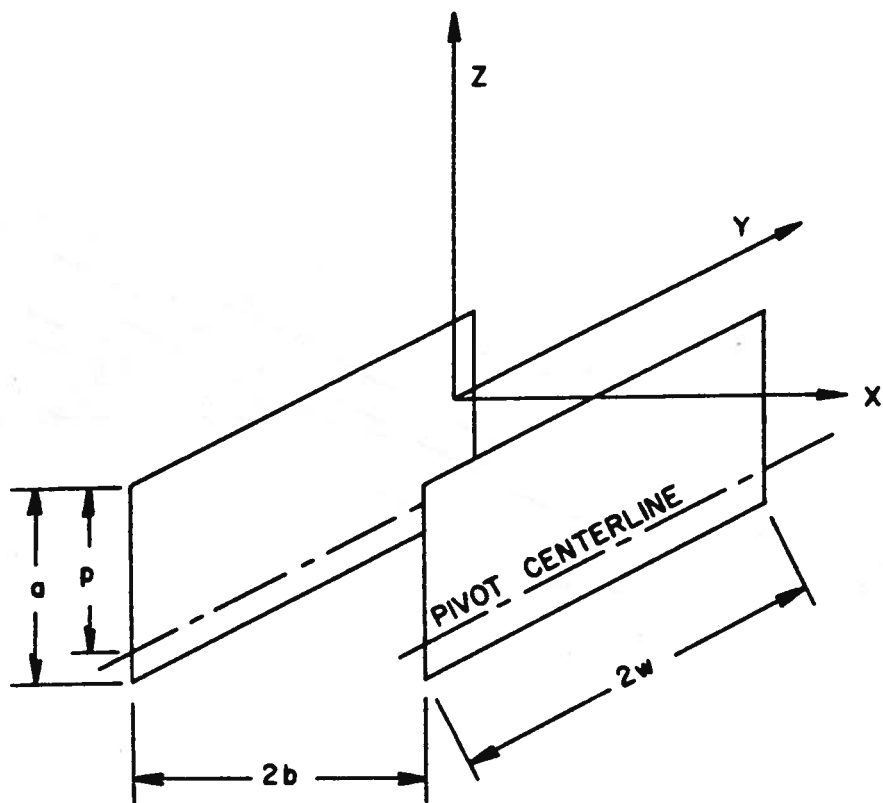


Fig. 2. Coordinate system and dimensions for a flap-type absorbing device.

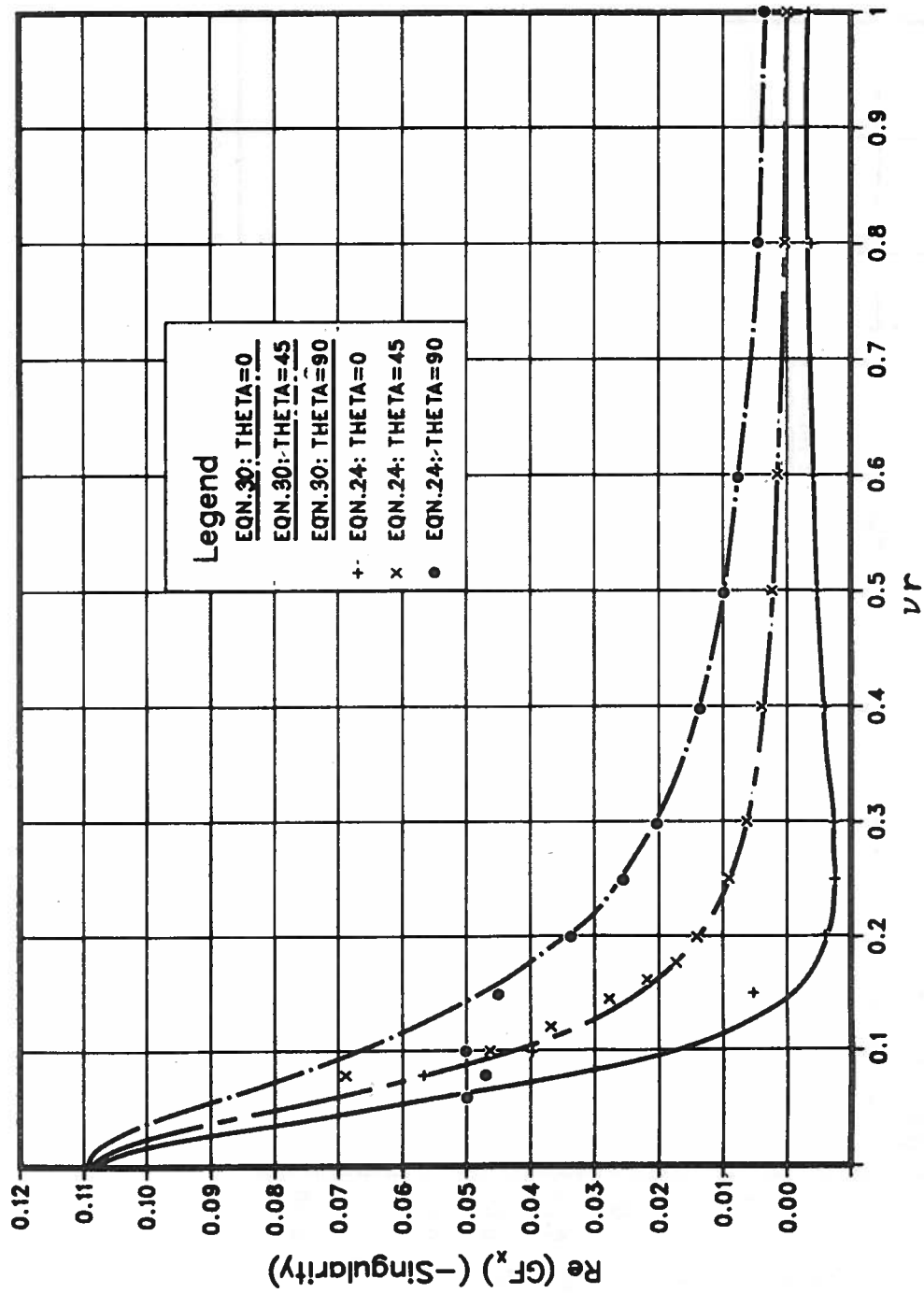


Fig. 3a. Comparison of Green's function values.

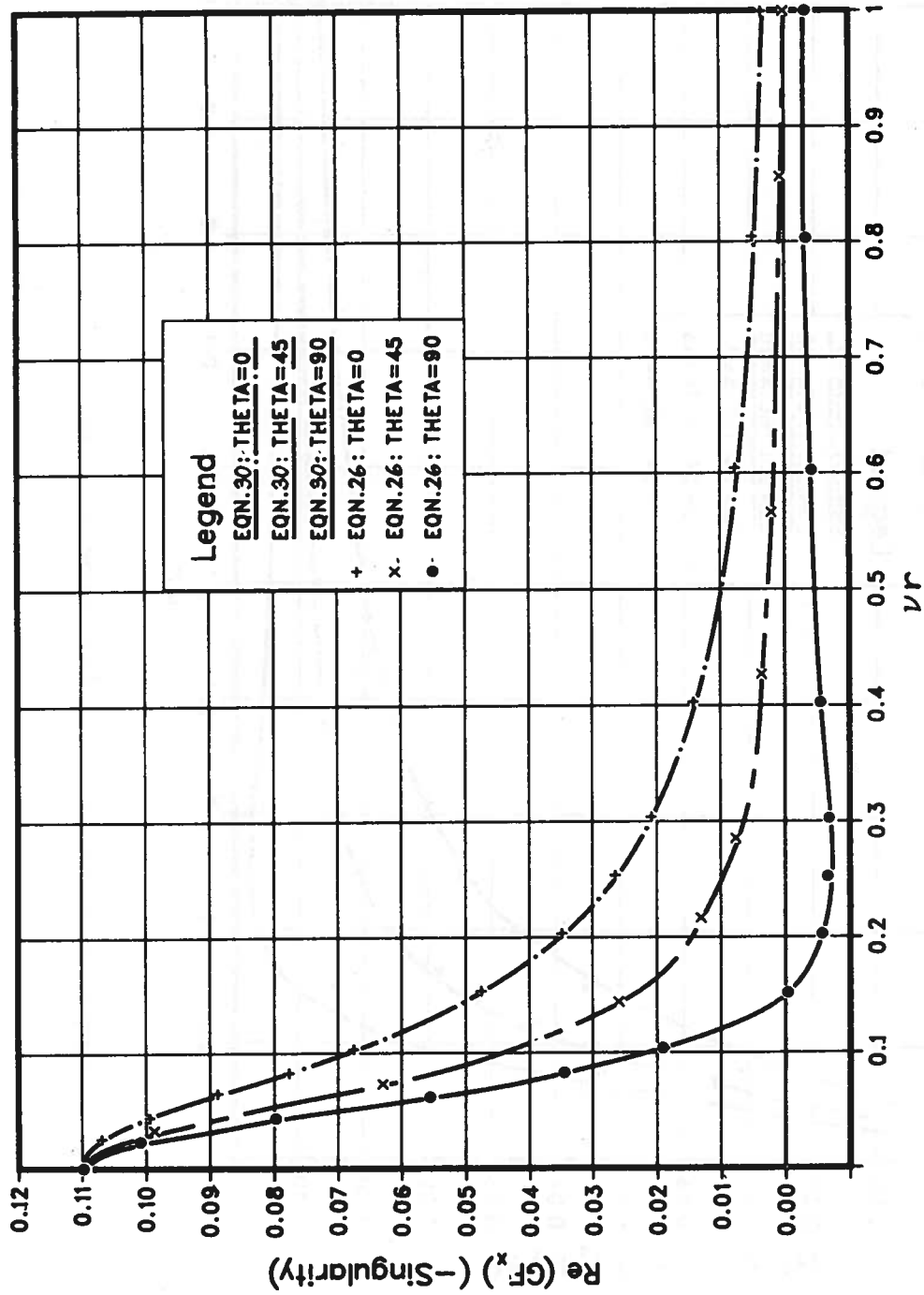


Fig. 3b. Comparison of Green's function values (continued).

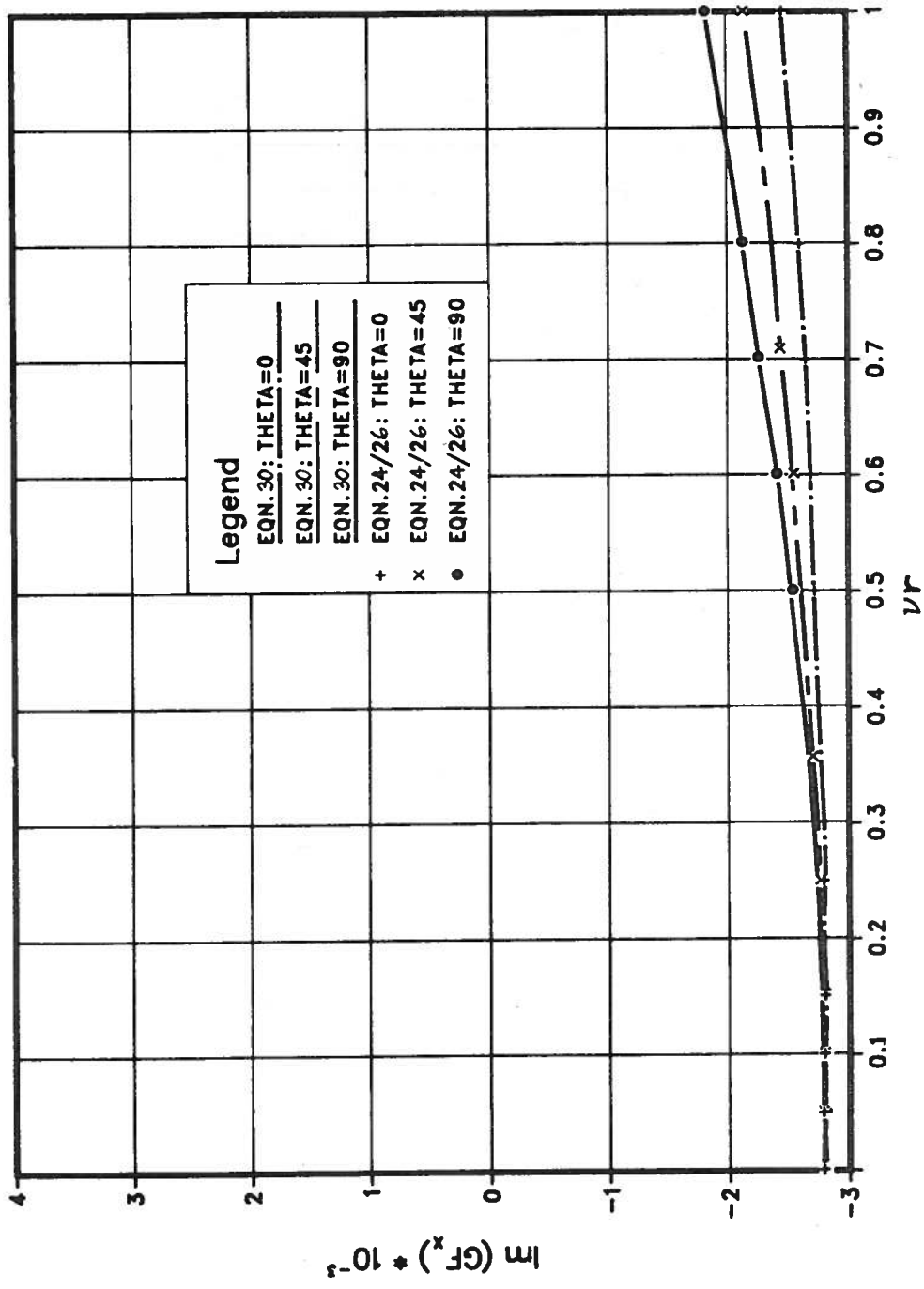


Fig. 3c. Comparison of Green's function values (continued).

FLAP 1

1	$n+1$			
2				
3				
n	$2n$			mn

FLAP 2

$mn+1$				
$(m+1)n$				$2mn$

Fig. 4. Quadrilateral numbering scheme.

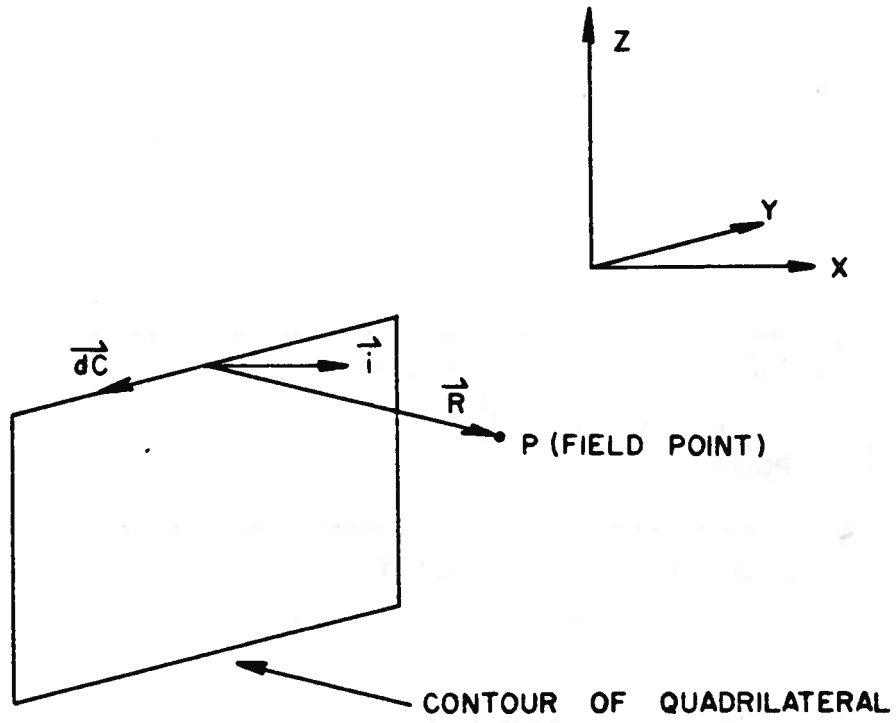


Fig. 5. Application of Biot-Savart law to calculation of singular terms of dipole Green's function.

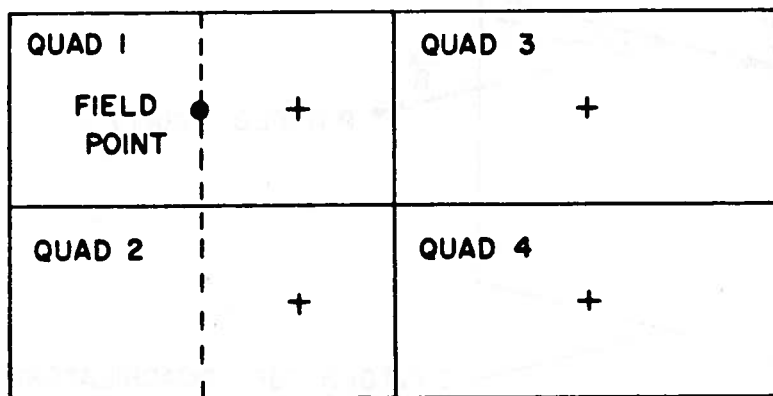


Fig. 6. Half-quadrilateral scheme for use of mid-point rule integration of wave terms on local "stack" of quadrilaterals.

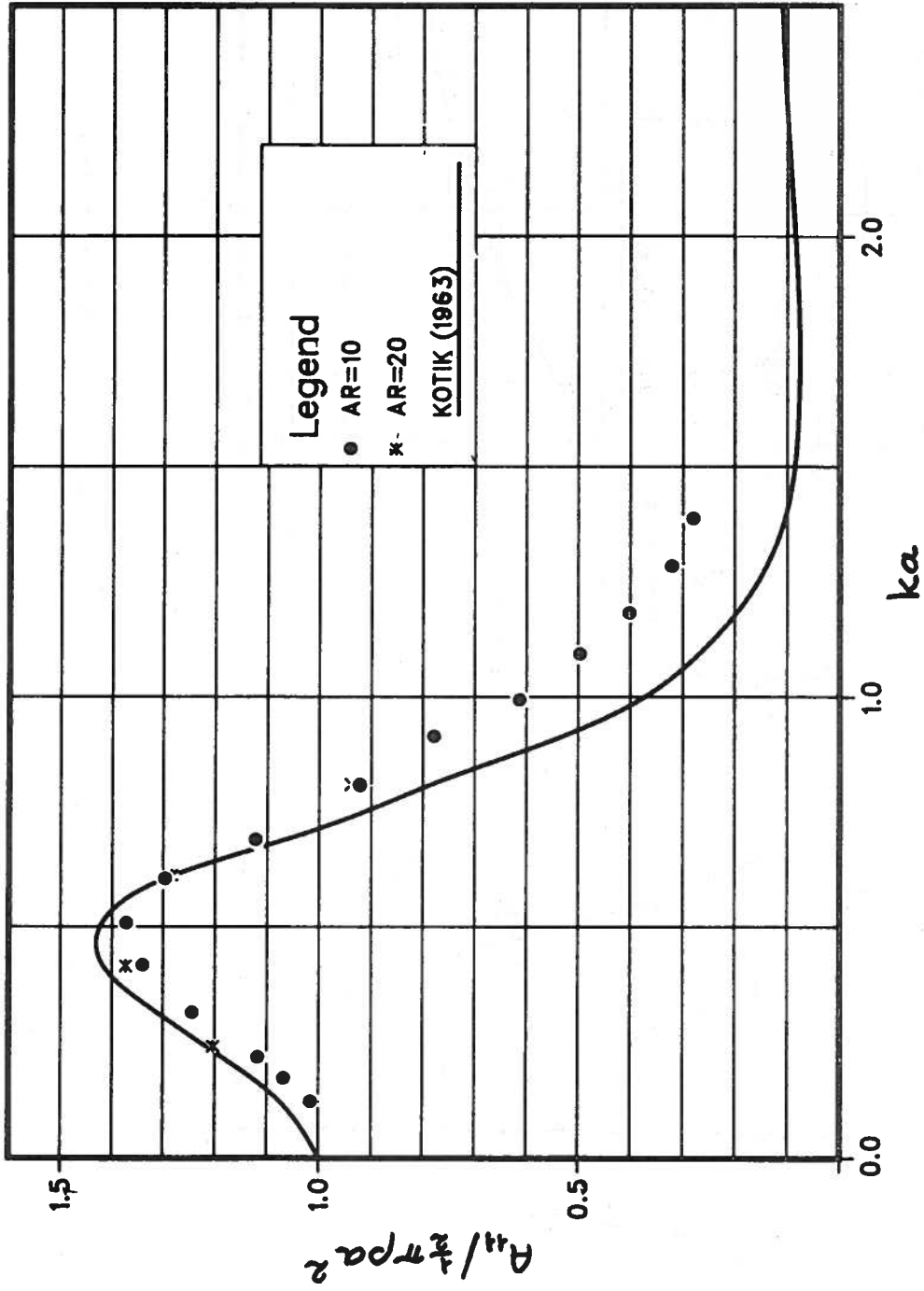


Fig. 7. Comparison of added mass coefficients versus Kotik's 2-D prediction (sway).

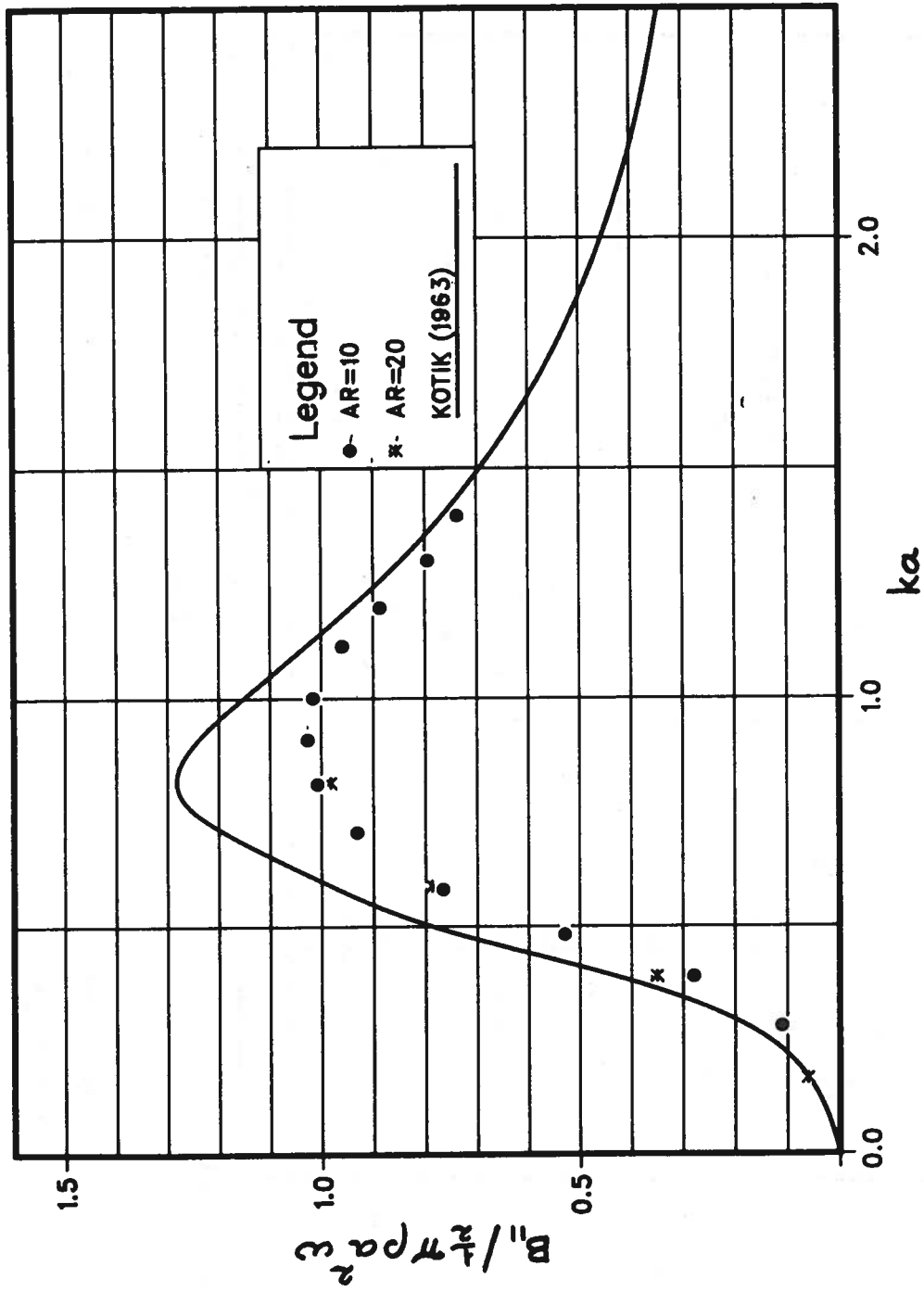


Fig. 8. Comparison of damping coefficients versus Kotik's 2-D prediction (sway).

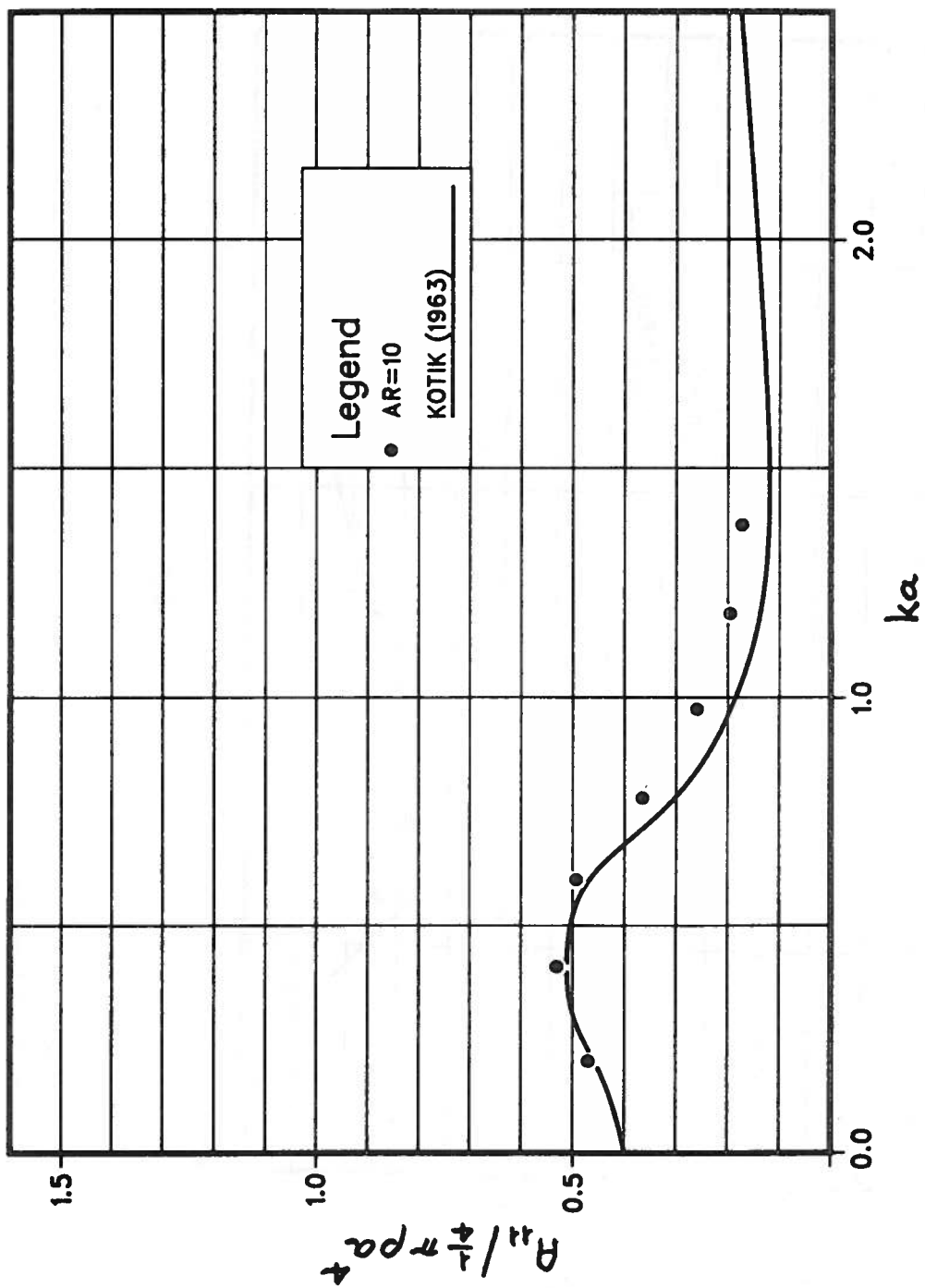


Fig. 9. Comparison of added inertia coefficients versus Kotik's 2-D prediction (roll).

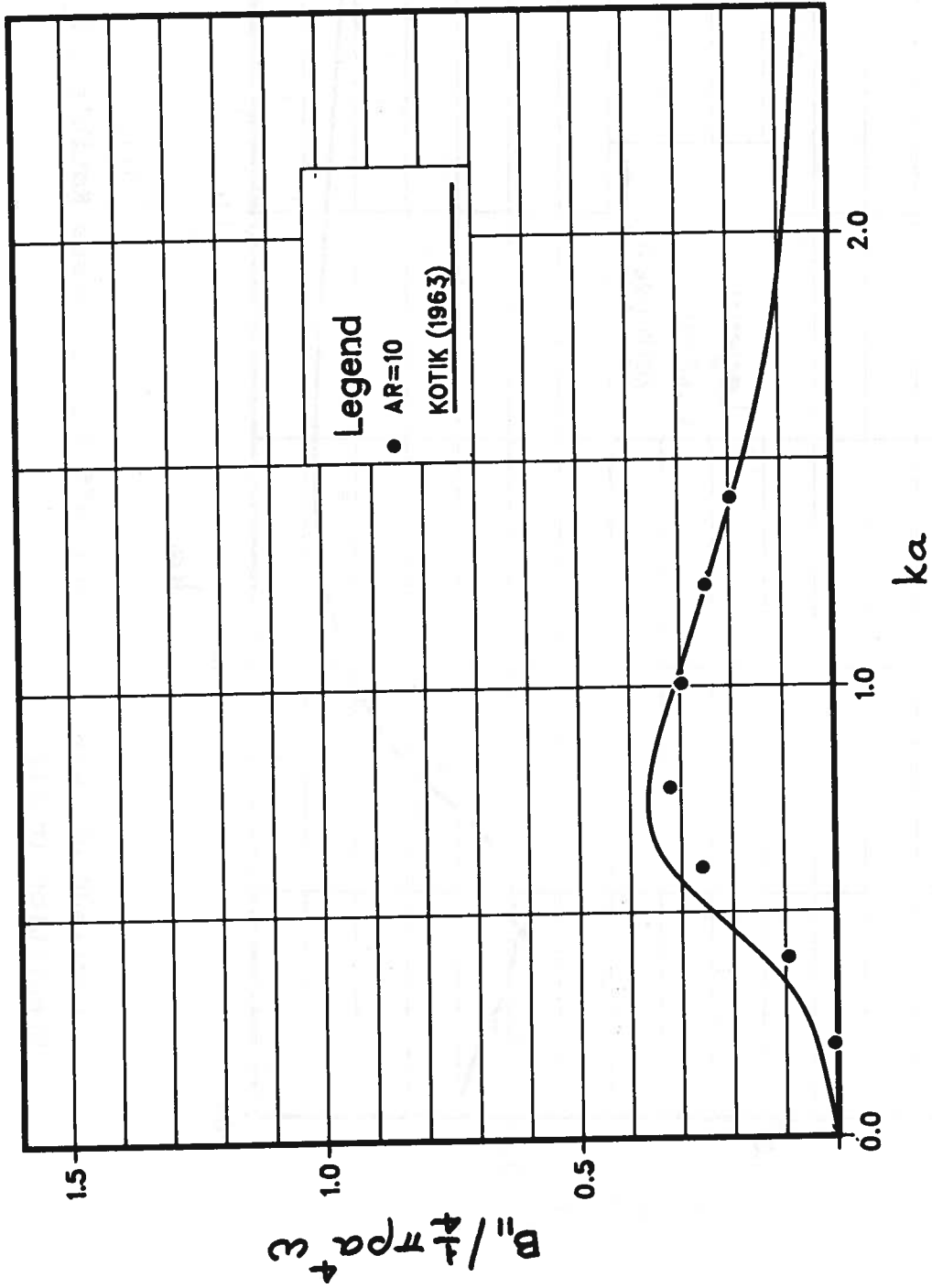


Fig. 10. Comparison of damping coefficients versus Kotik's 2-D prediction (roll).

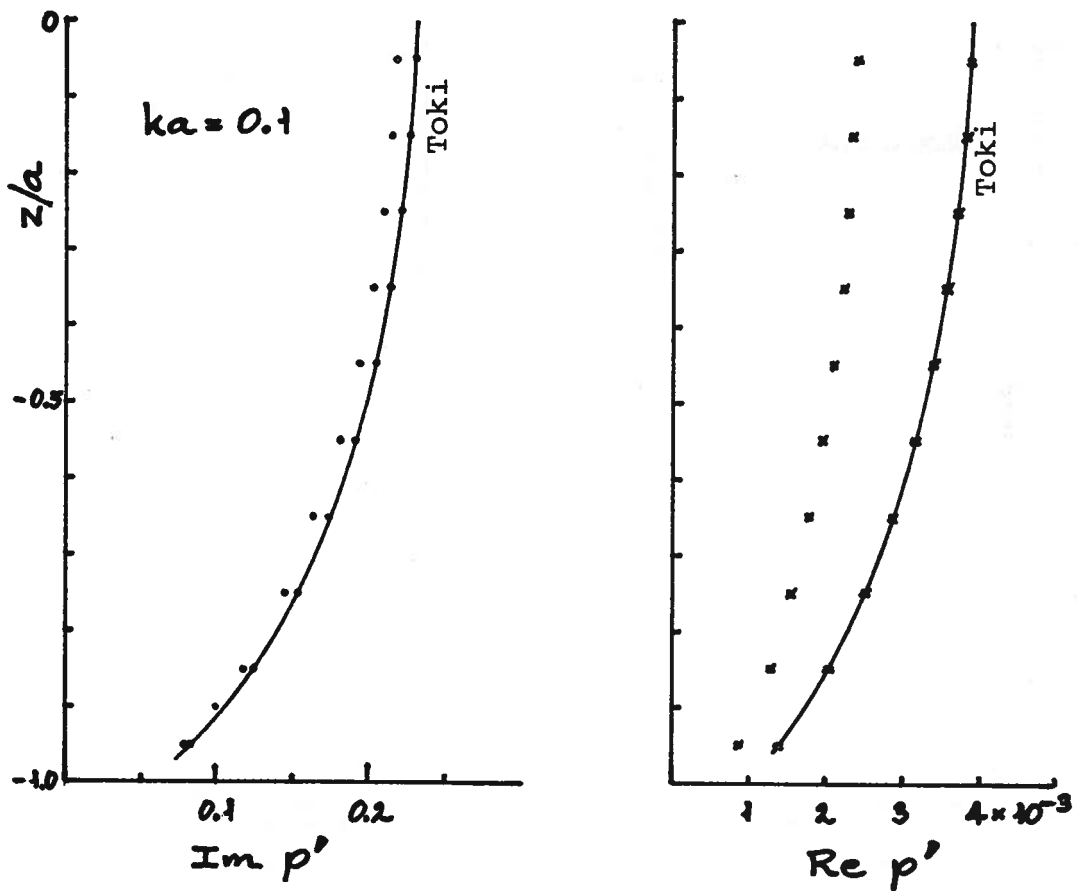


Fig. 11a. Comparison of depthwise radiation pressure distribution at midspan versus Toki's 2-D prediction. Note: $p' = 4\pi\omega\gamma/g|X|$.

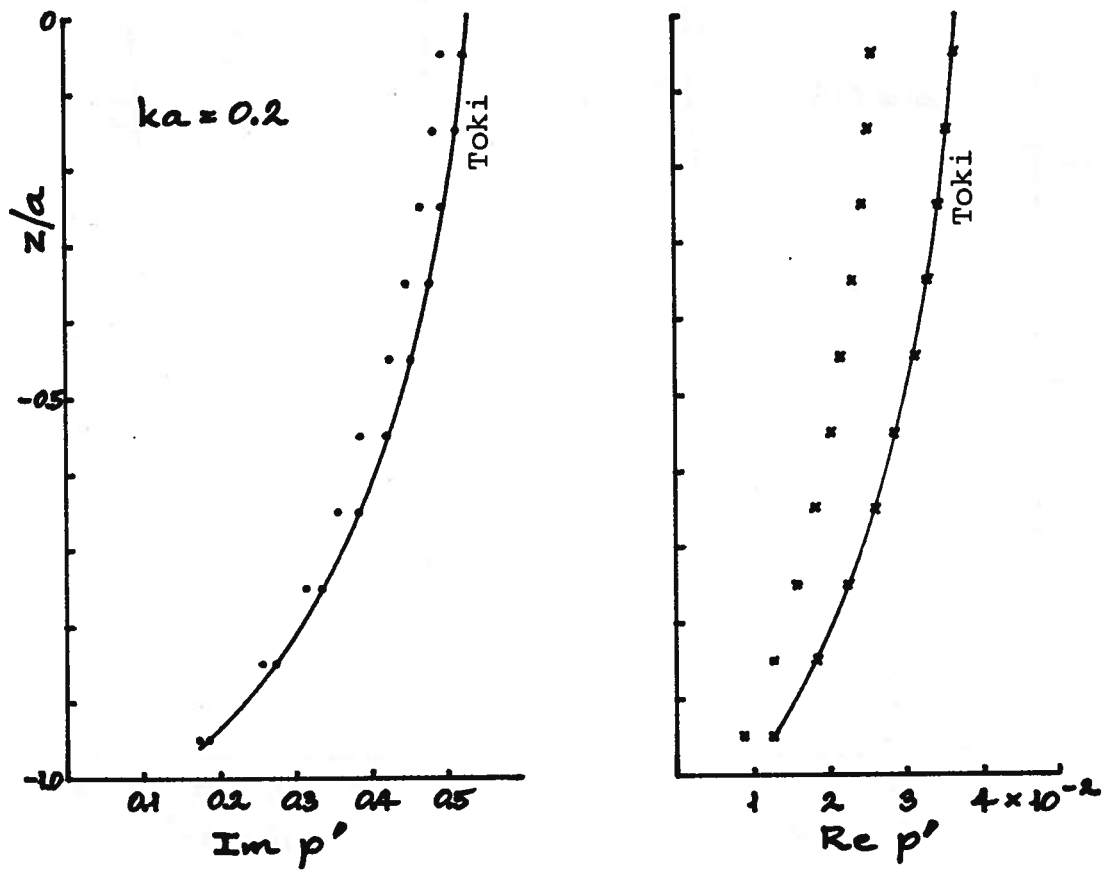


Fig. 11b. Comparison of depthwise radiation pressure distribution at midspan versus Toki's 2-D prediction (continued).

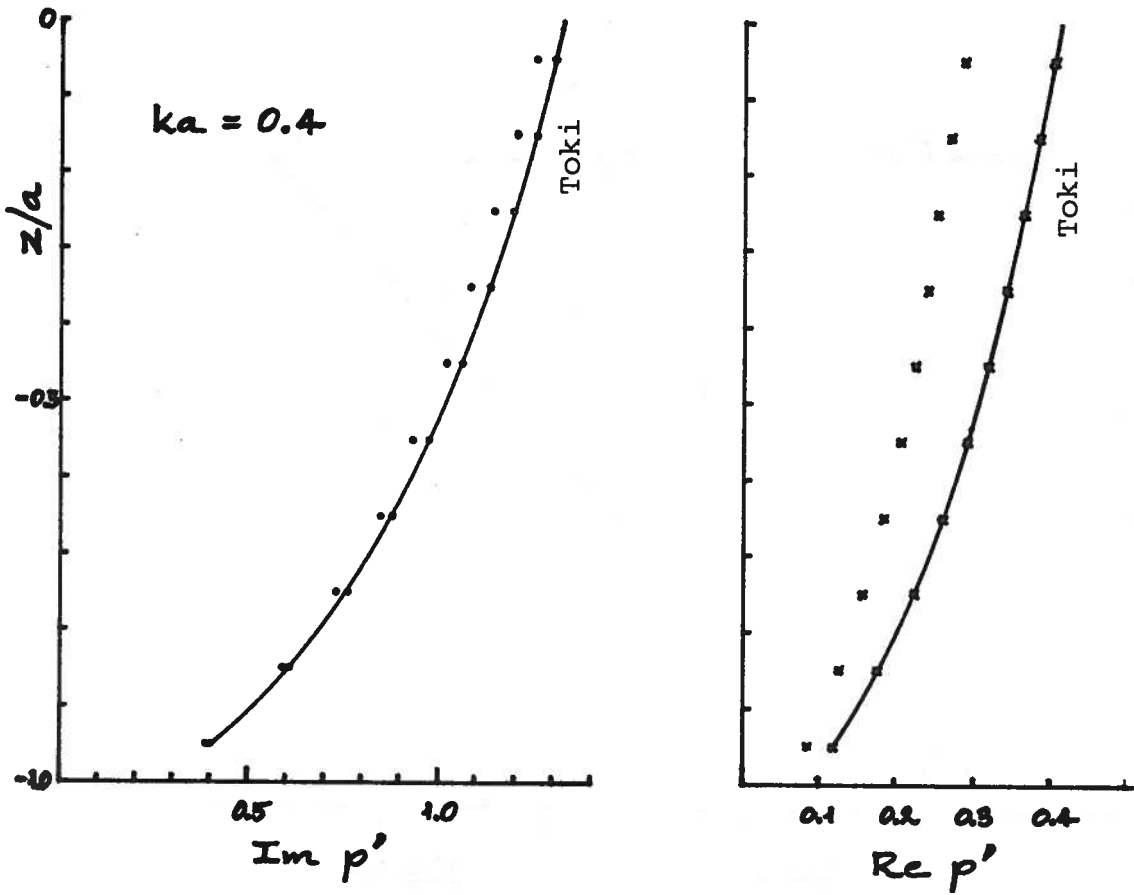


Fig. 11c. Comparison of depthwise radiation pressure distribution at midspan versus Toki's 2-D prediction (continued).

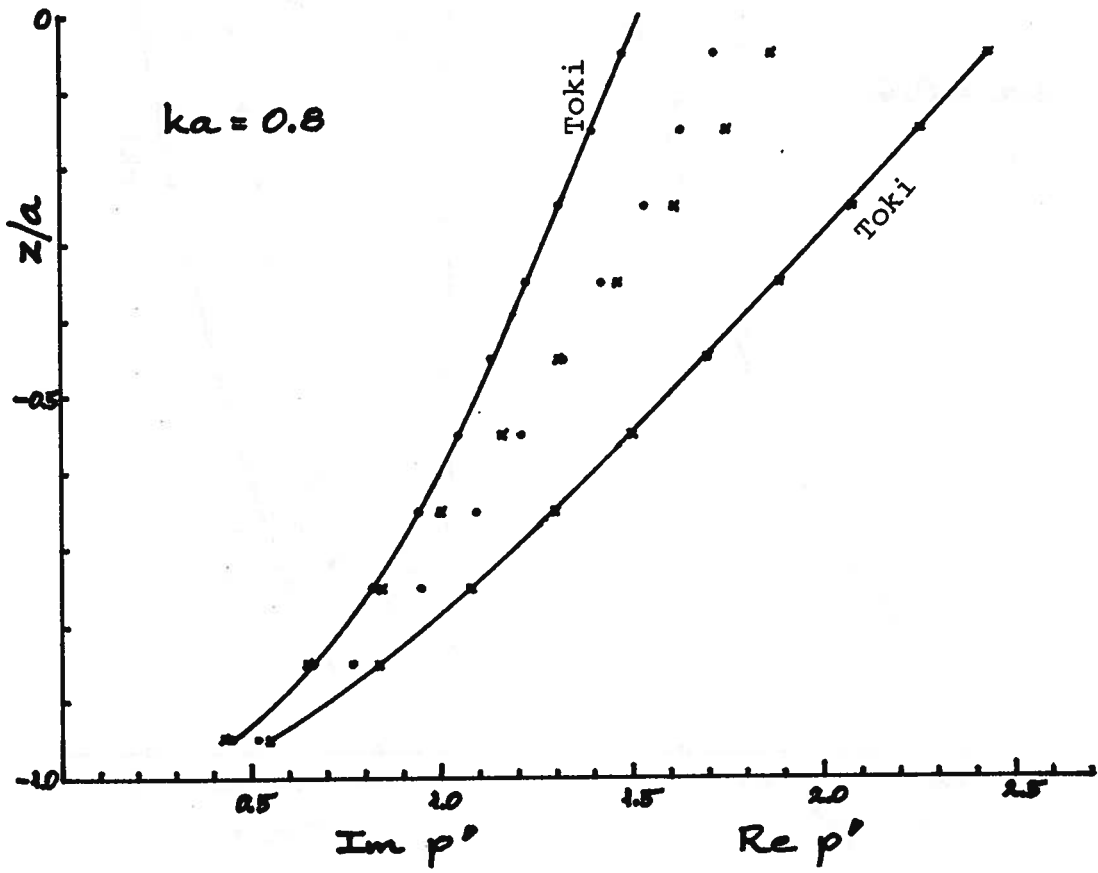


Fig. 11d. Comparison of depthwise radiation pressure distribution at midspan versus Toki's 2-D prediction (continued).

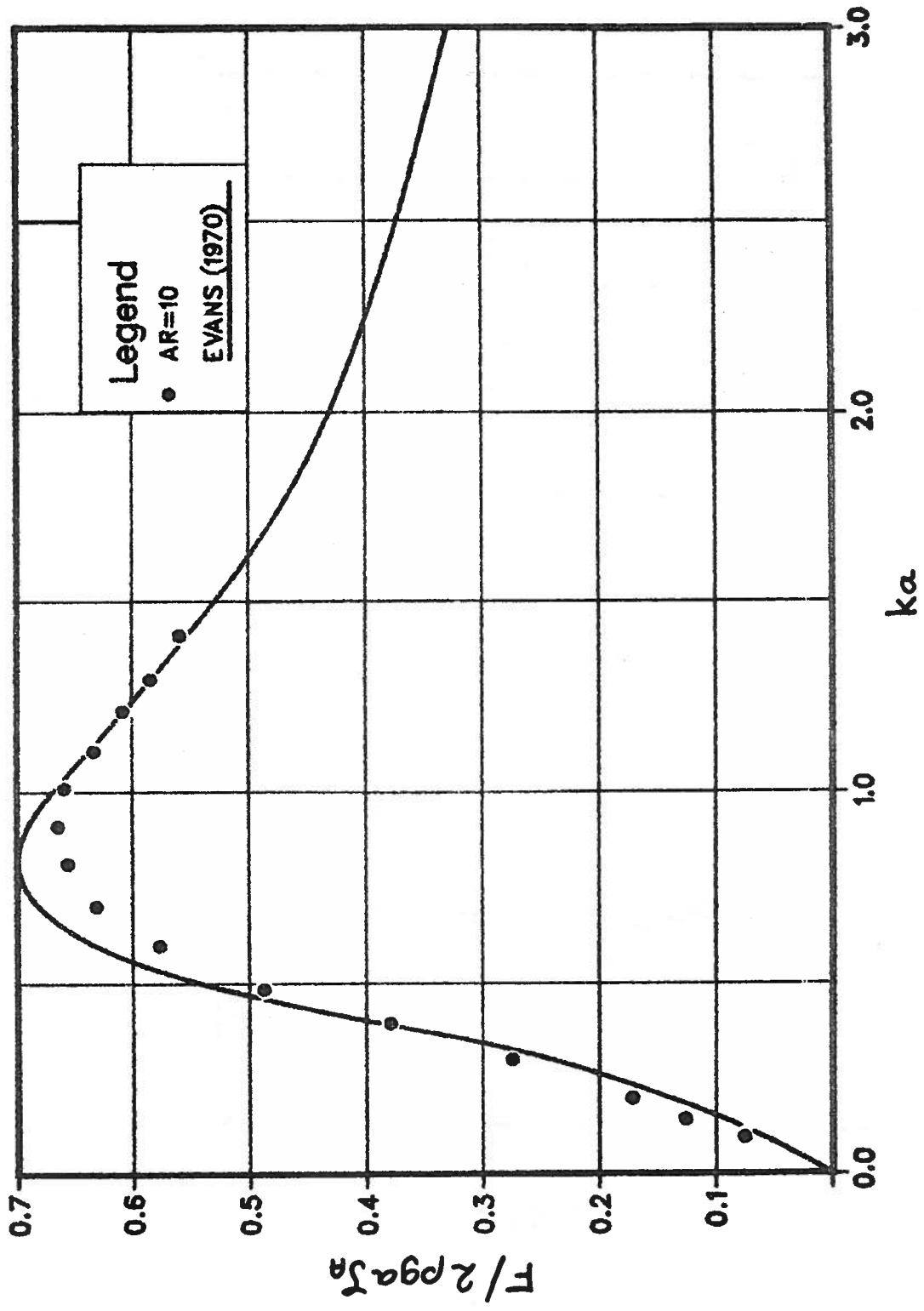


Fig. 12. Comparison of exciting force versus Evans' 2-D prediction (sway).

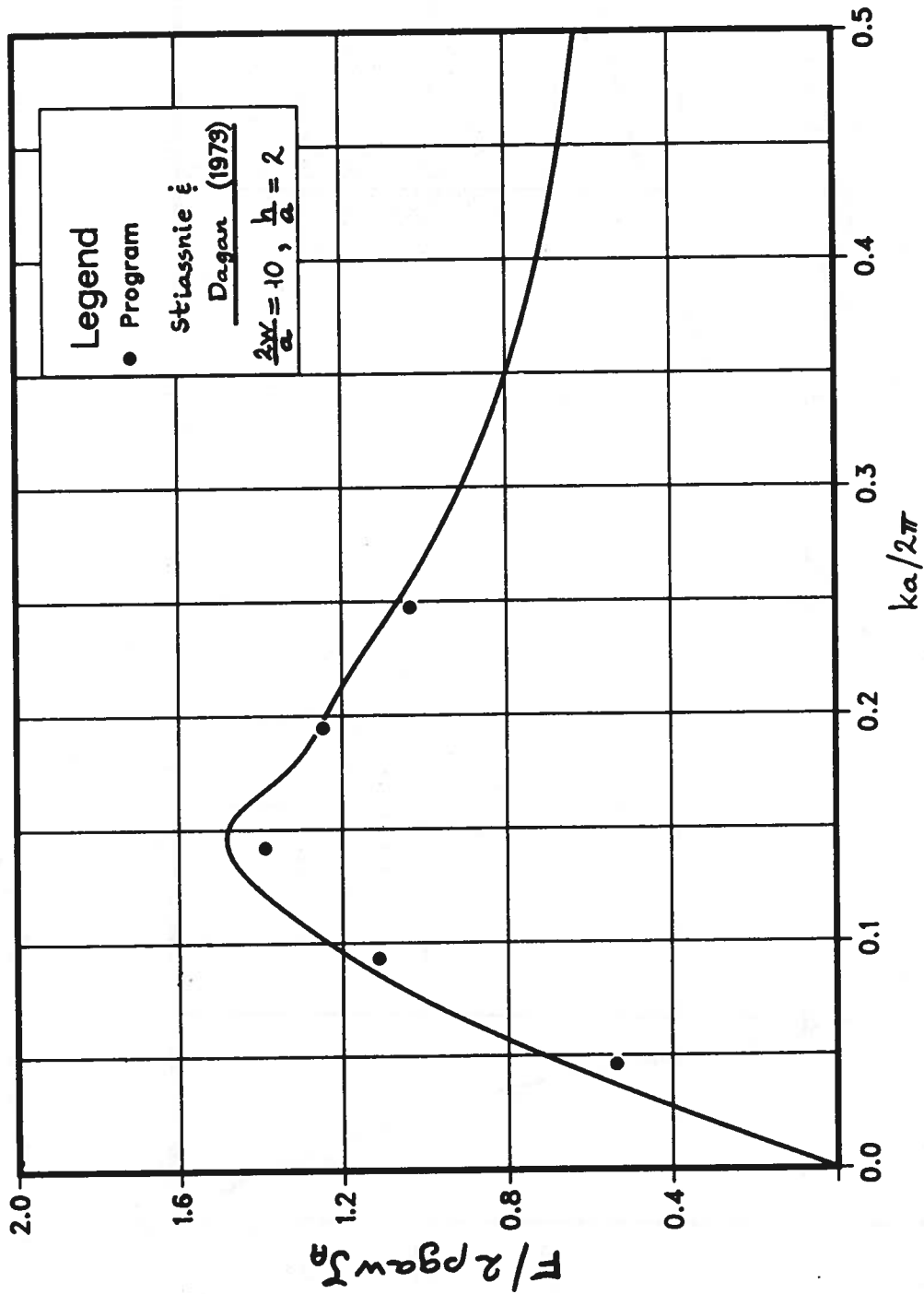


Fig. 13. Comparison of exciting force (sway) versus Stiasnie and Dagan's 3-D result, for a flap aspect ratio of 10, normal encounter.

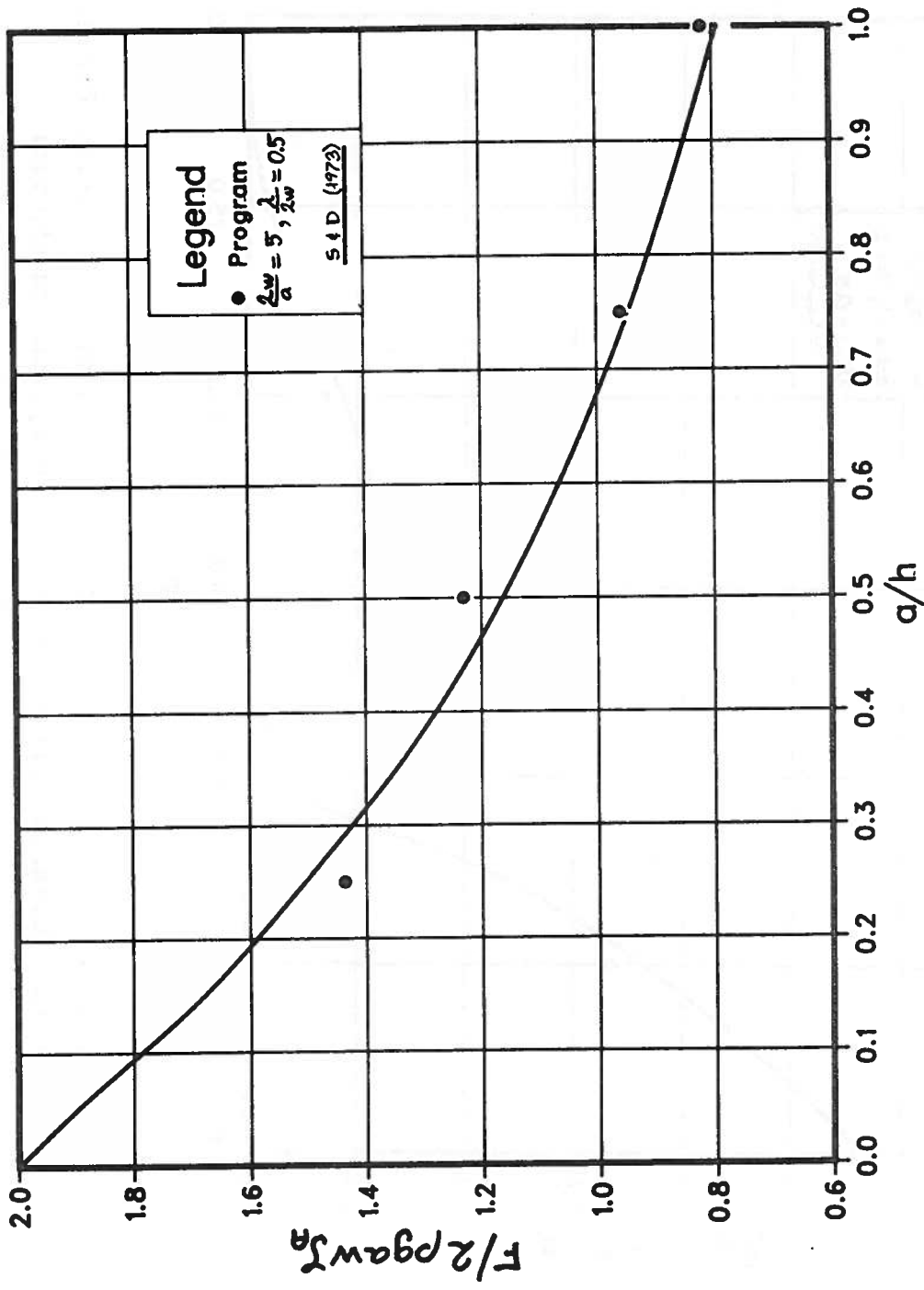


Fig. 14. Comparison of effect of draft/depth ratio on exciting force, versus Stiassnie and Dagan's 3-D result (normal encounter).

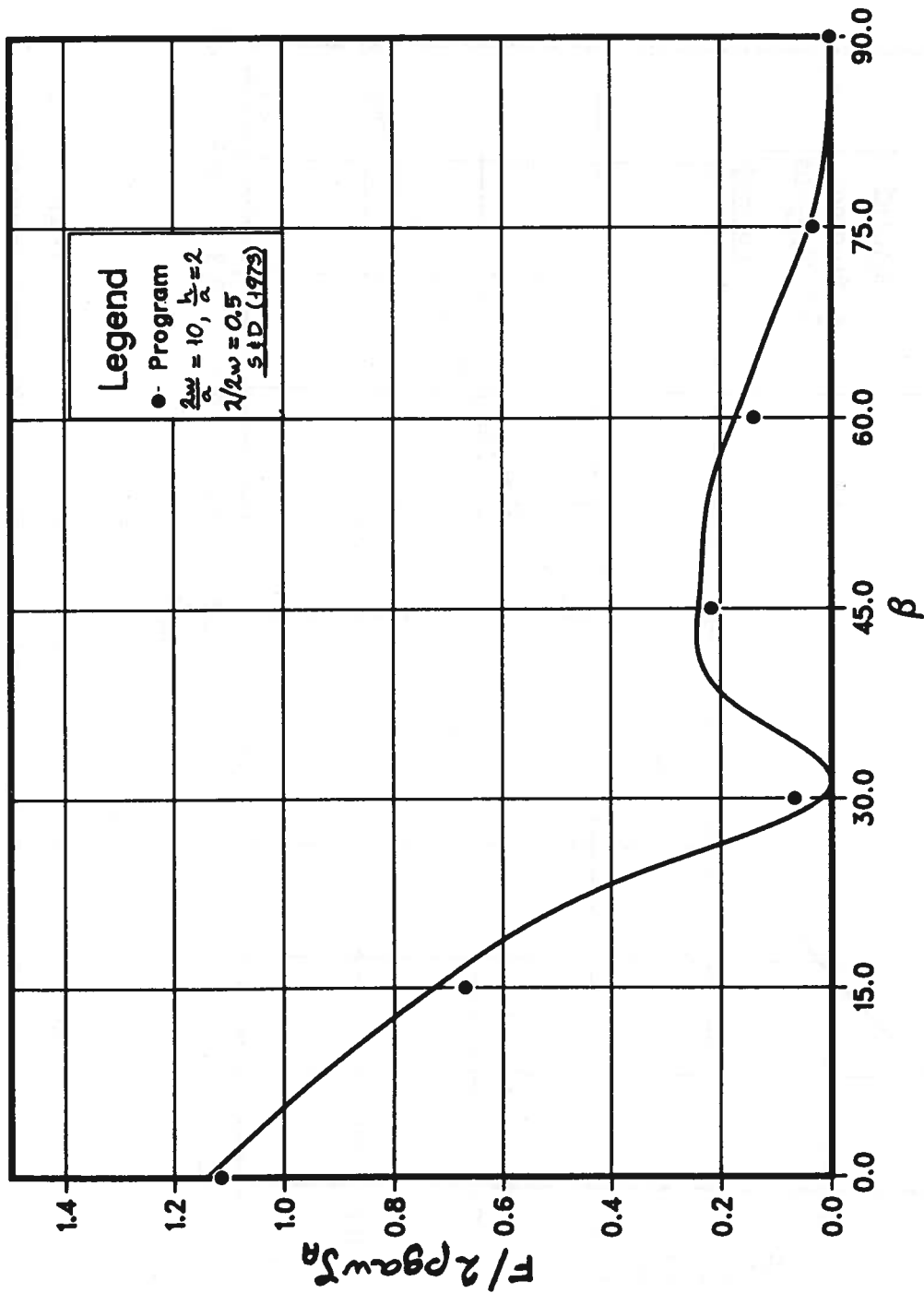


Fig. 15. Comparison of effect of angle of encounter on exciting force, versus Stiassnie and Dagan's 3-D analytical prediction.

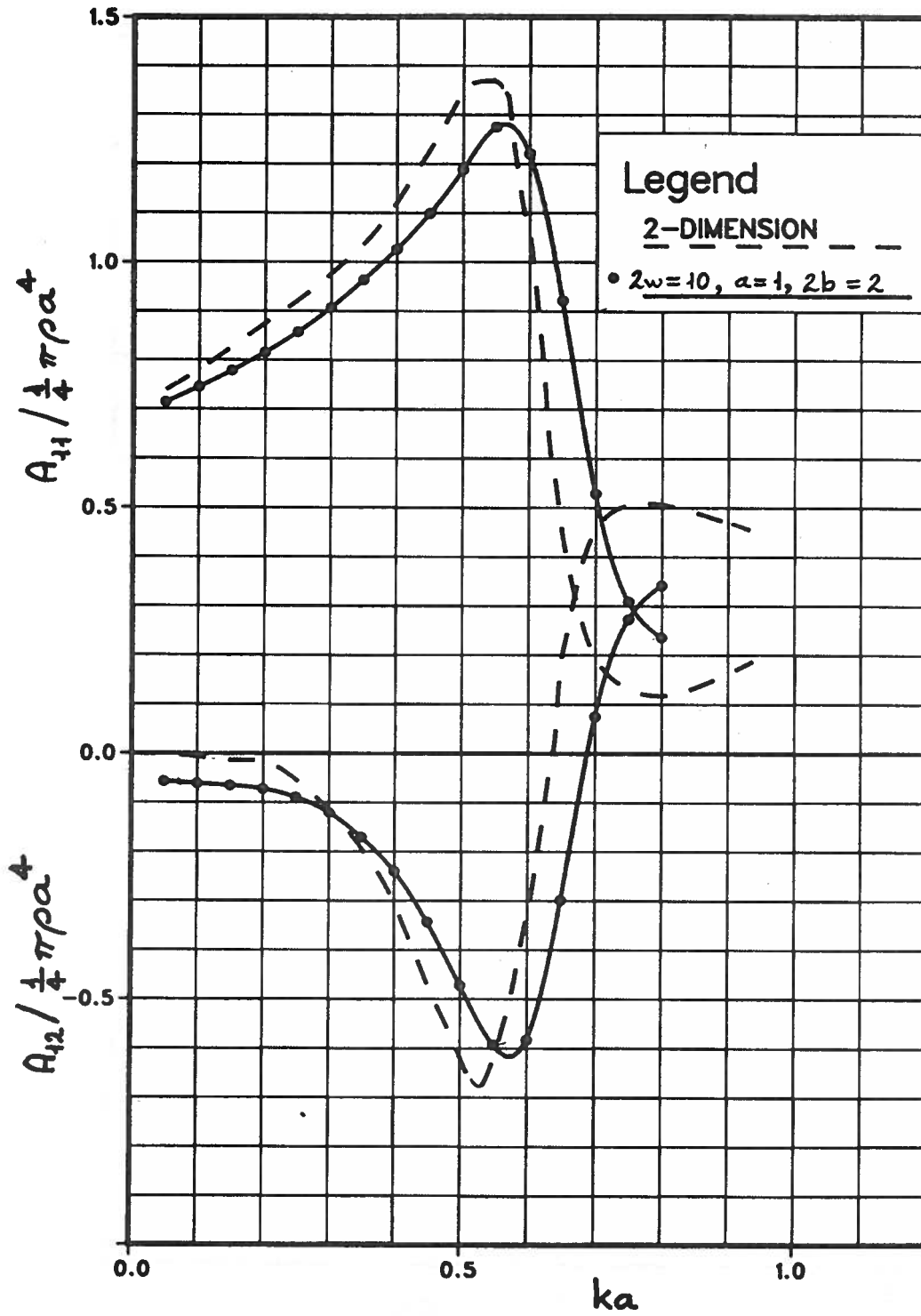


Fig. 16. Comparison of added mass and acceleration coupling coefficient for a twin flap versus Srokosz and Evans' 2-D prediction.

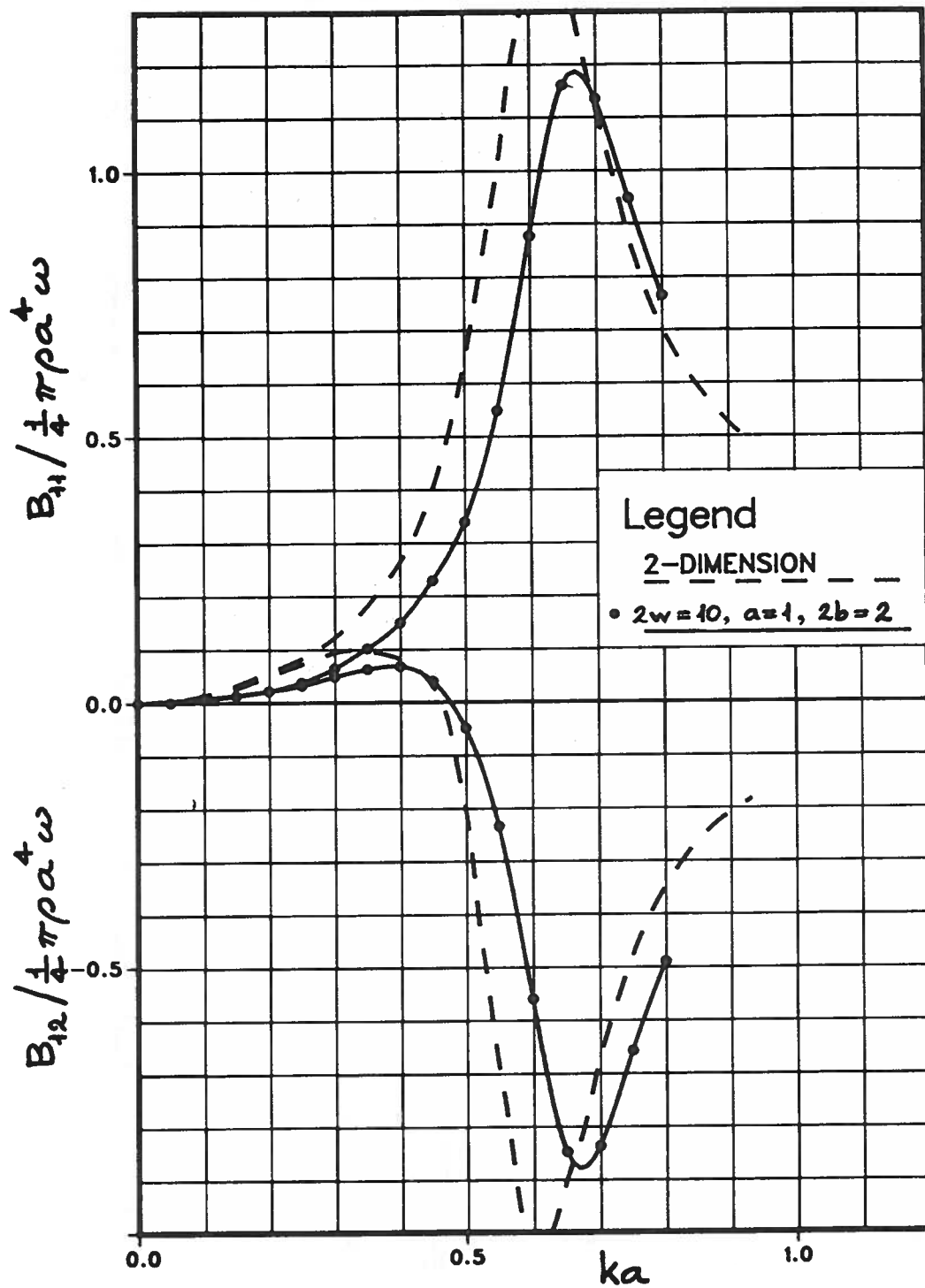


Fig. 17. Comparison of damping and velocity coupling coefficient for a twin flap versus Srokosz and Evan's 2-D prediction.

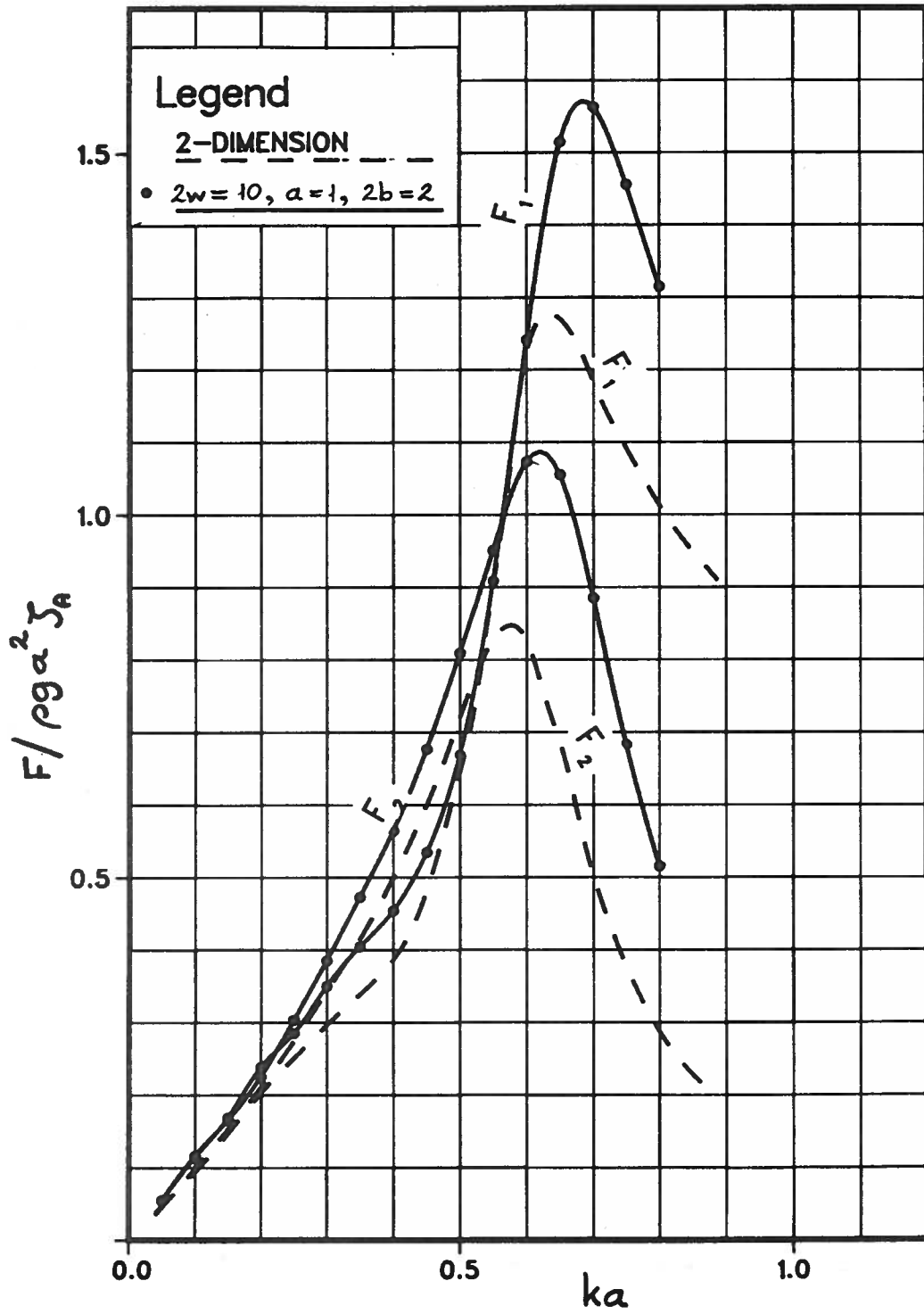


Fig. 18. Comparison of exciting force magnitudes for a twin flap versus Srokosz and Evans' 2-D prediction.

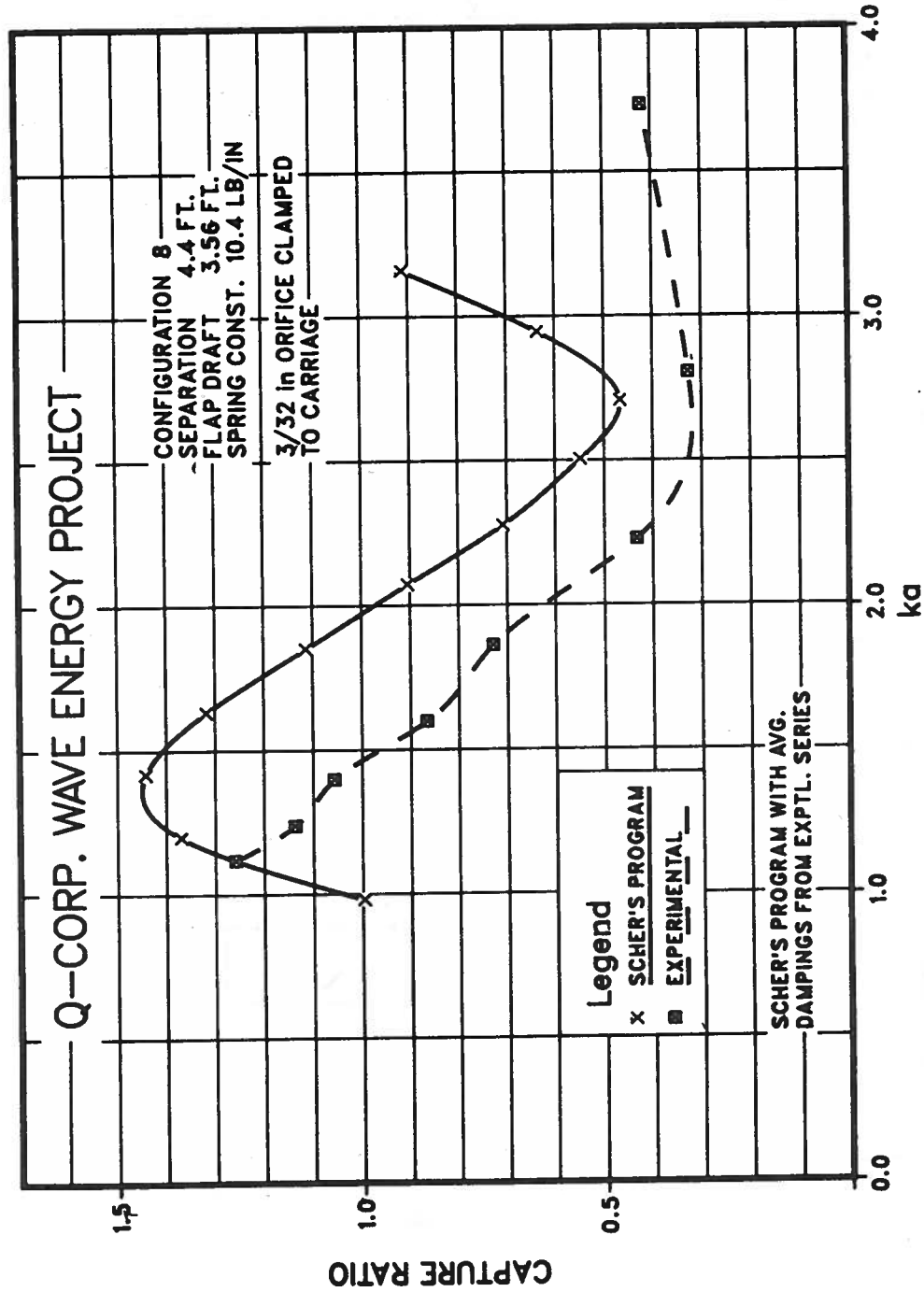


Fig. 19. Comparison of absorption cross-section per unit flap width versus experimental results for a finite width twin-flap device.

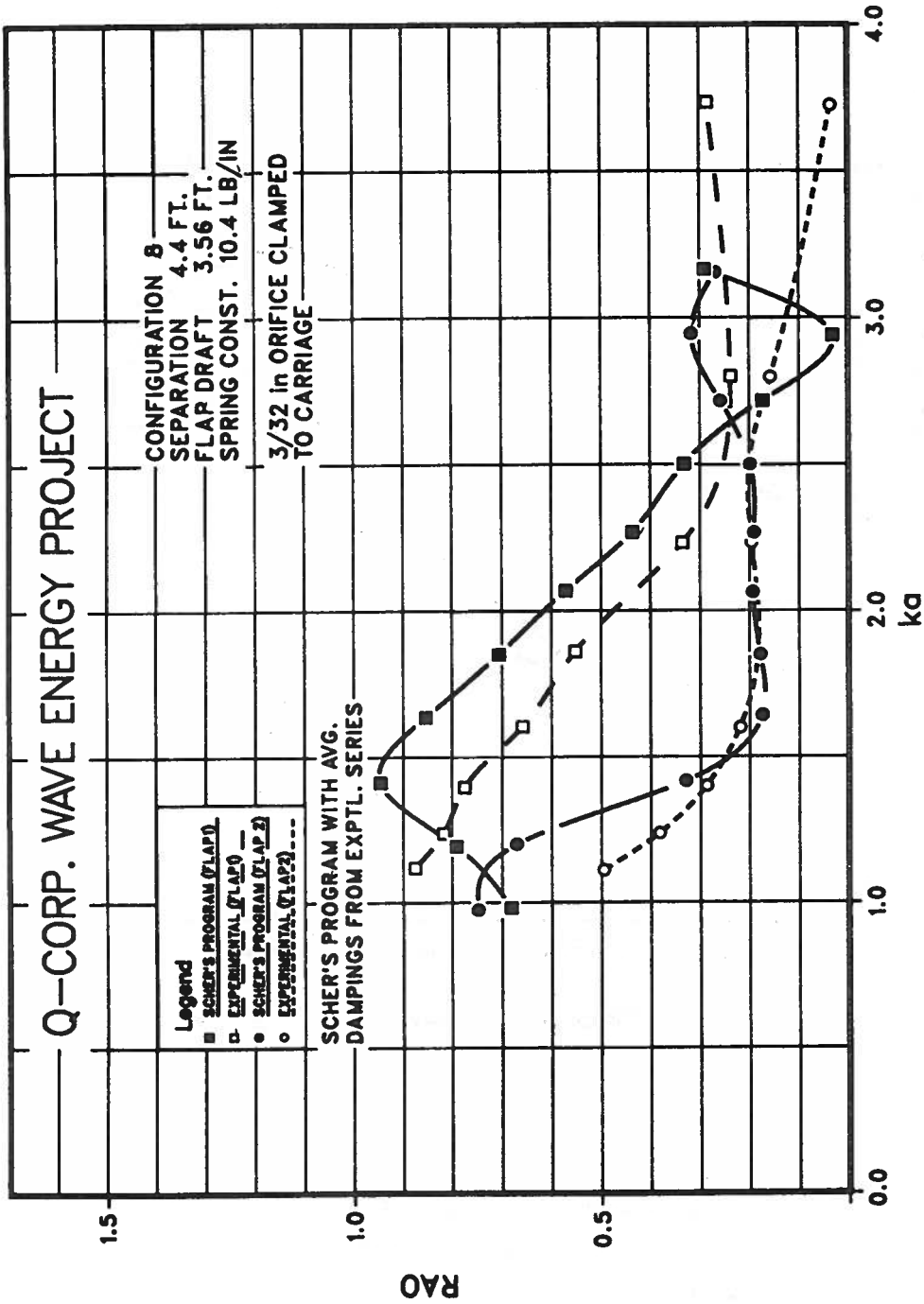


Fig. 20. Comparison of flap motion response amplitude operators versus experimental results for a finite width twin-flap device.

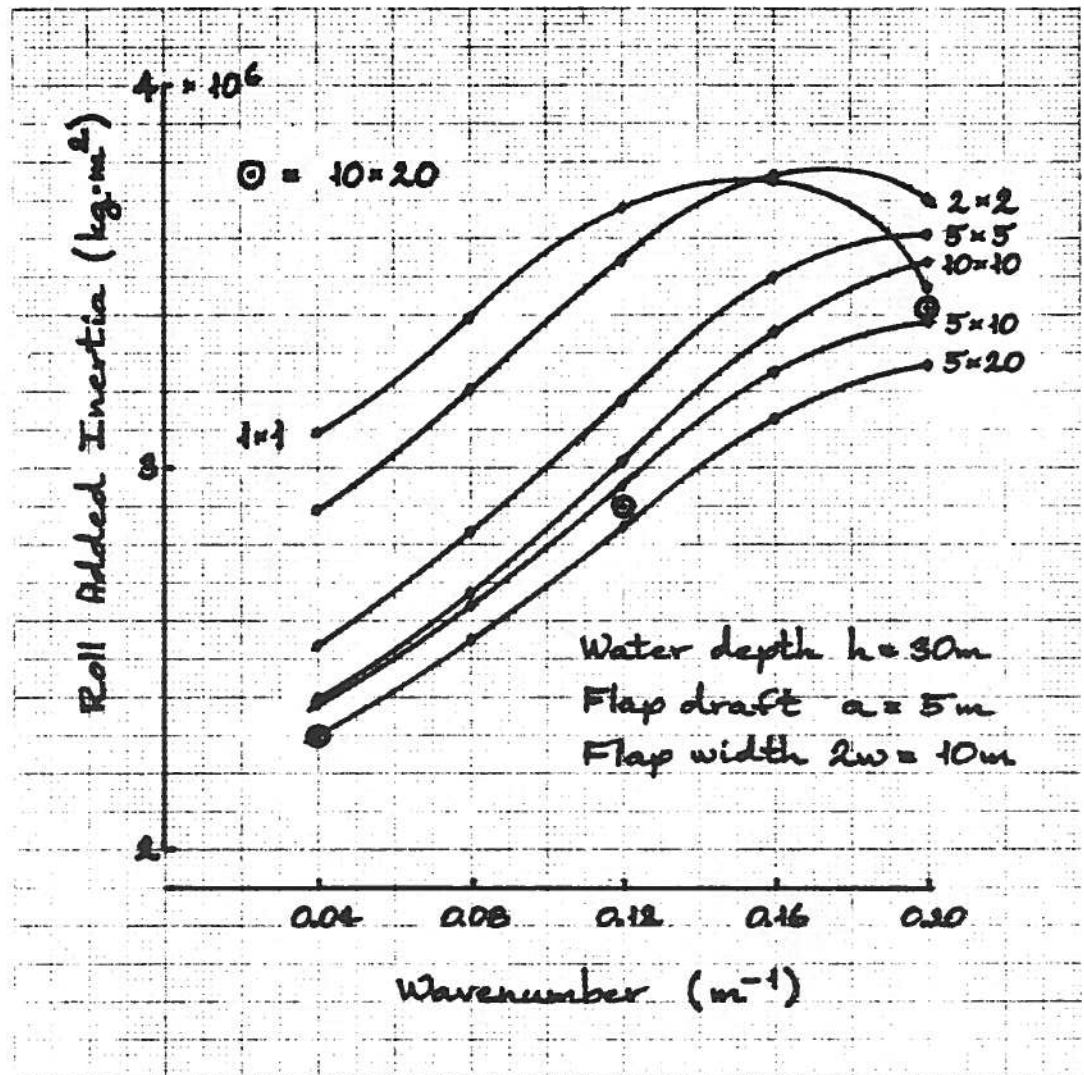


Fig. 21. Typical sensitivity to quadrilateral arrangements for a single flap: added inertia.

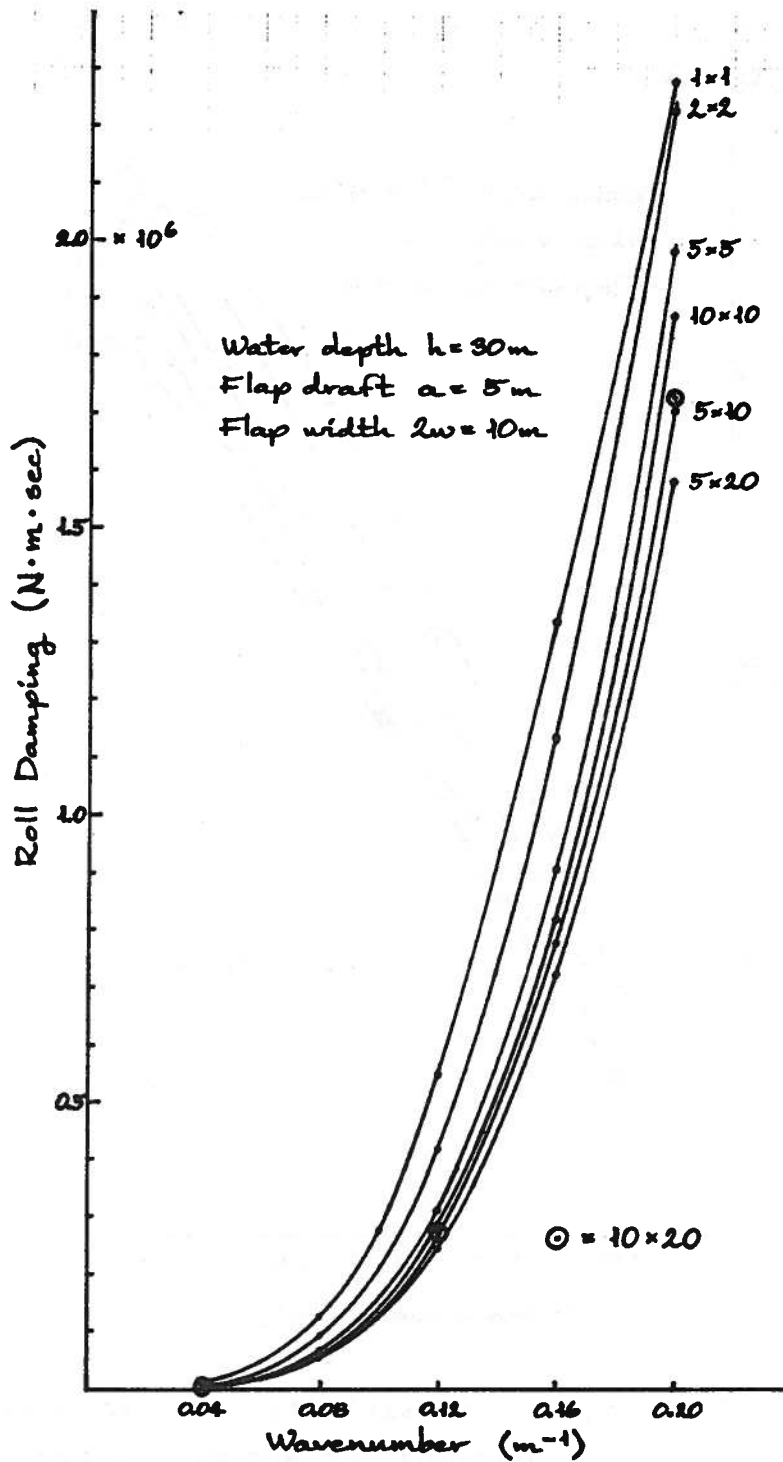


Fig. 22. Typical sensitivity to quadrilateral arrangements for a single flap: damping coefficient.

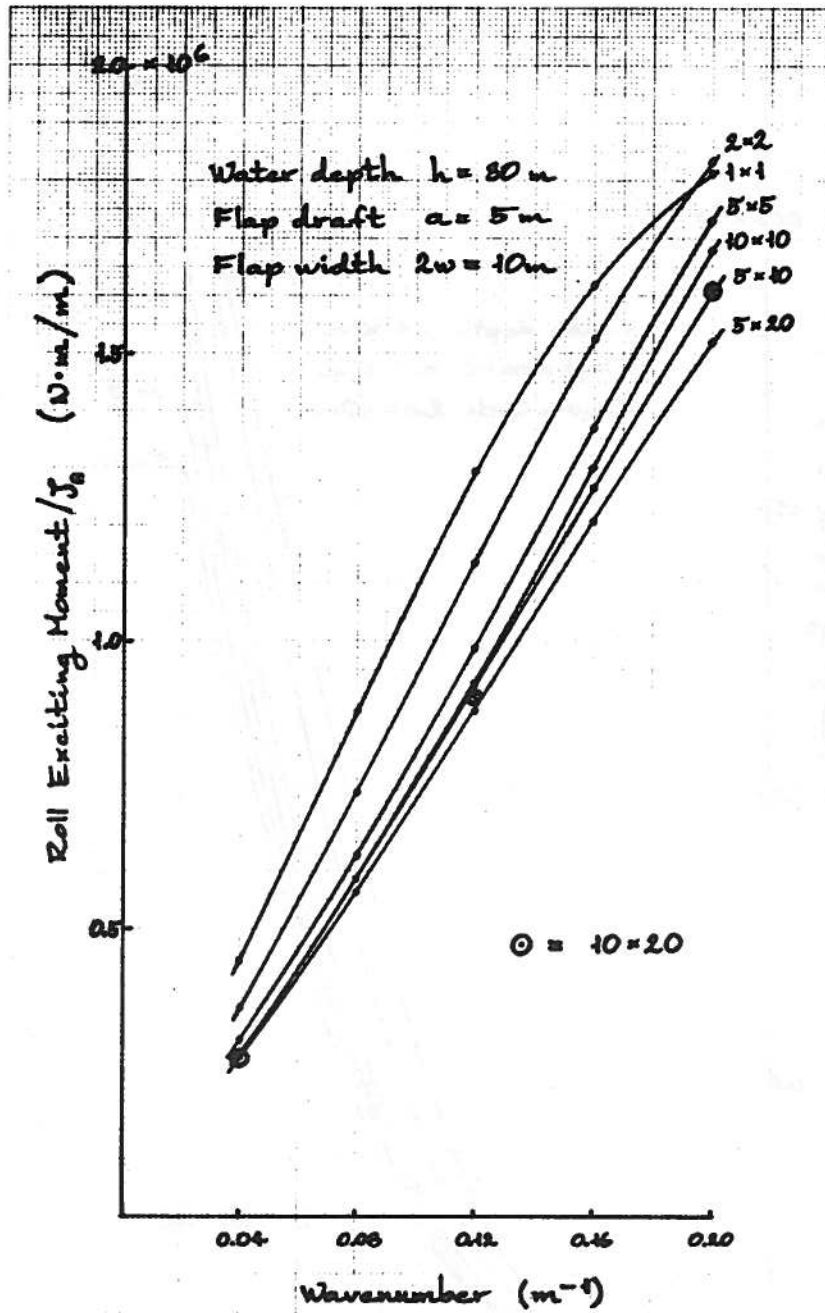


Fig. 23. Typical sensitivity to quadrilateral arrangements for a single flap: exciting force.

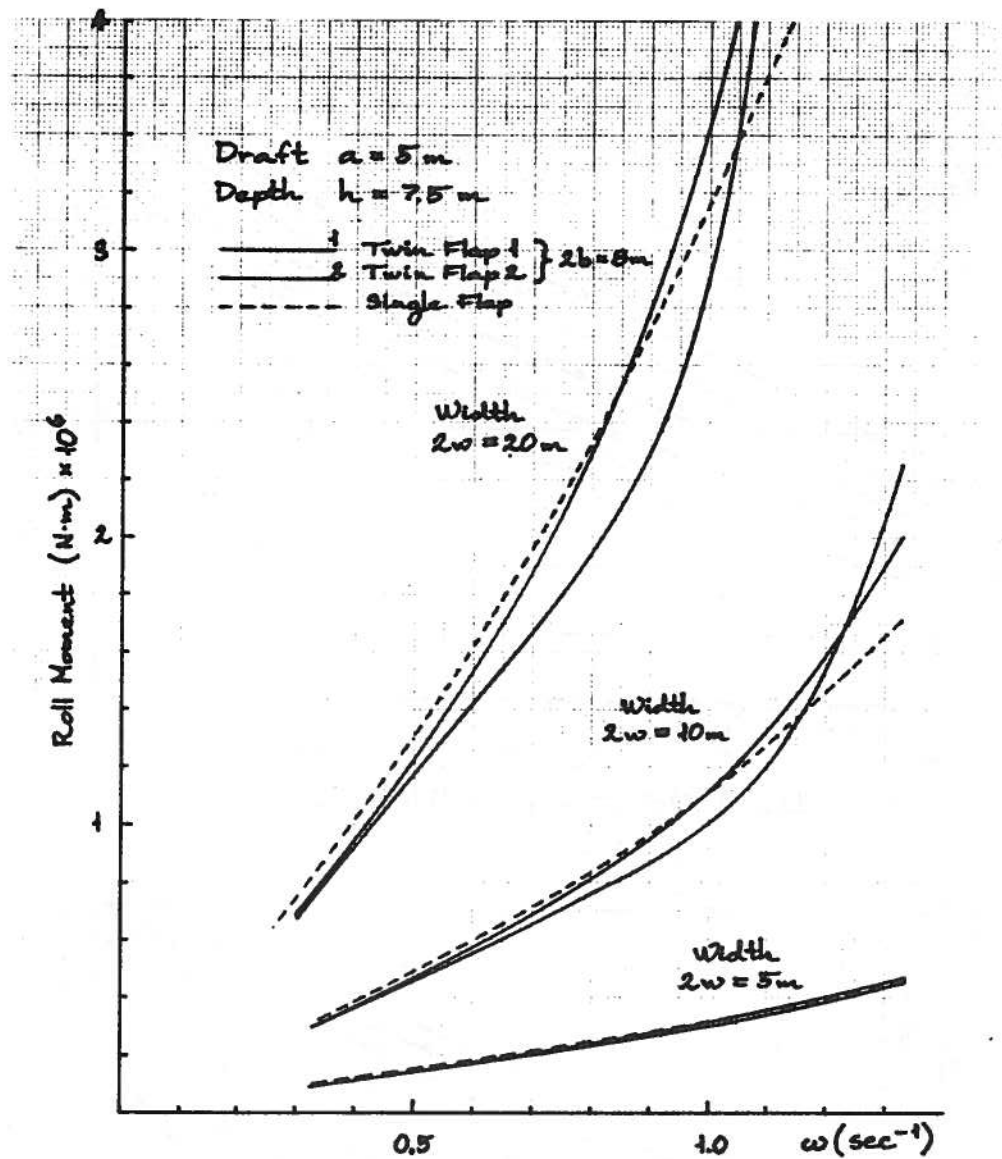


Fig. 24. Three-dimensional exciting force magnitude comparisons, single versus twin flap, at three flap widths.

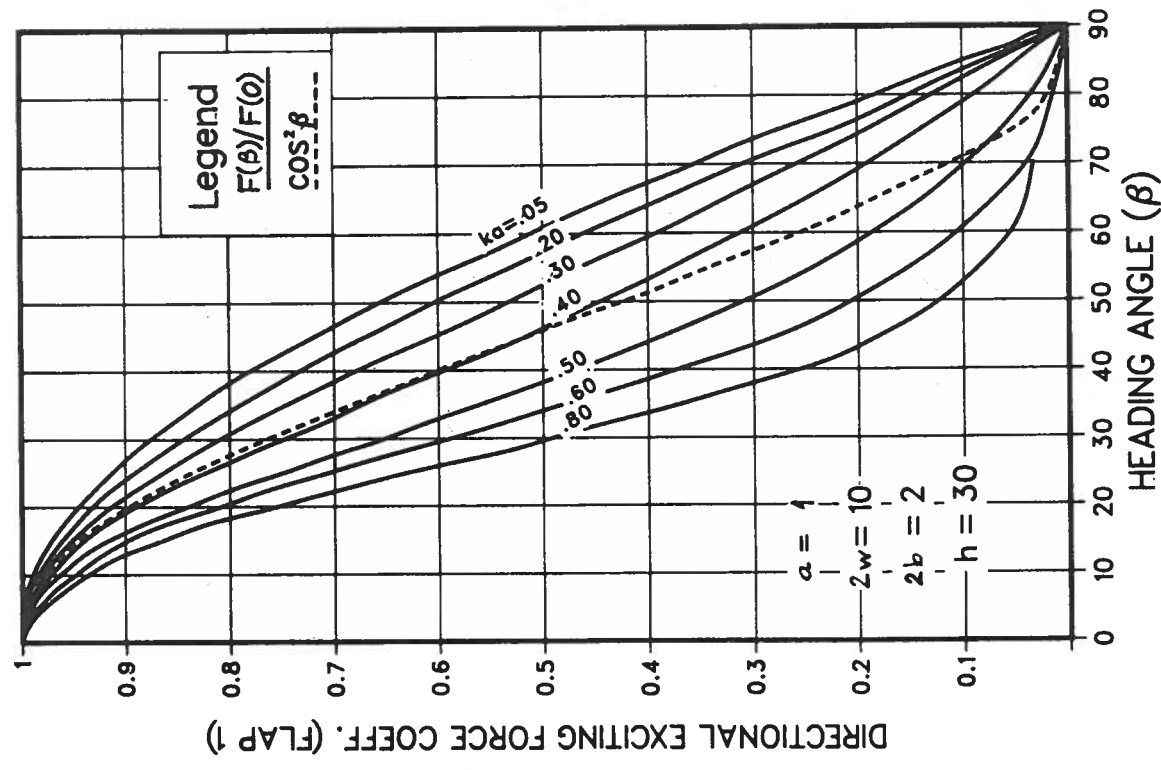
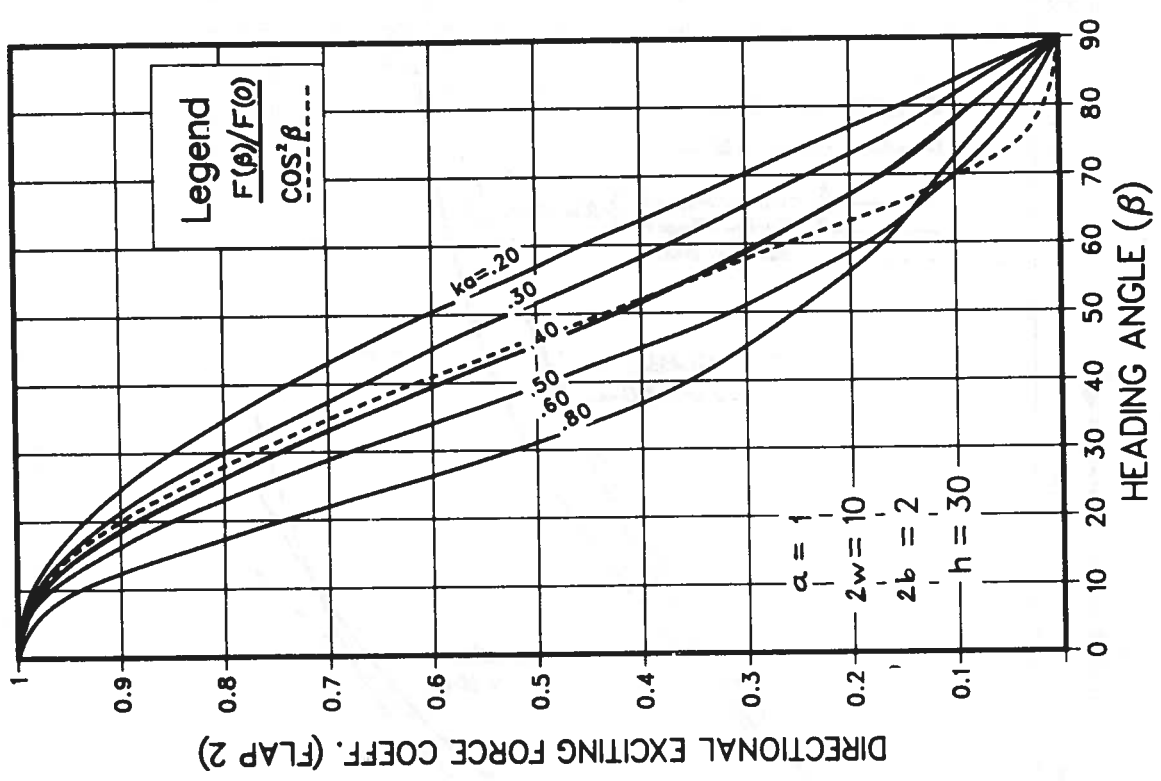


Fig. 25a. Twin flap exciting force magnitudes and phase relationship versus encounter angle.

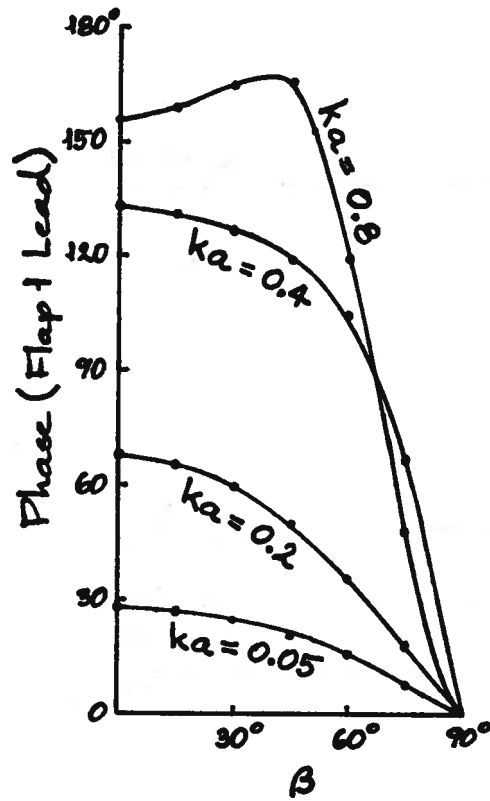


Fig. 25b. Twin flap exciting force magnitudes and phase relationship versus encounter angle (continued).

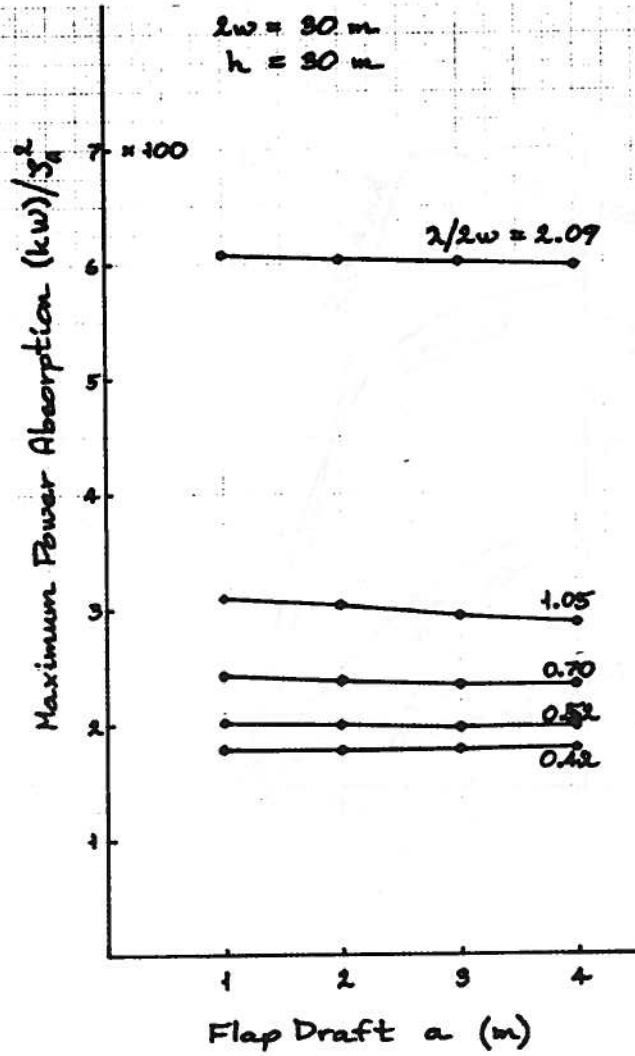


Fig. 26. Maximum absorption versus draft for a high aspect ratio flap, deep water.

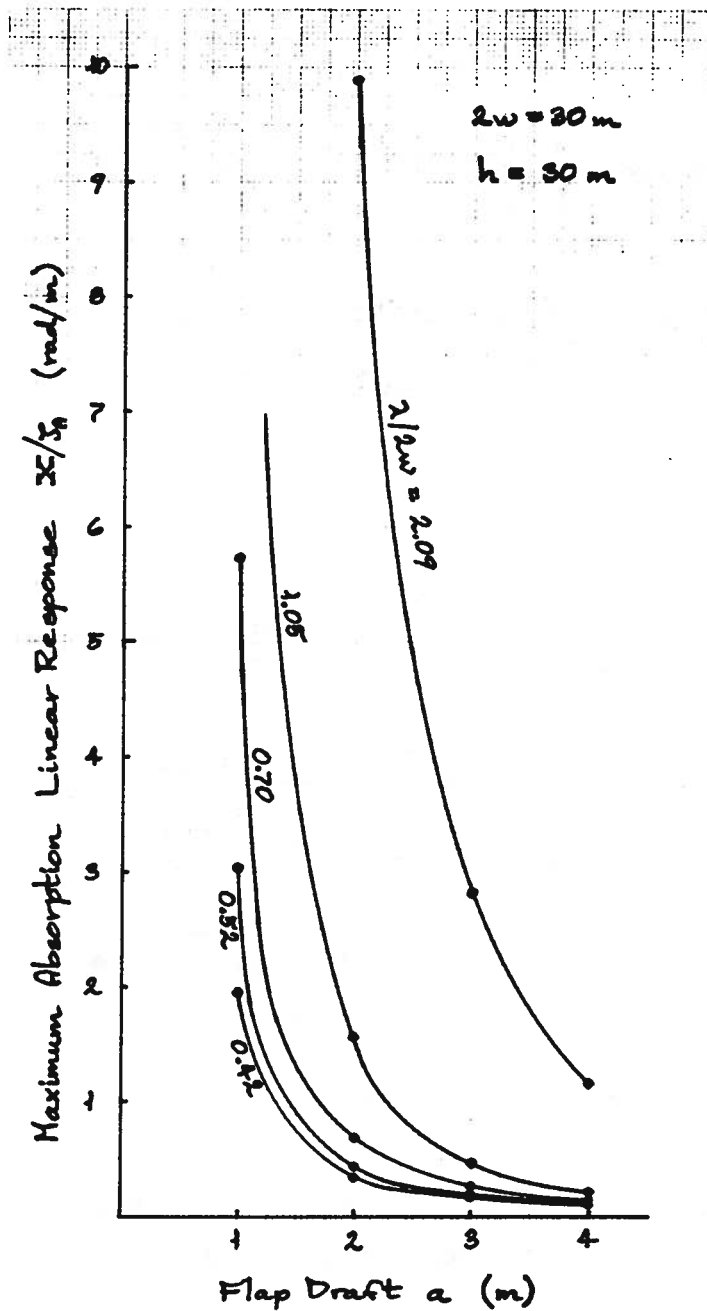


Fig. 27. Motion amplitude at maximum absorption versus draft for a high aspect ratio flap, deep water.

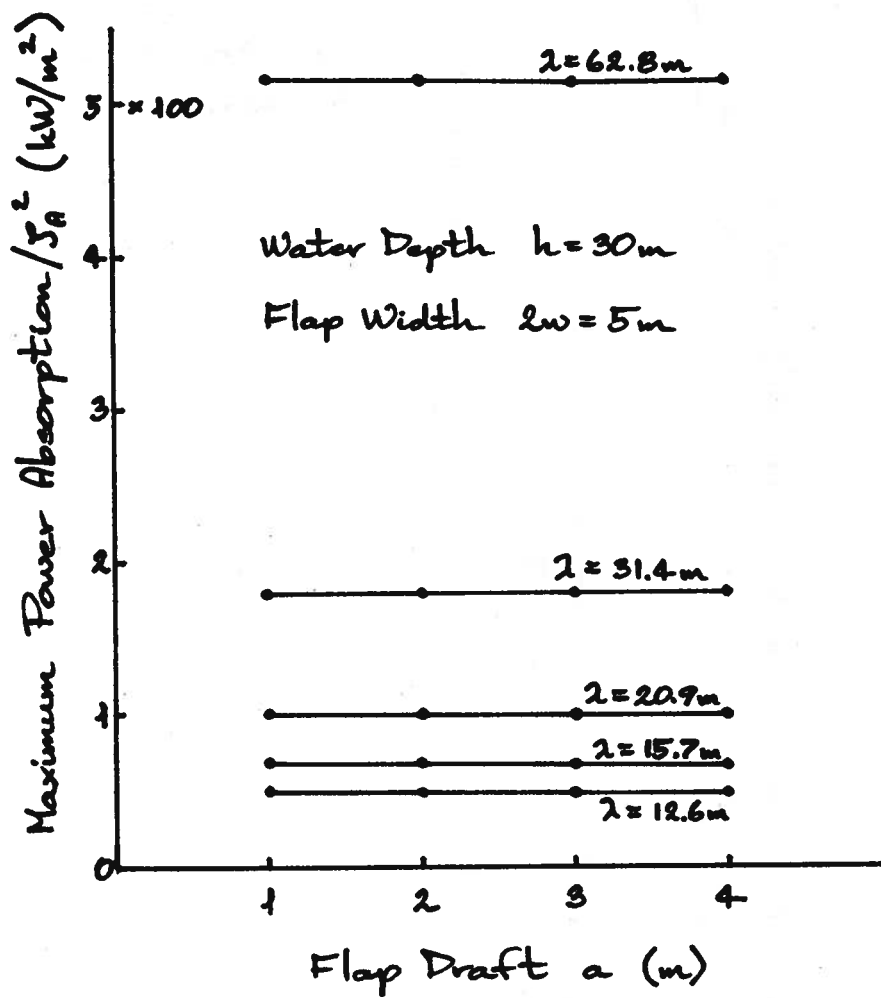


Fig. 28. Maximum absorption versus draft for a low aspect ratio flap, deep water.

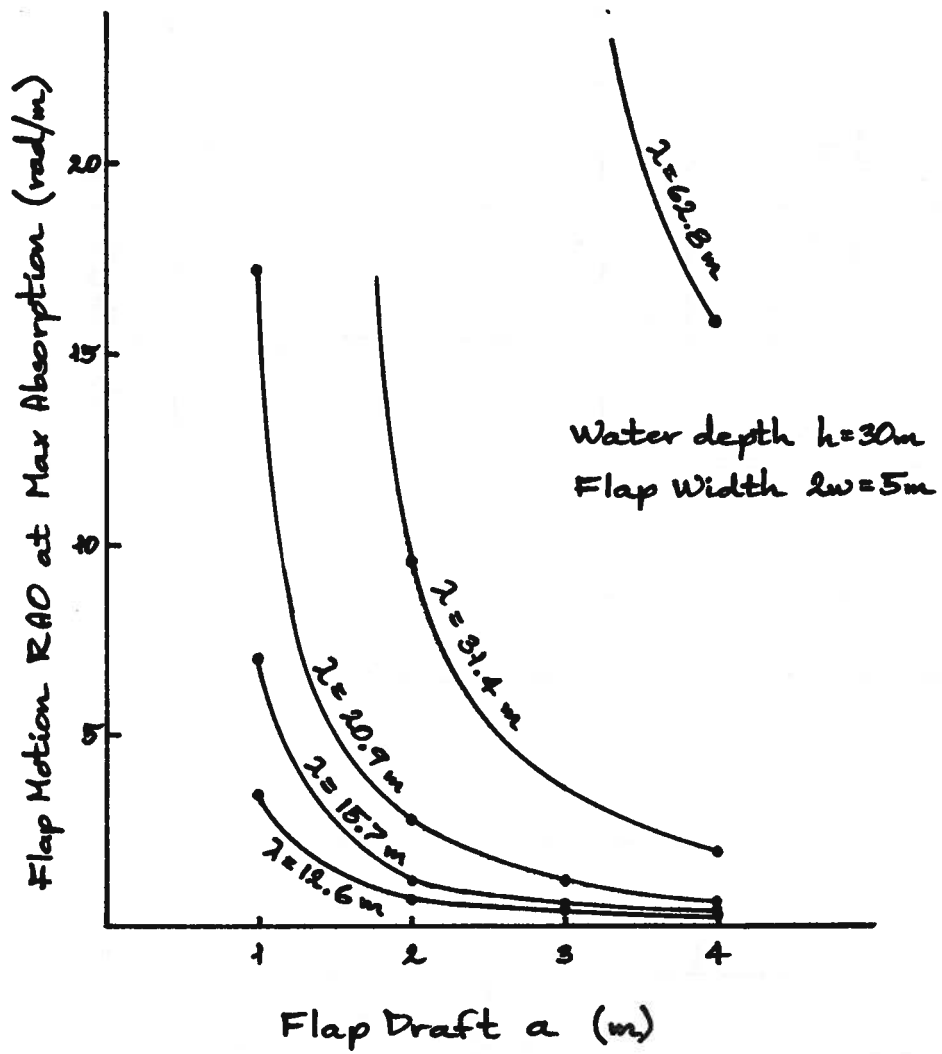


Fig. 29. Motion amplitude at maximum absorption versus draft for a low aspect ratio flap, deep water.

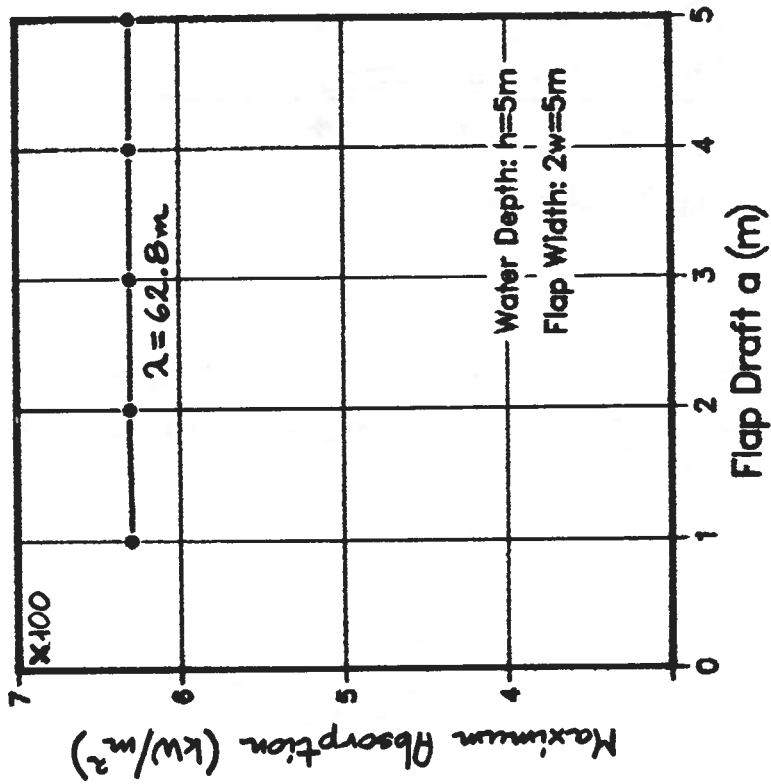
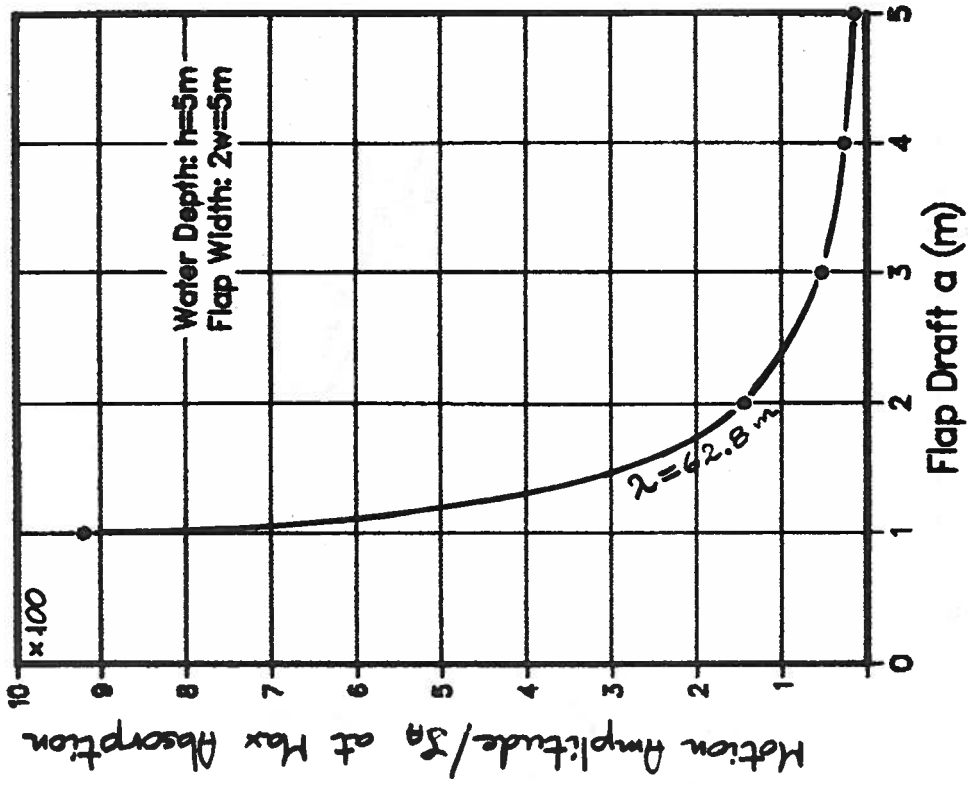


Fig. 30. Maximum absorption and motion amplitude versus draft for a low aspect ratio flap, shallow water.

Water Depth $h = 7.5\text{ m}$
 Flaps: $5\text{ m} \times 10\text{ m}$

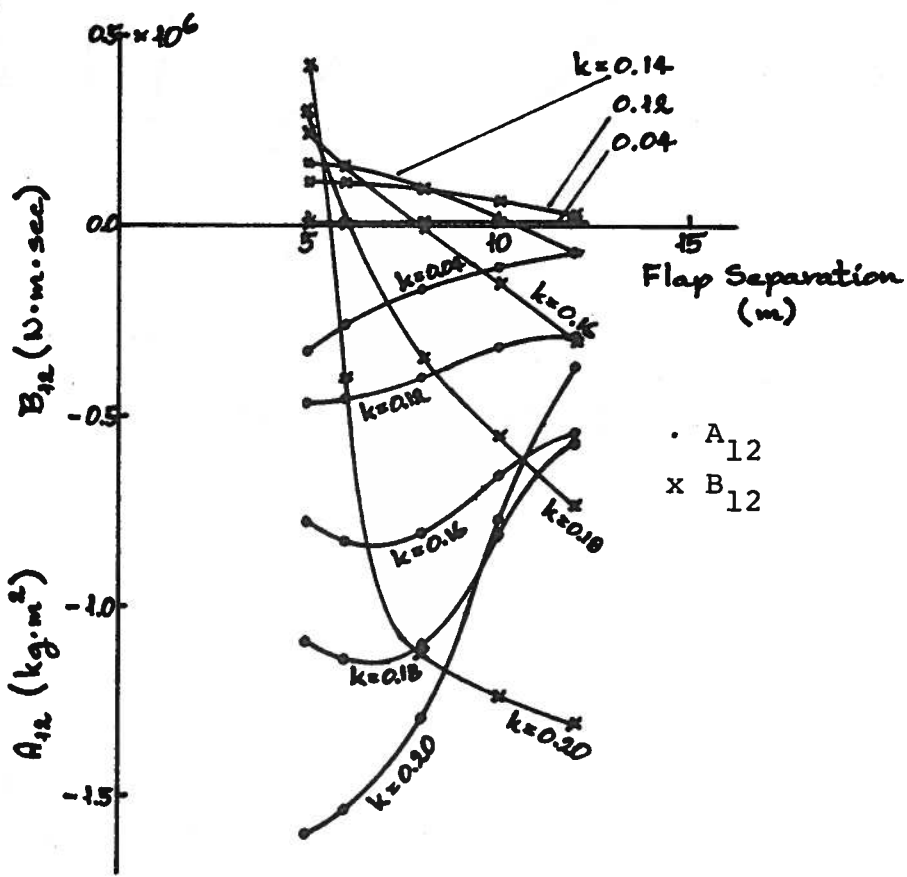


Fig. 31. Coupling force coefficients versus separation for a twin flap.

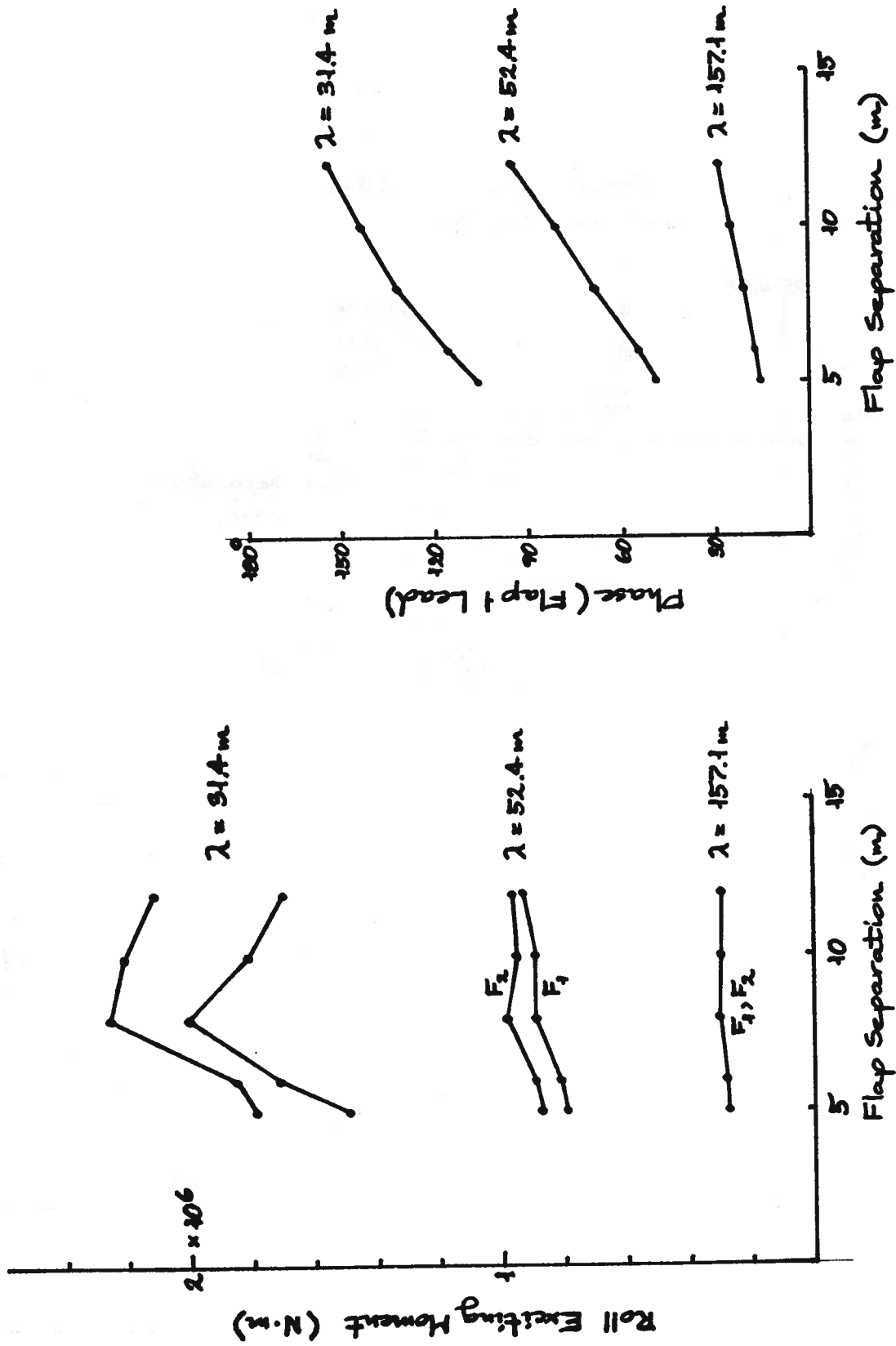


Fig. 32. Exciting force magnitudes and phase versus separation for a twin flap.

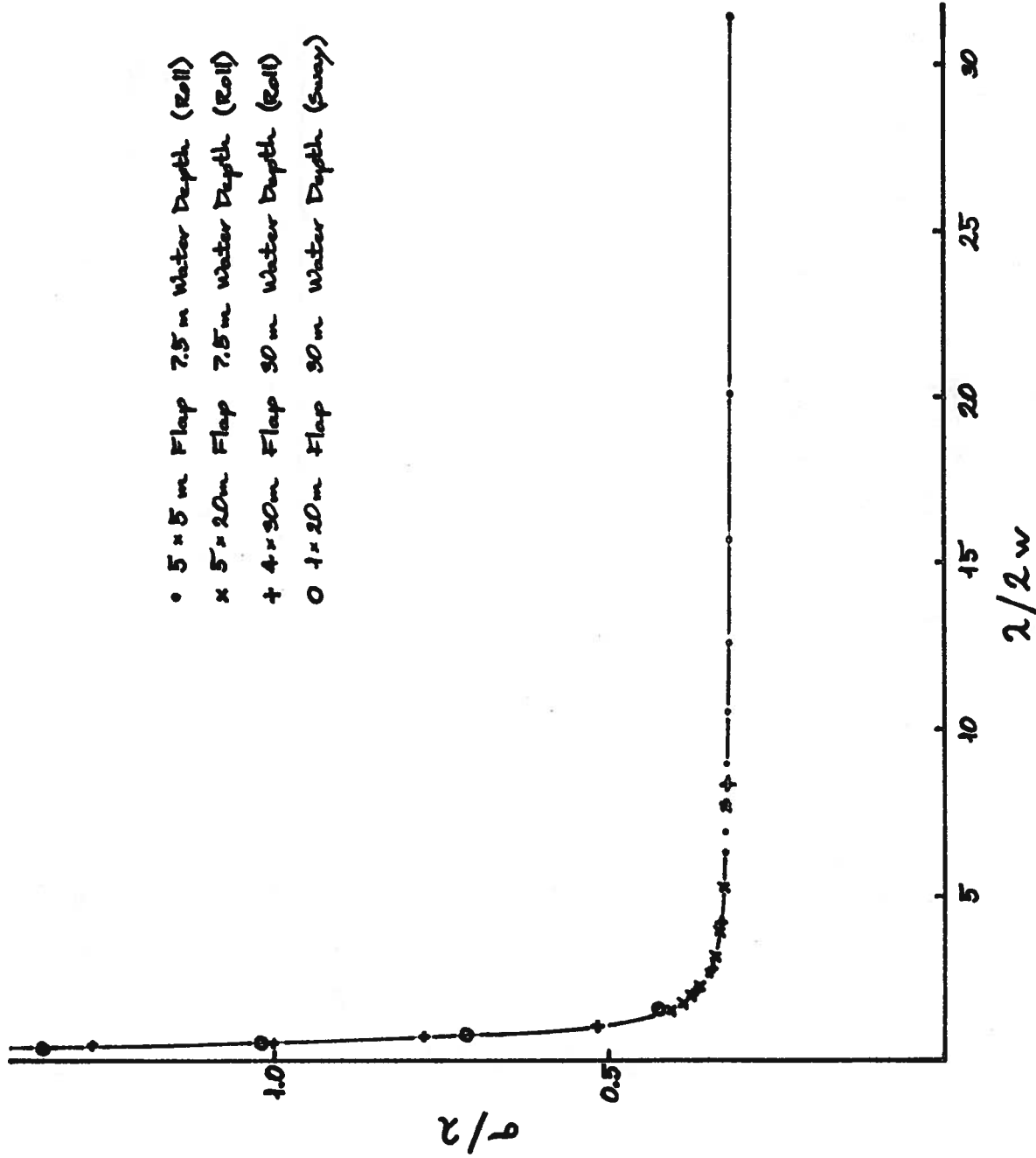


Fig. 33. Absorption cross-section/wavelength ratio, as a function of wavelength/device width.

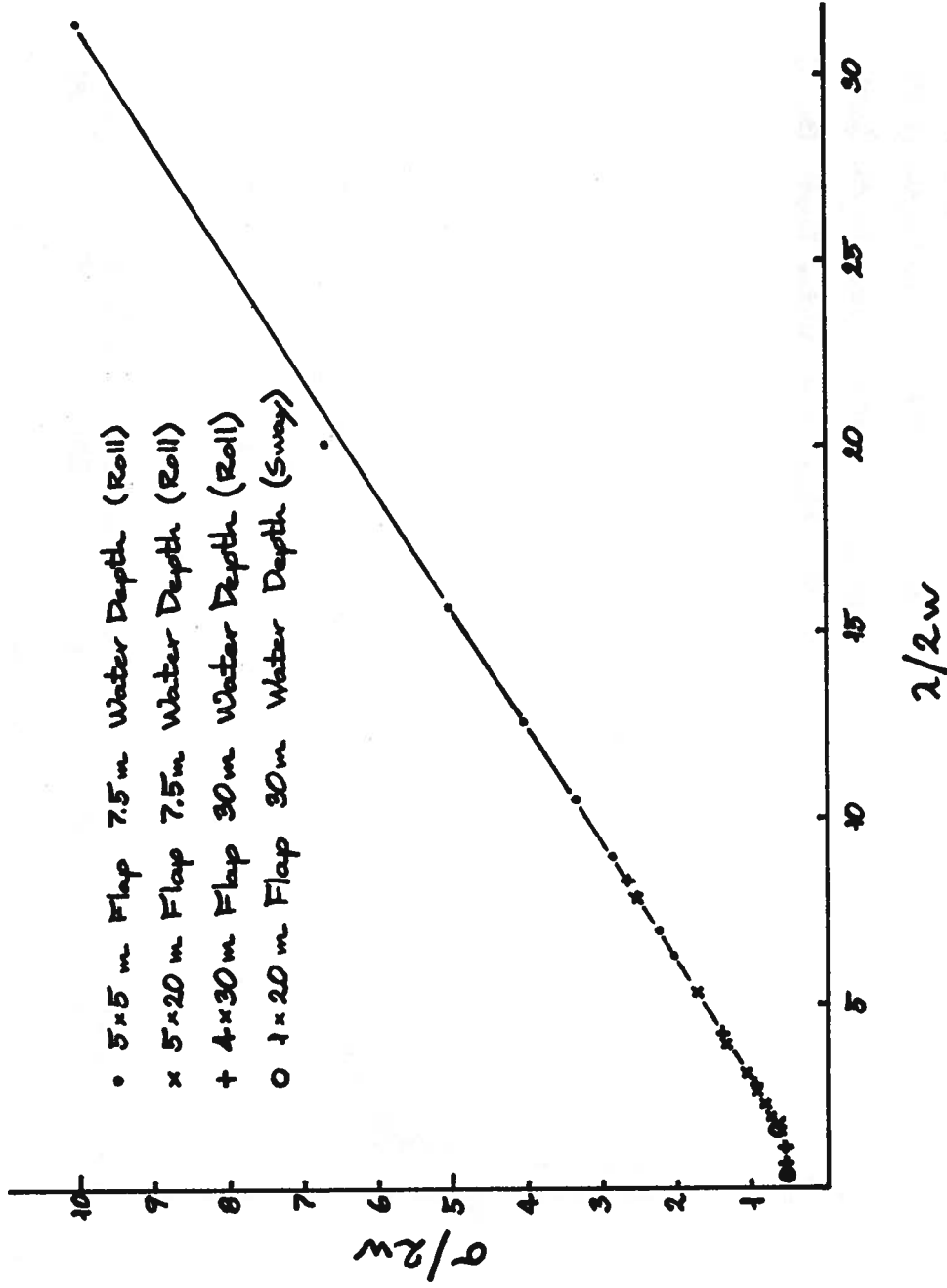


Fig. 34. Absorption cross-section/device width ratio, as a function of wavelength/device width.

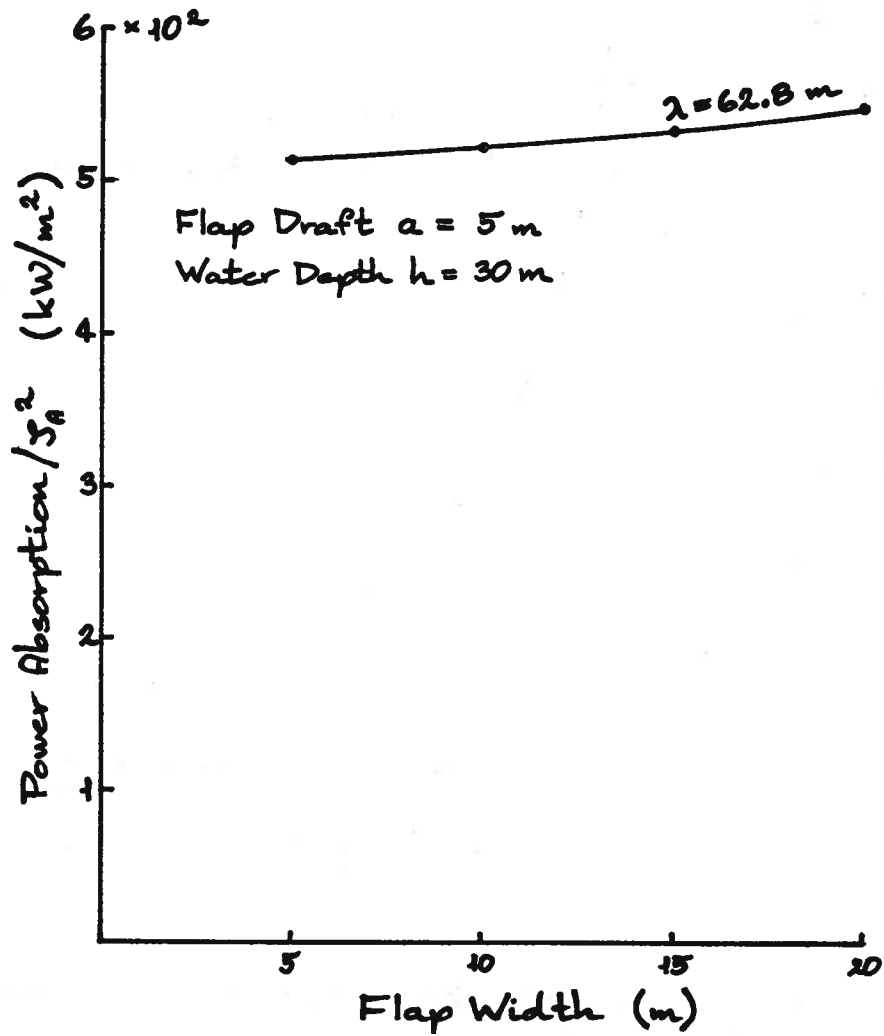


Fig. 35. Maximum absorption versus flap width for a single flap, deep water.

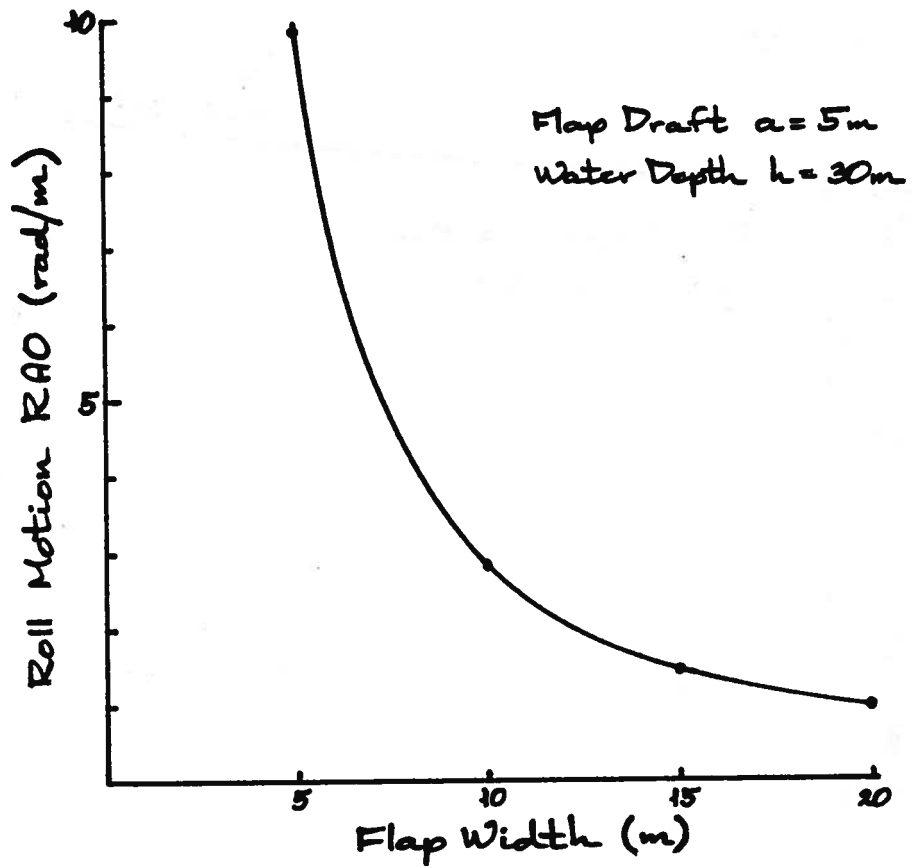


Fig. 36. Motion amplitude at maximum absorption versus flap width for a single flap, deep water.

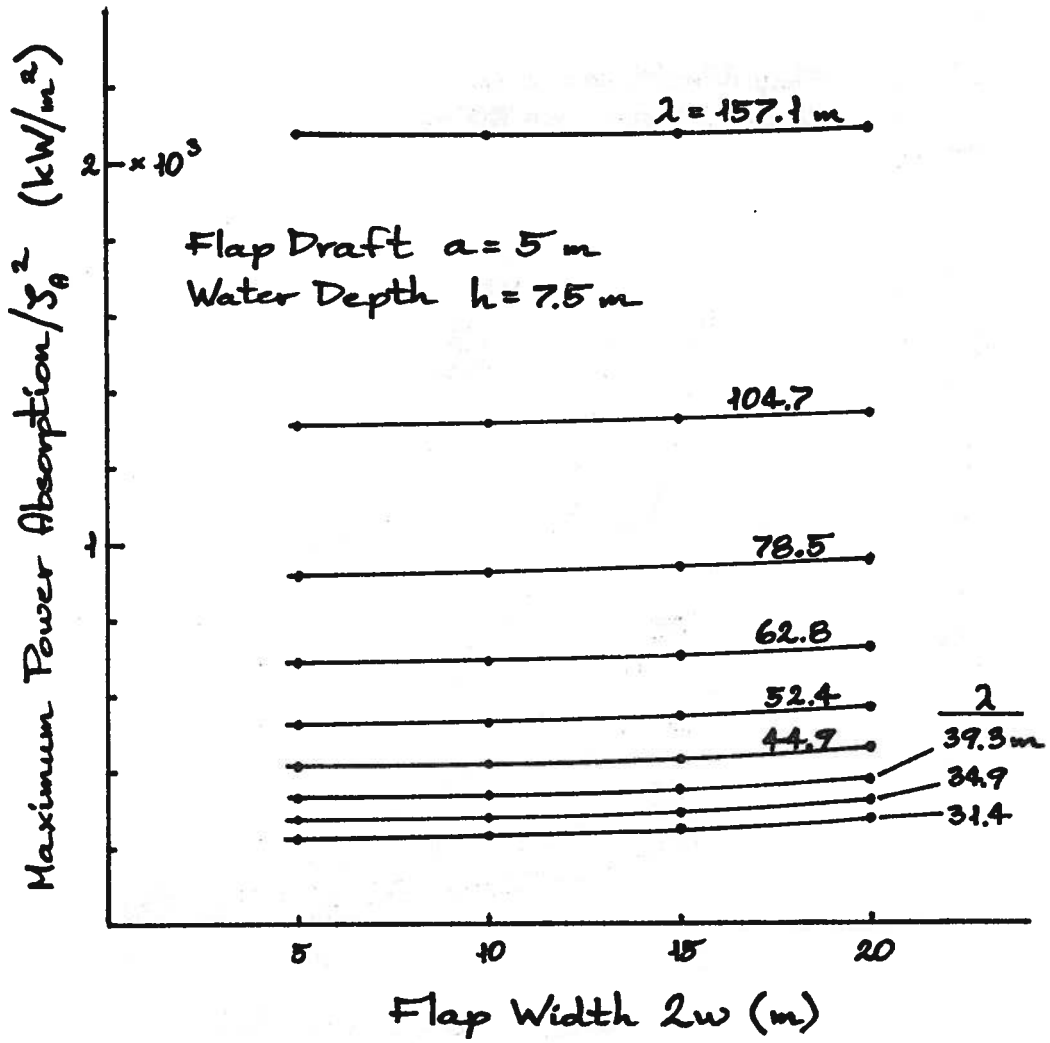


Fig. 37. Maximum absorption versus flap width for a single flap, shallow water.

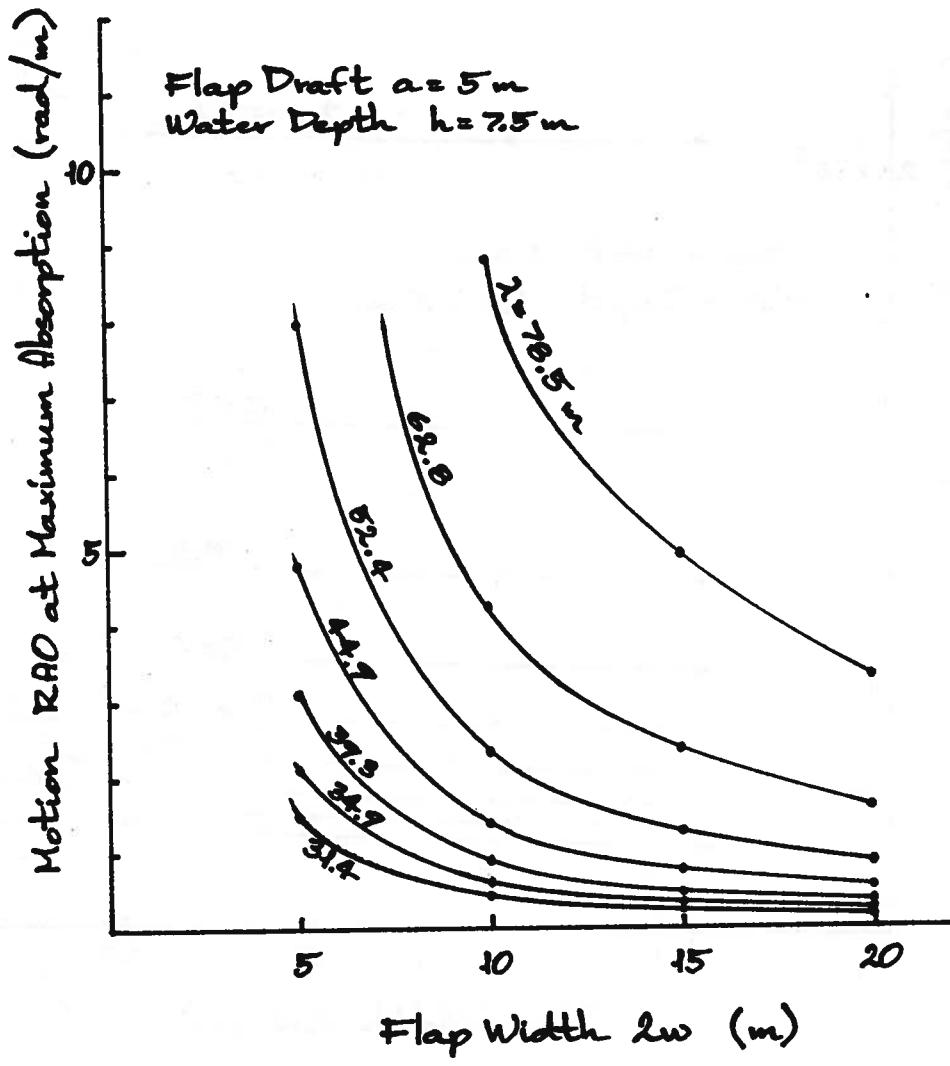


Fig. 38. Motion amplitude at maximum absorption versus flap width for a single flap, shallow water.

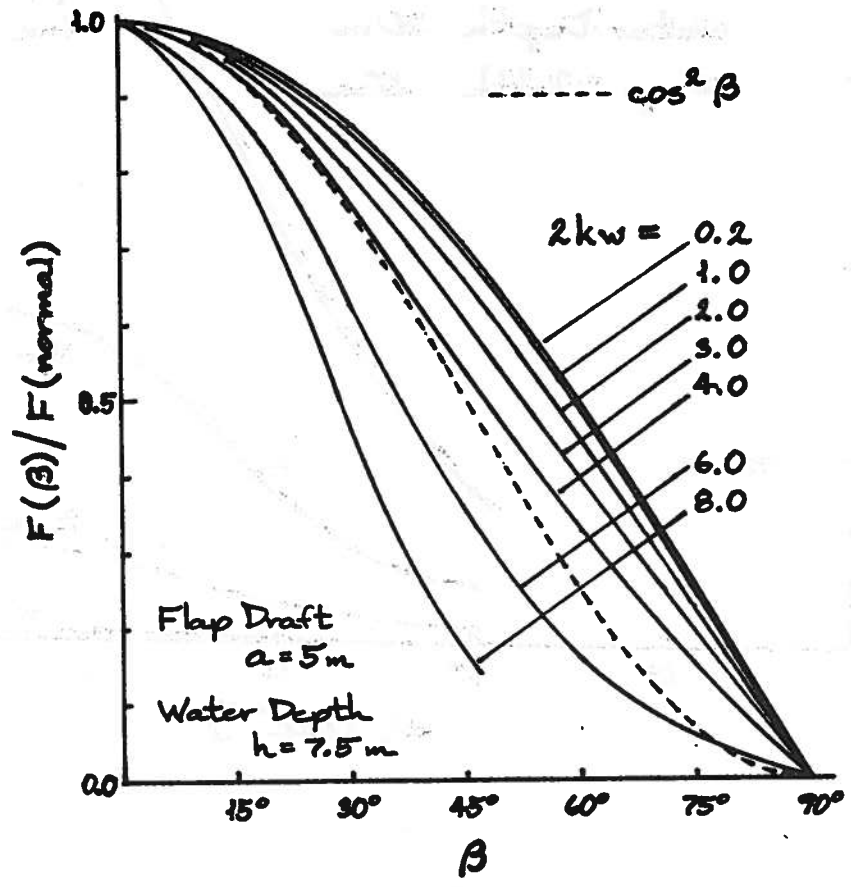


Fig. 39. Exciting force versus encounter angle for single flaps.

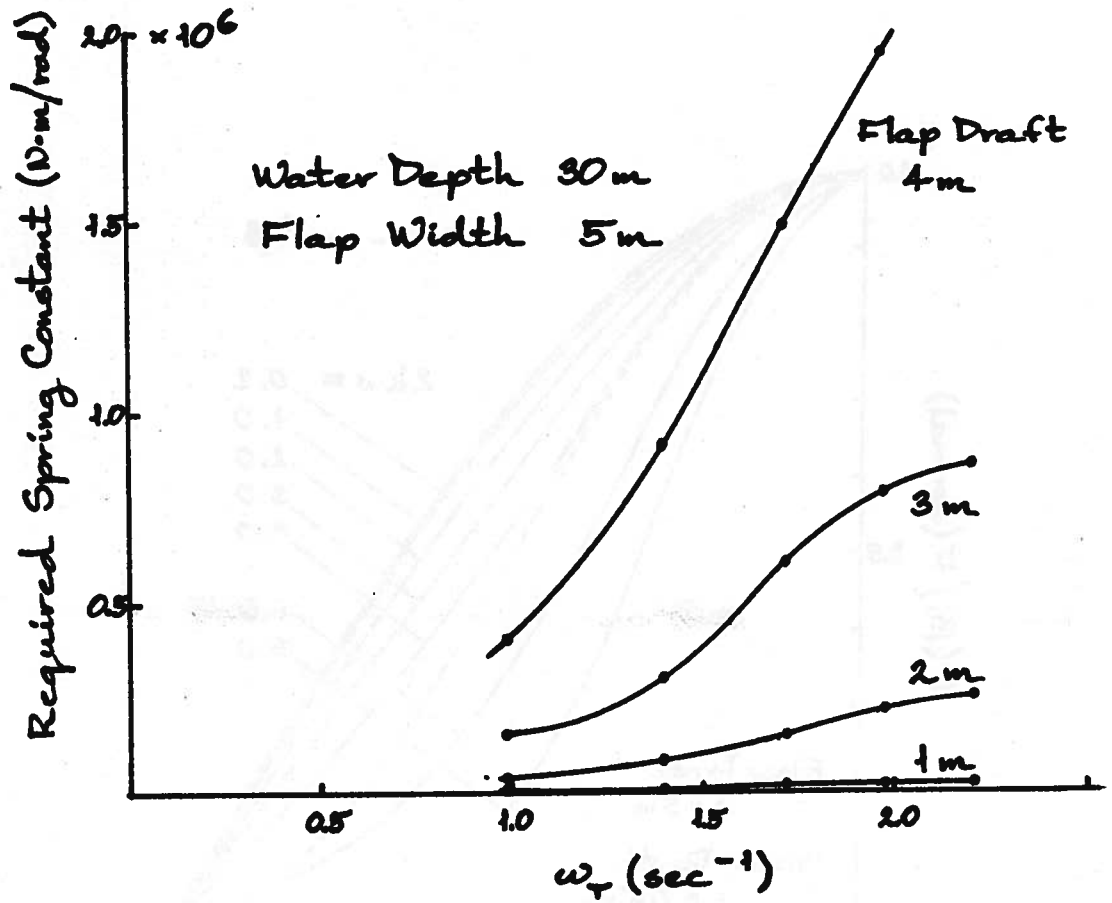


Fig. 40. Required spring constant versus tuned frequency, showing the effect of flap draft on tuning.

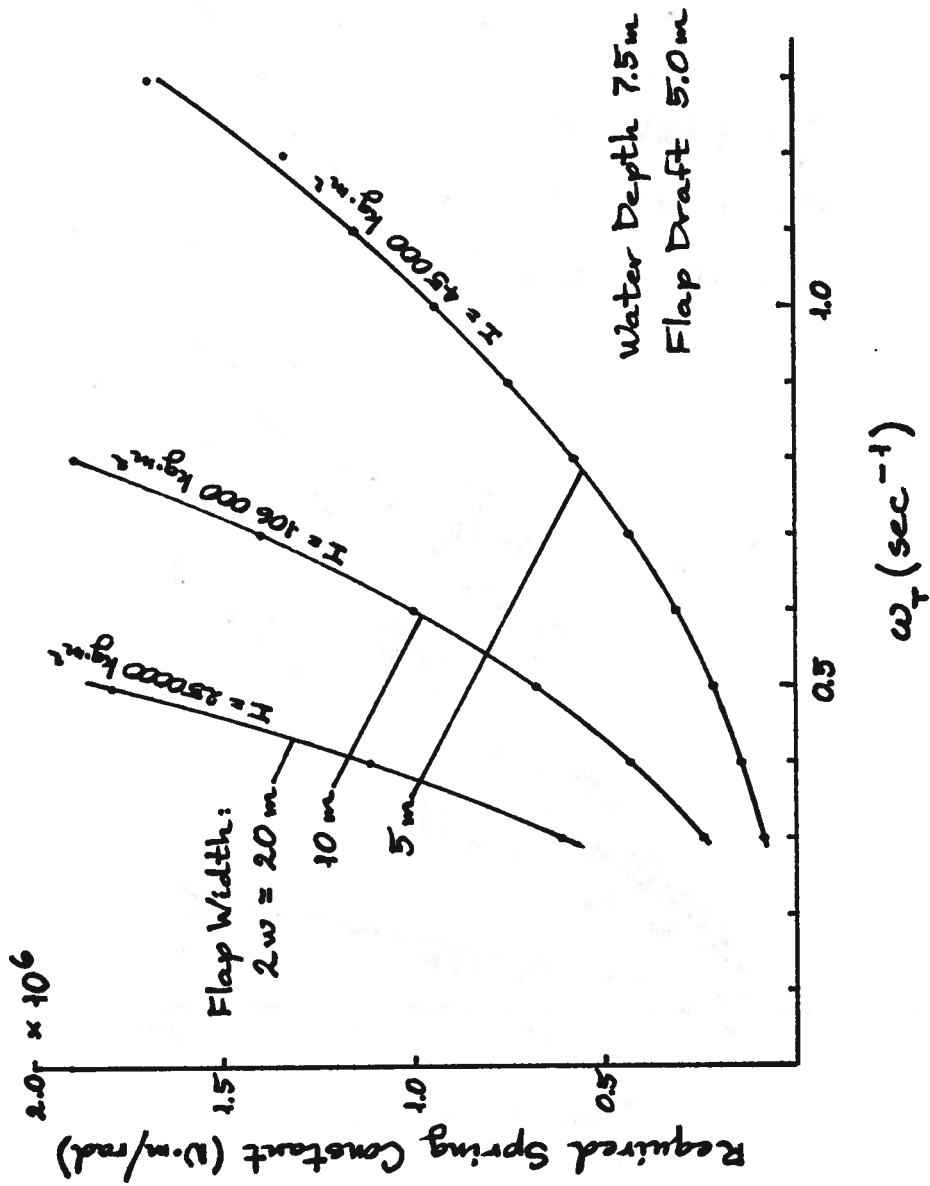


Fig. 41. Required spring constant versus tuned frequency showing the effect of flap width on tuning.

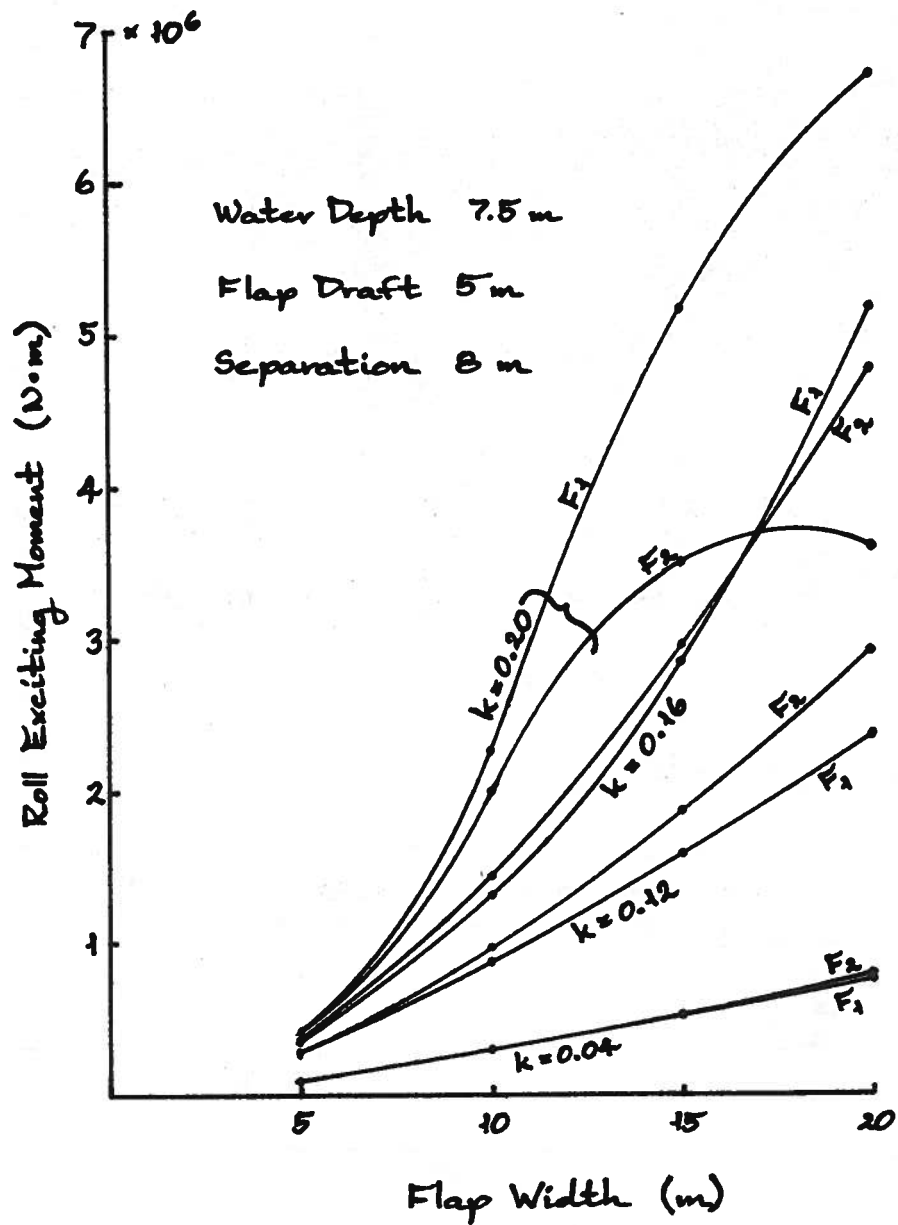


Fig. 42a. Exciting force magnitudes and phase versus flap width for a twin flap.

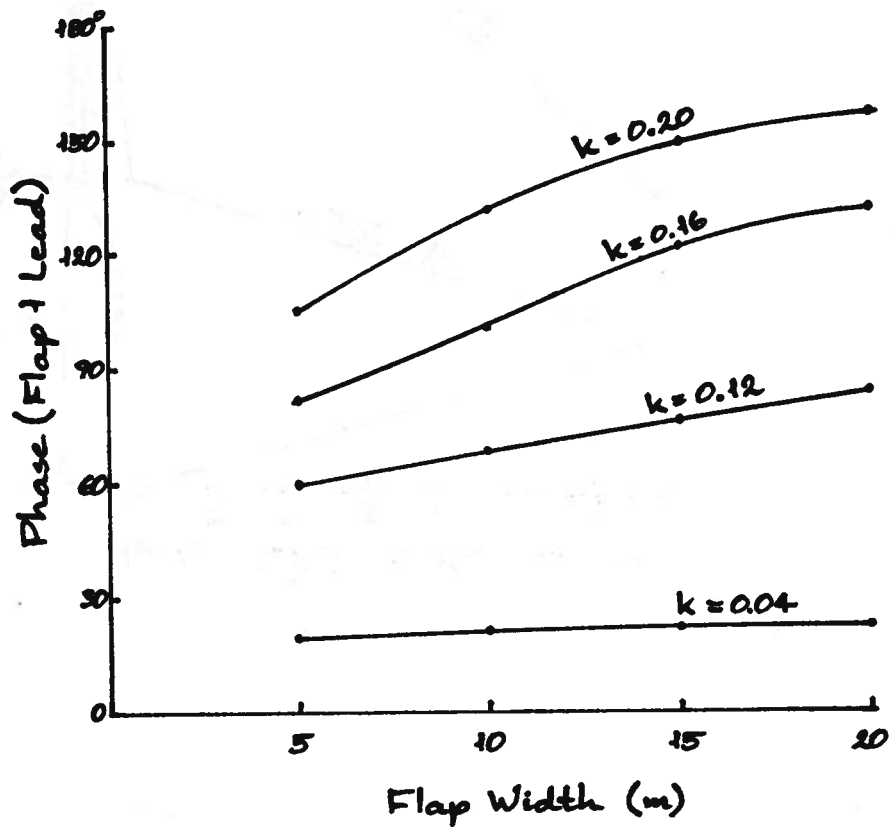


Fig. 42b. Exciting force magnitudes and phase versus flap width for a twin flap (continued).

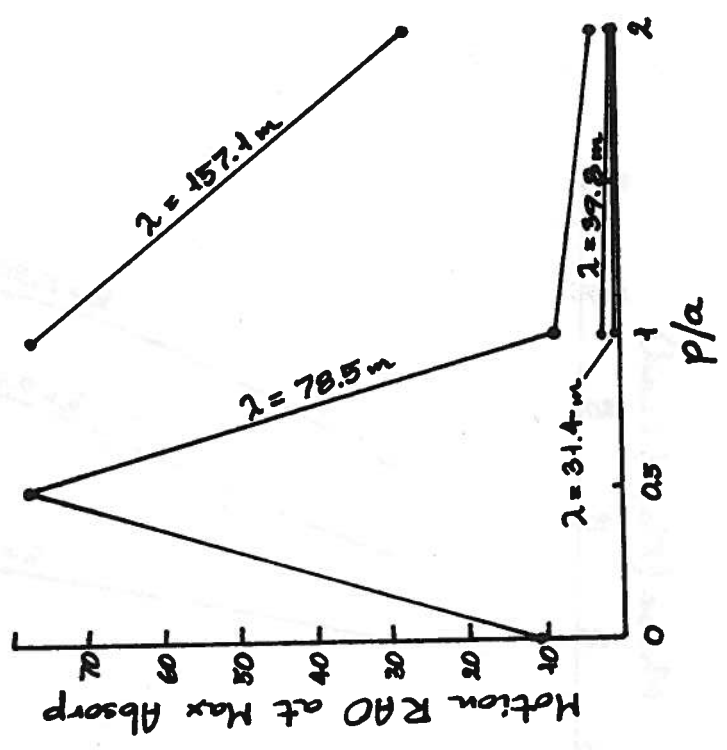
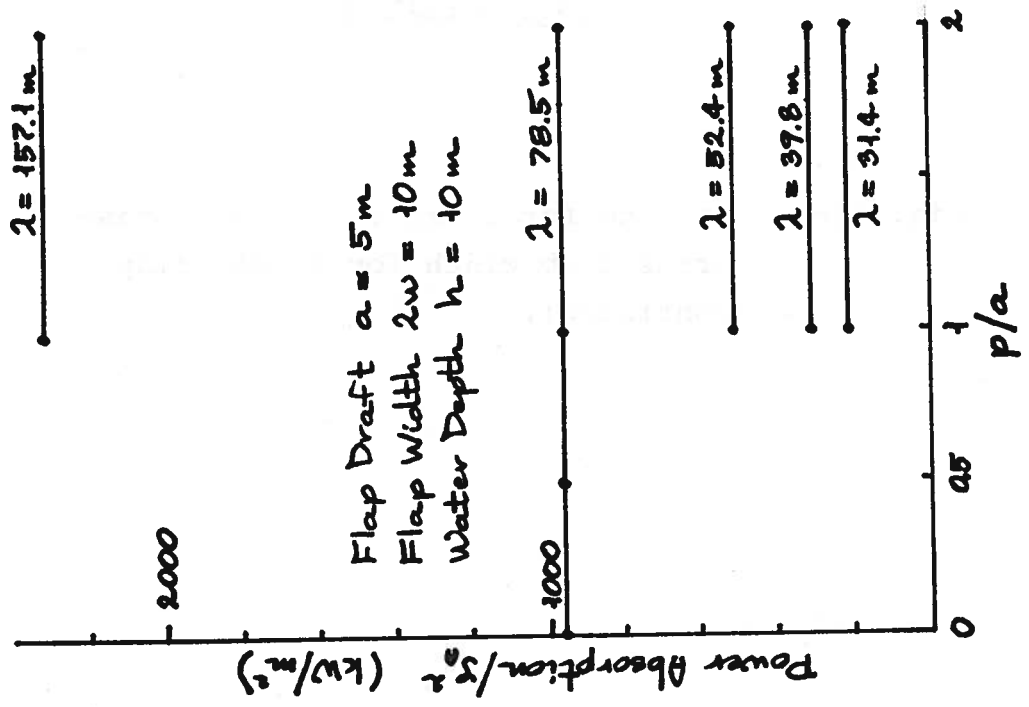


Fig. 43. Maximum absorption and motion amplitude versus pivot depth/draft ratio.

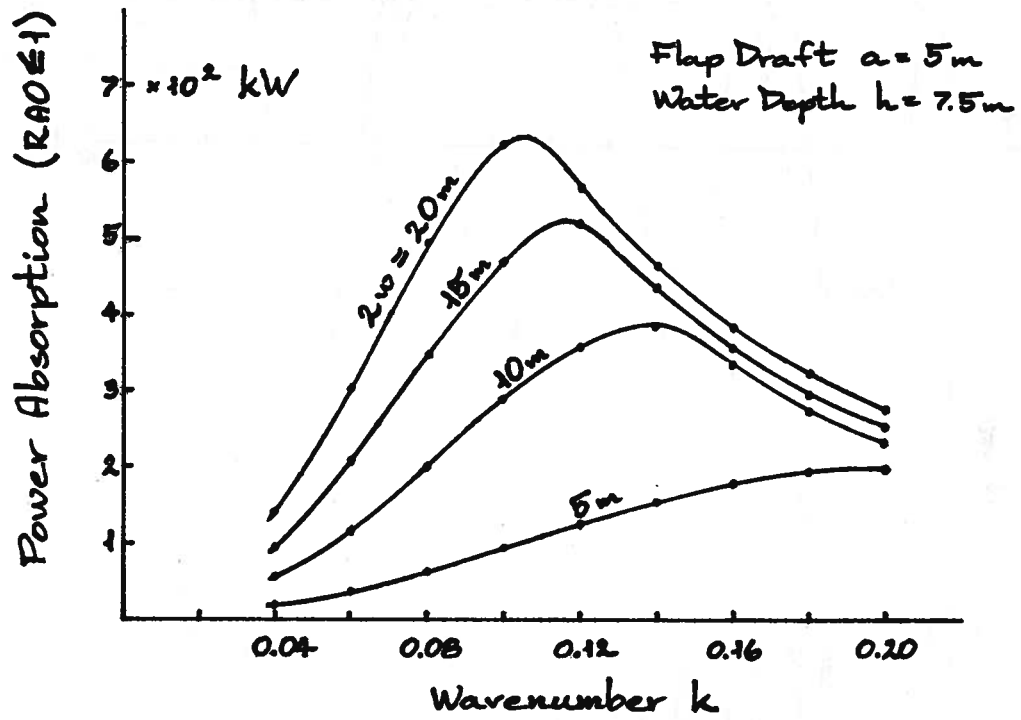


Fig. 44. Absorbed power with a maximum stroke constraint ($RAO = 1$) obtained by overdamping, versus flap width.

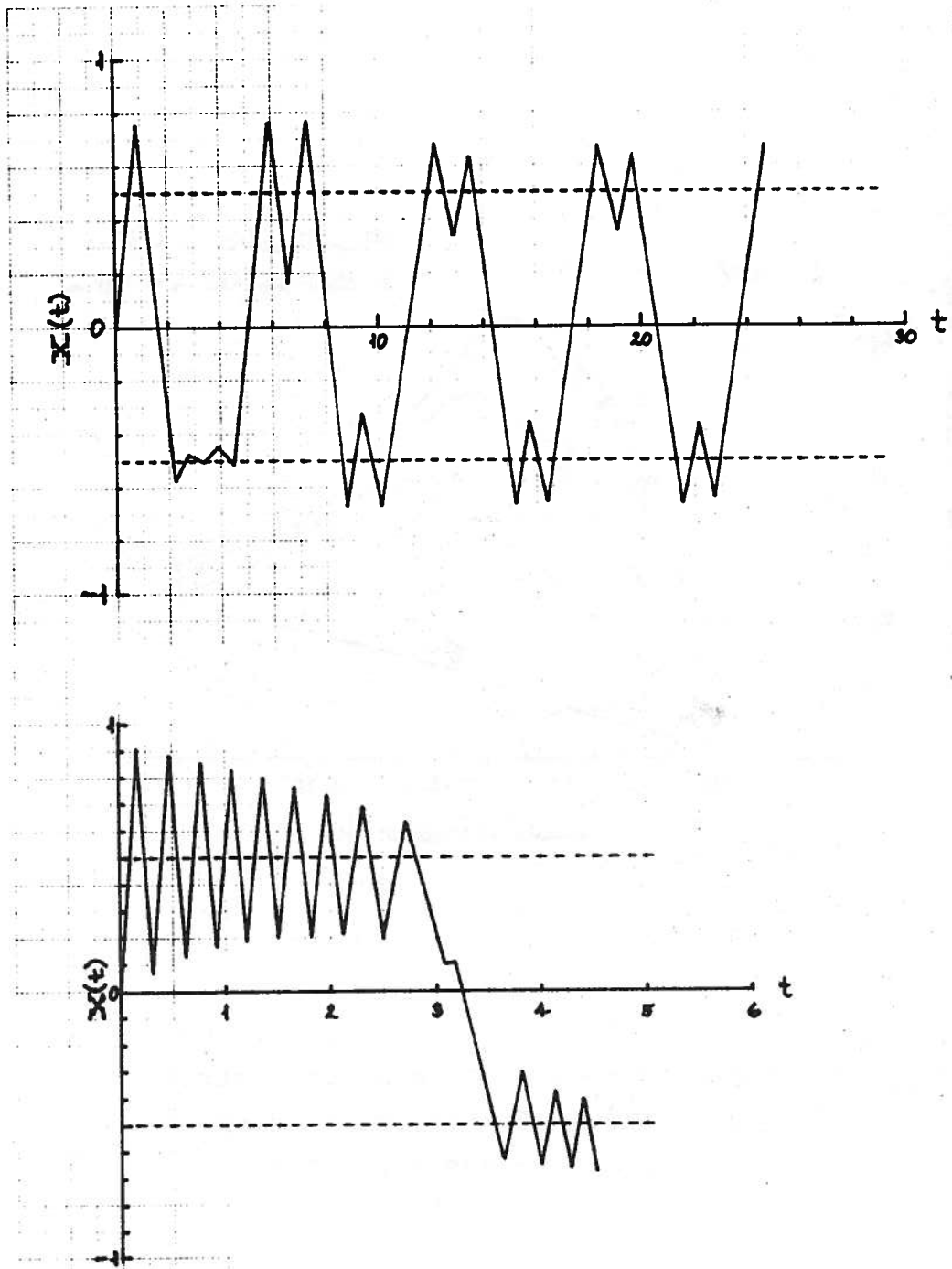


Fig. 45. Bouncing off the stops with a nonlinear spring stroke limiter at low exciting-force frequencies.

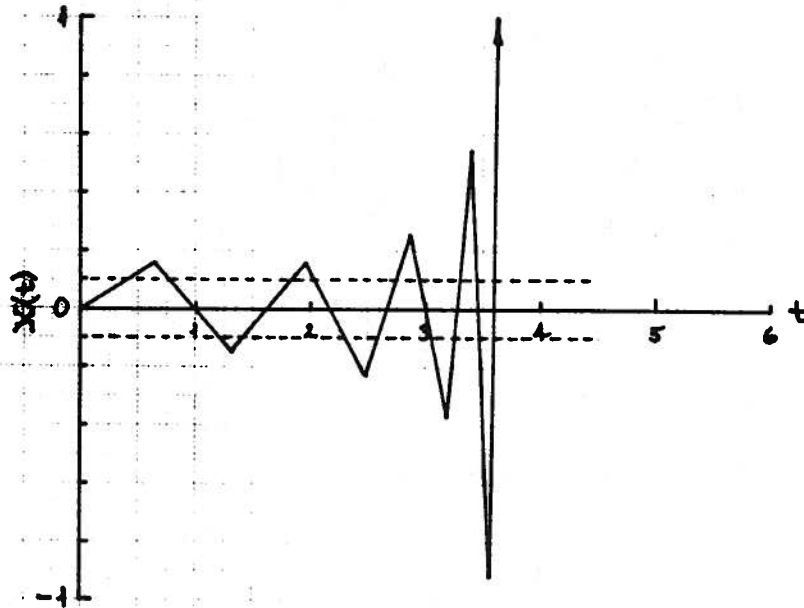


Fig. 46. Instability of a time-step simulation at resonant frequency with a nonlinear spring stroke limiter.

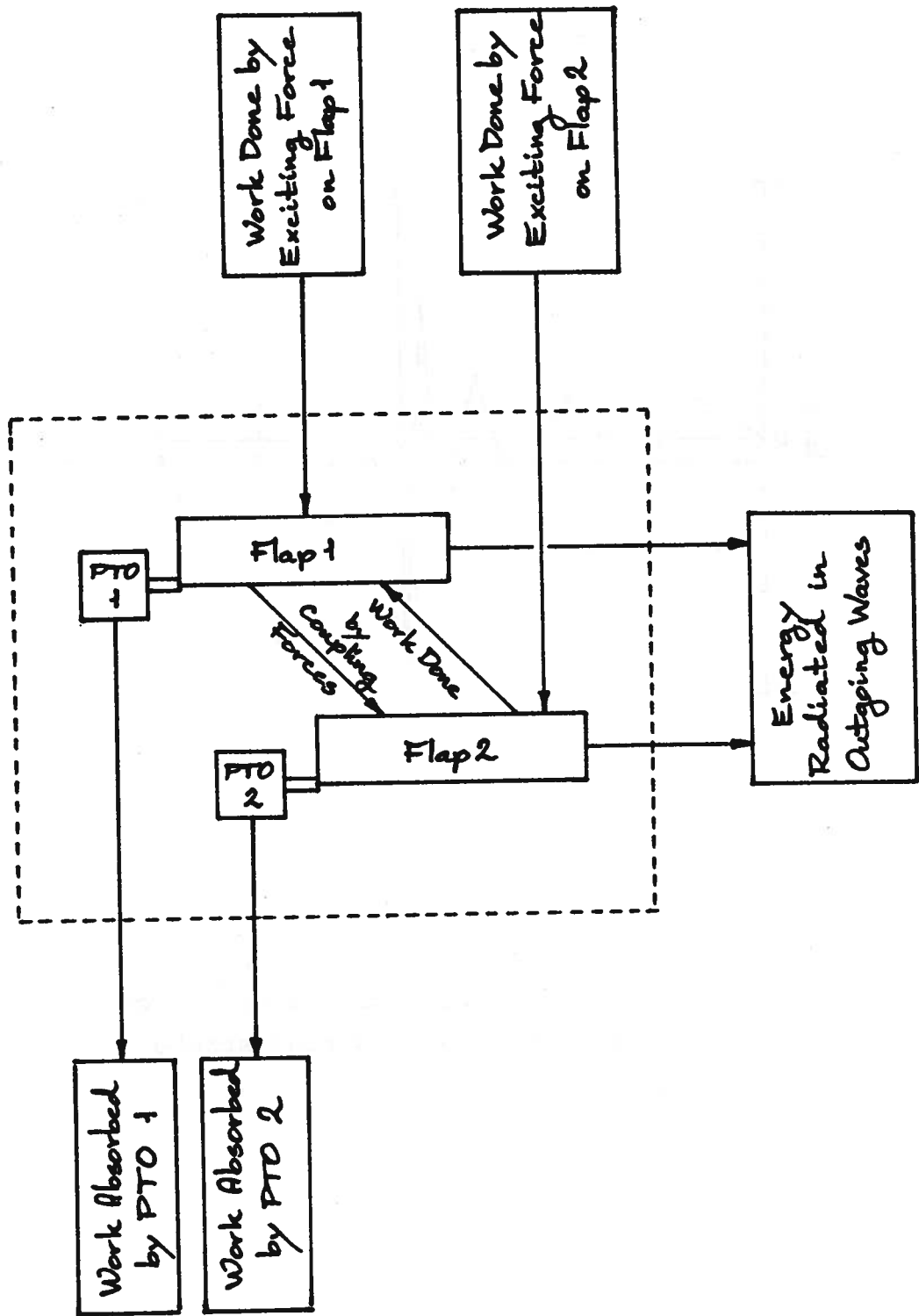


Fig. 47. Energy budget schematic for a twin-flap system.

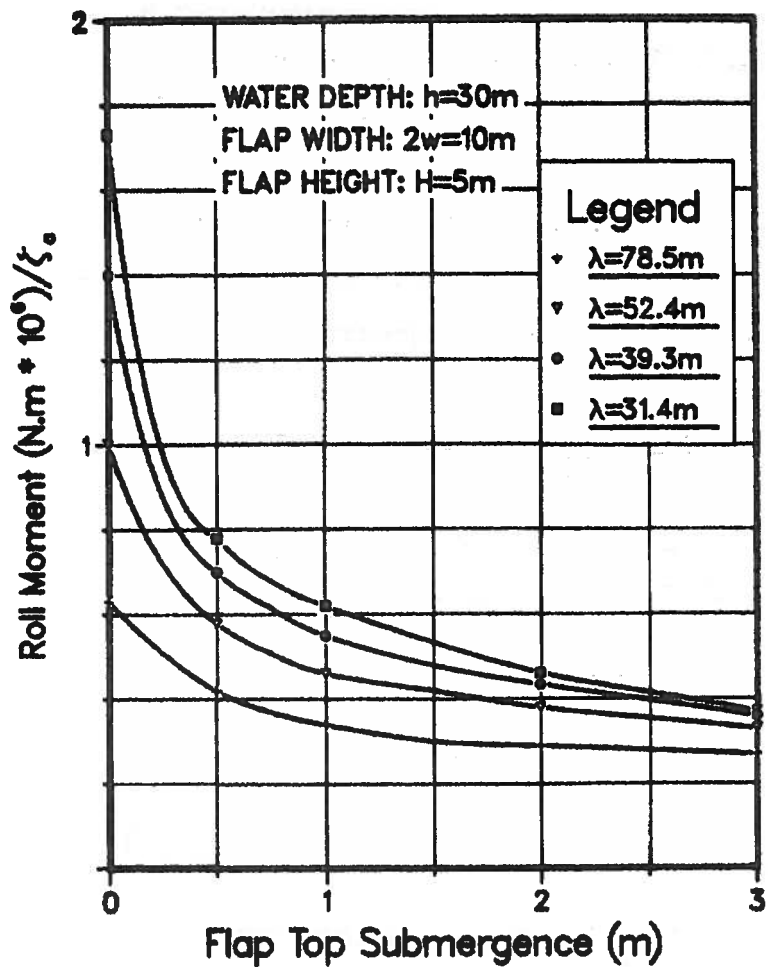


Fig. 48. Exciting force versus flap top submergence, deep water.

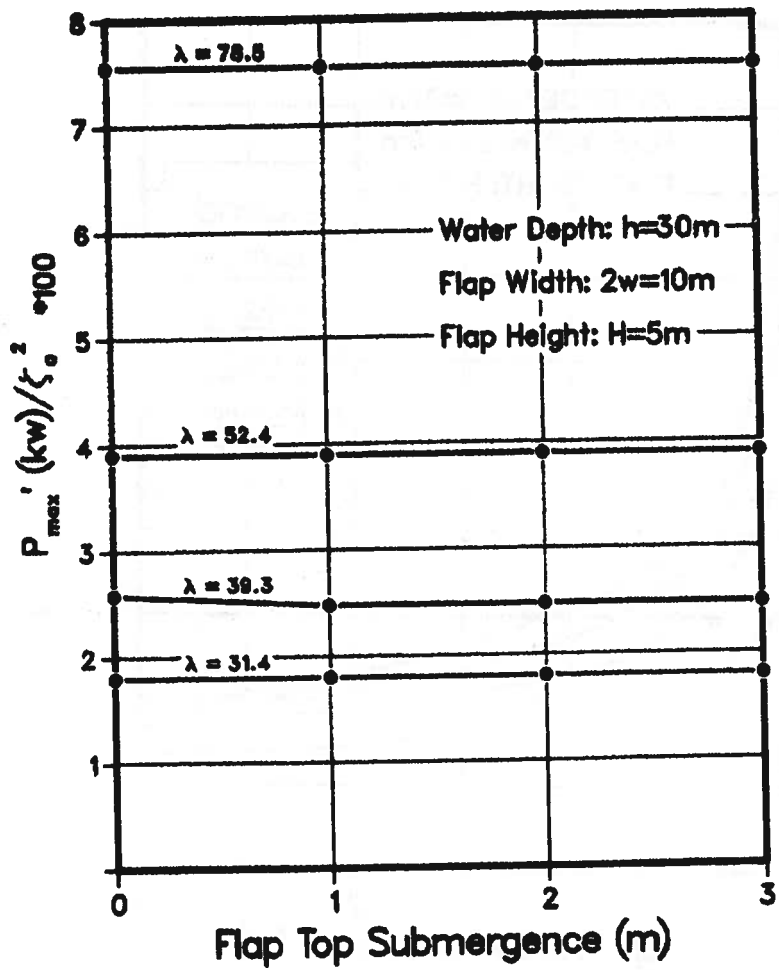


Fig. 49. Maximum absorption versus flap top submergence.

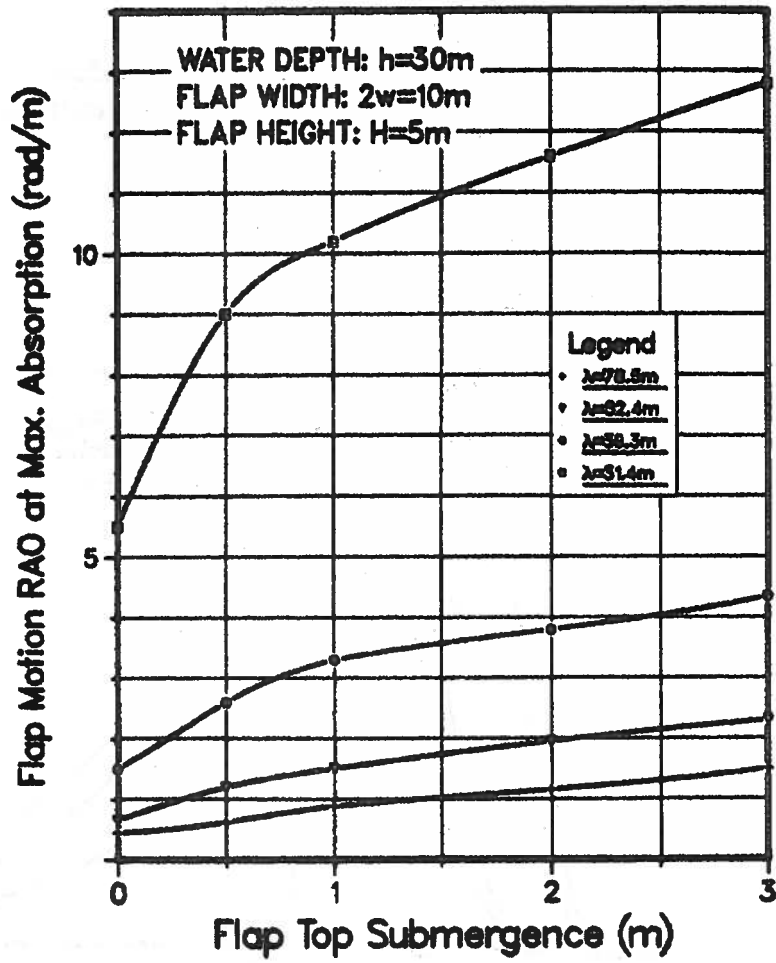


Fig. 50. Motion amplitude at maximum absorption versus flap top submergence.

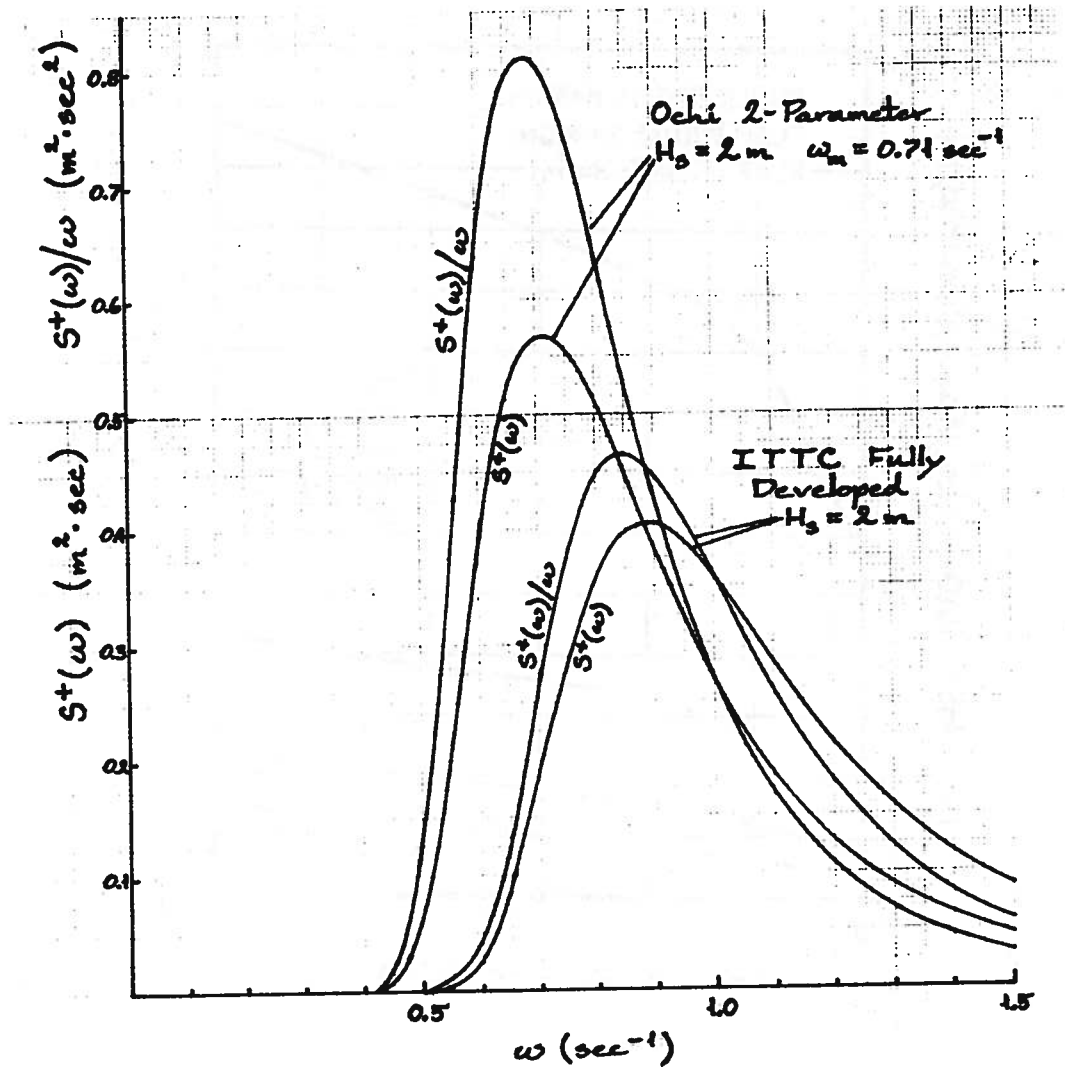


Fig. 51. Two spectra for 2 m significant wave height, showing both variance spectral density and power density.

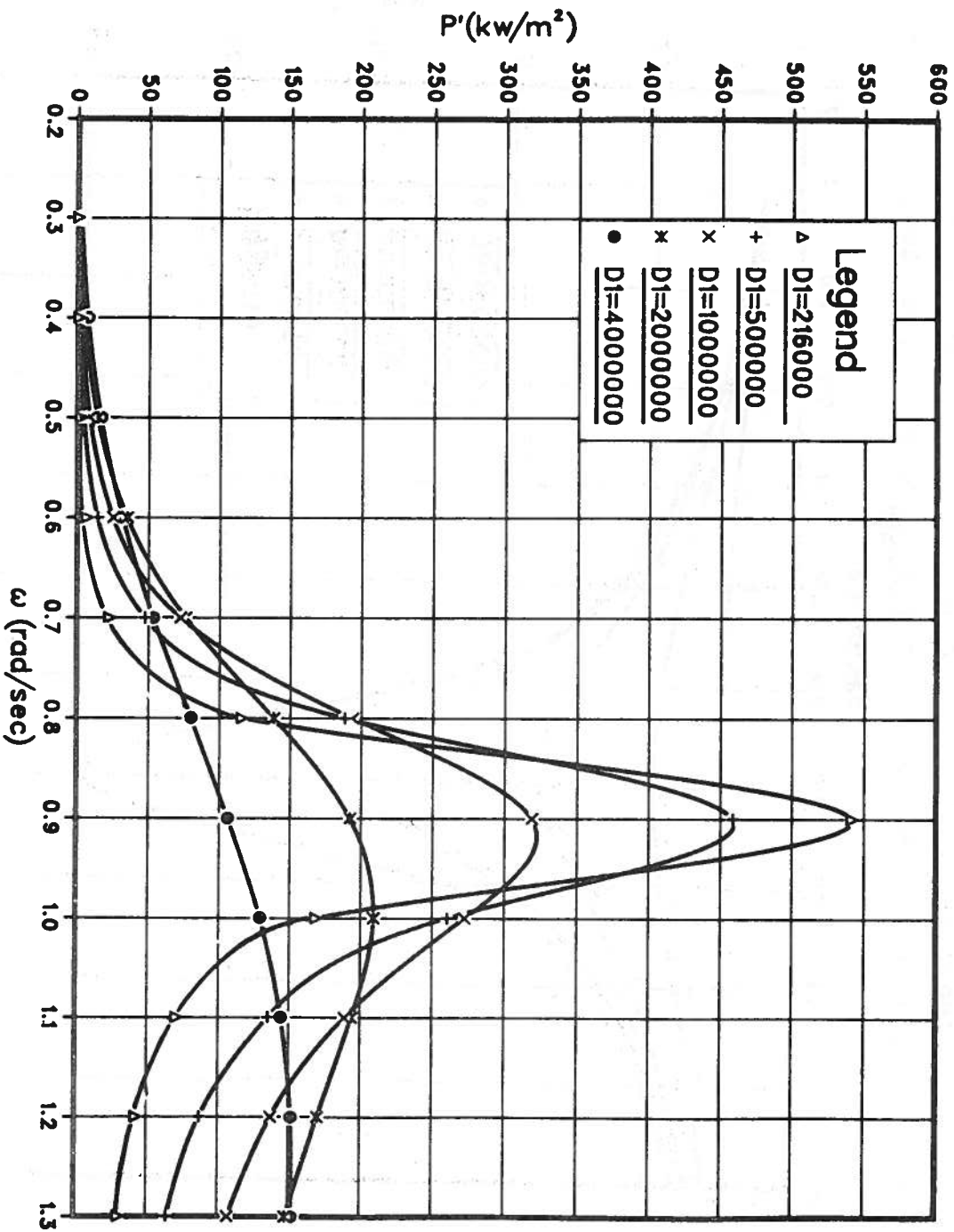


Fig. 52. Specific power absorption curves for a 5 x 10 m flap, water depth 7.5 m, tuned to a frequency of 0.9 rad/sec, at various dampings.

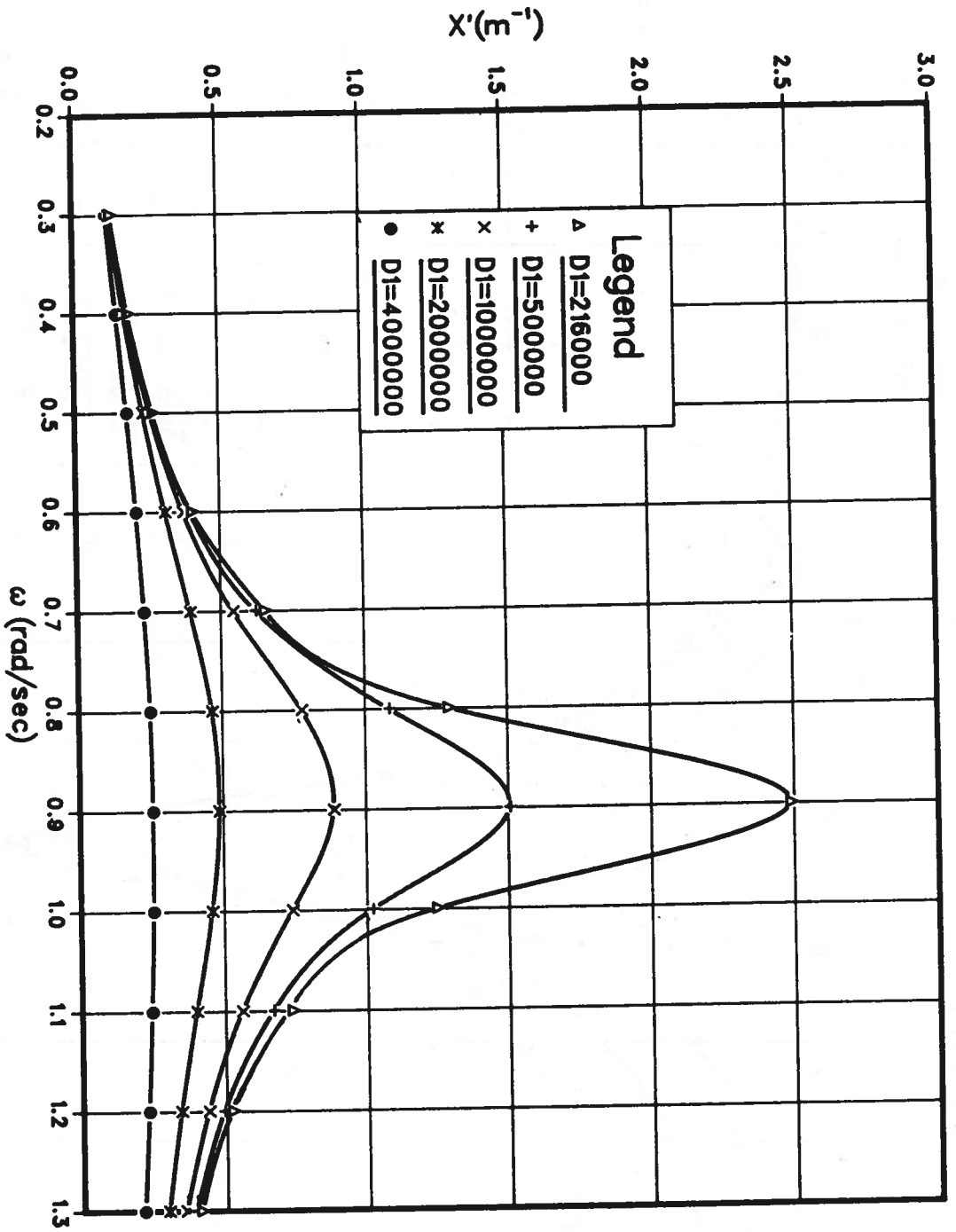


Fig. 53. Motion amplitudes for a 5 x 10 m flap, water depth 7.5 m, tuned to a frequency of 0.9 rad/sec, at various dampings.

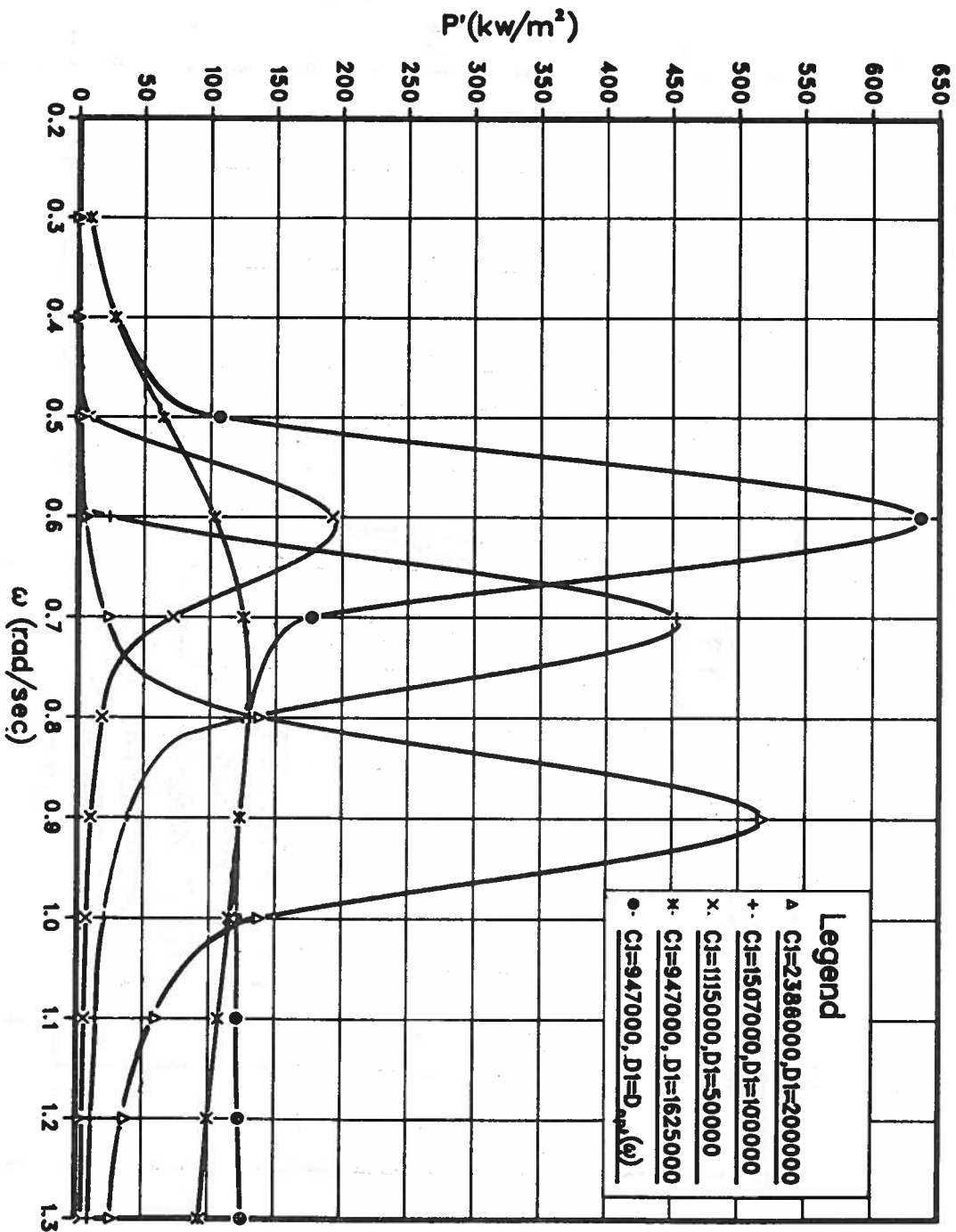


Fig. 54. Specific power absorption curves for a 5 x 10 m flap, water depth 7.5 m, at various tunings and dampings.

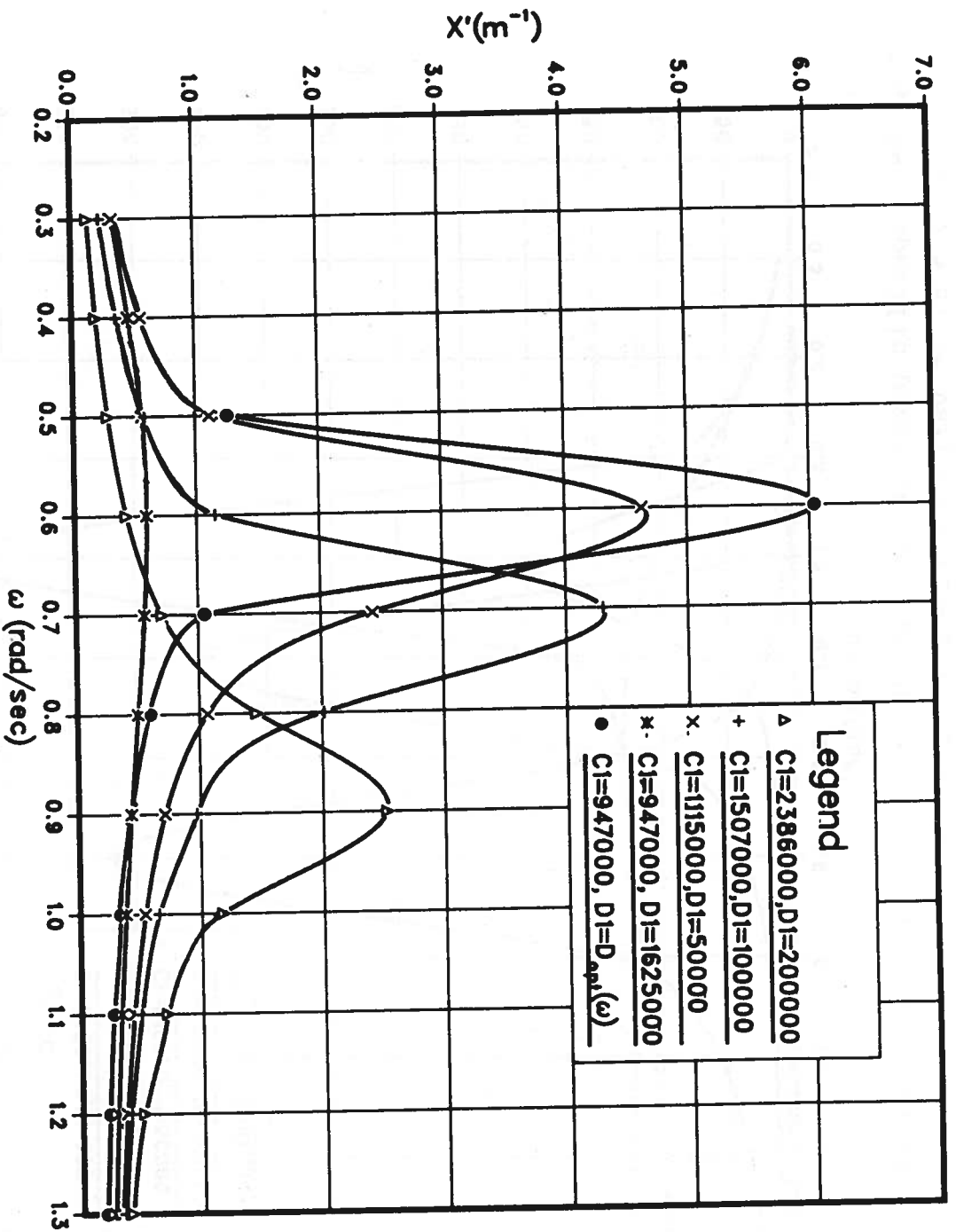


Fig. 55. Motion amplitudes for a 5 x 10 m flap, water depth 7.5 m, at various tunings and dampings.

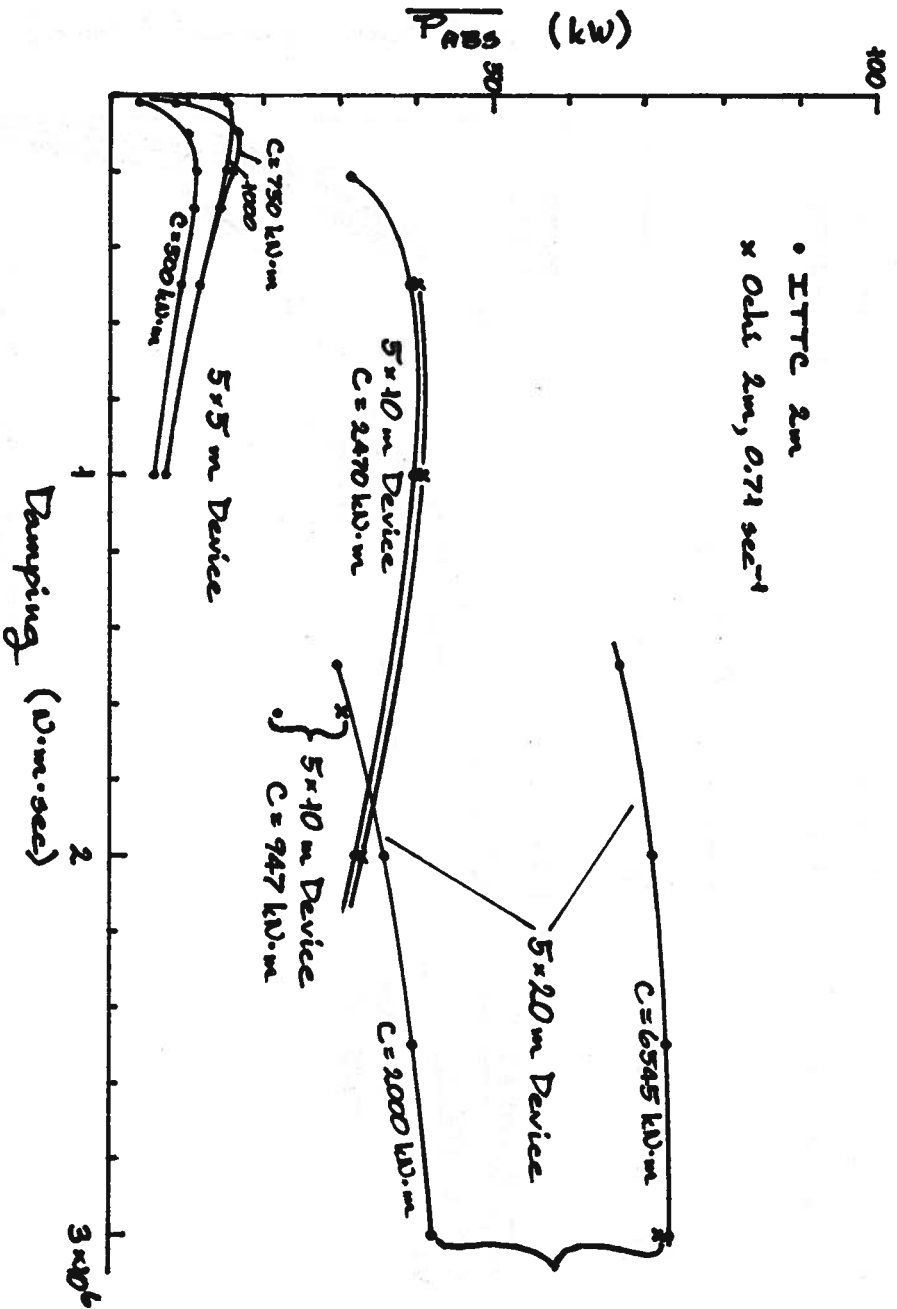


Fig. 56. Average power absorption in 2-m significant wave height versus damping for three device sizes, various tunings.

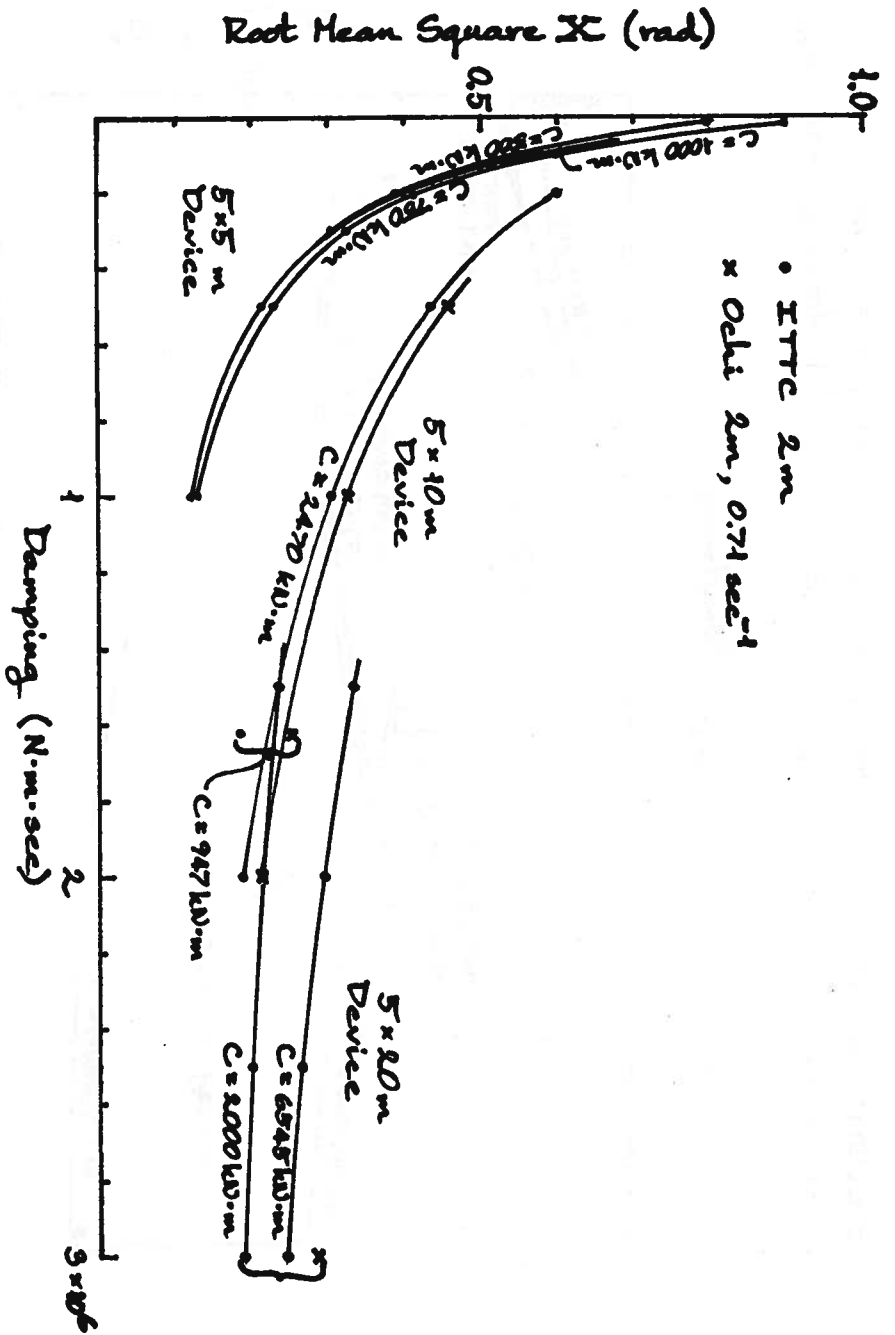


Fig. 57. Root-mean square motion in 2 m significant wave height versus damping for three device sizes, various tunings.

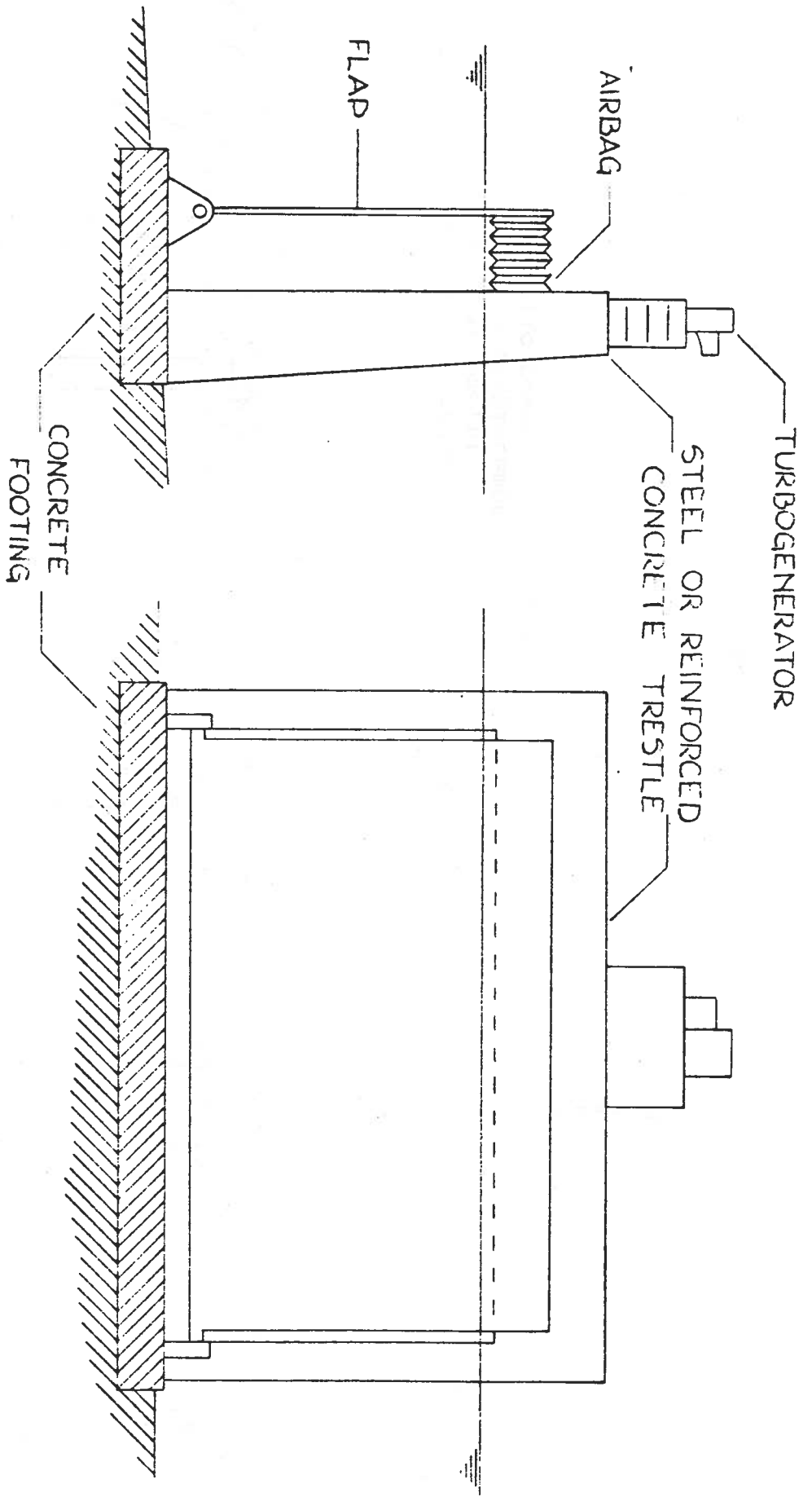
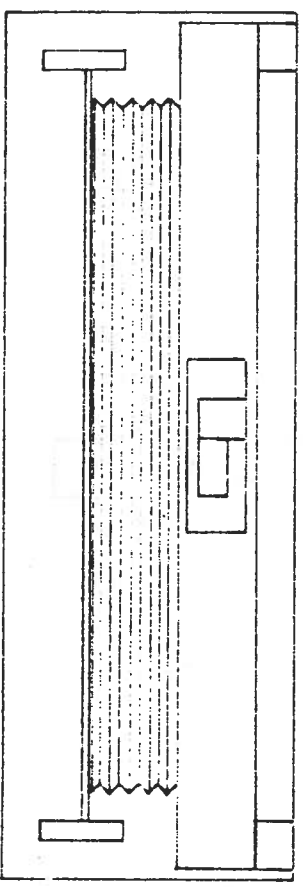


Fig. A1. Flap device arrangement with a top-mounted airbag and turbine power takeoff system.



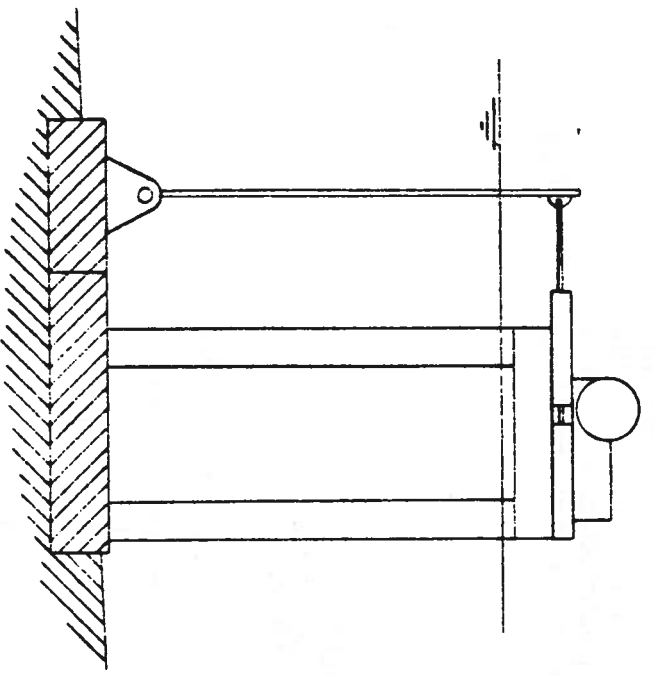
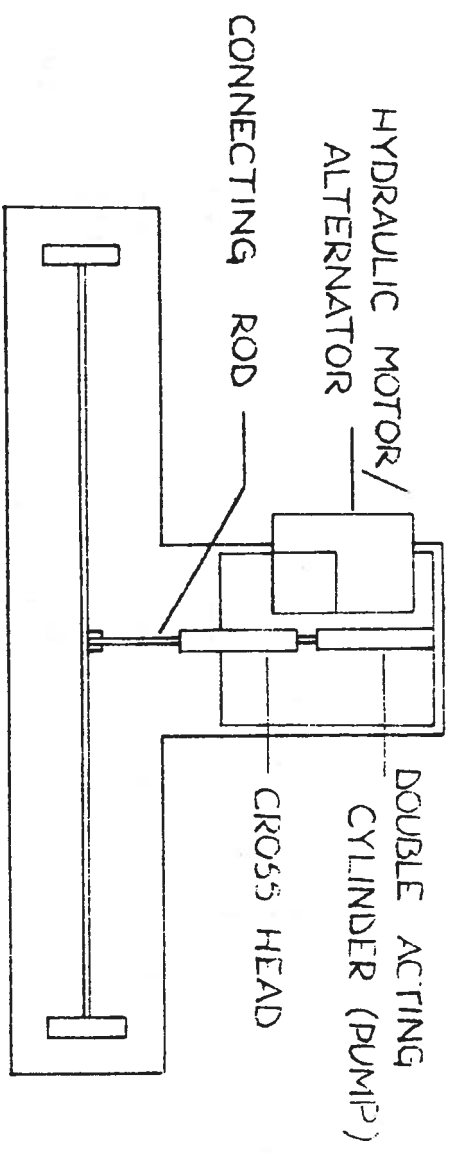
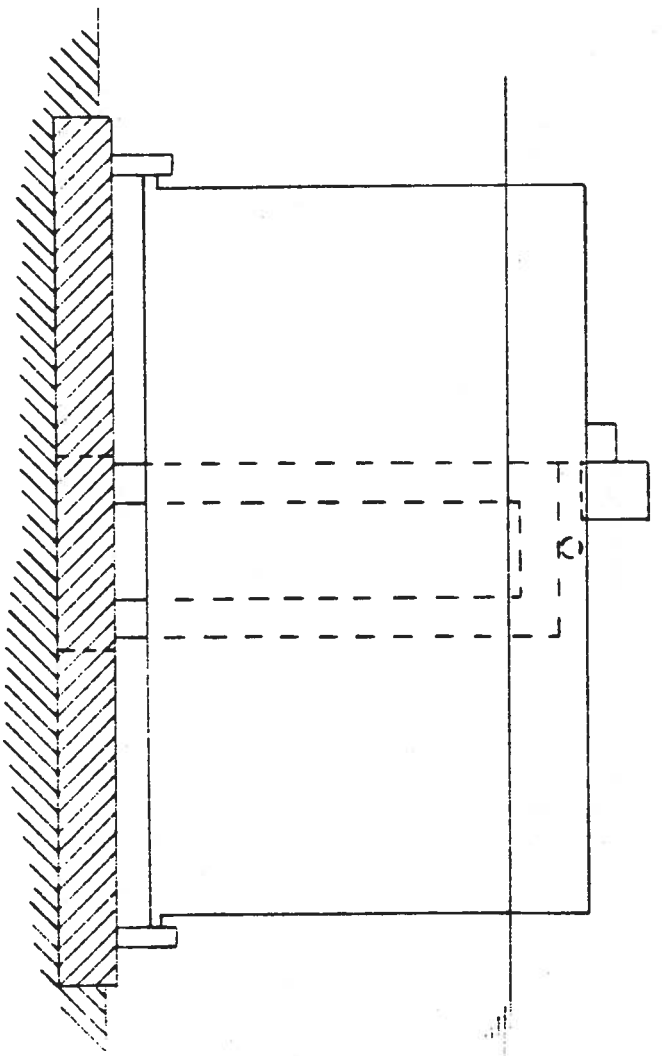


Fig. A2. Flap device arrangement with a top-mounted positive-displacement hydraulic power takeoff.



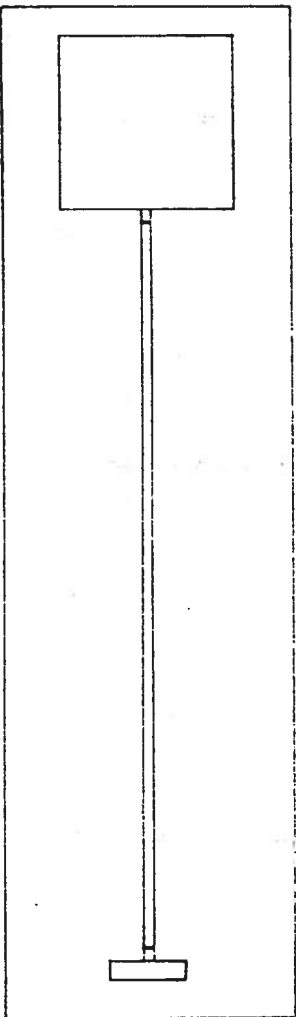
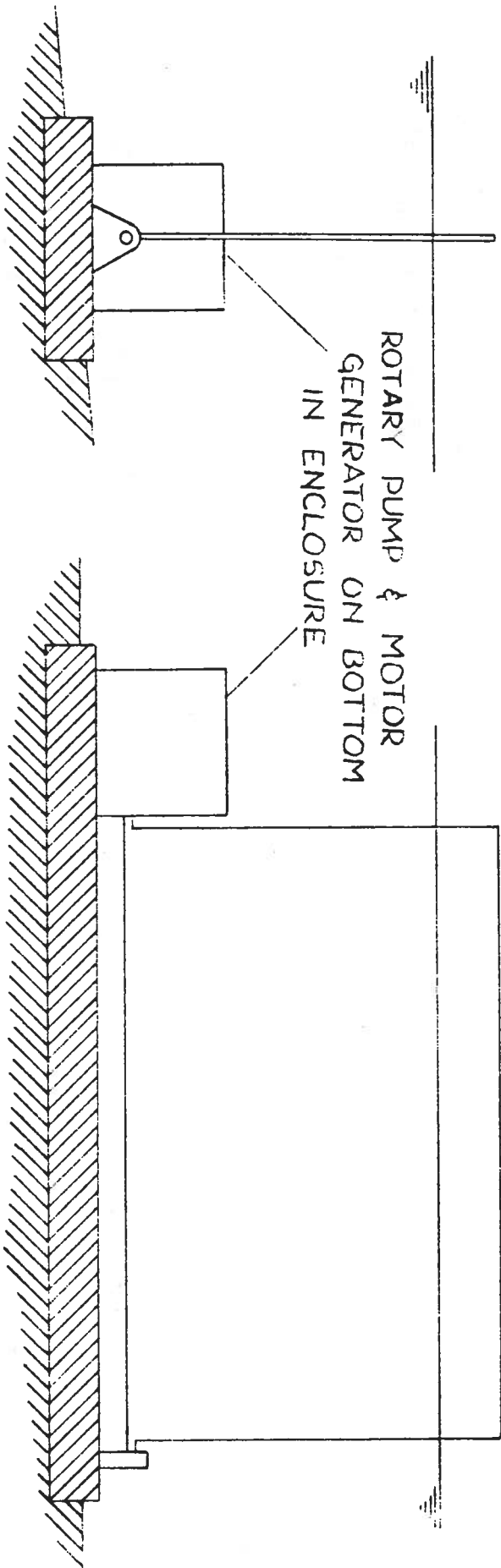


Fig. A3. Flap device arrangement with a bottom-mounted hydraulic power takeoff in an underwater enclosure.

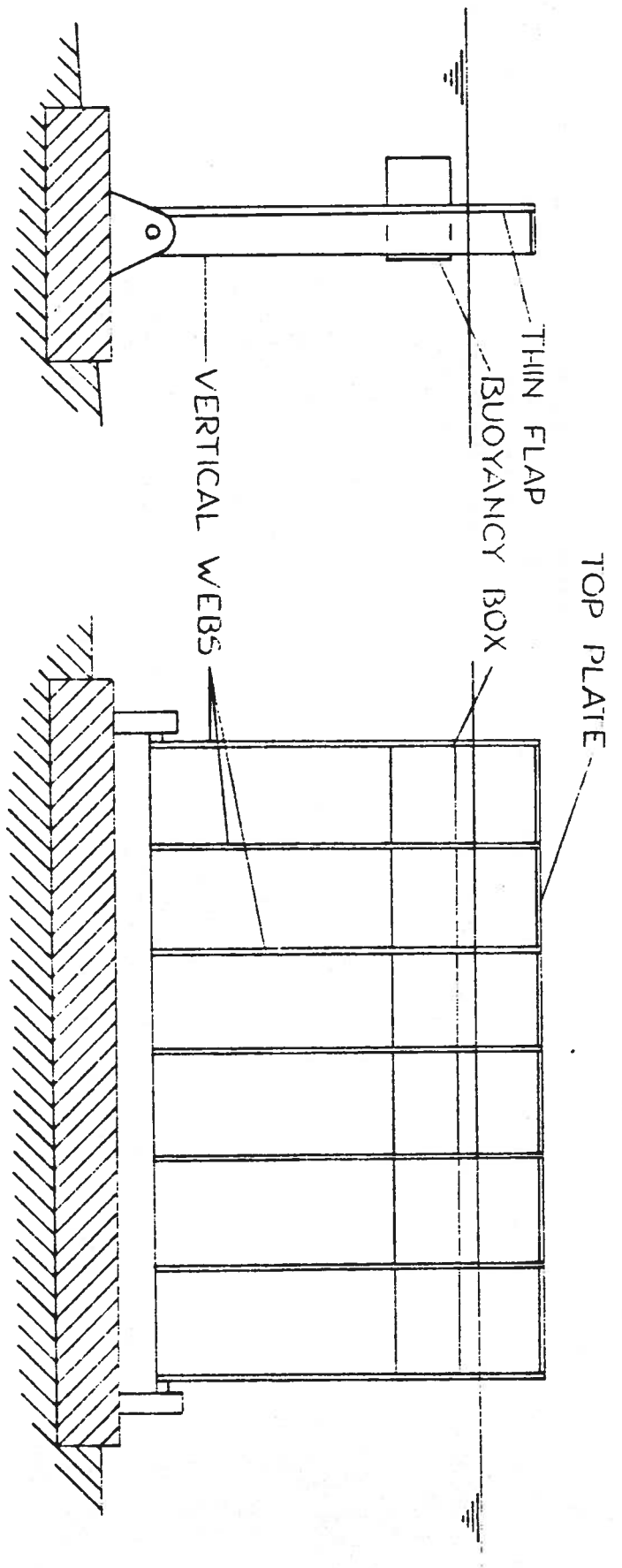
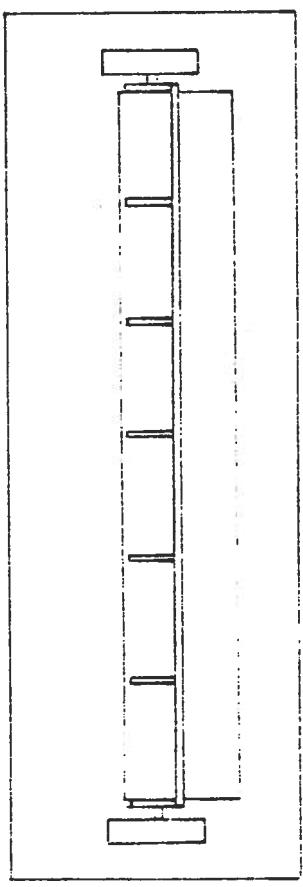


Fig. A4. Stiffened single plate flap with a buoyant member for restoring force.



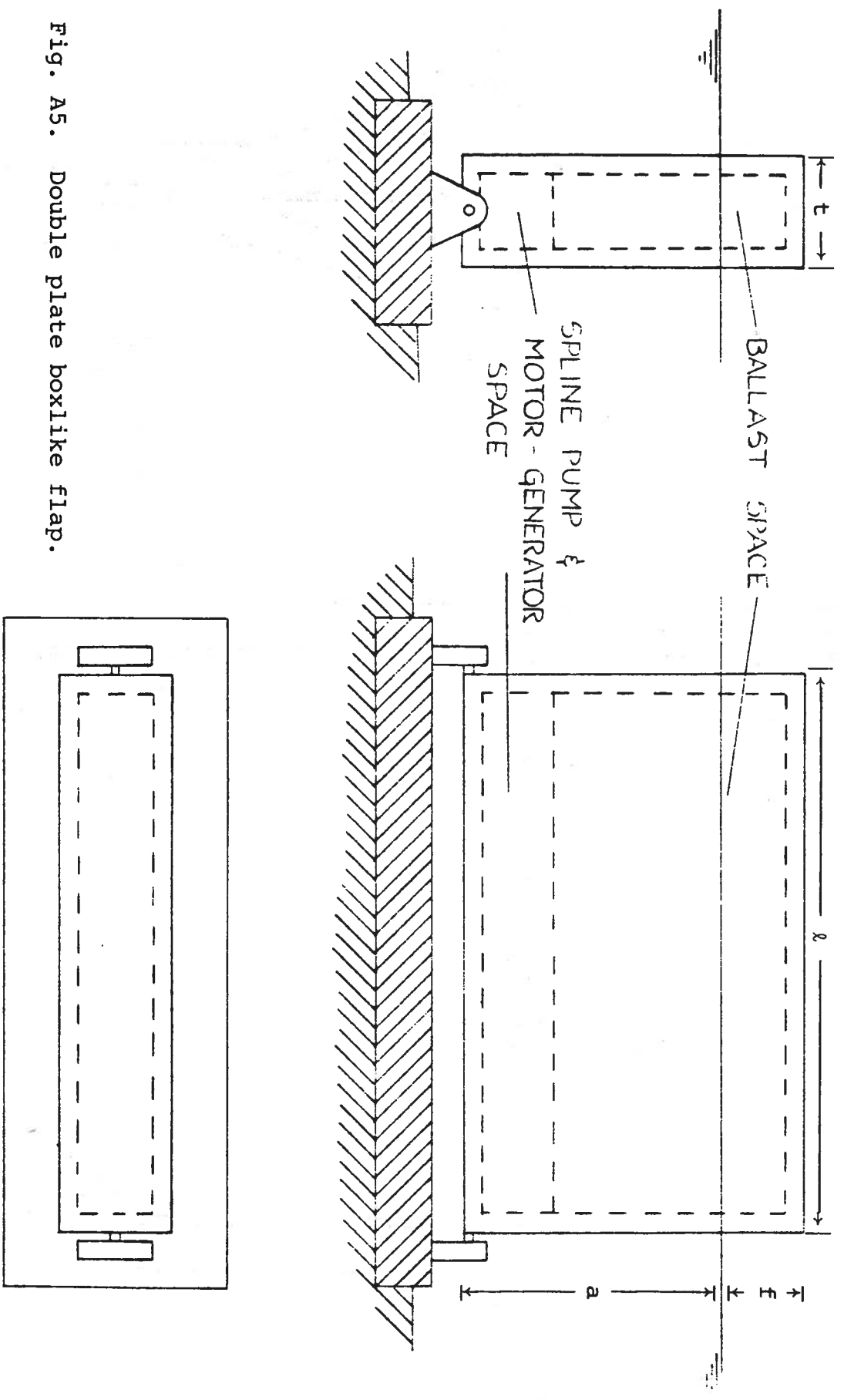


Fig. A5. Double plate boxlike flap.

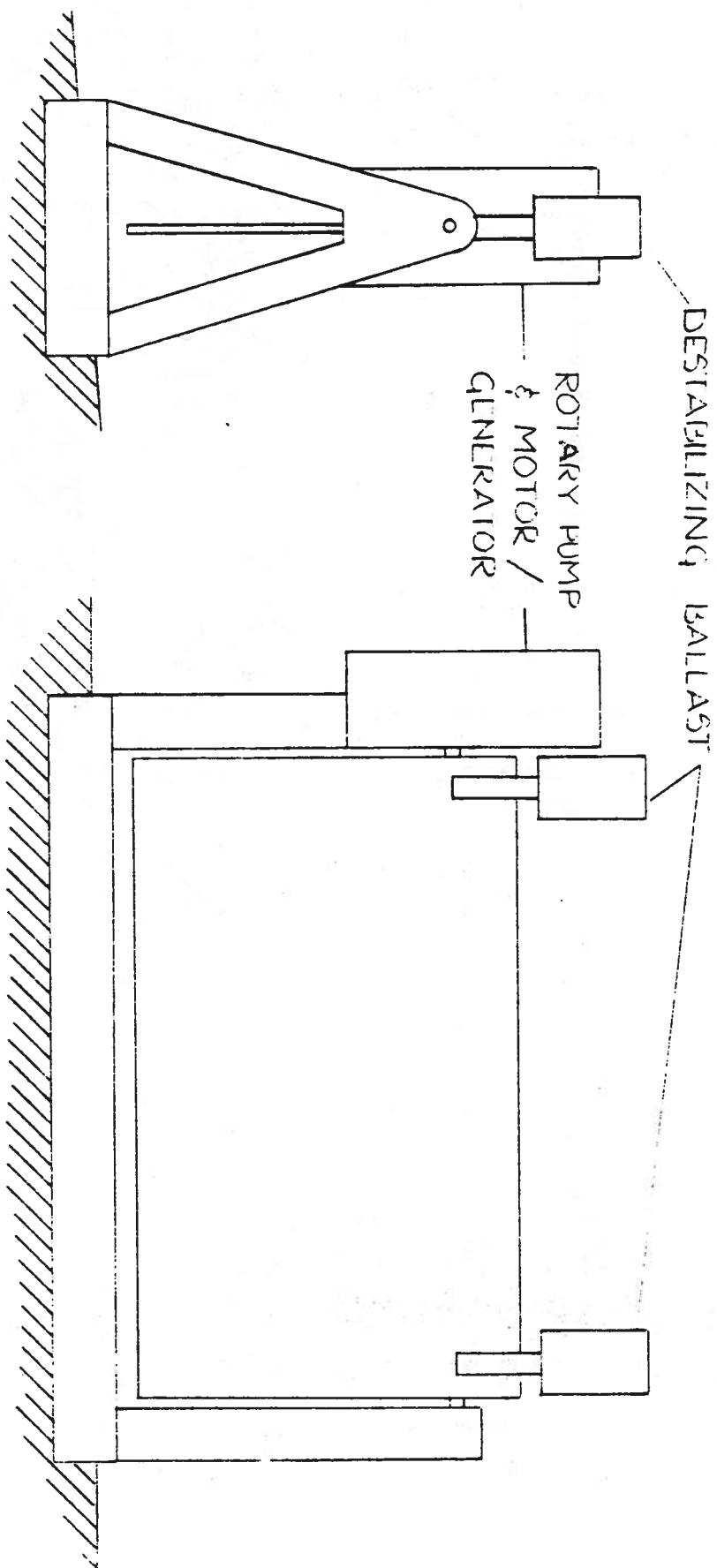
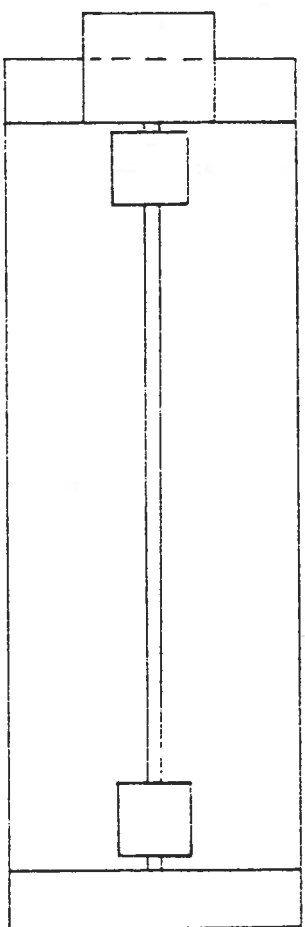


Fig. A6. Pendulous top-pivoted flap.



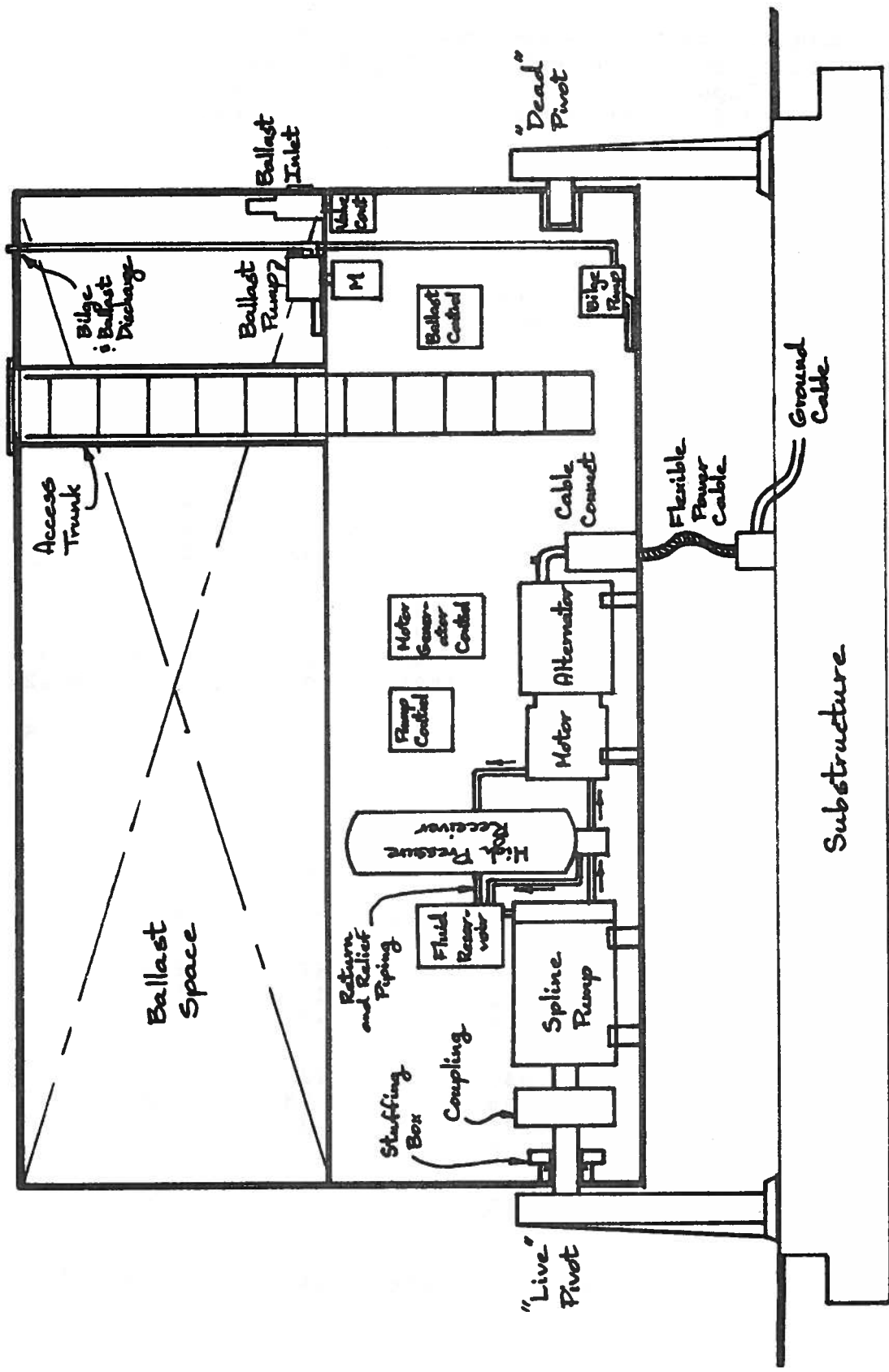


Fig. A7. Arrangement of a positive displacement hydraulic power takeoff and auxiliary systems inside a bottom pivoted boxlike flap.

Table I. Typical comparisons of power absorption and flap motions for single and twin flap devices, normal encounter. Flaps 5 m draft, 10 m width, separation 8 m, water depth 7.5 m, intrinsic inertia 106,000 kg·m².

<u>Flaps</u>	<u>ω</u>	<u>C1</u>	<u>C2</u>	<u>D1</u>	<u>D2</u>	<u>P_{ABS}'</u>	<u>X₁'</u>	<u>X₂'</u>				
1	0.6	999		43		1045	11.7					
				100		875	7.0					
				200		604	4.1					
				400		363	2.2					
				800		200	1.2					
				951		171	1.0					
				1600		105	0.60					
						750	417	193	1.6			
						500	833	101	0.82			
						250	1249	69	0.55			
						100	1499	58	0.46			
						0	1666	52	0.42			
				2	0.6	999	999	43	43	990	2.5	11.1
								0	43	1229	4.4	12.7
0	999	604	0.15					8.9				
0	0	95	0.39					0.42				
		500	500					700	700	199	0.82	0.95
		957	∞					35	0	1019	12.7	0
								100	0	786	6.6	0
								200	0	520	3.8	0
								400	0	304	2.1	0
		∞	957					0	400	331	0	2.1
1	0.9	2465						217		544	2.5	
								500		459	1.5	
								862		350	1.0	
										1000	1643	127
						500	2195	98	0.33			
						250	2471	88	0.30			
						0	2748	80	0.27			
				2	0.9	2465	2465	217	217	871	1.4	2.8
								0	217	1059	2.6	3.5
								217	0	415	2.2	4.4
0	0	146	0.23					0.29				
		2642	2642									

Table II. Typical comparison of single and twin flap directionality effects. Flaps 5 m draft, 10 m width, separation 8 m, water depth 7.5 m, intrinsic inertia 106,000 kg·m².

<u>F1</u>	<u>ω</u>	<u>β</u>	<u>C1</u>	<u>C2</u>	<u>D1</u>	<u>D2</u>	<u>P_{ABS}'</u>	<u>X₁'</u>	<u>X₂'</u>
1	.338	0	302		940		54	1.0	
		15					51	0.97	
		30					41	0.87	
		45					27	0.71	
		60					13	0.50	
		75					3.6	0.26	
		2					.338	0	300
15	94		0.97	0.97					
30	75		0.87	0.86					
45	50		0.71	0.70					
60	25		0.51	0.49					
75	6.6		0.26	0.24					
1	.918		0	302		940			
		15	57				0.38		
		30	45				0.34		
		45	29				0.27		
		60	14				0.19		
		75	3.7				0.10		
		2	.918				0		300
15	105			0.33	0.42				
30	83			0.30	0.37				
45	53			0.24	0.29				
60	26			0.17	0.20				
75	6.7			0.09	0.10				
1	1.33			0	302		940		
		15	48	0.24					
		30	37	0.21					
		45	23	0.17					
		60	11	0.11					
		75	2.7	0.06					
		2	1.33	0					
15	89			0.26	0.22				
30	67			0.23	0.19				
45	41			0.18	0.15				
60	19			0.12	0.10				
75	4.8			0.06	0.05				

Table III. Typical comparison of twin flap variations near an optimum tuning and damping. Flaps 4 m draft, 5 m width, separation 4 m, water depth 30 m, intrinsic inertia 27,000 kg·m².

<u>Flaps</u>	<u>ω</u>	<u>C1</u>	<u>C2</u>	<u>D1</u>	<u>D2</u>	<u>P_{ABS}'</u>	<u>X₁'</u>	<u>X₂'</u>
1	.988					514	15.8	
2	.988	410	412	-2.6	5.7	929	27.2	25.9
		410	413	-2.1	4.6	1027	27.2	28.2
		411	413	-2.1	4.6	1046	33.5	31.3
		411	413	-1.9	4.2	1063	29.6	30.4
		411	413	-1.8	3.9	1088	31.3	32.2
		411	414	-1.8	3.9	1104	37.5	35.3
		411	414	-1.7	3.6	1121	37.2	35.9
		411	414	-1.6	3.4	1132	40.1	38.2
		411	416	0	2.1	1049	37.3	32.0
		410	414	-1.6	3.4	906	20.3	27.2
		410	416	0	2.1	969	25.3	24.1

Table IV. Summary of effects of spectral parameters on design parameters. Increases in the given spectral measure (with the other measures unchanged) have the suggested effect on each design feature. Arrows indicate an increase or decrease, - indicates no significant effect, LC indicates "less critical."

<u>Spectral Measure</u>	<u>Design Parameter</u>						
	<u>Geometry</u>	<u>Draft</u>	<u>Width</u>	<u>Tuning</u>	<u>Damping</u>	<u>Rating</u>	<u>Struct</u>
Average Power Density		↑	↑	-	↑	↑	↑
Central Frequency		↓	↓	↑	-	-	-
Power Broadness		↑	-	LC	↑	↓	-
Directionality Measure		-	↓	-	-	↓	↓

APPENDIX: PROTOTYPE WAVE ABSORBING SYSTEMS

The design of a small operational prototype system is a possible next step toward the practical application of a flap-type device. This step has already been taken for several other device concepts, notably:

(a) The 1-m diameter, 50-m long (nominally one-tenth scale) Salter duck array tested in Loch Ness during 1977 and 1978 (reported in Ref. 27).

(b) The one-tenth scale Cockerell raft, Wavepower Ltd., tested in the Solent in 1978 (described in Ref. 43).

(c) The 80-m long wave-power ship KAIMEI (Ref. 8).

Needless to say, there are obvious economic reasons to proceed through an operational prototype stage, rather than attempting to go directly from laboratory or tank-test experiments to the design of a full-scale power generating installation. Apart from the high costs and risks of making a large jump in device size, there are also valuable lessons to be learned from a prototype device. There are at least three key differences between such an operating device and experimental tank models:

(1) An operational prototype, if it can be designed to

produce useful power (rather than merely measuring the capacity for power production), will give some insight into the practical problems of design and operation of an entire generating system, quite beyond the hydrodynamic behavior of the absorbing body alone.

(2) A prototype system, installed in an actual sea location (or at least in a site that gives a good distribution of "sea-like" conditions, as Loch Ness was supposed to do), provides a basis for long-term data collection that probably cannot be obtained at reasonable cost in an experimental facility, even with sophisticated wavemaking apparatus.

(3) A prototype system at sea is exposed to other environmental factors (in addition to the wave climate) that cannot be conveniently duplicated in the laboratory. The experience gained in meeting these environmental factors will be extremely valuable in subsequent larger scale designs.

For these reasons, the prototype stage is important to the potential development of wave energy resources, regardless of the device type proposed. However, before this stage can be undertaken, several underlying design decisions must be made. Apart from questions of device geometry, and the issue of floating versus fixed platforms, both of which have been addressed in preceding sections, there remain two basic elements of the system to decide upon: the

type and arrangement of power takeoff and conversion machinery, and the provision of suitable restoring forces for tuning the device. Each of these factors will be discussed below. Following this discussion, the outline of a proposed operational prototype flap device will be presented, together with a method for estimating its economic performance.

Type and Arrangement of Power Takeoff Machinery

The type of power takeoff machinery employed has a substantial impact on the geometry of the device, both with regard to the flaps themselves and their supporting structures. In past work, three main types of power conversion machinery have been most often proposed for the intermediate transformation of the low-frequency oscillatory power absorbed from ocean waves into electrical power. These are:

1. Positive-displacement hydraulic systems driving conventional alternators.
2. Turbomachinery, either hydraulic or pneumatic, also driving conventional alternators.
3. Specialized, directly coupled, low-speed induction generators, often based on superconducting components.

Of these alternatives the last is still highly speculative, and will receive no further consideration here. Each of the other two types has produced a large number of

proposed variants, differing primarily in the details of the hydraulic or pneumatic pumping system supplying fluid under pressure to the motor or turbine driving the generator.

Both high-pressure hydraulic and low-pressure pneumatic or hydraulic systems offer particular advantages and disadvantages as applied to flap-type wave-power absorbers. Both the Salter duck and the Cockerell raft prototype devices mentioned above were fitted with positive-displacement hydraulic systems, the damping forces actually provided by hydraulic cylinders. In the latter case, the pressurized hydraulic fluid operated a piston-type hydraulic motor driving an automotive alternator. By contrast, the much larger KAIMEI device used air turbines, driven by the alternate compression and decompression of air contained between the free surface and the floating structure of the vessel.

The generic characteristics of these types of machinery have been discussed in depth elsewhere; in Ref. 43 for example. While the detailed design of the power takeoff system is outside the scope of this presentation, some basic considerations in the selection of a power takeoff will be given here, with specific application to flap-type absorbers.

Requirements for Power Takeoff Systems for Flap-Type Absorbers

The essential function for any power takeoff system for wave power absorbers is the conversion of power in the form of a low-frequency, random response due to wave forces into a suitably uniform and high-frequency (or even steady) output. In the case of a conversion system driving a conventional alternator, the desired properties of the conversion process may be listed as follows:

1. Rectification. The conventional alternator must be driven in one direction, regardless of the direction of motion of the absorbing body. Rectification may be achieved by suitable valving of a fluid flow between a pump and motor (or turbine), by the use of unidirectional turbomachinery (such as the Wells turbine), or mechanically by a system of pawls or overriding clutches.

2. Torque conversion. A typical prototype installation would probably be based on a standard alternator rated at between 800 and 3600 rpm, while the flap might be oscillating at 0.1 Hz or even less. Thus the required step-up in speed is unusually high. This torque conversion can be accomplished efficiently either by positive-displacement hydraulic systems or by turbomachinery.

3. Cycle smoothing. For practical reasons, a conventional alternator obviously should not have to stop and start on each stroke of the oscillating body. Thus, the

power takeoff system must perform some short-term energy storage over a fraction of the cycle, while the body stops and reverses direction. Similarly, in random seas, the power-conversion system may be called upon to perform further short-term energy storage to secure smoothing of the input to the alternator. Smoothing can be obtained in the power-conversion process by: (a) Interconnecting several oscillating bodies to a single alternator drive, and depending on the phasing of the body motions to develop the required degree of smoothing at the alternator. (b) Energy storage by pumping fluid into a high-pressure receiver or an elevated reservoir. (c) Energy storage in the inertia of moving parts, such as a flywheel or the generator itself.

4. Provision for variable stroke of the absorbing body. The alternator must be able to reach its approximate rated speed for a wide range of root-mean-square response of the oscillating body. In order to obtain rated alternator speed in a range of seastates, of course, the alternator load must be varied. Normally, this can be done by varying the excitation of the alternator, however, the intermediate conversion machinery must also be able to provide the variable torque conversion necessary. Furthermore, because of the large variation of time-averaged absorbed power with changes in ambient seastate, the conversion machinery must be able to achieve reasonable efficien-

cy over a relatively wide range of power input.

5. Controllability of external damping coefficient.

In order to make use of variable damping or phase control (which have been discussed in a previous section) to control the absorbed power and the motion of the flap in a random sea, the power takeoff must be capable of relatively rapid modulation of the load in response to gross changes in motion amplitude. For practical reasons, positive-displacement hydraulic systems are better suited to this rapid variation than are turbomachinery-based systems.

6. Reliability and long period between required maintenance. Because of the remote location of the absorbers, and the consequent difficulty and added expense of maintenance and repair operations, the conversion machinery must be capable of operating reliably for long periods without intervention. In this regard, turbomachinery is probably a better choice than relatively sensitive high-pressure hydraulics.

In addition to these specialized requirements, a suitable wave-power conversion system, like all other power conversion devices, must also achieve a favorable balance between nominal efficiency and first cost.

Hydraulic versus Pneumatic Conversion Machinery

As mentioned above, the two most commonly proposed forms of intermediate power conversion using fairly conventional components are positive-displacement hydraulic and low-pressure turbine systems, either hydraulic or pneumatic. Positive-displacement hydraulic systems have been proposed by Salter (Ref. 5), Cockerell (Ref. 7), Q-Corporation (Ref. 45), and Evans (Ref. 46), among others. The Salter duck configuration was originally envisioned as incorporating a large-diameter spline pump between the moving body and a supporting "backbone". More recent versions of the Salter device include hydraulic pumps driven by the precession forces of large gyroscopes, permitting the entire power takeoff to be fitted inside a watertight compartment within the moving body. Prototype models of the Cockerell wave-contouring raft have been fitted with standard hydraulic cylinders between adjacent sections, acting as the pumps in the system. In early feasibility studies for flap-type absorbers, hydraulic cylinders were also envisioned as the pumping mechanism (Ref. 45). The Bristol submerged cylinder device (Ref. 46) is also depicted as using hydraulic cylinders in the mooring system to absorb power from the responses of the cylinder in heave and sway. Most of these systems also incorporated positive displacement hydraulic motors with variable stroke (swash-plate or radial piston) to drive the generator, although hydraulic

turbines have also been mentioned.

Regardless of the detailed type and arrangement of the pump, positive displacement hydraulic systems offer the following advantages (Ref. 47):

1. Compactness, particularly for high-pressure systems (this is of special value for a small prototype).

2. Relatively high component efficiencies over a range of pump delivery rates.

3. Rapid variability of device damping over a wide range of settings, for example, by varying the stroke of a swash-plate motor, or by throttling the outlet from the pump.

4. Closed system, not requiring intake of seawater or exterior air.

To weigh against such advantages, however, positive-displacement hydraulic systems also present certain problems, among them:

1. Positive displacement systems may require more complex cycle smoothing arrangements than turbine alternatives, involving an additional component such as a high-pressure receiver.

2. High-pressure hydraulics are sensitive to hydraulic fluid quality and contamination, and require a high standard of manufacturing precision.

3. In general hydraulic power takeoffs impose higher

local loadings on the flap structure at the power takeoff attachment points than can be achieved by other forms of machinery. Thus, the flap structures are subjected to overall bending or torsional moments that may require "thick" flaps for structural soundness.

Water turbine systems have been proposed in connection with submerged oscillating water-column (OWC) systems, and described by Meir (Ref. 48), and Moody (Ref. 49), the HRS rectifier described by Rance (Ref. 50), and the Lockheed Dam-Atoll (Ref. 51). In these systems, the water turbine is actuated directly by wave-induced flow, without the intervention of a mechanical pump, and is connected directly to the alternator. Unidirectional rotation of the turbine is usually achieved by flap valves, by spill-over of water through an entrapped air volume (in the OWC concept), or by employing a unidirectional device such as a Wells turbine (Ref. 52). Cycle-smoothing in these systems depends mainly on the inertia of the turbine-alternator combination.

A later variant of the Cockerell raft (described in Ref. 43) is a hybrid system, using a positive displacement spline pump to deliver seawater against the pressure of an entrapped air volume in a high-mounted reservoir, from which the water then exits through a turbine, thus obtaining both cycle smoothing and unidirectional flow to the turbine. Presumably, the same type of arrangement could be applied to a flap-type system. In fact, the flap device

would then be tantamount to a single-hinge Cockerell raft rotated into a vertical plane.

The advantages of water turbine systems include relative simplicity, few moving parts, distribution of loads on the structure, and high efficiency at rated load due to the possibility of using large, efficient turbines. Various types of turbine have been suggested for this application (Ref. 43). However, power takeoff systems involving seawater-driven turbomachinery are characterized by one practical drawback: the exposure of turbine elements to deterioration and fouling in the salt-water environment. For this reason, in part, many systems have resorted to the use of low pressure air turbines in lieu of seawater turbines.

Air turbines have been proposed for a number of systems in which air is compressed within a floating or fixed chamber by the vertical motion of the free surface itself, e.g., Masuda (Ref. 8). Such systems have made use of flap valves or unidirectional turbines for flow rectification, and one of their key advantages is the absence of any moving parts except for the turbine and its associated valving. By locating the turbine high enough above the waterline, problems of salt-spray ingestion can be minimized. Cycle smoothing is usually obtained by the inertia of the turbogenerator itself; however, the compression of the air within the chamber can also serve as a form of short-term

energy storage for smoothing.

For systems in which power is absorbed by horizontal motions of an absorbing body, such as a flap-type absorber, the free surface itself can no longer be used to act as an air compressor, and some alternative form of actuator must be used as a pump to supply air to the turbine. Flexible air bag systems have been proposed by French (Ref. 53) and Bellamy (Ref. 54). Some experience in the design and manufacture of large flexible air bags has been gained in connection with marine hovercraft and surface effect ships.

For application to a flap-type wave absorber, a flexible bag device could be located entirely above water, between the upper part of the flap and a supporting structure. Thus, power takeoff forces could be distributed almost uniformly over the width of the flap, eliminating most horizontal bending moments on the flap and perhaps permitting some savings in structure weight. As with water turbines, the rectification of turbine motions can be accomplished either by flap valves on the turbine inlet ducting or by the use of an inherently unidirectional turbine, such as the Wells turbine, Ref. 52. It should be noted that a flap fitted with a flexible bag is, in effect, a Lanchester "clam," Ref. 54.

As should be apparent from this discussion, any number of power takeoff systems can be devised to suit a flap-type absorbing body. Each has certain advantages, and the final

selection of one concept over another can only be made on the basis of engineering judgement supported by far more detailed design studies than have been conducted here. At such an early stage, then, there is always some risk attached to choosing a particular type of machinery. At present, however, a prototype system based on positive displacement hydraulics is felt to be most suitable for a flap type device. The rationale for this choice is as follows:

(1) A hydraulic system of relatively small size and low power output can still be made relatively efficient, while small turbines cannot.

(2) A hydraulic system offers a wide range of damping and load-matching characteristics, including the ability to lock the flap in position, which a turbine does not.

(3) A fairly powerful hydraulic system using either direct-acting hydraulic cylinders or a spline pump can be built around commercially available marine units. Components of marine steering gear may be particularly useful in the role of the low-speed pump. For example, straight cylinders, or radial-piston or spline machines, which are normally used as high-torque actuators rather than pumps, may be adapted. For the high-speed alternator drive, a swash-plate machine (often used as a pump or a motor in marine applications, especially in cargo handling systems) is a reasonable choice, and its variable stroke answers many of

the requirements listed in the preceding section.

(4) A hydraulic system, particularly one based on a rotary pump (such as a radial piston or spline machine), offers an advantage with regard to the need for protective stroke limitation. For example, a radial piston device can provide continuous all around motion (the flap will not be able to go quite that far), while a two-vane spline pump can give nearly 90° of throw either way. However, the restriction of flap motion that may be imposed by power takeoff machinery components, regardless of type, is also a function of their location, which is the subject of the next section.

Location of Power Takeoff Machinery

The location of power takeoff machinery is also a key factor in the design of the system. Three possible schemes are shown in Figs. A1-A3. Arrangement I is based on pneumatic conversion using a high-mounted flexible bag with a rectifying turbine. Arrangement II is based on a positive-displacement hydraulic conversion system using a high-mounted double-acting hydraulic cylinder as the pump, with a swash-plate motor driving the alternator. Arrangement III is also based on a positive-displacement hydraulic system: however, the high pressure fluid is delivered by a low-mounted rotary pump, and the entire power takeoff system is arranged in a watertight enclosure.

The advantages of locating all power takeoff machinery above the waterline include the following: (1) ease of access for maintenance; (2) lower forces on power takeoff components due to the large moment arm; (3) simplicity of underwater components (the flap pivot, which absorbs no power, is the only moving part below the waterline). However, above water location of the machinery also has some important drawbacks. The high location requires large additional supporting structures above water, and the machinery must be protected against both weather and high waves, the shelter therefore requiring some degree of watertightness and considerable structural strength. In addition, the use of a top-mounted power takeoff imposes an inherent and rigid stroke limitation on the flap, which must be positively protected independent of hydrodynamic limitations. (Obviously, the use of a severely stroke-limited pump, such as a hydraulic cylinder or even an air bag, implies the need for similar protection against hitting the limit).

By contrast, the placement of power takeoff machinery below the waterline requires little or no additional structure, particularly if all components are housed within the flap. The use of a suitable rotary spline pump gives a stroke limit of over 180 degrees, which in practice would mean that the stroke would be limited only by the flap encountering the bottom. With this arrangement, then, protection against overstroke damage can be obtained largely

by hydrodynamic damping and by the natural reduction of wave exciting force as the flap inclines to a large angle.

Clearly, however, underwater location of the power takeoff machinery has certain disadvantages. It severely restricts access. The forces on the rotary pump components are extremely large, due to the small moment arm involved. The pivots and associated shafting arrangements are also much more complicated in the underwater arrangement, since at least one of the pivots must transmit torque from the flap to the power takeoff, and water-excluding seals must be provided. These will undoubtedly require a bilge pump to free the machinery compartment of the inevitable leakage. Finally, if the power takeoff is located inside the oscillating flap, instead of in a fixed enclosure, then the connection to the power transmission line will require a flexible connector from the flap to the fixed cable, either through the side or bottom of the flap, or coaxially through one of the pivots. The alternative of providing a reliable sliding contact in the pivot, and sealing it against seawater, seems even less attractive.

Power Conversion Machinery and Conversion Efficiency

In the development of a wave-power absorbing systems, the issue that often receives the first and greatest attention is the hydrodynamic problem: configuring a body to obtain high absorbed power in a given wave environment with

respect to device dimensions and other limitations. The absorbed power, however, is clearly only the first step in the transformation of wave power to useable power.

Given the absorption characteristics of a particular device, the problem of designing a suitable secondary conversion system remains. In particular, to obtain a balanced, economical design, the absorption capabilities of the device must be matched by the conversion characteristics of the power takeoff system.

The desired qualities of a power takeoff system have already been mentioned in a previous section, mainly in connection with its function as an external damper on the absorbing device, and consequently as a control on the motion of the flap. In model experiments, in fact, this role is often the only one: since the measurement of absorbed power is the primary aim, it is not usually important that the absorbed power be converted into useful form. Obviously, as part of a practical wave-energy generating system, the power takeoff must also perform efficient secondary conversion into useful and transmittable form.

Conversion efficiency for an individual absorbing device will be defined as the power output at the connection from the device into the initial transmission line. Complete full-scale power generation systems based on multiple absorbing units, such as proposed in Ref. 56, for example, might include further transmission components at locations

remote from the absorber, or at shore stations, such as step-up transformers, rectifiers, and inverters. These components, although obviously quite important to the overall economic merit of a full-scale wave-power system, should be discussed separately.

For a prototype system, particularly if it consists of a single device located relatively close to shore, it seems likely that a high-voltage a.c. transmission system (3300 or 4250 V) would be used directly to the shore station, rather than transforming and rectifying for a long distance d.c. transmission. Details of the transmission system for a full-scale, multiple-unit system have been considered by Glendenning (Ref. 30), Wallace and Whittington (Ref. 55), and McIlhagger (Ref. 56).

The conversion losses for a device using positive displacement hydraulics driving an electric generator can be grouped into the following components:

- (1) Mechanical friction in the flap bearings and drive to the pump.
- (2) Mechanical and volumetric (leakage) losses in the pump.
- (4) Losses in the piping and valves between pump, high-pressure receiver, and motor.
- (5) Losses in the alternator.

Typical losses in large, water-lubricated shaft bearings, such as marine stern-tubes, are about 2 percent.

For shafting which must stop and start repeatedly under significant normal loads as in the case of an oscillating flap, it is quite possible that frictional losses will be substantially higher than for continuously rotating shafts. In the absence of conclusive data, a bearing efficiency of 96 percent, corresponding to twice the loss for a typical stern-tube application, might be assumed.

The two basic elements of any system of this type are the hydraulic pump and motor, although other components are also necessary to smooth the output from the pump in order to provide a near constant motor speed, and to control the load on the motor. The characteristics of positive displacement hydraulic system have been described in detail by Turnbull (Ref. 47) and Korn (Ref. 57). The generic component efficiencies given below are also cited by Shaw, Ref. 43. The assumed efficiencies of electrical components are taken from Ref. 30.

There are many types of positive displacement hydraulic pumps and motors, falling into two major categories: those suitable mainly for low-speed, high torque applications, and those intended for relatively high speed and low torque. In most conventional marine applications, the pump is of the latter type, being driven either by an electric motor or directly by a diesel engine, while the hydraulic motor is connected to a low-speed, high-torque load, such as a steering gear, windlass, or unloading boom actuator.

In a wave-energy absorber the reverse is true: the pump is driven by the low-frequency, high-torque oscillating motion of the absorbing body, while the motor is connected to a high-speed alternator.

Two common types of low-speed positive-displacement hydraulic device are applicable as the pump component in a wave-power conversion system, namely, the radial piston pump and the spline pump. An axial piston machine, usually in the form of a variable stroke swash-plate motor, has been proposed by Salter and others as the most suitable for providing high-speed output for electrical generation.

Pressures in most standard commercially available positive displacement systems are relatively high, usually less than about $0.007 \text{ m}^3/\text{sec}$, corresponding to a power output of about 135 kW. For the purposes of a prototype wave-power system, at least, it would probably be advantageous to use standard marine or industrial hydraulic components where possible, even if this constraint limited the maximum output to a smaller value than might be economically ideal for a full-scale power generation installation.

Even for full-scale applications, however, it may be that an array of relatively small independent units can compare favorably with a single large device. This is especially true when the absorption cross section substantially exceeds the width of the device, as is the case for point absorbers or short flaps operating near

resonance with optimum damping. Thus, the use of numerous small units in the 100-200 kW range may not be as much of a handicap as it might seem at first glance.

A typical axial piston hydraulic motor operating at constant speed can achieve better than 95 percent over-all conversion efficiency at ideal torque, and can remain above 90 percent efficient over quite a wide range of output torques, generally from 50 to 500 percent of the peak-efficiency torque. The efficiency falls off more rapidly with variation in motor speed, however, which implies that smoothing of the output from the pump may be advantageous to the efficiency of the system in spite of pipe and valving losses associated with a pressure receiver.

The critical efficiency for a suitably smoothed system, in which the motor is able to operate at a fairly constant speed and torque, is then the efficiency of the low-speed pump itself. Obviously, the speed of the pump, and therefore the delivery rate, varies constantly over the stroke even in regular response. Furthermore, in random seas the maximum speed will also vary greatly from stroke to stroke.

Both spline and radial piston pumps can provide about 95 percent maximum efficiency at best pressure and flow rate. If approximately constant output pressure is maintained (within about 20 percent) by delivering to a high-pressure receiver of adequate volume, pump efficiencies of over 90 percent can be maintained for flow rates from about

10 to 500 percent of the maximum-efficiency rate. For larger variations of flow above the ideal rate, better efficiencies can be obtained by increasing the output pressure; however, this is not generally possible without a more complicated system of connections or receivers.

For the purposes of estimating power output in typical seastates, conservative values of average hydraulic pump and motor efficiency are suggested: namely 88 percent and 92 percent, respectively. It should be noted that the average pump efficiency in random seas is degraded primarily by the large excursions forced by higher waves, resulting in a larger fraction of the total flow occurring at rates substantially higher than ideal. Thus, a decrease in overall hydraulic efficiency in higher seastates will actually produce a more level load on the electrical generator.

In addition to losses in the pump and motor, further fluid losses will occur in the piping between components. However, by the use of a compact arrangement of power take-off machinery, with short piping runs, these losses can be held to a low level. An average loss of 4 percent may be assumed for the purposes of power output estimates.

A typical a.c. synchronous generator has an efficiency at rated output of about 95 percent, dropping off only slightly at over and underload conditions. An average efficiency of 92 percent will be assumed. It should be mentioned here that most investigators have adopted synchron-

ous machines on the grounds of efficiency, size, and cost, rather than on the basis of obtaining synchronous a.c. output from multiple absorbing units. The random nature of wave absorption in real seastates will probably preclude the idea of synchronizing multiple units with the grid, unless extremely large hydraulic accumulators are used to achieve complete smoothing of the generator output. For this reason, multiple-unit systems are usually based on rectifying each individual output to d.c. at a central location, placing the rectified outputs in series, and then using high-voltage d.c. final transmission.

Based on the above assumptions, the average conversion efficiency for an absorbing unit will be calculated as follows:

Mechanical efficiency of pump drive	0.96
Pump efficiency	0.88
Piping and valve efficiency	0.96
Motor efficiency	0.92
Generator efficiency	0.92
Over-all conversion efficiency	0.69

This figure may be used with reasonable confidence for moderate seastates, corresponding to outputs between about 50 percent and 200 percent of generator rating. The principal effect of a more energetic seastate is to require a higher damping to maintain reasonable motion amplitudes of the flap. This implies that the load on the generator and

possibly the pitch of the swash-plate motor must be increased, the latter depending not only on the amplitude of the flap motion but also on the average frequency, since the time averaged delivery rate from the pump will depend on the average number of strokes per minute as well as the average length of the stroke. Presumably, then, this departure from rated conditions will entail reduced conversion efficiencies, although the extent of this effect has not been calculated here. However, it appears that in high seastates it would be better to allow the device to operate at reduced absorption (by deliberate detuning of the restoring force) so that the power-takeoff could continue to work at its rating. As mentioned previously, it may also be possible to reduce the absorption by allowing the flap to submerge in higher waves.

Apart from the effects of increasing average absorbed power on conversion efficiency, which would be encountered even in regular waves, the effects of random seas on secondary conversion should be considered. In a relatively broad-banded sea, for example, the use of controlled damping or phase control would be desirable for maximum power output during momentary lulls. For the present, it will be assumed that large transients in the absorbed power would be "shed" above some cutoff value, by allowing the hydraulic pump or receiver to "blow off" at a preset pressure,

allowing the motor to remain below the maximum overload power. An approximate method of estimating the time-averaged loss of output due to a cutoff power has been presented by Glendenning (Ref. 58). This will be discussed at greater length subsequently.

Finally, conversion performance in random seas will depend to some extent on the capacity of the high pressure receiver. A detailed analysis might be undertaken to determine the relationship between receiver capacity and the expected frequency of required blow-off in a given sea-state. Presumably, a larger receiver would be able to store more of the energy from a larger power transient without blowing off, and would also allow the motor to continue to work at a reasonably high rating during a longer momentary lull in the absorbed power. This quantitative work will require a far more detailed analysis of the power takeoff machinery.

Restoring Forces

The performance of any oscillating wave absorber depends to a great extent on the tuning of the system. As has been shown from from Eqs. 44 and 45, for a system having a single degree of freedom the conditions for maximum power absorption in waves of a given frequency are:

- (i) power takeoff damping equal to "loss" damping (i.e., radiative damping plus system losses, such as friction),

and (ii) Restoring force and mass set for resonance at the given frequency. Thus, the primary function of the restoring force is to tune the device. In addition, of course, the restoring force also provides the stability of the system in the absence of exciting forces, and resists any steady forces that would tend to move the system away from its mean position.

For small-scale models, restoring forces can be provided quite easily by physical springs, as in Refs. 10 and 26. Even in full-scale, for certain completely submerged devices such as the Bristol cylinder, Ref. 46, the absence of hydrostatic stability necessitates mechanical springs of some form, located either underwater or on supporting structures above the surface, and such springs have in fact been proposed. Problems associated with extremely large mechanical springs may include:

1. High first cost.
2. Reliability and maintainability.
3. Heat dissipation.
4. Transference of spring reaction forces into structure.

In many cases, however, full-scale systems can use hydrostatic restoring forces to provide the equivalent of springs. In particular, full-scale devices acting in heave or roll modes at the free surface are most suitable for the application of hydrostatic restoring force: among these

are the Salter duck, Cockerell raft, and rolling flap-type absorbers. In fact, the use of hydrostatic restoring forces is a strong argument for adopting a roll arrangement as opposed to sway for flaps at full scale.

In order to generate a hydrostatic restoring moment, of course, a bottom-pivoted flap must have a certain amount of buoyancy, although it need not have any waterplane area at all. For example, the configuration shown in Fig. A4 can be given positive stability in spite of having essentially no waterplane area. In this case the flap itself can be constructed mainly as a stiffened flat plate, with a boxlike or cylindrical buoyant member below the waterline. The net righting moment at any angle of inclination can be written as

$$M_r = (bz_b - wz_w) \sin \theta \quad (A1)$$

where w is the total weight of the flap, b is the total buoyancy, and z_w and z_b are the centroids of weight and buoyancy, respectively, about the pivot.

For small angles of inclination, this can be linearized as

$$M_r = (bz_b - wz_w) \theta \quad (A2)$$

so that the effective spring constant is

$$C = \left. \frac{dM_r}{d\theta} \right|_0 = bz_b - wz_w \quad (A3)$$

It must be recognized, of course, that the hydrodynamic coefficients (added mass, damping, and exciting force) will be affected by the presence of the buoyant member,

however, a detailed analysis of this effect will not be further considered here.

An alternative arrangement, using the entire flap as a buoyant member, is shown in Fig. A5. The moment of buoyant force for such a boxlike flap can be written as

$$b(\theta)z_b(\theta) = M_b(\theta) = \frac{1}{2} \rho g l t a^2 \frac{\tan \theta}{\sin \theta} \quad \text{for } \theta < \cos^{-1}\left(\frac{a}{a+f}\right)$$

$$b(\theta)z_b(\theta) = M_b(\theta) = \frac{1}{2} \rho g l t (a+f)^2 \sin \theta \quad \text{for } \theta > \cos^{-1}\left(\frac{a}{a+f}\right)$$

(A4)

where the relevant dimensions are as shown in Fig. A5.

Again, for small angles of inclination, this can be linearized as

$$M_r = \frac{1}{2} \rho g l t a^2 \theta - w z_w \theta \quad (A5)$$

giving a spring constant of

$$C = \left. \frac{dM_r}{d\theta} \right|_0 = \frac{1}{2} \rho g l t a^2 - w z_w \quad (A6)$$

The use of a "thick" flap, of course, will also have an effect on the hydrodynamic coefficients versus the assumed thin geometry implied by modelling the flaps as distributions of normal dipoles. A measure of this change can be judged, at least for preliminary purposes, from the 2-D work of Papanikolaou, Ref. 59. A comparison of the sectional hydrodynamic coefficients for rectangular sections of relatively large draft/beam ratios (typically, greater than 2) shows that the effect of changing flap thickness,

at a constant draft, on the section forces or moments is slight. Therefore, it may be assumed that small flap thicknesses, will not have any great effect on the power absorption or motion characteristics of a flap device, other than through the restoring force and tuning.

A boxlike flap structure has certain practical advantages in addition to hydrostatic tuning. Structural concerns, such as twisting and lateral bending of the flaps, for example, are alleviated by the use of a box structure. Furthermore, the interior of the flap may be an attractive location for the power takeoff and conversion machinery.

It has been noted that the restoring moment of the flap can be changed by ballasting the flap. This effect can be seen most easily by adding the weight moment of flooding water to the weight terms in Eqs. A3 and A6, leaving the buoyancy terms unchanged. Obviously, the ballast space should be located as high in the flap as possible, in order to secure a maximum change in spring constant with a minimum amount of flooding water. (This means that a smaller ballast pump will be capable of changing the tuning in a given amount of time.) In fact, the reduction in spring constant is somewhat larger than indicated by Eqs. A3 and A6 if there is a free surface in a partially flooded tank, but for relatively thin spaces this effect can be shown to be slight.

More importantly, the effect of flooding on the

natural frequency of the flap is made even stronger by the fact that ballast not only decreases the net righting moment by adding weight and raising the center of gravity, but also by increasing the flap moment of inertia about the pivot. Therefore, not much ballast will be necessary to secure a large reduction in tuned frequency from the unballasted condition.

The over-all result of dependence on hydrostatics for restoring moments is significant for flap-type absorbers. Flap-type absorbers of practical dimensions and proportions may be limited in the maximum spring constant that can be obtained in relation to inertia, especially when the added inertia is large. Thus, there will be a practical upper limit to the tuned frequency that can be obtained with hydrostatics alone. The implication, then, is that hydrostatically sprung single flap systems can be set for maximum power absorption in relatively long waves, but not in waves that are too short.

For completeness, it should be stated that a rolling flap can also be pivoted at or near the top of the flap, rather than at the bottom. In this case, positive stability (and consequently high restoring moment) is obtained by surplus weight rather than by surplus buoyancy, as shown in Fig. A6. With a pendulous flap, of course, no net buoyancy is required for a positive righting moment, so the flap can

remain structurally thin. However, variable tuning would still depend on the ability to add or subtract weight on the flap, and this in turn would require ballast or movable counterweights somewhere, as shown in the figure.

However, high-pivoted flaps have a number of undesirable characteristics as opposed to bottom-pivoted designs. They cannot be ballasted to submerge without moving the pivot itself. Furthermore, large amplitude motions of a flap with a top pivot would tend to bring the flap closer to the free surface, where local wave induced pressures are greatest, rather than depressing the flap and thereby reducing the pressures most rapidly. Viscous losses can be expected to increase due to the large motion of the bottom edge of the flap. Finally, top-pivoted designs of the fixed variety would require taller, more heavily stressed, and presumably more expensive supporting structures. For these reasons, top-pivoted rolling flaps will not be discussed further here.

Elements of an Economic Model

For the purposes of determining economic feasibility, or to compare two alternative designs on a rational basis, the following two economic elements must be estimated:

- (1) Average annual energy production.
- (2) Average annual cost.

In the following brief sections, we will discuss some methods for arriving at estimates of these two elements for a particular device in a given family of spectra.

Average Annual Energy Production

The average power absorbed by the flap and the power actually converted into a useful form are obviously two different things, and not merely because of the intervention of conversion machinery, with some associated losses, as has been discussed previously. If, in fact, the conversion efficiency were the only thing standing between average absorption and average output, then to determine the annual output we could reasonably begin with a definition of "average average" absorption, as follows:

$$E[\overline{P_{ABS}}] = \sum_j P_j \int_{-\pi}^{\pi} \int_0^{\infty} S_j^+(\omega, \theta) P_{ABSj}'(\omega, \theta) d\omega d\theta \quad (A7)$$

where the summation is over a set of discrete seastates, j ,

each of which is characterized by a probability of occurrence p_j and a directional spectrum $S_j^+(\omega, \theta)$. Furthermore the specific absorption P_{ABSj}' is subscripted with j to imply that there may be an alternative curve of P_{ABS}' applied to each spectrum, since the tuning and damping may in fact be adapted to each spectrum, even for a fixed geometry. That is,

$$P_{ABSj}'(\omega, \beta) = P_{ABS}'(\omega, \beta; \underline{G}, \underline{T}_{Oj}, \underline{D}_{Oj}) \quad (A8)$$

where \underline{T}_{Oj} and \underline{D}_{Oj} denote the optimal (constrained) tuning and damping for the spectrum j . It should be noted here that the facing of the device might be construed as a part of the geometry vector \underline{G} , in the sense that it cannot be changed to suit the daily conditions.

Now, if the conversion efficiency were the only difference between absorbed power P_{ABS} and output power P_{OUT} , then we would be justified in simply writing down that $\overline{P_{OUT}} = \overline{P_{ABS}} \eta_c$ and $E[\overline{P_{OUT}}] = E[\overline{P_{ABS}} \eta_c] = E[\overline{P_{ABS}}] \eta_c$, if conversion efficiency were assumed to be a constant over all operating conditions. However, even if the conversion efficiency were invariant with respect to input frequency (which may or may not be true even over the low frequency range of ocean waves, because of the variation of flap and pump speeds with wave frequency), and with respect to load, (which is probably not true, because of frictional losses), the relationships above would still be only first approxi-

mations, for statistical rather than mechanical reasons.

As Glendenning (Ref. 58) has pointed out, for a linear device which loads the flap as a damper with a constant coefficient, the flap motion and velocity are Gaussian random processes, subject to the assumptions of linear theory. The latter, at least, must also be a zero mean process unless we are prepared to let the flap walk off. On the other hand, the instantaneous power absorption is by definition proportional to the square of the velocity. Thus, the absorbed power is certainly not a Gaussian process, and it is to be hoped it is not zero mean.

In any case, with the instantaneous absorbed power as a random variable Glendenning considers the fact that with finite ratings on various components of the power-takeoff system, there will be times when the power process crosses the threshold of some components capability. It is assumed that when this happens, absorbed power is "lost" like an unwelcome guest, and the component is relieved of the necessity to work at overload.

Fortunately, even though the absorption is not Gaussian, it is possible to determine the fraction of time that it exceeds a certain specified value: the expected fraction of time that the instantaneous absorbed power $P_{ABS}(t)$ is greater than some value P_{crit} is just the probability that the velocity of the flap $V(t)$ is more extreme than $\pm V_{crit}$, where V_{crit} is $(P_{crit}/D)^{1/2}$, D being the effective

damping coefficient of the power takeoff. Now the velocity V is Gaussian, with zero mean and variance given by the spectrum of the motion response:

$$\sigma_V^2 = \int_0^{\infty} \omega^2 S_X^+(\omega) d\omega \quad (\text{A9})$$

Thus, the probability that V exceeds V_{crit} can be calculated easily once the spectrum of the response is known. Calling this probability $F(V_{\text{crit}}, \sigma_V)$, we can say that with probability $1-F$, the device is not overloaded and the instantaneous output should be

$$\begin{aligned} P_{\text{OUT}}(t) &= P_{\text{ABS}}(t) \eta_c \\ &< P_{\text{crit}} \end{aligned}$$

and with probability F the device is overloaded and the output is P_{crit} . From the form of the Gaussian distribution, Glendenning derives a so-called "overload" efficiency, based on the ratio between component rating and the mean of absorbed power. This "efficiency," which is a statistical rather than a mechanical effect, is defined as

$$\eta_o = \overline{P_{\text{OUT}}} / (\overline{P_{\text{ABS}}} \eta_c) \quad (\text{A10})$$

where the conversion efficiency appearing in the denominator (a genuine mechanical ratio of power in to power out) may in fact be a function of $\overline{P_{\text{ABS}}}$. Since η_o depends on the relationship between the fixed component rating and the environment (the mean absorption) it must be a number that varies from one seastate to another, regardless of what the

conversion efficiency does. Therefore, a proper expression for the expected output energy per year is:

$$E[EPY] = E[\overline{P_{OUT}}] \times A \times 8766 \text{ hr/yr} \quad (\text{A11})$$

$$E[\overline{P_{OUT}}] = \sum_j p_j \eta_o(P_{crit}, \overline{P_{ABSj}}) \eta_c(\overline{P_{ABSj}}) \overline{P_{ABSj}}$$

where $\overline{P_{ABSj}}$ is just the double integral from Eq. A7, and A is an availability factor, reflecting lost production time due to the system being out of service either because of breakdown or scheduled maintenance and repair. (Strictly speaking, A should be a random variable, too, because of the probabilistic nature of system failure. However, this will not be considered in detail here. If data were available, the variable A could be replaced by its expected value for the purposes of long-term economic predictions.)

In this formulation, the role of the power rating P_{crit} means that one can design a flap and power system combination that will operate at its rated power with probability nearly 1 in all seastates above a certain energy density. This can always be done by combining a relatively large flap (or a small, lightly damped flap moving through large amplitudes) with a puny generator. This may or may not be a sound strategy, depending on whether flaps or power takeoffs dominate the costs of a system. However, it does make the calculation of the average annual energy production much more straightforward. In fact, for large

seastates, there is no real point in using the entire method represented by Eq. All: above a certain incident power, $\overline{P_{OUT}}$ is simply going to be P_{crit} .

Now, one could argue that a small-generator approach wastes a lot of energy that could otherwise be converted into useful power. However, "waste" is not really a proper word if the design is relatively inexpensive per unit of rating. After all, incident wave energy is free: it is the average annual cost of the subsystems between the wave and the the generator, the subsystems needed to hold the ensemble in place against wave forces, and the undeniable extra annual cost of an offshore versus land location, that must be compared with the average annual costs of the alternative prime mover and its fuel.

Average Annual Cost

The average annual cost is defined as the annual operating cost plus the annual cost of capital recovery, based on a target rate of return (which may include a risk premium), the tax rate and depreciation scheme used, the economic life of the project. For wave energy systems in general (from case studies summarized in Ref. 43) the average annual costs are expected to be more sensitive to capital recovery costs than for conventionally fueled plants, because of the absence of the large fuel cost item. How-

ever, significant operating costs have been predicted for wave energy systems, as well. For this reason, some method of investigating both initial and operating costs, and more particularly the variation of these costs with respect to design variables, is required. In most design cost estimating, the final objective is to make a very accurate estimate of the cost of the project, as for a contract bid; or just a fairly accurate estimate, as for a comparison study between different but reasonably familiar systems, such as ships. In either case, the method usually depends on precedent, either in the form of a few related cases or a large number of data points that can be regressed to give an estimating relationship.

In this case, however, precedent does not exist, comparable structures and even mechanical systems are few, and the thing has not been designed, much less built. In spite of this, a cost is needed to make an evaluation of this device. Even more important than the absolute values of cost items, however, which change from time to time and which have a great deal of scatter depending on who is buying and who is selling, the cost model should contain the proper recognition of physical design variables insofar as they would tend to affect the cost of the device.

The first task is identify the principal cost groups for a flap-type device, with its associated supporting structures and power-takeoff equipment. The following out-

line of groups is proposed, for a device of the type shown in Fig. A7:

(1) Flap structure. This includes all materials incorporated into the flap to resist the global and local loads imposed by wave forces, excess buoyancy forces, and hydrostatic pressure on the shell. It excludes all fittings for pivots and items of internal outfit.

(2) Flap internals. For a boxlike flap, this item includes essentially nonstructural steel material, such as access trunks and ballast tank plating other than the shell of the flap. It excludes all steelwork directly related to the support of power takeoff equipment.

(3) Flap pivots. This item includes all structural pivot components (such as steel shafting and tubing) whether attached to fixed structure or built into the flap, which are subject to the horizontal and vertical forces imposed by waves and excess buoyancy.

(4) Pivot supporting structures. This item includes all fixed steel structures connecting the pivots to the substructure.

(5) Substructure. This item consists of the steel or concrete structures that hold the flap in position on the seabed. It may include pilings as well.

(6) Pivot bearings, seals, and stuffing boxes.

(7) Internal shafting and couplings. This item includes the shafting that carries the reaction torques

from the power takeoff pump into fixed structure. It may also include any flexible couplings that are required to isolate the pump from misalignment or over-all structural forces.

(8) Machinery foundations. This item includes all nonstructural steelwork whose primary function is to locate and support power takeoff and conversion components.

(9) Low-speed hydraulic pump.

(10) Hydraulic high-pressure receiver. This item includes the receiver and its associated pipework and valves, but excludes all active control systems.

(11) Hydraulic fluid reservoir.

(12) Hydraulic motor and electrical generator set.

(13) Power takeoff system controls and sensors. This item includes all remote or automatic controls, including those for the ballast system mentioned in the next item.

(14) Ballast and bilge pump systems. This item includes pumps, motors, piping, valves, and through-hull fittings, but excludes remote or automatic control.

(15) Auxiliary systems. This item includes several miscellaneous outfit components not related to structural, tuning, or power-conversion requirements: for example, navigational aids and warning devices, access ladders and manholes, internal lighting if any, lifting arrangements, etc.

(17) Power connection and underwater cable.

(18) Springs. This item includes all mechanical,

pneumatic, or hydraulic devices intended to provide restoring moments in addition to hydrostatics, if fitted.

Each of these cost groups will contain both material and labor components. The groups are now described and discussed in greater detail, with a brief explanation of suggested preliminary estimating methods and sources of further information.

Flap structure. The flap structures must be designed to withstand forces under more extreme wave conditions, as distinct from the design conditions for the power takeoff components. Therefore, for the purposes of a rough weight and cost estimate, the relevant loads on the flap structure must be defined and estimated, at least in a preliminary way. These loads arise from two distinct sets of forces: wave forces, and hydrostatic forces that would exist even in the absence of waves. The weight of flap structural components may be dominated by either primary stresses (e.g., those stemming from over-all bending moments) or by local stresses, depending on arrangements. This is also the case for a ship hull, so that many of the design arguments may be approached from the ship designer's point of view. The discussion begins with primary stresses.

A horizontal bending moment arises from wave forces, and is especially large if the flap is supported only by pivots at its ends. For regular waves of a given frequency

and amplitude, the maximum first-order horizontal force on the flap may be approximated from the roll exciting moment amplitude calculated by the hydrodynamic program, by dividing by a lever arm. In deep water, this arm is never less than the half-draft, the limit in long waves, as shown by Evans (Ref. 15). In shallow water, a strong argument could be made for using the half-draft, because the pressure due to the incident wave becomes more nearly constant with respect to depth.

A better approach, of course, would be to modify the existing program to calculate the total horizontal force as well as the roll moment, since this merely involves an additional use for the pressure (or dipole) distribution which has already been calculated. This has not been done at this point, mainly because of a preoccupation with energy absorption and flap motion responses. However, Eq. 38, modified by removing the lever arm terms, would provide these horizontal forces.

As an additional problem, a sound flap structure should be designed on the basis of long-term extreme values of a random process, as suggested by Ochi (Ref. 60), rather than by selecting a "design" wave and configuring the structure to withstand the deterministic loads imposed by it. Nevertheless, the use of such a simplified design method is firmly entrenched in ship design practice, and constitutes a reasonable method for making first estimates.

The problem, then, becomes one of identifying a "reasonable" design wave for structural purposes. In preliminary ship design, the design wavelength and height for estimating maximum wave bending moments are both usually related to the length of the ship. For a relatively short wave-absorbing body in nearly normal wave encounter, this approach is not valid: the wave bending moment can hardly be assumed to be maximum in waves of flap length. However, within a given spectrum for an extreme sea condition, the wave exciting force spectrum can be determined from the wave spectrum and the squared exciting force in unit wave amplitude as a function of frequency, a quantity which is available from the hydrodynamic model. The root-mean-square exciting force, and thus anticipated extreme values, can be calculated based on this output spectrum, following Ochi's method.

In the absence of a full spectral analysis of wave forces, a design wave force for a wave absorber may be selected on the basis of the maximum torque of the hydraulic system. This implies that in large waves, the power take-off will "blow-off" at a certain pressure, allowing the flap to incline and relieve some of the pressure due to the incident wave. In this regard, the flap is significantly different from a ship. The maximum torque of the power takeoff can be adjusted, of course, by setting the pressure on the relief valve, but it seems reasonable to assume that

it will be substantially larger than the torque at rated power output. Let this overload torque setting be denoted by

$$\Gamma_{\text{over}} = K \Gamma_{\text{rated}} \quad (\text{A12})$$

where K is a constant (greater than one) to be decided upon after an analysis of overload power loss following the method of Glendenning (Ref. 58), and Γ_{rated} is the maximum instantaneous torque when the pump is delivering its nominal mean rated power.

The torque at rated power can be determined from the maximum instantaneous power output in the rated condition and the corresponding angular speed of the pump. For harmonic motion of the flap, the maximum instantaneous power can be shown to be twice the mean power, and the peak torque on the pump at rated power output can then be written as

$$\Gamma_{\text{rated}} = 2\bar{P}/\omega S \quad (\text{A13})$$

where P is the rated mean power output from the pump, ω is the angular frequency (wave frequency), and S is the rated half-stroke (a motion amplitude). The horizontal force on the flap corresponding to overload torque on the pump can be calculated by dividing the torque by the assumed lever arm of the wave forces about the pivot, approximately half the flap draft, as stated above. The values of ω and S used in Eq. A13 are obviously of great importance. For a

conservative flap structural design, the lowest wave frequency of economic interest can be used, but what of S ?

From the point of view of reducing the torque on the pump, and the corresponding force on the flap, it is advantageous to have the flap move through a large amplitude, contingent on absorbing a given power. The extent to which large motions may reduce the absorbed power cannot be predicted on the basis of linear results, however. Until more information, either analytical or experimental, is obtained on this point, the designer must use a reasonable estimate of the imposed stroke limit, realizing its effect on the rated torque.

In any case, if the horizontal force amplitude is denoted by F_h , then the mid-span horizontal bending moment between two end pivots (assuming pinned end conditions) is

$$M_B = (1/8) F_h \ell \quad (A14)$$

assuming a uniform distribution of load over the width of the flap, ℓ .

The use of pinned end conditions implies that the short pivot bearings at either end of the flap are mounted compliantly. This kind of arrangement will clearly require an internal flexible coupling between the pivot and the pump, so that misalignment forces are not transmitted. However, more rigid bearing mountings would entail locally concentrated bending moments on the flap, and on the pivots

themselves. This would cause additional problems of bearing wear and frictional losses, and would still not necessarily eliminate the need for a flexible coupling. Therefore it seems wiser to accept a system that allows for angular misalignment at the flap ends from the very outset.

The assumption of a uniform load distribution over the width of the flap is not conservative for estimating the bending moment, since the actual distribution must tend to zero at the ends. However, if a more detailed widthwise distribution of wave loads is desired for structural calculations, the hydrodynamic model can be modified to produce this load distribution as well, using the dipole distribution already calculated for the hydrodynamic coefficients, Eq. 38.

With regard to the number of pivots, it should be noted that making the pivots more numerous, or even continuous along the bottom of the flap, will reduce the horizontal bending moment on the flap by transferring the loads directly into the substructure. However, such arrangements will increase the complexity of the pivot system, may also have a complicating effect on the power takeoff and flap design, and will tend to make bearing alignment more critical. Nevertheless, this is a design detail that should be given more careful study at a later stage.

The flanges, that is, the front and back plates of the flap and their horizontal stiffeners, must be heavy if the

bending moment is large, especially because the flap thickness t is the small dimension. If the flap is considered as a simple beam in bending, and if the bending moment is as estimated above, then the required effective flange thickness at midspan, distributed over the depth of the flap, is given by

$$H_f = \frac{1}{8} \frac{F_h \ell}{(a+f) t \sigma} \quad (A15)$$

where a is the flap draft and f the freeboard, and σ is the working stress of the flap material. Thus the flange thickness can be seen to be sensitive to the flap dimensions ℓ and t , especially since the horizontal force can be expected to increase with ℓ , assuming that the designer increases the rated torque of the pump (at least) to match the smaller motion amplitude of a wider flap at a given power output. In addition, in short waves, an increased flap width does increase the available power absorption, and the designer may wish to increase the rating and torque to follow suit.

For relatively short flaps, however, it may turn out that the over-all horizontal bending moment leads to a required flange plating thickness that is small. In such a case, the actual plating thickness used will generally be determined by local pressure loads, both hydrodynamic and hydrostatic. The required plating thickness will then be dependent on the frame spacing, and may be calculated by

methods that are well known from preliminary ship design, such as those in Ref. 61.

Similarly, the required thickness of top, bottom, and end plating may be determined by hydrostatic requirements. For long, two-pivot flaps, subject to high midspan bending moments, this plating may be significantly lighter than the front and back plates, except where local reinforcement is needed in way of pivot bearing attachment points, power takeoff machinery foundations, and other local loads.

Since the high-frequency tuning of the device (without mechanical springs) depends on excess buoyant moment (spring constant) and to an extent on flap inertia, there will be some advantage in minimizing unnecessary flap weight, particularly top weight, provided that doing so does not unduly complicate the design and increase the costs. (In this regard, it is very much like a ship design.) Therefore, it may be desirable to reduce plating thicknesses in areas of low primary stress, away from the midspan of the flap, except where local reinforcement is necessary. However, this is a design detail that will not be given further consideration at this point.

A second bending load on the flap arises from excess buoyancy. However, at small angles of inclination the the resulting stresses in the top and bottom plating should be relatively small because the flap depth is so much larger than the thickness. However, the excess buoyant force may

become large when a high maximum tuned frequency is sought. Furthermore, the resulting bending moment stresses are transferred to the front and back flanges at higher angles of inclination. Thus, a complete design would have to include a check of this bending moment.

In addition, there is yet a third over-all bending moment due to the lever between the center of wave force and the power takeoff torque. However, the corresponding beam (whose length is only of the order of flap draft) is short and relatively stiff. Thus, the stress due to this component is likely to be low. Finally, the effect of torsional moment on the flap due to the power takeoff reaction is also neglected.

By straightforward geometry, the weight of the shell plating may be approximated for steel as

$$W = 77 \text{ kN/m}^3 [2(a+f)\ell H_f + 2(a+f+\ell)tH_e] \quad (\text{A16})$$

where H_f is the thickness of the front and back (flange) plating, and H_e is the thickness of top, bottom, and end plating. A conservative working stress for normal ship steel may be taken as $1.4 \times 10^8 \text{ N/m}^2$, approximately 20,000 lb/in². For required stiffeners, the shell weight can be increased perhaps 15 to 20 percent, as a first estimate.

The weight of the flap may finally be translated into cost by using a steel material cost, average labor content, and unit labor cost, including indirect costs. Suggested

values, based on Ref. 62 and updated to Jan 1984 dollars, are \$520/tonne material, 80 man·hr/tonne, and \$22.50/man·hr. This labor content and cost are typical of shipbuilding standards. However, these labor estimates may be high for a simple structure consisting almost entirely of flat plate panels and straight stiffeners. A more accurate labor cost estimate should probably be based on weld length and number of parts, rather than pure steel weight. However, this would require a more detailed design than has been developed at this point. In any case, as will be seen below, the costs of the flap structure itself are not the largest and most sensitive items, at least for a small prototype device.

Flap Internals. The weight of access and ballast tank boundaries might be assumed to vary as lt and will be small by comparison with the outer shell and its stiffeners. A few percent of the flap structural weight should suffice as an approximation. Similar cost factors can be applied.

Pivots. The weight of pivots should tend to vary with both the horizontal force due to waves and power takeoff reaction torque, and the vertical force due to excess buoyancy, since it is the pivots that must hold the flap down. If the total length of pivots is short, as assumed for structural reasons, and relatively insensitive to flap dimensions, then the weight and cost will be primarily dep-

endent on the cross-sectional area required to support the load in shear. However, there will be an additional torsional load on at least one pivot to carry the pump torque into the flap structure. This load may then dominate the design of the pivot.

The total nontorsional load on the pivots may be estimated as the resultant of the design horizontal force determined from the pump reaction torque, as above, and the vertical force due to excess buoyancy, which may be calculated separately once the flap dimensions and rough weights are established. For safety, it may be assumed that each of the two pivots will be sized to support the entire flap load. A working stress in shear of 7.0×10^7 N/m² (approximately 10,000 lb/in²) can be assumed for normal shafting materials.

For the torsional requirement, the maximum torque from Eq. A13 can be used, together with the well-known formula for the required radius of a shaft in torsion:

$$r = (2T/\pi\sigma)^{1/3}$$

where σ is the working shear stress. For the combined shear and torsional requirements, a somewhat more detailed analysis of the stress is required. However, a quick but rough method of adding the requirements is available from section 5 of Ref. 61, dealing with spade rudder stocks.

The total weight of pivots may be quite small. However, such forged and machined components are very expen-

sive per unit weight. From unpublished data used in the compilation of Ref. 62, a value of \$7500/tonne seems appropriate as a first estimate.

Pivot supports. These components should vary in required scantling as the total force times the distance from the top of the the substructure to the centerline of the pivot. These will be small but relatively complicated fabrications. Without detailed estimation, the cost is suggested as approximately half of the pivot cost.

Substructure. The nature of the required substructure will vary widely depending on the soil characteristics of the site, the water depth, and other geometrical factors. However, in frictional soils (sand, for example) the base for the pivot supports is envisioned as a mass-concrete structure, with a minimum weight of approximately the excess buoyancy force in the unballasted (high-tuned) condition, plus the horizontal force. A total material plus fabrication cost of \$220/tonne can be used as a first approximation, based on Ref. 63.

Bearings and Seals. This should be a small cost item and may be considered as relatively insensitive to flap dimensions, other than those that affect the pivots themselves. In the absence of any firm data, a value of a quarter to a half of the pivot cost is suggested.

Interior shafting and Couplings. The weight and cost of these items should be functions of the maximum torque or holding torque of the hydraulic pump. Simple dimensional analysis shows that the weight, and therefore (for estimating purposes) the cost, should vary approximately as the torque to the power of $2/3$. Accordingly since this behavior matches that of the pump itself, this cost may be included with that of the pump unless the length of shafting is excessive, which is a design feature to avoid in any case.

Machinery Foundation Steel. Because of the compactness of the flap, these items should be small, they may be grouped with the flap structural weight.

Hydraulic Pump. Unlike the structure of the flap, the pump may be sized directly according to the power takeoff requirements. There is very little data to go on, but the cost of the pump should vary approximately as torque to the two-thirds. The rated torque Γ_R (N·m) may be taken to vary with $\bar{P}_R/\omega S$, where \bar{P}_R is the rated power (watts), S is the nominal flap motion amplitude (radians) and ω is the wave angular frequency. Because the pump is such a high-torque machine, it would not be surprising to find it expensive. An estimator of $\$12 \Gamma_R^{2/3}$, installed, is proposed, based on Ref. 64.

Hydraulic Fluid Components. By dimensional analysis,

a high pressure receiver has a required weight approximately proportional to its volume times the working pressure, that is, roughly proportional to the rated power. Detailed information is lacking, but a preliminary estimate of \$100/kW should suffice, based on a preliminary rough design. A fluid reservoir, by contrast, is usually supplied directly coupled to the pump.

Hydraulic Motor and Electrical Generator Combination.

These items are grouped together because they rotate at the same speed. The cost is estimated from equivalent diesel-generator installations, giving approximately \$750/kW at 100 kW rating for the prime mover and generator alone, without switchboard, distribution systems, or uptakes, as derived from preliminary work for Ref. 62. Because the cost of the motor/generator set is expected to vary roughly as the rating to the two-thirds, at fixed rpm, an estimator of $\$35 P_r^{2/3}$, installed, is derived from these figures.

Controls. Because the degree of control incorporated is so variable, no firm estimator for this component is known. However, it should be relatively flat with respect to the other design variables. A value of \$10,000 buys a reasonable microcomputer and some peripherals. The details of the control system must await a more detailed design study of its requirements.

Ballast and Bilge Pump Systems. This item should be primarily composed of two small pumps and their associated piping, inlets and discharges. A flat \$2400 is estimated for a pair of 150 gpm pumps, with their associated valves and piping, installed (F. Ashcroft, University of Michigan, personal communication). The flow rate from either of these pumps corresponds to a deballasting rate of about 30 tonne/hr.

Auxiliary Systems. This group should be relatively insensitive to device dimensions, since it contains such items as a watertight hatch, mooring cleats to secure a workboat, light and sound signals, a radar reflector, and possibly a mast for same. The problem of what will happen to these last few devices (let alone the workboat) if they are mounted on a flap that submerges periodically has not been solved. However, if they must be placed on an independent structure or buoy, then this cost should probably be estimated separately, although it is certainly represents a part of the cost of the prototype system. A total value of \$1500 has been extracted for navigational lights, radar reflector, an aluminum tube mast, and a single deck manhole, from various marine catalogs. No interior lighting is envisioned for a small prototype system.

Connector and Underwater Cables. Because this item is strongly related to the site rather than to the device it

should be estimated separately. The costs of seabed cables are known to be very high. An estimate of \$40,000/km was given in Ref. 13, for a low-power transmission line, installed. Updated to 1984 costs, this would correspond to approximately \$54,000/km. This alone constitutes a good reason to keep the machine near the shore. The costs of the cable connector should be fairly small by comparison.

Springs. Since no mechanical or pneumatic devices are necessary for a flap with sufficient hydrostatic springing, this item may be conveniently neglected unless the urge is on for a higher tuned springing. They will be expensive.

Finally, the cost of installing this contraption in an offshore location. This must vary widely, but the idea is to build the entire device, complete with substructure, in the yard. Emplacement costs will vary with the distance to the site, of course, but even a modest crane barge with a lift capacity of only about 100 tonnes must charter for several thousand dollars per day. Accordingly, a rate of \$10,000 plus \$20/tonne of substructure weight (the largest single weight item) is charged against this item as a starting guess. This, however, neglects the cost of any pile-driving, or dredging and backfilling, that may be necessary to hold the device in critical soils. In addition, the effect of water draft is excluded, so that even this approximation is restricted to relatively shallow water

sites only.

Annual Capital Recovery. For the average annual cost, a capital recovery factor of 0.18 corresponds to a return of 10 percent after tax, 50 percent income tax, straight line depreciation, and a 20 year life, fairly typical assumptions for a ship. However, it is somewhat doubtful whether this kind of economic thinking is particularly appropriate for a prototype device whose primary reason to exist is research rather than energy production.

Nevertheless, it may be interesting to see what kind of production costs are estimated for such a small device, especially since there is at least the possibility that larger systems may be built around arrays of devices of not much greater size than the prototype. Such systems, of course, would presumably incorporate a more advanced form of power transmission system, possibly involving separate platforms for the transformers and rectifiers, as suggested in Ref. 28. However, the costs of such a full-scale system are even more conjectural than those of the prototype, and will not be discussed further at this point.

Annual Operating Costs. Annual operating costs have been estimated as follows, based on Ref. 64:

Flap structure maintenance: 5 percent of flap structure, pivot, and pivot-support costs.

Substructure maintenance: Nil.

Machinery maintenance and repair: \$15/kW of pump rated power, plus \$12/kW of motor/generator rated power.

Transmission cable maintenance and repair: 5 percent of transmission cable cost.

Insurance: 1.25 percent of total investment.

Finally, of course, the costs, both initial and operating, of research activities associated with the prototype device should be evaluated in detail before any prototype project is undertaken. However, since these costs are not directly associated with power production, it would not be correct to apply them against the average cost per kW·hr.

A Design Example

As an example, consider the wave environment of South Uist, in the Outer Hebrides, as reported in Ref. 28. The seastate distribution for this location consists of 391 cells (significant wave height and energy-averaged period), of which 135 cells registered a probability of occurrence of at least 0.001. Of these, an aggregate probability of 0.654 was represented by 41 states, clustered between significant wave heights of approximately 1.33 to 3.33 m, with energy-averaged periods from 6 to 10 sec. The modal significant wave height was approximately 2 m, with seastates between 1.67 and 2.33 m accounting for an aggregate probability of 0.377.

Accordingly, a reasonable range of design seastates is selected as consisting of 2 m significant wave height states with periods from 6.5 to 10 sec, the modal period at the wave height being about 7.2 sec. A hypothetical site is selected in a water depth of 7.5 m, and it is assumed that the energy density in 2 m significant wave height states is not significantly altered due to the water depth.

Because of the water depth, the flap draft is, of course, firmly limited to 7.5 m. However, in order to keep the pivot well clear of the bottom, an initial flap draft of only 5 m is chosen, together with a flap width of 20 m, consistent with a desire to retain a 2-pivot arrangement and a relatively small device as a prototype.

As shown in Fig. 56, at a tuned spring constant of 6545 kN·m/rad, and a damping of 3000 kN·m·sec, a 5 x 20 m flap device is capable of absorbing approximately 74 kW in 2 m significant seas between 7 and 8.8 sec modal period, corresponding to energy-averaged periods between approximately 7.9 and 9.9 sec. This range covers a large part of the 2 m probability range, and for longer periods the device can be ballasted to maintain a near resonant condition.

A rated pump output of 135 kW is chosen, corresponding to 1.9 times the average absorbed power, and Ref. 54 indicates an "overload efficiency" of 0.73 for this normalized rating. Allowing for losses in shafting, pump, and piping,

as mentioned in a previous part of this appendix, the motor/generator set is sized at 55 kW.

In the design seastate range, 2 m significant wave height, the alternator will be operating at an output of about 37 kW, allowing for the further losses in the hydraulic motor and the generator itself. This design condition, as mentioned above, represents an aggregate probability of almost 0.38.

In more energetic seastates, which account for approximately 0.41 probability, the flap and pump will be overdriven, while the motor/generator will operate at rated power. For example, in increasing from a seastate of 2 m significant wave height at an energy-averaged period of 7.2 sec, to 2.5 m significant at 8.2 sec (typical modal values for South Uist), the incident energy density increases nearly 80 percent. If this higher energy were to be absorbed at an unchanged cross-section, then the fixed pump rating would drop from 1.9 to 1.07 of the mean absorption, corresponding to a reduction in "overload efficiency" from 0.73 to 0.54. The motor would then be receiving approximately 58 kW. Thus, for a fixed motor rating of 55 kW, the flap and pump will begin to unload not far above the design seastate. (It is not claimed that this is an optimal generator-sizing: that is a question for further study.)

In less energetic seastates, accounting for a total probability of about 0.21, the power output will obviously

be reduced, simply because of the incident wave energy reduction. Furthermore, since the frequency content of lower energy seastates shifts toward the high frequency end, the power absorption cross-section may also tend to decline, as shown in earlier sections, due to mistuning. Of course, in these lower seastates, the "overload efficiency" will be nearly 1. Based on the assumption of a constant cross-section, however, it is estimated that for the lower seastates in the South Uist sample, below 2 m significant wave height, an average power output of 15 kW can be obtained.

The average power output can now be calculated from the three groups of conditions (design, high-energy, and low-energy) weighted by their probabilities. The result is a 40 kW average. On this basis, the motor/generator set is already rated 38 percent higher than its average output.

Now, we can turn to some of the estimated costs. The estimated rated torque on the pump (Eq. A13) is 1154 kN·m, based on $\omega = 0.45 \text{ sec}^{-1}$ and $S = 0.52 \text{ rad}$ (30°). Because the pump is already rated so much higher than the motor generator, no further overload capacity need be assumed. The corresponding horizontal force is 462 kN, and the midspan bending moment (Eq. A14) is therefore 2308 kN·m. With an assumed box-flap thickness of 2.6 m, this bending moment is too small to require thick flange plating, and accordingly a minimum steel thickness of 5 mm is applied

for the entire shell. The resulting box weight, (Eq. A16) including 15 percent for internal stiffening, is 146 kN, about 14.9 tonne. Reckoning on another 8 percent for internals, access and tanks, the steel weight in the flap is about 16.1 tonne. The buoyancy in seawater is about 267 tonne, giving an approximate excess buoyancy of about 2620 kN, less the weight of the power installation if fitted inside the flap. This box thickness, then, gives the required spring constant without recourse to mechanical springs.

The design force on the pivots is taken as the resultant of the wave and buoyancy force, about 2660 kN. If each of the two pivots is to be able to take the entire force, surely conservative, the required diameter of each pivot is only 22 cm. However, the torque requirement for the live pivot requires a 44 cm diameter shaft; accordingly, one pivot of each diameter will be specified. If each pivot is 75 cm long, the live pivot weighs 0.90 tonne, and the dead pivot 0.22 tonne.

The rated torque of the pump is 1154 kN·m, as given above, and the motor/generator is rated at 55 kW.

Finally, the substructure weight is set at the sum of the horizontal and vertical forces, namely, 3082 kN, or about 314 tonne. Now, according to the cost expressions given previously, we can estimate the following initial cost breakdown:

Flap Structure:	\$ 37 400
Pivots:	8 400
Pivot Supports:	4 200
Bearings and Seals:	2 100
Spline Pump and Coupling:	132 000
Receiver and Reservoir:	13 500
Motor-Generator:	50 600
Ballast System:	2 400
Auxiliary Systems:	1 500
Substructure:	69 100
Installation:	16 300
Total	\$ 337 500

(less shore cable)

These costs correspond to approximately \$6100/kW based on the generator rating. This is quite high. However, it is a very small plant, and there may be substantial advantages of scale available, particularly in the power takeoff and conversion groups, which are the most expensive items.

The average annual cost breakdown can now be given as follows:

Annual Capital:	\$ 60 800
Structure Maintenance:	2 500
Machinery Maintenance:	2 700
Insurance:	4 200

Total Average Annual Cost: \$ 70 200

Now if the device is able to operate at an average of 40 kW, as assumed above, with an availability of 95 percent, the corresponding cost per kW·hr is approximately 21¢, neglecting the costs of the transmission line. Even for a very short transmission line, say only 1 km, an additional estimated annual capital expense of \$9700, maintenance and repair of \$2700, and increased insurance cost of \$700 are incurred. The corresponding average annual cost is then \$83,300, for a cost per kW·hr of 25¢.

This figure is in the higher range of wave-energy devices, summarized in Ref. 43. It should be mentioned here that the usual cost figures given in this field are for extremely large, conjectural systems, rather than for the prototypes. Furthermore, the usual sources of economic data and projected costs are people who are trying to establish wave-power as a credible energy resource. It would hardly be surprising, therefore, to find that some cognitive bias exists in these numbers.

However, the device described here is very small, and some improvement should be possible. On the other hand, the cost is still in the neighborhood of twice the prevailing estimate of costs for conventional oil-fired, and three times the cost of coal-fired installations (Ref. 43). Thus, the time may not yet be ripe for the widespread application of wave power on a commercial basis. However,

there remains a great deal of interest in this subject in many quarters, and the subject is far from closed.